

NASA CONFERENCE PUBLICATION

NASA CP-2165

NASA-CP-2165 19810006429

SPACE PLASMA PHYSICS ACTIVE EXPERIMENTS

Summary of First Active Experiments
Working Group Meeting, September 23-24, 1980,
Marshall Space Flight Center, Alabama

FOR REFERENCE

NOT TO BE TAKEN FROM THIS ROOM

Edited by W. T. Roberts
Space Sciences Laboratory

October 1980

LIBRARY COPY

JAN 06 1981

**LANGLEY RESEARCH CENTER
LIBRARY, NASA
HAMPTON, VIRGINIA**

Prepared by

NASA — George C. Marshall Space Flight Center
Marshall Space Flight Center, Alabama 35812

1. REPORT NO. NASA CP-2165	2. GOVERNMENT ACCESSION NO.	3. RECIPIENT'S CATALOG NO.	
4. TITLE AND SUBTITLE Space Plasma Physics Active Experiments		5. REPORT DATE November 1980	6. PERFORMING ORGANIZATION CODE
		8. PERFORMING ORGANIZATION REPORT #	
7. AUTHOR(S) Edited by W. T. Roberts	10. WORK UNIT NO.		
9. PERFORMING ORGANIZATION NAME AND ADDRESS George C. Marshall Space Flight Center Marshall Space Flight Center, Alabama 35812		11. CONTRACT OR GRANT NO.	
		13. TYPE OF REPORT & PERIOD COVERED Conference Publication	
12. SPONSORING AGENCY NAME AND ADDRESS National Aeronautics and Space Administration Washington, D.C. 20546		14. SPONSORING AGENCY CODE	
		15. SUPPLEMENTARY NOTES Prepared by Space Sciences Laboratory, Science and Engineering Directorate	
16. ABSTRACT This document is a compilation of the material presented at the first meeting of the Spacelab Space Plasma Physics Active Experiments Working Group on September 23-24, 1980, at the Marshall Space Flight Center.			
17. KEY WORDS		18. DISTRIBUTION STATEMENT Unclassified—Unlimited <i>W. T. Roberts</i>	
19. SECURITY CLASSIF. (of this report) Unclassified	20. SECURITY CLASSIF. (of this page) Unclassified	21. NO. OF PAGES 262	22. PRICE NTIS

FOREWORD

The material included in this document was presented at the first meeting of the Spacelab Space Plasma Physics Active Experiments Working Group on September 23-24, 1980, at the Marshall Space Flight Center (MSFC). Representatives were present for all of the experiments which were selected in November 1979 except for the Atmospheric Lyman-Alpha Emissions (ALAE) experiment. The ALAE writeup in this document is a combination of the ALAE experiment description for Spacelab 1 plus additional material provided by the Principal Investigator.

Because these active experiments to be performed on future Spacelab missions represent a new mode of space plasma physics experimentation in the 1980's, it was decided to publish the presentation material as an initial active experiments reference manual. The individual experiment reports in this document may then be used by scientists who have an interest in the types of instruments that may be flown on future Spacelab missions. The reports also provide initial listings of parameters such as instrument design concepts, instrument capabilities, and planned experiments to be performed.

It will also become obvious that these experiments are highly inter-related; thus, one set of instruments (e.g., particle accelerators and experiment transmitters) require coordinated measurements or observations from other instruments (e.g., free flyers and optical spectrometers). Because the reports provide data on instrument operations, components, etc., they may also be used by engineering teams performing initial mission analysis and planning.

Finally, although they are not in the same state of definition as the other experiments, it was decided to include the Chemical Release Module (CRM) and the Tethered Satellite Facility in this group of future active experiments.

It is anticipated that this document will be updated periodically as the definition of the instruments and experiments matures.

W. T. Roberts
Executive Secretary
Active Experiments Working Group

TABLE OF CONTENTS

		Page
I.	ATMOSPHERIC LYMAN-ALPHA EMISSIONS (ALAE) J. L. Bertaux - CNRS, France	1
II.	ATMOSPHERIC EMISSION PHOTOMETRIC IMAGING (AEPI) S. B. Mende - Lockheed Palo Alto Research Laboratory	9
III.	IMAGING SPECTROMETRIC OBSERVATORY (ISO) D. G. Torr - Utah State University	27
IV.	ENERGETIC NEUTRAL ATOM PRECIPITATION (ENAP) B. A. Tinsley - University of Texas, Dallas	57
V.	WIDE ANGLE MICHELSON DOPPLER IMAGING INTERFEROMETER (WAMDII) G. G. Shepherd - York University, Toronto	75
VI.	ENERGETIC ION MASS SPECTROMETER (EIMS) B. A. Whalen - NRC, Canada	91
VII.	SPACE EXPERIMENTS WITH PARTICLE ACCELERATORS (SEPAC) T. Obayashi - ISAS, Japan	107
VIII.	THEORETICAL AND EXPERIMENTAL STUDY OF BEAM PLASMA PHYSICS (TEBPP) PHYSICS (TEBPP) H. R. Anderson - Rice University	117
IX.	WAVES IN SPACE PLASMAS (WISP) R. W. Fredricks - TRW	139
X.	THE WISP/HF SYSTEM H. G. James - Communications Research Centre, Canada	171
XI.	MAGNETOSPHERIC MULTIPROBES (MMP) J. L. Burch - Southwest Research Institute	185
XII.	RECOVERABLE PLASMA DIAGNOSTICS PACKAGE (RPDP) S. D. Shawhan - University of Iowa	213
XIII.	CHEMICAL RELEASE MODULE (CRM) D. L. Reasoner - Marshall Space Flight Center	237
XIV.	TETHER FACILITY P. M. Banks - Utah State University	247

SECTION I. ATMOSPHERIC LYMAN-ALPHA
EMISSIONS (ALAE)

SPACELAB EXPERIMENT : ALAE

ATMOSPHERIC LYMAN-ALPHA EMISSIONS

J.L. BERTAUX (PI,SA) ; FLORENCE GOUTAIL (CO-1,SA)
G. KOCKARTS (CO-1,IASB)

SCIENTIFIC OBJECTIVES

1. DEUTERIUM (DAY SIDE)

- VERTICAL DISTRIBUTION
- EDDY DIFFUSION COEFF. K AT 100 KM
- TEMPERATURE (100 → 200 KM ?),

2. PROTON PRECIPITATIONS

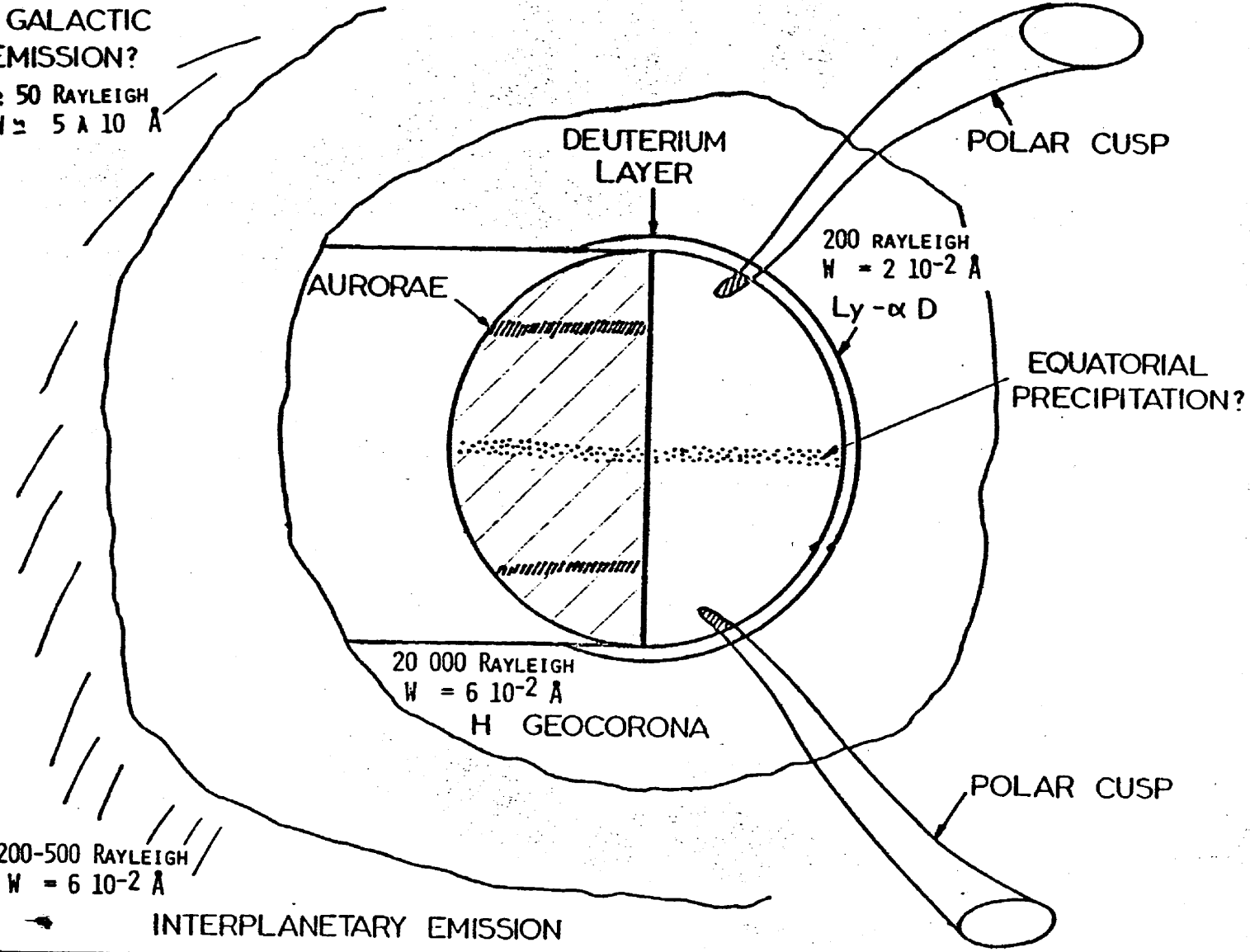
- AURORAL ZONES
- EQUATORIAL ZONES
- POLAR CUSP FOOT
- PROTON GUN OBSERVATIONS.

3. ATMOSPHERIC HYDROGEN

- NADIR : TOTAL H COLUMN
- ZENITH : EXOBASE TEMPERATURE.

GALACTIC
EMISSION?

≈ 50 RAYLEIGH
 $W \approx 5 \text{ \AA} \text{ } 10 \text{ \AA}$



POLAR CUSP

DEUTERIUM
LAYER

AURORAE

200 RAYLEIGH
 $W = 2 \cdot 10^{-2} \text{ \AA}$

Ly - α D

EQUATORIAL
PRECIPITATION?

SUN

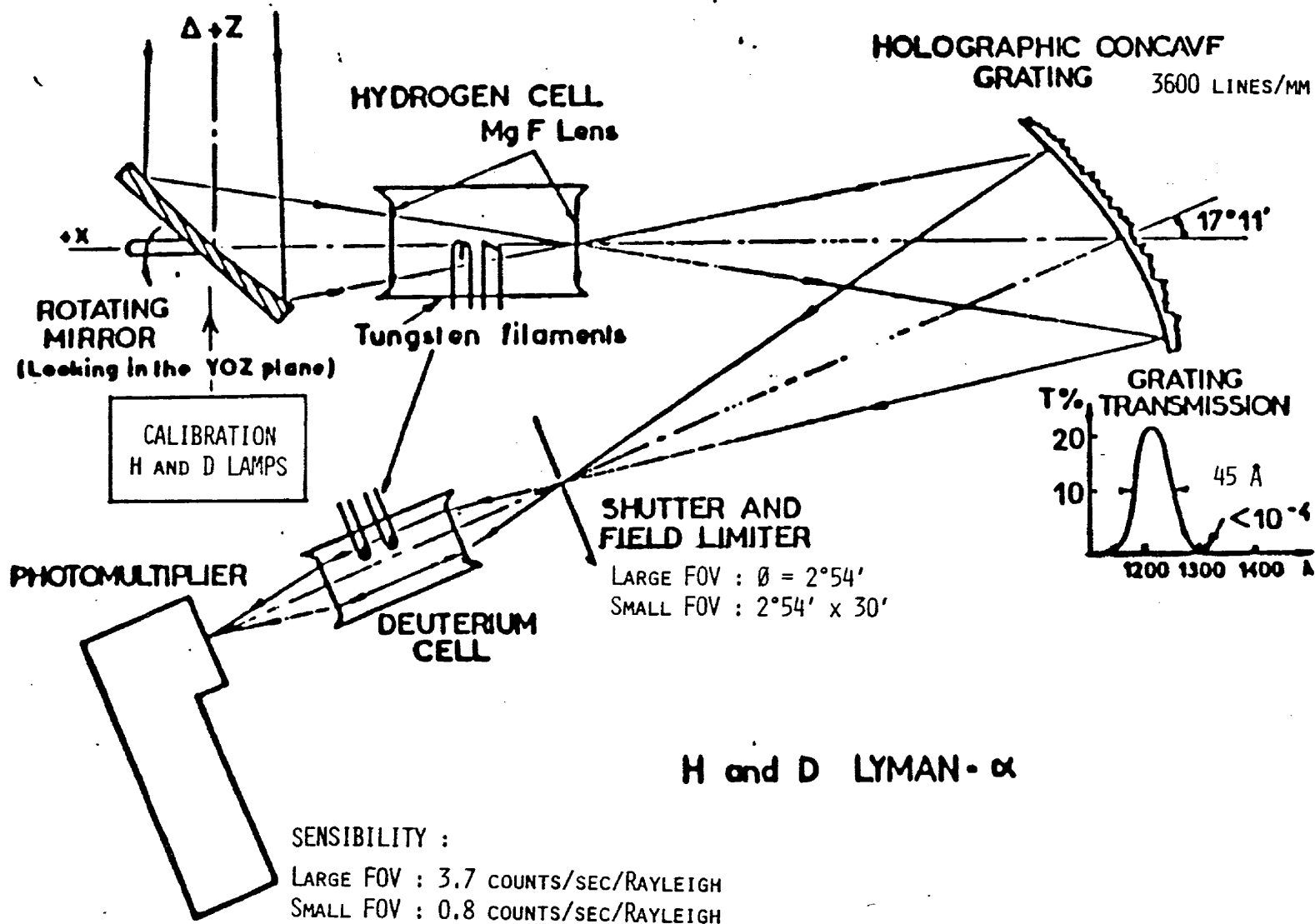
20 000 RAYLEIGH
 $W = 6 \cdot 10^{-2} \text{ \AA}$

H GEORONA

POLAR CUSP

200-500 RAYLEIGH
 $W = 6 \cdot 10^{-2} \text{ \AA}$

INTERPLANETARY EMISSION



INVESTIGATION ON ATMOSPHERIC H AND D THROUGH THE
MEASUREMENT OF THEIR LYMAN- α EMISSIONS
(1ES017)

J. L. Bertaux
Service d'Aéronomie du CNRS, France

The scientific objective of this experiment is to study various sources of Lyman- α emission in the atmosphere, in the interplanetary medium, and possibly in the galactic medium. The instrument is a spectrophotometer associated with two absorption cells, one filled with hydrogen, the other with deuterium (Fig. 1).

The main source of Lyman- α as seen from Spacelab is the result of resonance scattering of solar photons by atmospheric atomic hydrogen. This emission has been studied thoroughly with previous space experiments and is considered as "noise" in the present investigation; it is eliminated with the help of the hydrogen absorption cell run at a high absorption level. The other sources of Lyman- α are then studied (Fig. 2).

Lyman- α emission of atomic deuterium (D) is identified with the help of the deuterium absorption cell. Its intensity and line-width are measured, yielding the vertical distribution of D from 90 to approximately 250 kilometers and its temperature. From this vertical distribution, the eddy diffusion coefficient K around 100 kilometers is derived and mapped on the whole sunlit Earth.

Lyman- α emission resulting from charge exchange is possibly present at various places: auroral zones, equatorial zones, and possibly at the foot of the polar cusps, where the solar wind interacts directly with the neutral atmosphere. The foot of the polar cusps could be located precisely through observations of these regions with a scanning mirror.

Some emission is also expected from the plasma guns placed on board Spacelab.

Interplanetary hydrogen (which comes from the nearby interstellar medium) is a source of Lyman- α . It prevents astronomical observation of diffuse galactic Lyman- α emissions. With the help of the absorption cell, the level of diffuse galactic emission will be determined. The use of the absorption cell on Spacelab is also a test for determining if the presence of geocoronal and interplanetary emission will prevent future astronomical observations of Lyman- α emissions.

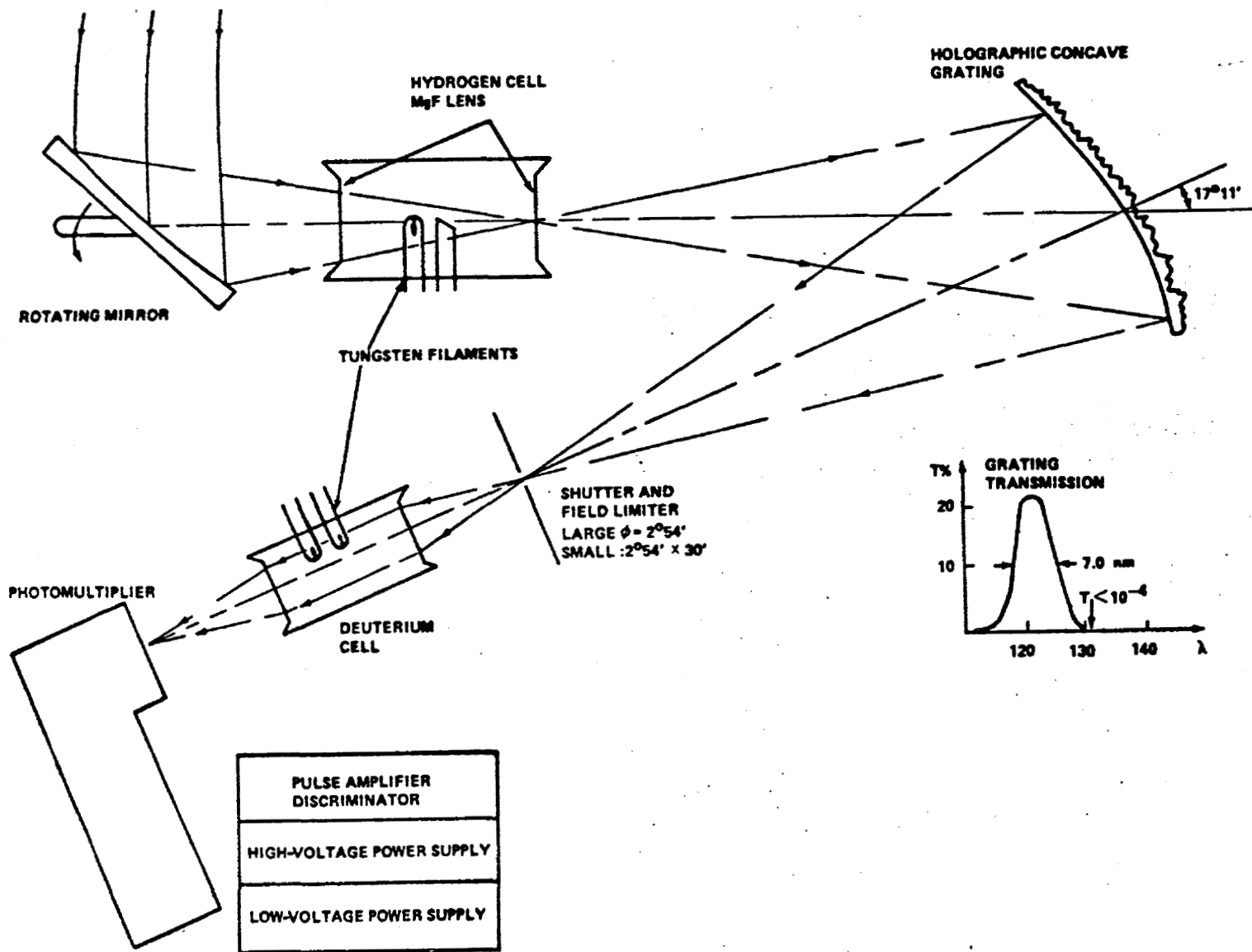


Figure 1. Schematic of instrument for measurement of hydrogen and deuterium Lyman- α emission.

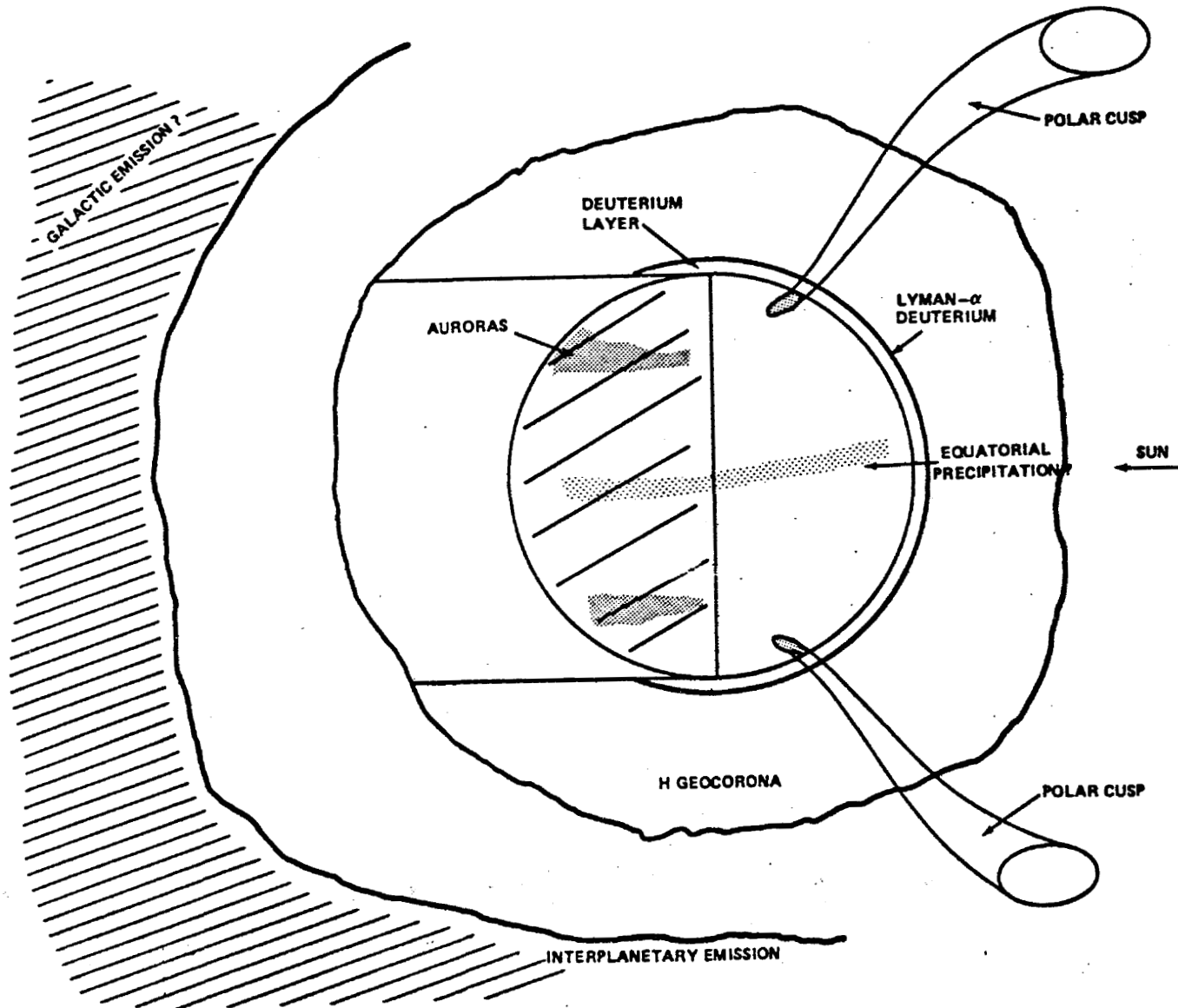


Figure 2. Sources of Lyman- α emissions.

SECTION II. ATMOSPHERIC EMISSION PHOTOMETRIC
IMAGING (AEPI)

Active Experiment Working Group
Meeting

September 23, 1980

Atmospheric Emission Photometric Imaging
on Spacelab
(AEPI)

Presented by

S.B. Mende

Lockheed Palo Alto Research Laboratory
3251 Hanover Street
Palo Alto, California 94304

ATMOSPHERIC EMISSIONS PHOTOMETRIC IMAGING ON SPACELAB

Dr. S. B. Mende, Principal Investigator (415) 493-4411, Ext. 5786
Dr. W. G. Sandie, Co-Investigator Ext. 5638
Lockheed Palo Alto Research Laboratory
Palo Alto, CA 94304 (415) 493-4411

Dr. R. H. Eather, Co-Investigator
Physics Department, Boston College
Chestnut Hill, Massachusetts 02167 (617) 969-0100, Ext. 3595

Dr. G. R. Swenson, Co-Investigator (205) 453-3040
K. S. Clifton, Co-Investigator (205) 453-2305
Space Science Laboratory
George C. Marshall Space Flight Center
Huntsville, Alabama 35812

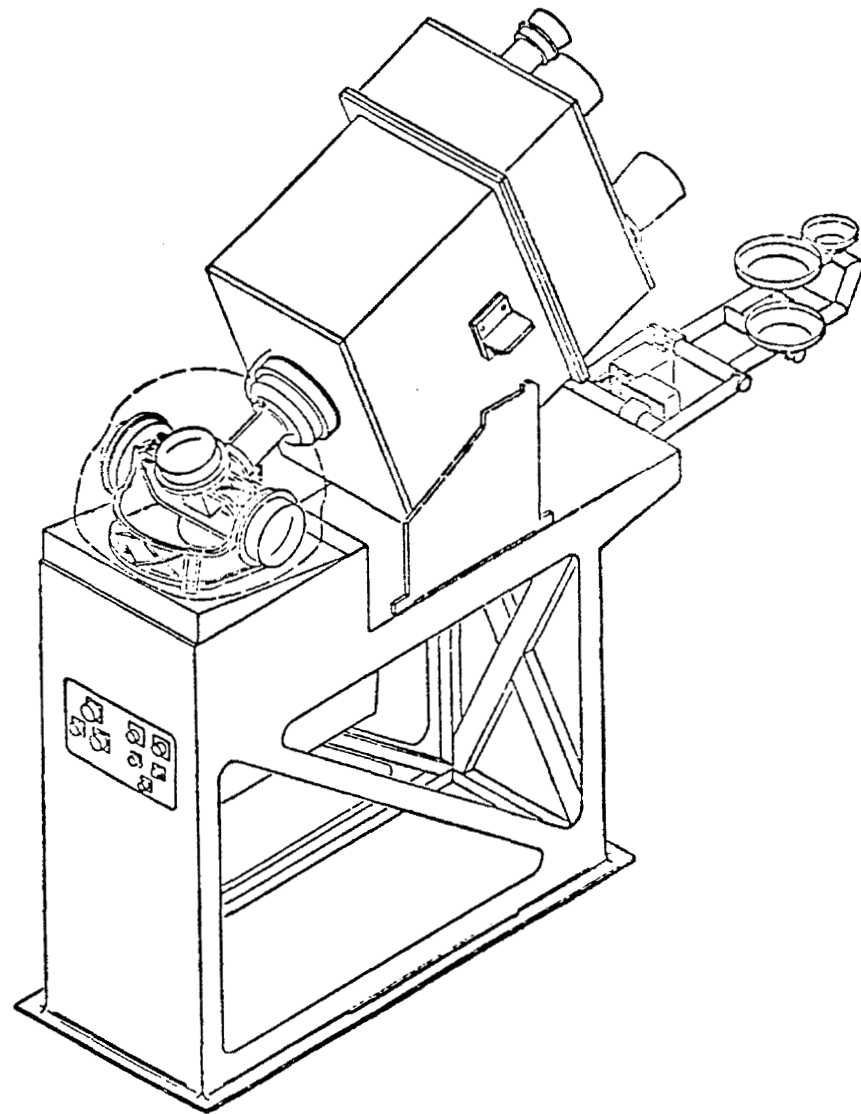
Dr. P. M. Banks, Co-Investigator (801) 752-4100, Ext. 7761
Physics Department
State University of Utah
Logan, Utah 84322

Dr. M. Mendillo (617) 353-2640
Department of Astronomy
Boston University
Boston, Massachusetts 02215

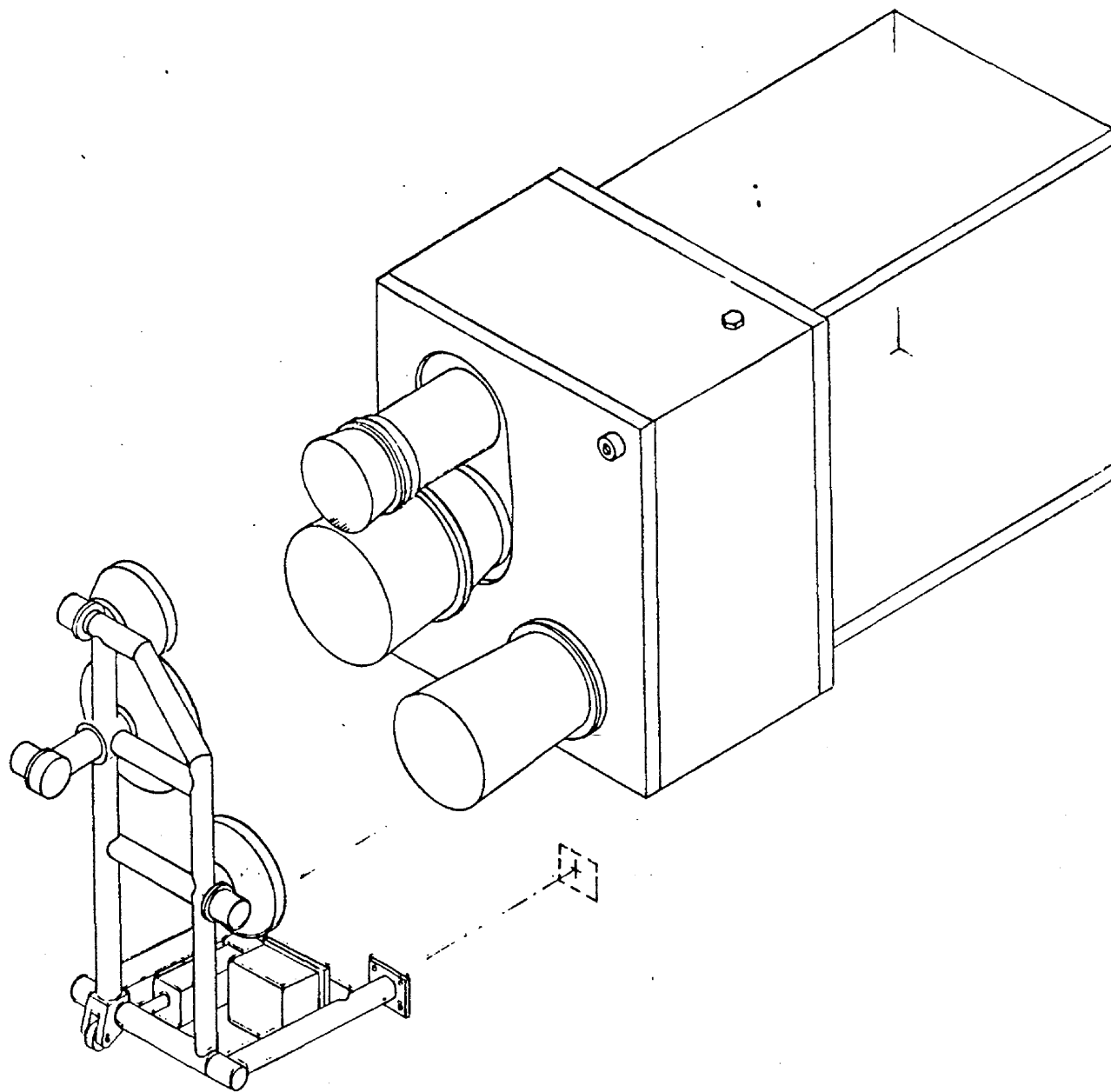
Dr. R. Orville (518) 457-3935
Department of Atmospheric Science
Earth Science Building - ES 214
The University at Albany
Albany, New York 12222

Dr. John Meaburn
Department of Astronomy
University of Manchester
M139PL England

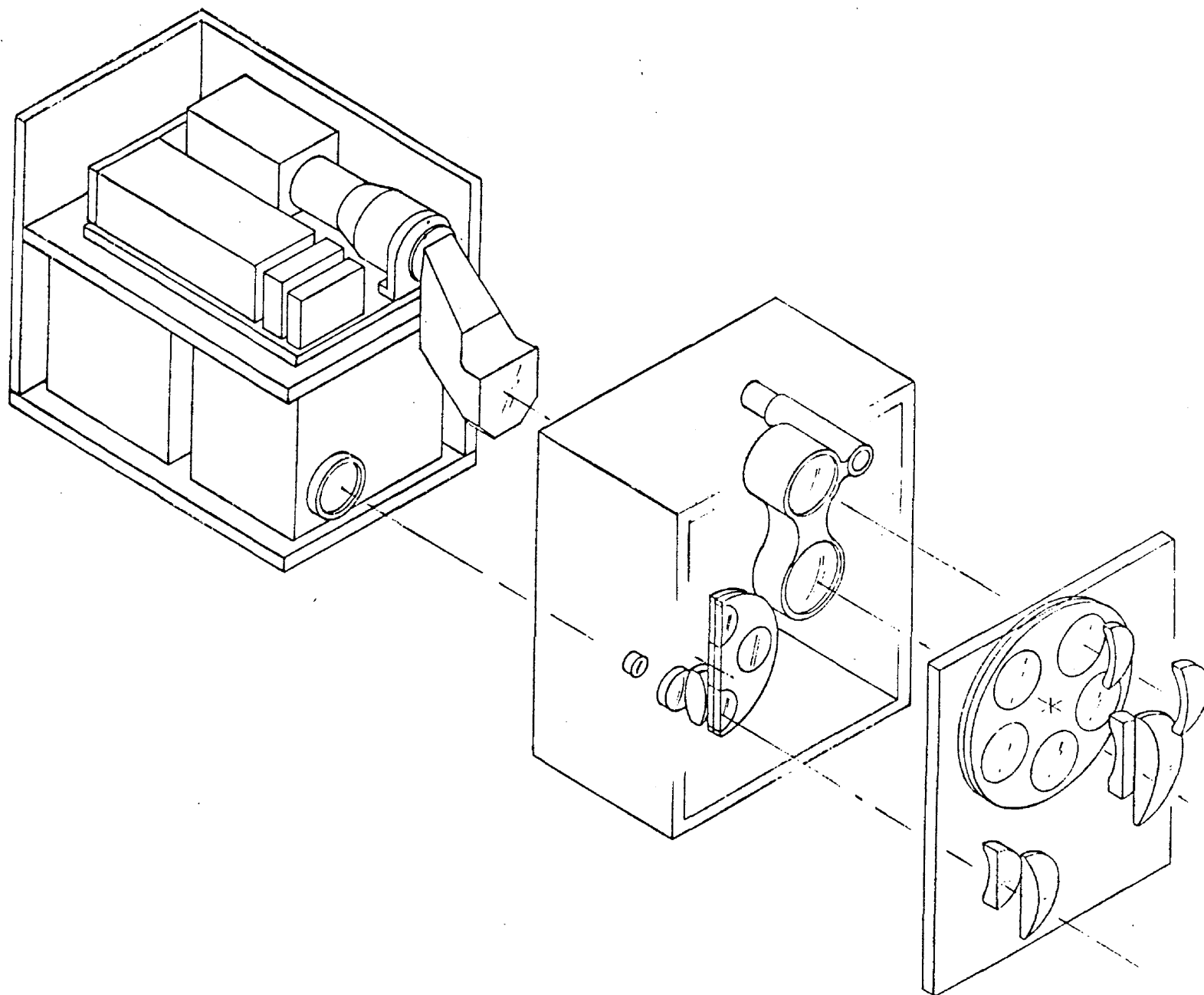
AEPI Experiment



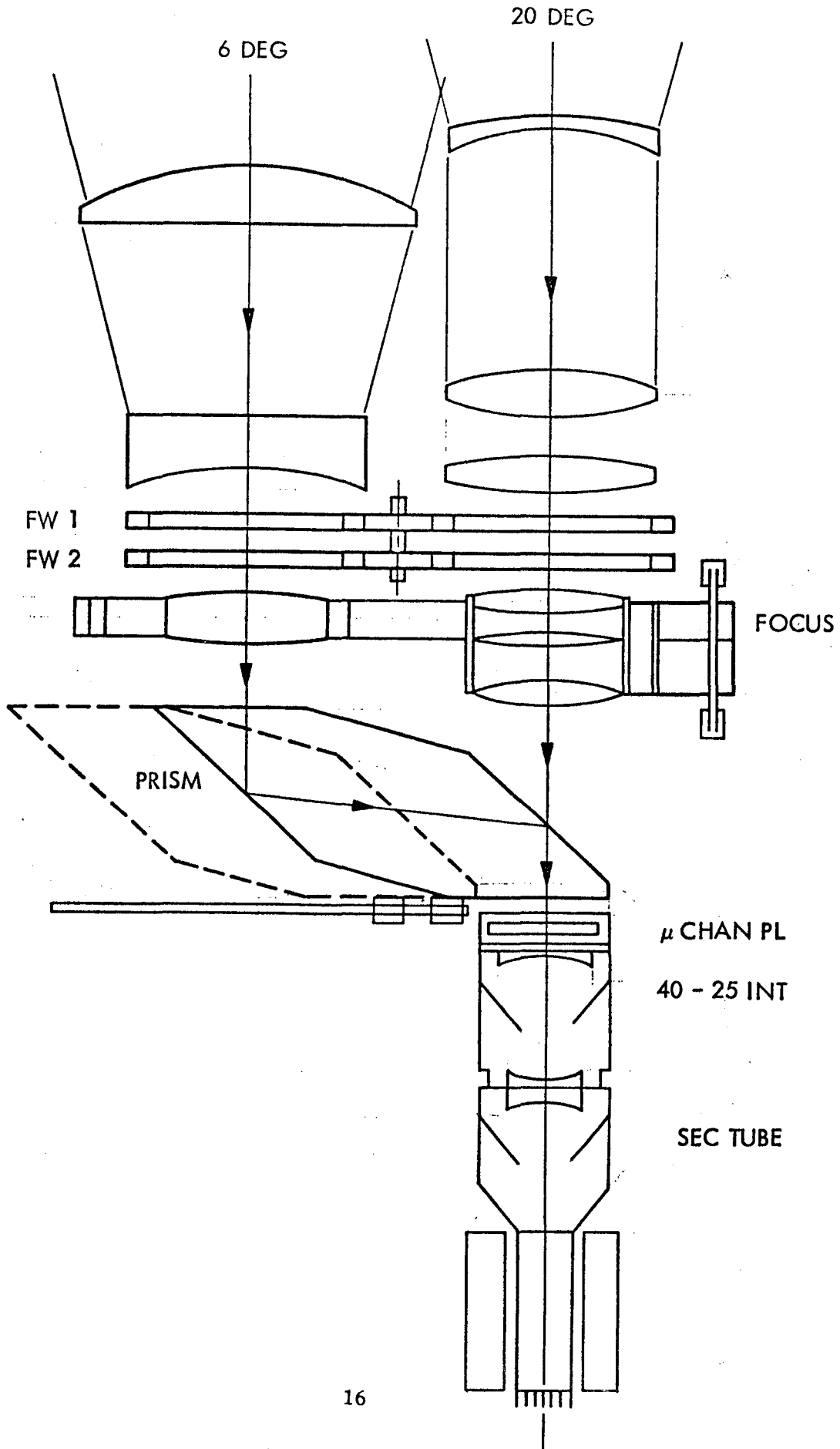
AEPI Detector Assembly



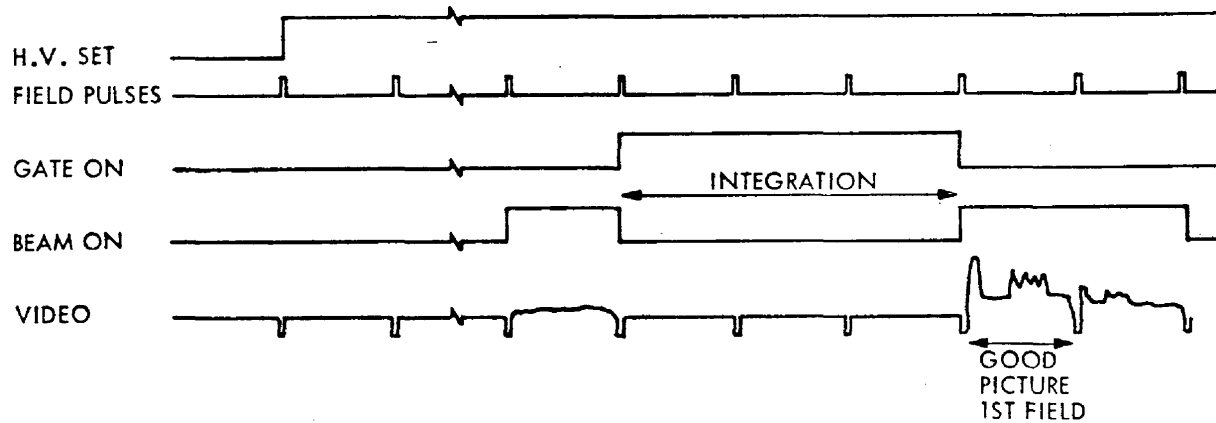
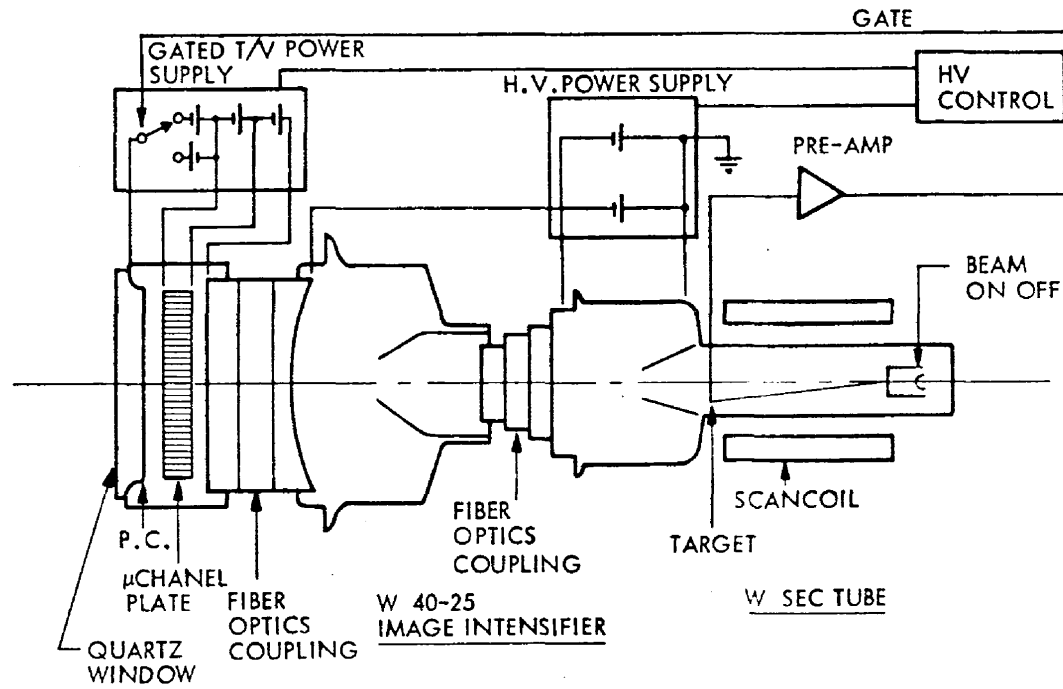
AEPI DETECTOR ASSEMBLY



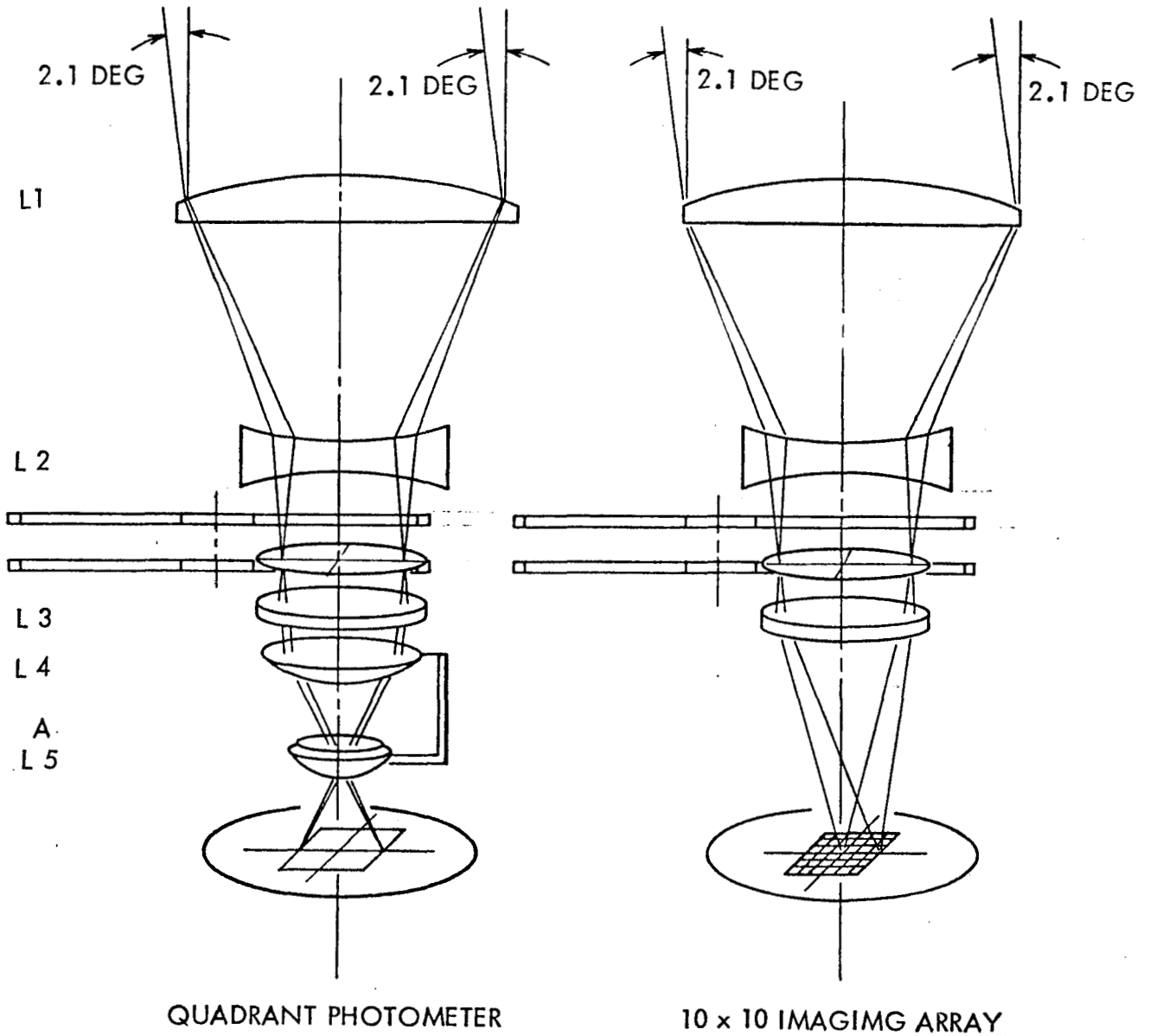
AEPI TV Optics



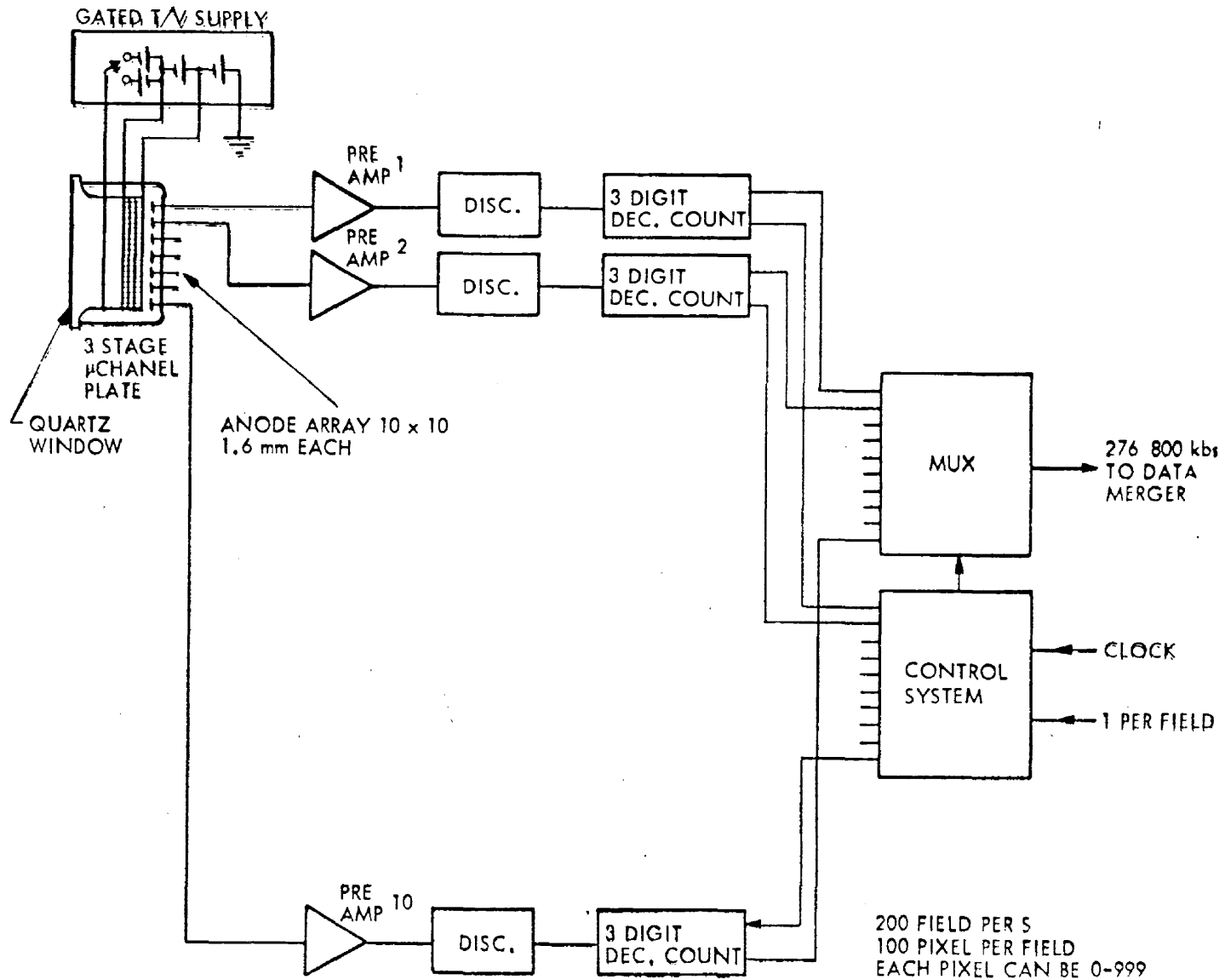
AEPI LLL-TV

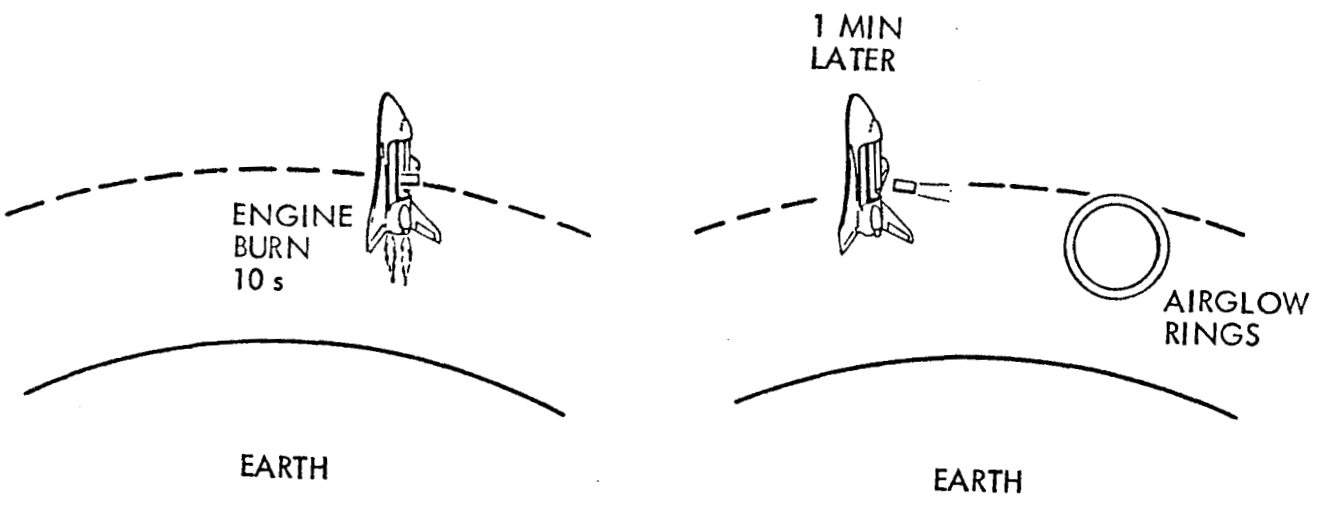


AEPI Photon Counting Array



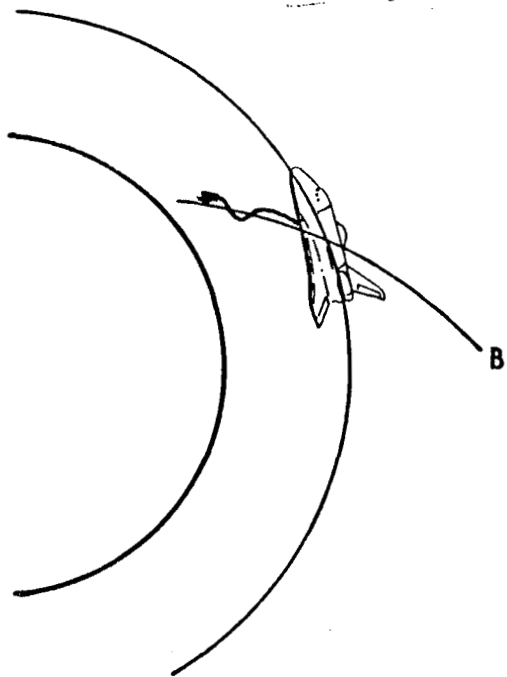
AEPI PHOTON COUNTING ARRAY



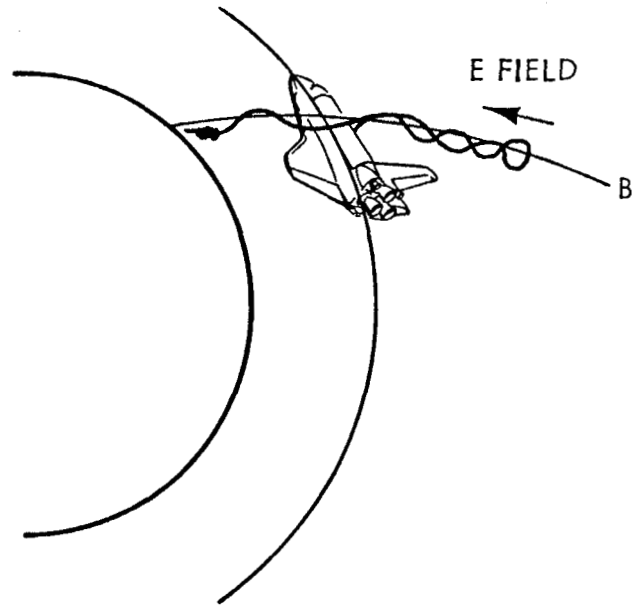


IONOSPHERIC AIRGLOW MODIFICATIONS

Joint experiments with the electron beam accelerator.

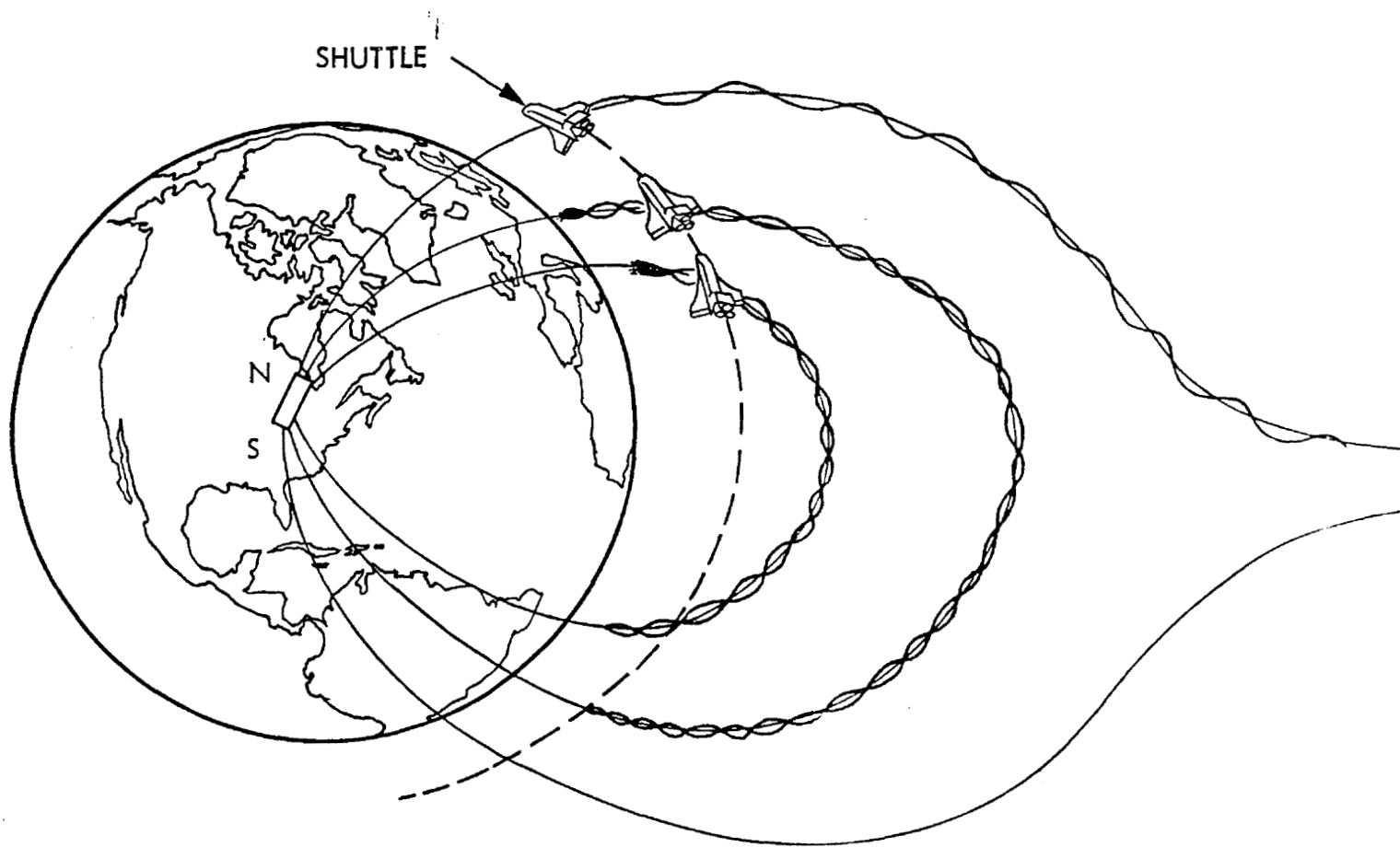


ARTIFICIAL AURORA

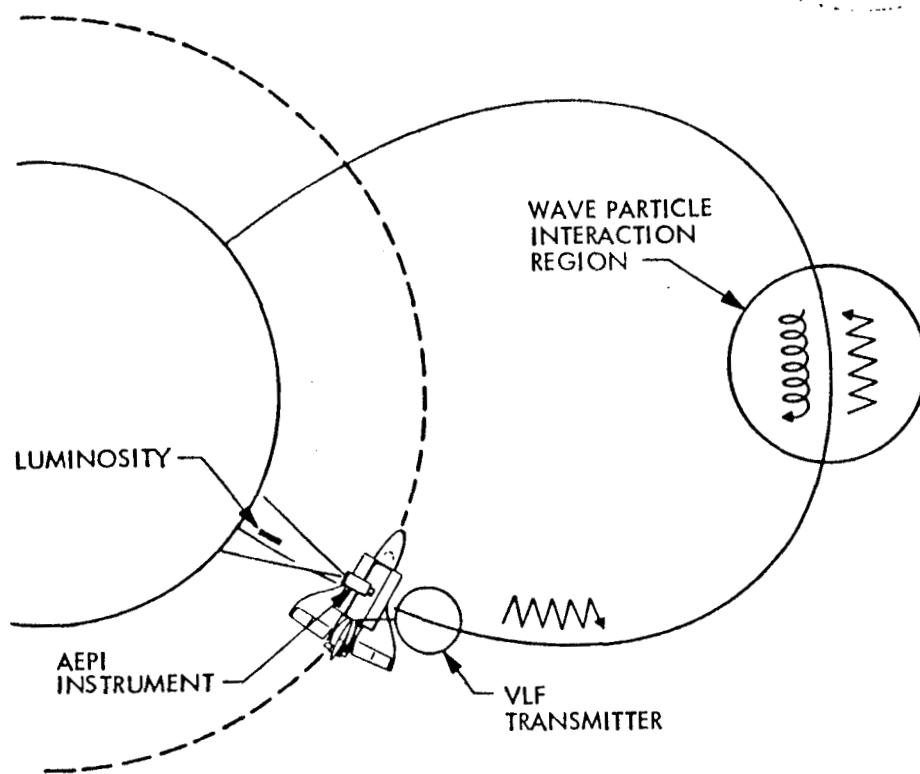


PARALLEL ELECTRIC FIELD

ECHO Experiment



The experiment aimed at the observation of the on-board VLF transmitter-induced precipitation.



DESCRIPTION OF THE INSTRUMENT

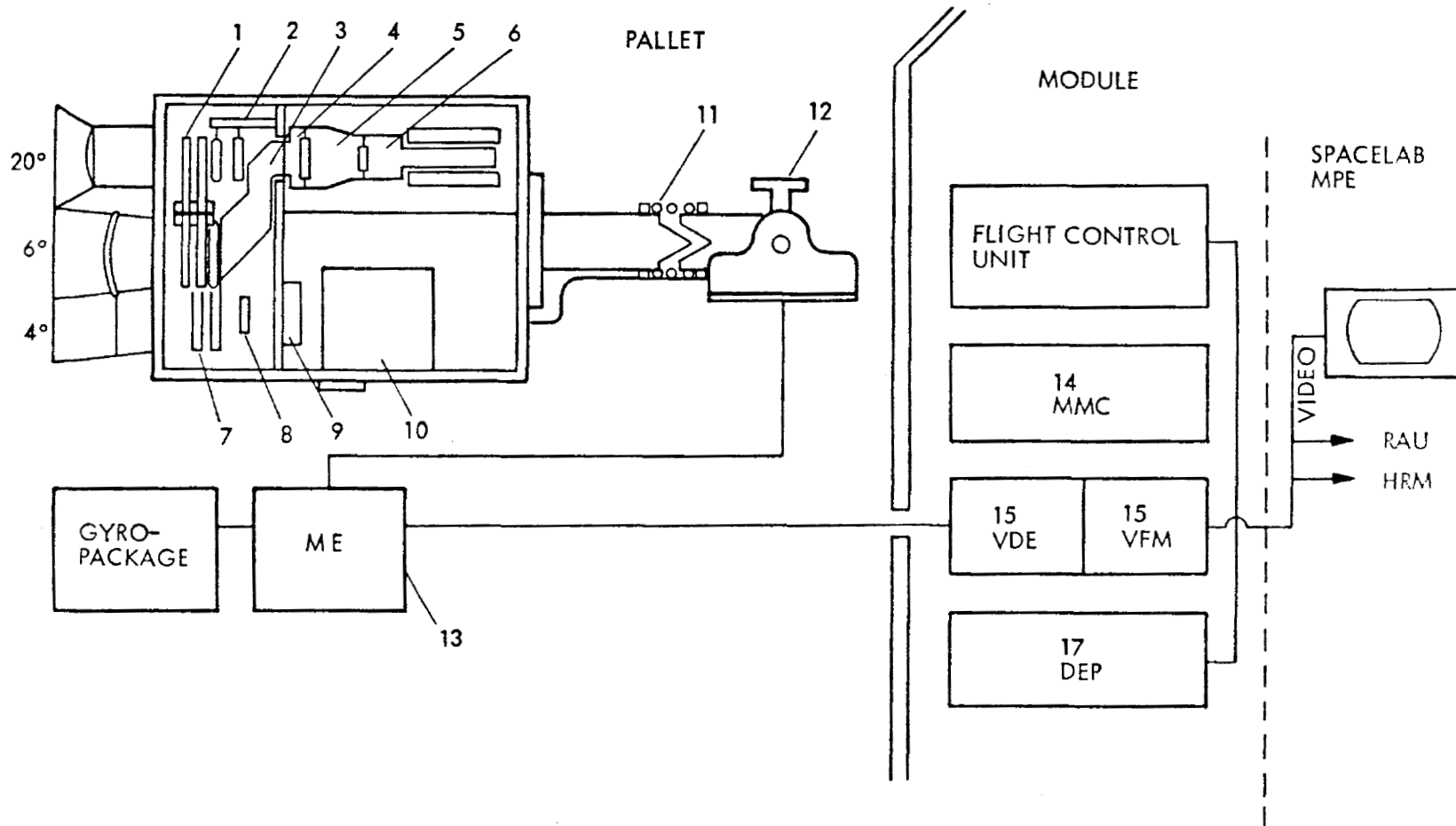
The AEPI system is illustrated in Fig. 6 . There are two parallel detector systems. The top system is a TV system using the image intensified S.E.C. tube as the detector. The bottom system, the photon counting array (P.C.A.), uses a microchannel plate intensified anode array tube and is equivalent to a 100 channel photomultiplier. For the television, the filters are selected by means of a filter-wheel set (1). For the selected waveband, an appropriate focus is chosen by focussing system (2). The field of view of the TV system is interchangeable between 20 and 6 degrees, by means of a moveable prism (3). The quartz window μ -channel plate intensifier (4) is fiber optically coupled to a 40-25 demagnifying tube (5) which is in turn coupled to the S.F.C. tube (6). The PCA channel has a fixed field of view of 4° . The waveband selection is achieved by means of the filter wheel (7). The PCA has a remote control interchangeable photometric converter optics (8) which converts the imaging array into a multichannel photometer. The μ -channel plate array tube (9) amplifies the photons into detectable counts for the PCA electronics (10). The entire system is pointed by a two-axis gimbal, the (MAST) mount (12). The load isolator (11) is a decoupling device for launch to save the mount from excessive launch loads. The mount electronics package (13) will provide the appropriate signal conditioning between the mount servos the dedicated experiment processor (DEP) (17) and the mount manual control (MMC) (14). The video data encoder (15) annotates the video with housekeeping information, both in readable alphanumeric characters and in decodable signal bars. The video field memory (16) is a single frame digital store which freezes the picture for inspection. The VDE and VFM electronics include an adjustable cursor which is displayed on the video frame in the TV. This can be used by the payload or mission specialist for manually controlling the pointing mount. The data output is fed to the Spacelab furnished video monitor, the high-rate multiplexer HRM, and the remote acquisition unit RAU of the Spacelab computer. The properties of the AEPI detector system is tabulated in Table I-1.

The flight equipment which will be acquired during this program consist of the gyro-package and the Interactive flight control unit panel. The gyro package is necessary because of the inadequate attitude reference supplied by the current Spacelab systems. The interactive flight control unit panel enables the payload/mission specialist to issue direct commands to the experiment DEP to manually set up camera parameters. The instrument as it is currently flown on Spacelab relies very highly on pre-programming of the DEP with very limited flexibility on the part of the mission/payload specialist to make changes to the operating programs. Much of the experimental objectives require the man in the loop to update the system operation after each detection trial.

TABLE I-1. THE PROPERTIES OF THE AEPI DETECTOR SYSTEM.

	TV SYSTEMS	
TV Standard:	525 TV lines maximum	
Field of View:	6°	20°
F/Number	2.5	2.0
Resolution (300 lines)	$.02^\circ (3.5 \times 10^{-4})$	$.07^\circ (1.16 \times 10^{-3} \text{ rad})$
Range 150 Km	5.2 m	170 m
300 Km	105 m	340 m
500 Km	175 m	580 m
Minimum Sensitivity (1 sec exposure)	60 R	40 Rayleigh

FIGURE 6
AEPI SYSTEMS CONFIGURATION



1. TV FILTER WHEEL
2. DYNAMIC CHROMATIC CORRECTOR
3. FIELD-OF-VIEW CHANGE PRISM
4. μ-CHANNEL PLATE INTENSIFIER
5. DE-MAGNIFYING TUBE
6. S.E.C. TUBE

7. FILTER WHEEL (PCA)
8. PHOTOMETER CONVERTER
9. PHOTON COUNTING ARRAY (PCA)
10. ELECTRONICS PCA
11. LOAD ISOLATION
12. MAST TWO-AXIS GIMBAL

13. MAST ELECTRONICS
14. MOUNT MANUAL CONTROL
15. VIDEO DATA ENCODER
16. VIDEO FIELD MEMORY
17. DEDICATED EXPERIMENT PROCESSOR

PHOTON COUNTING ARRAY

Mode	10 x 10 Image array	Quadrant Photometer
Field of View:	4.25° x 4.25°	6° diameter circular
F Number	2.5	2.5
Resolution	.42° (0.073 rad)	6° (0.1 rad) diameter circular
Range 150 Km	1.1 Km	15 Km
300 Km	2.2 Km	30 Km
500 Km	3.6 Km	50 Km
Sensitivity	12.0 counts per Rayleigh per second	320 counts per Rayleigh per second per quadrant
Maximum counts rate (2 x 10 ⁵ per sec per anode)	2.4 M Rayleighs	2.4 M Rayleighs

**SECTION III. IMAGING SPECTROMETRIC
OBSERVATORY (ISO)**

TRACE CONSTITUENTS IN THE MIDDLE ATMOSPHERE
BY HIGH RESOLUTION UV SPECTROSCOPY

SUBMITTED BY:

PRINCIPAL INVESTIGATOR: DOUGLAS G. TORR (801)750-2779
UTAH STATE UNIVERSITY

CO-INVESTIGATORS: M. R. TORR (801)750-2865
UTAH STATE UNIVERSITY

T. M. DONAHUE (313)764-7220
G. R. CARIGNAN (313)763-2390
A. F. NAGY (313)764-9462
P. B. HAYS (313)764-6592
E. R. YOUNG (313)764-3335
S. K. ATREYA (313)764-3335
UNIVERSITY OF MICHIGAN

J. P. NOXON (303)499-1000, X3366
NATIONAL OCEANOGRAPHIC AND
ATMOSPHERIC ADMINISTRATION

J. C. G. WALKER (809)878-2612
ARECIBO OBSERVATORY, PUERTO RICO

PRIMARY DISCIPLINE: ATMOSPHERIC AND SPACE PLASMA PHYSICS

CENTER FOR ATMOSPHERIC AND SPACE SCIENCES
UTAH STATE UNIVERSITY
LOGAN, UTAH 84322

NOVEMBER 1980

THE IMAGING SPECTROMETRIC OBSERVATORY - ISO

BUILT FOR SPACELAB I

SL1 PRINCIPAL INVESTIGATOR: MARSHA R. TORR

REFLIGHT P.I. : D. G. TORR

(RESPONSIBILITY FOR INSTRUMENT REMAINS WITH M.R. TORR)

AFFILIATION: CENTER FOR ATMOSPHERIC AND SPACE SCIENCES
UTAH STATE UNIVERSITY

ISO SCIENCE

ISO IS A GENERAL PURPOSE INSTRUMENT WHICH CAN BE USED TO STUDY NUMEROUS ATMOSPHERIC PROBLEMS.

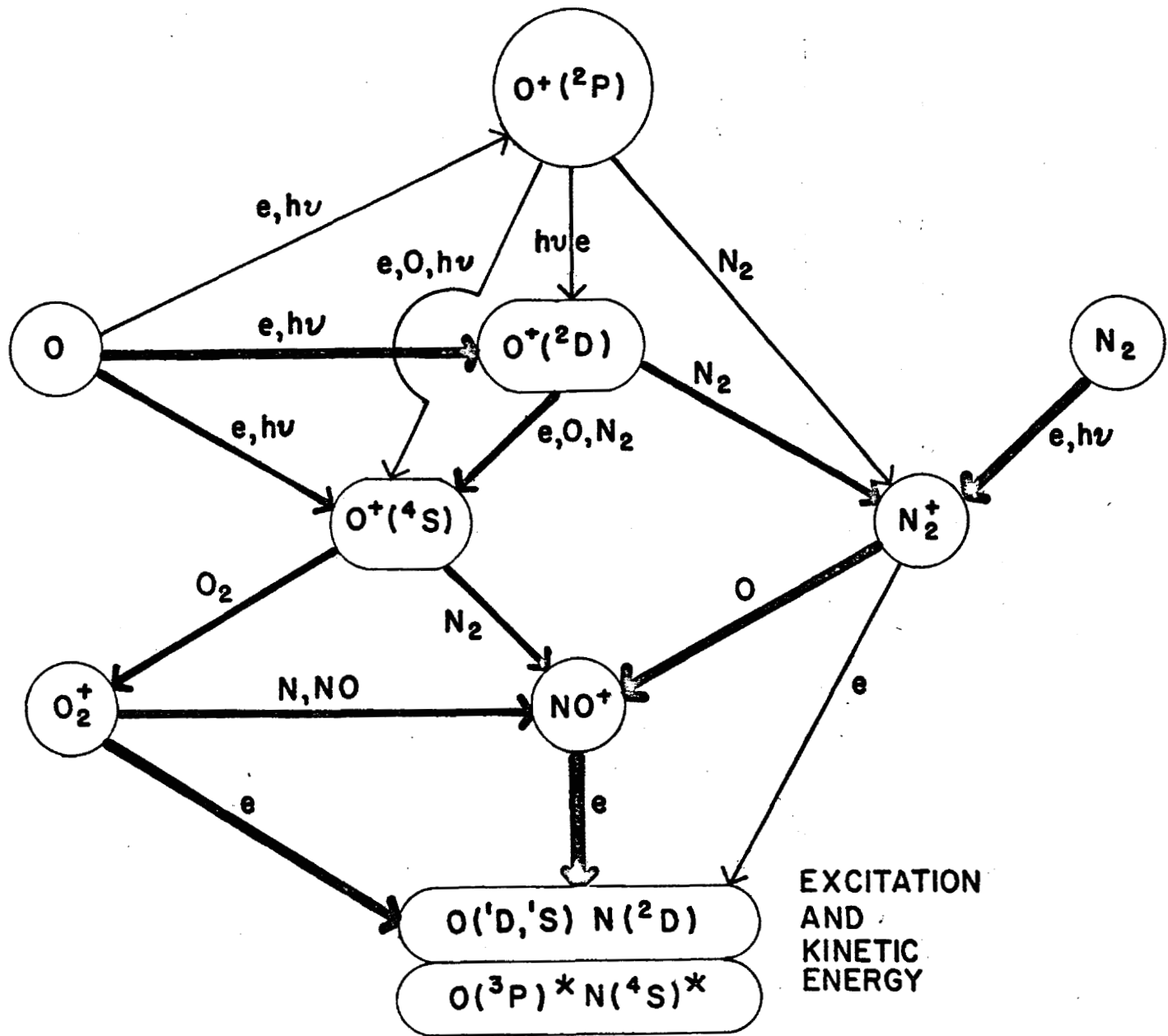
SPACELAB 1 WILL BE USED TO OPERATE MAINLY IN A SURVEY MODE.

FOR THE FIRST REFLIGHT WE PLAN TO SELECT A FEW SPECIFIC QUESTIONS TO ADDRESS. THESE MAY BE CHANGED LATER DEPENDING ON DEVELOPMENTS IN THE FIELD. ISO IS DESIGNED TO SELECT EXPERIMENT MEASUREMENT SEQUENCES BY SOFTWARE CONTROL.

WE HAVE CHOSEN TO CONCENTRATE ON THE CHEMISTRY OF SEVERAL METASTABLE AND VIBRATIONALLY EXCITED SPECIES, SINCE THESE ARE DIFFICULT TO STUDY IN THE LAB.

ISO WILL ALSO BE CAPABLE OF PROVIDING A DATABASE OF BASIC PARAMETERS TO USE IN MODELLING. THESE WILL BE DERIVED FROM THE INTENSITIES OF EMISSIONS WHOSE SOURCES AND SINKS ARE WELL KNOWN.

THERMOSPHERIC IONIC PROCESSES



THE N_2^+ PROBLEM

PROBLEM: CURRENT MODELS PRODUCE TOO MUCH N_2^+ IONIZATION

SOLUTION 1 : INCREASE THE RECOMBINATION RATE, BECAUSE N_2^+ IS VIBRATIONALLY EXCITED IN THE THERMOSPHERE

LAB RESULT: NO DEPENDENCE ON VIBRATIONAL EXCITATION - E. ZIPF

SOLUTION 2 : DECREASE CHARGE EXCHANGE OF $O^+(^2D)$ WITH N_2

LAB RESULT: NO. THE RATE COEFFICIENT IS LARGE $10^{-9} \text{ cm s}^{-1}$ - BIONDI'S GROUP, CONFIRMED BY NOAA GROUP.

CONCLUSION : THE REACTION OF N_2^{+*} WITH O MUST BE LARGER THAN N_2^+ WITH O

USE ISO TO CHECK THESE LAB RESULTS AND THE ABOVE HYPOTHESIS.

EXPERIMENT : DETERMINE WHETHER THE CHARGE EXCHANGE OF $O^+(2D)$ WITH N_2 PROCEEDS RAPIDLY ($k=10^{-9}$) OR SLOWLY ($k=10^{-10}$)

METHOD: MEASURE THE $O^+(2D)$ CONCENTRATION. THE TWO RATES WILL YIELD CONCENTRATIONS WHICH DIFFER BY NEARLY AN ORDER OF MAGNITUDE.

PARAMETER: EMISSION AT 3728.9A DUE TO THE TRANSITION $O^+(4S - 2D)$

THE MEASUREMENT WILL BE MADE IN A LIMBSCAN MODE WHERE THE SURFACE BRIGHTNESS WILL BE SEVERAL RAYLEIGHS TO TENS OF RAYLEIGHS DEPENDING ON K.

EXPERIMENT: MEASURE THE PRODUCTION OF N_2^+ DUE TO CHARGE EXCHANGE OF $O^+(^2D)$ WITH N_2

THE REACTION IS RESONANT IF N_2^+ IS FORMED IN THE $V=2$ LEVEL OF THE A STATE.

METHOD: OBSERVE PERMITTED TRANSITIONS OF N_2^+ ORIGINATING IN THE $V=1$ LEVEL OF THE A STATE, E.G.

1-0 AT 9212A

ISOLATE CHARGE EXCHANGE SOURCE BY MONITORING RESONANCE FLUORESCENCE PRODUCTION VIA:

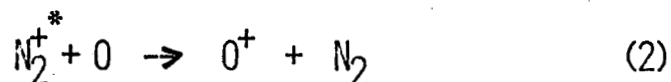
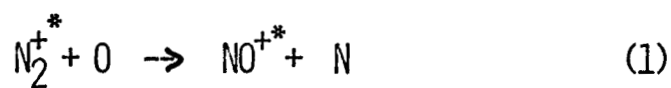
2-0 AT 7874A, 2-1 AT 9502A, 3-1 AT 8105A

MEASURE THE ROTATIONAL TEMPERATURE.

RESONANCE FLUORESCENCE GIVES A KINETIC THERMAL DISTRIBUTION
CHARGE EXCHANGE WILL GIVE A NON EQUILIBRIUM TEMPERATURE.

EXPERIMENT: INVESTIGATE THE DESTRUCTION OF N_2^+ BY REACTIONS WITH O

REACTIONS OF VIBRATIONALLY EXCITED N_2^+ WITH O HAVE NEVER BEEN STUDIED IN THE LAB. POSSIBLE CHANNELS INCLUDE:



REACTION (1) WILL PRODUCE VIBRATIONALLY EXCITED NO^+ IN $V > 2$.

THE RADIATIVE LIFETIME OF NO^{+*} IS OF THE ORDER OF MILLISECONDS

MEASURE: NO^{+*} EMISSIONS FROM $V \geq 4$ (I.E. LESS THAN 11,000Å)

DETERMINE WHETHER THESE INTENSITIES ARE CONSISTANT WITH PRODUCTION OF N_2^+ BY CHARGE EXCHANGE WITH O.

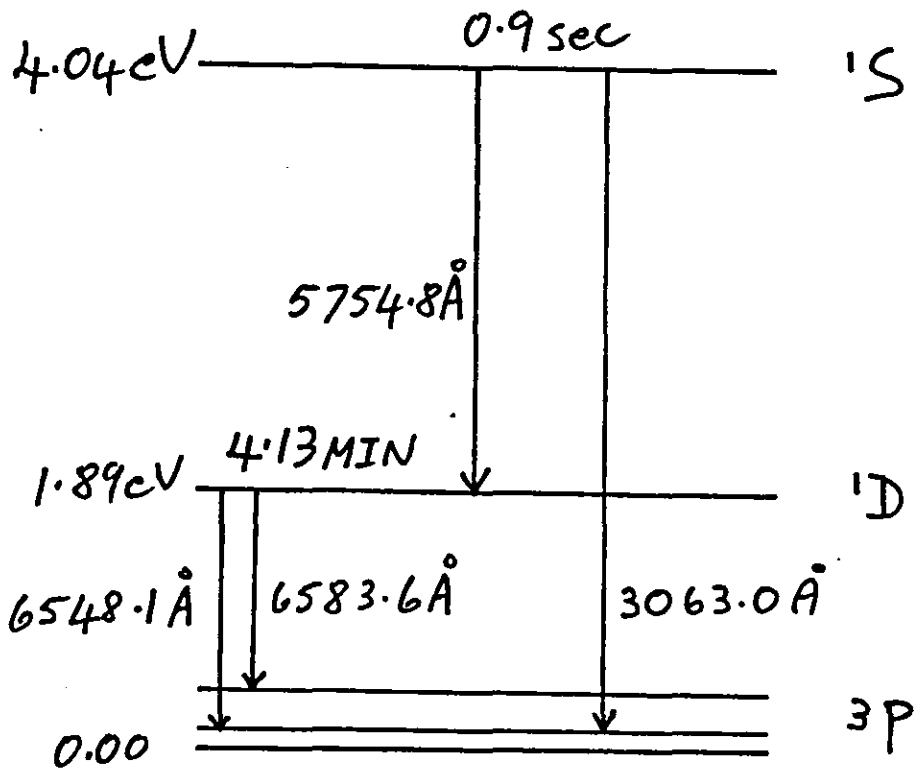
EXPERIMENT: STUDY THE CHEMISTRY OF METASTABLE N^+ IONS

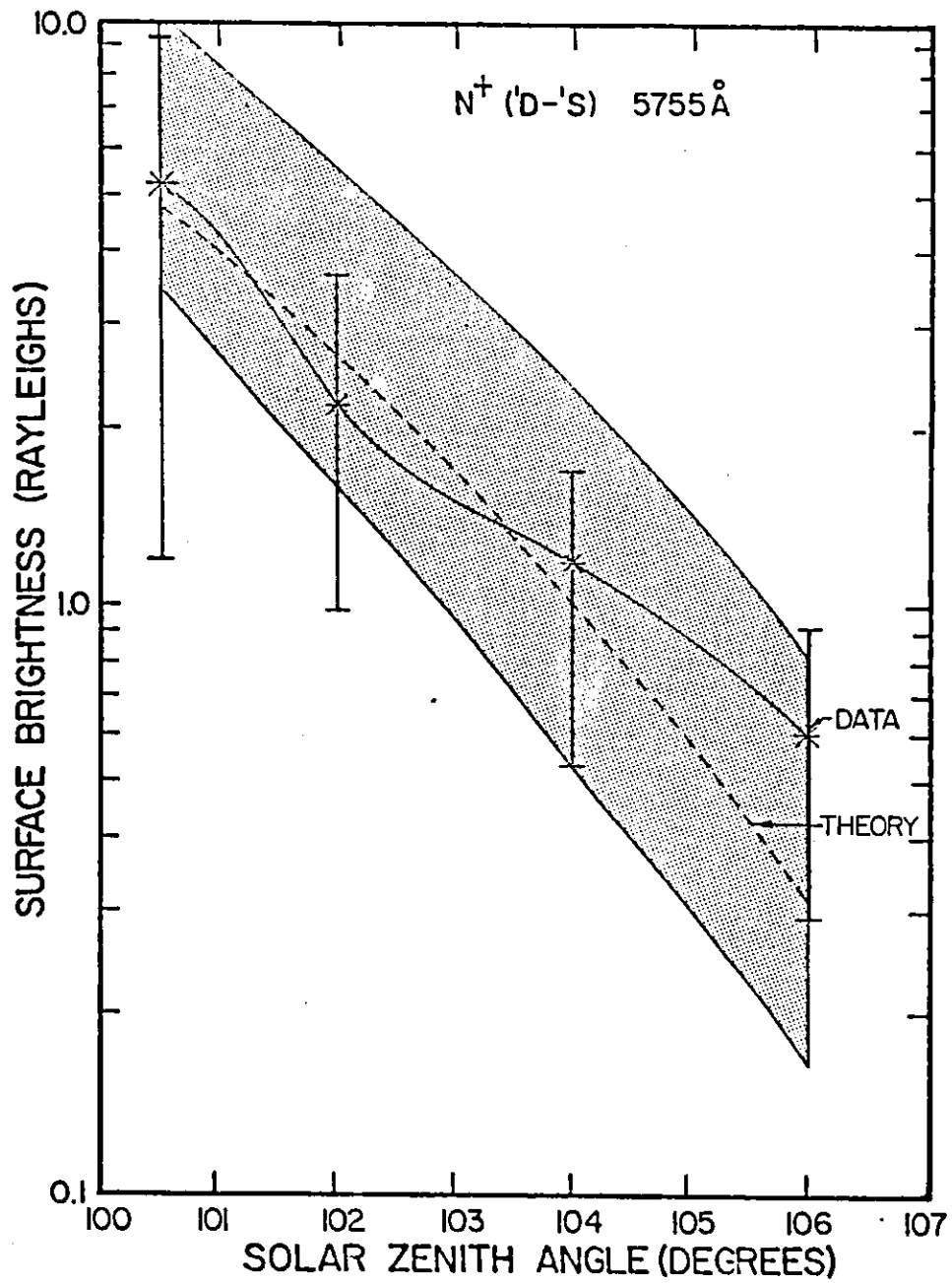
EMISSIONS: $N^+(^1D - ^1S)$ AT 5755 A 0.9 s
 $N^+(^3P - ^1D)$ AT 6548 A AND 6583 A 4.13 MIN

COMMENTS: THESE EMISSIONS HAVE BEEN DETECTED FROM THE
 GROUND, BUT WEAKLY. LIMBSCAN PLUS THE HIGH
 SENSITIVITY OF ISO WILL PERMIT US TO STUDY
 THE SOURCES AND SINKS IN DETAIL.

IT IS POSSIBLE THAT THESE METASTABLE SPECIES
MAY AFFECT THE CONCENTRATIONS OF OTHER
CONSTITUENTS SUCH AS $O(^1D)$ AND $O^+(^2P)$.

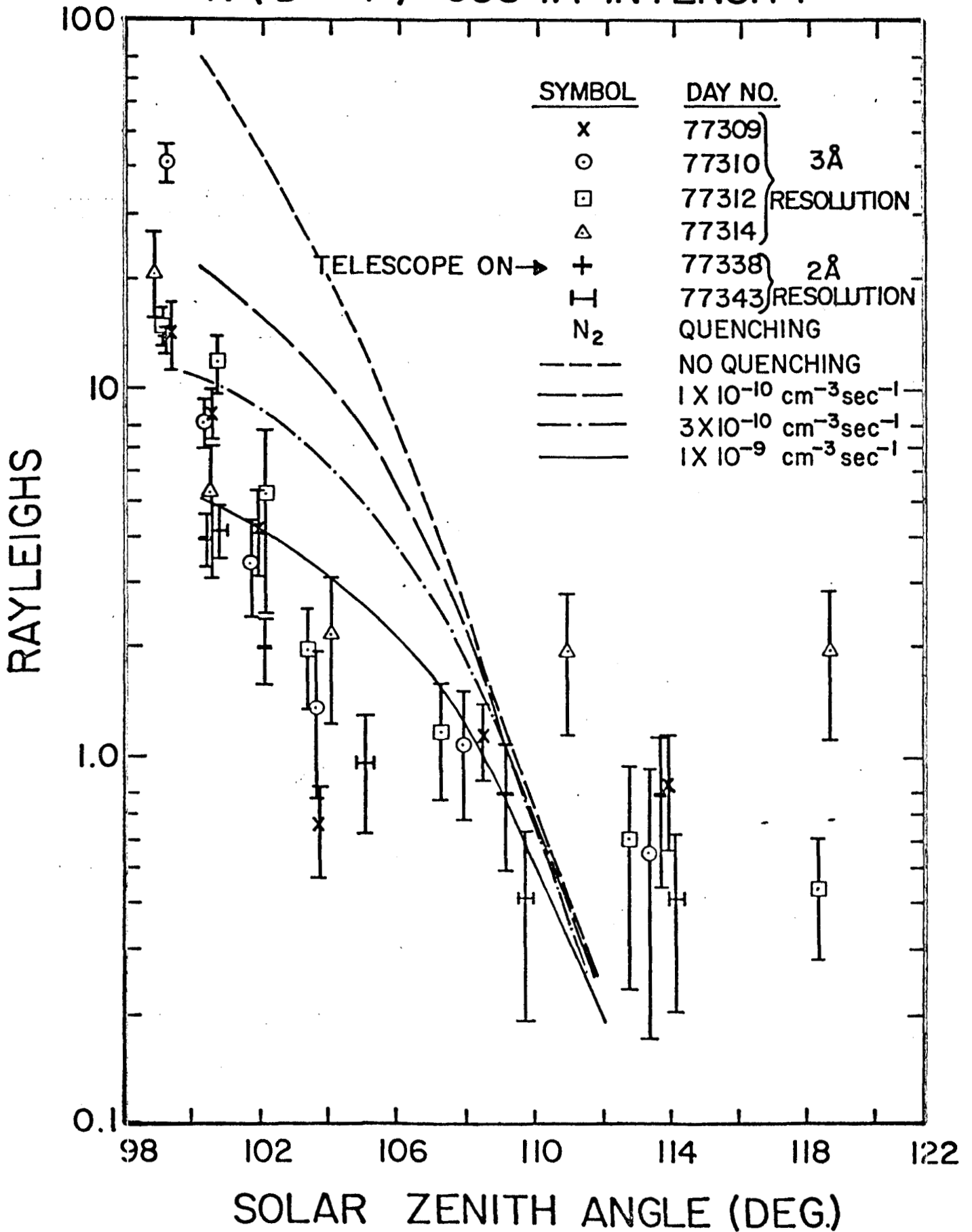
N^+





EVENING TWILIGHT

N⁺(1D-3P) 6584Å INTENSITY



EXPERIMENT: STUDIES OF O_2^+ IONS

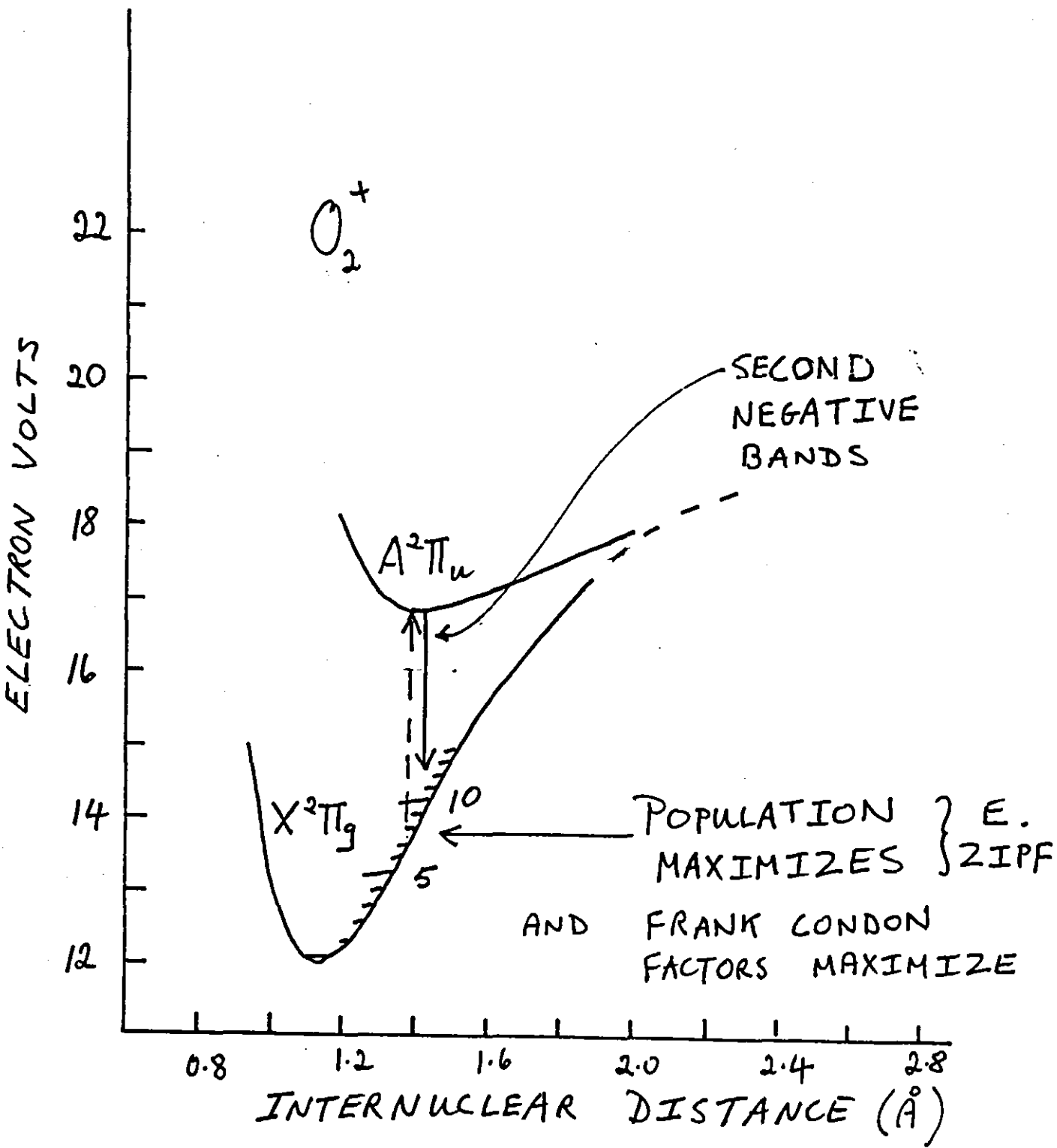
RECENT WORK BY E. ZIPF SUGGESTS THAT THERMOSPHERIC O_2^+ IONS RESIDE MAINLY IN VIBRATIONAL LEVELS BETWEEN 4 AND 16. THIS MEANS THAT THE POPULATION DISTRIBUTION WILL BE MORE CLOSELY ALIGNED WITH THE LEVELS WHERE THE FRANK CONDON FACTORS MAXIMIZE .

CONCLUSION: O_2^+ IS THEREFORE MUCH MORE SIMILAR TO N_2^+ THAN WAS PREVIOUSLY REALIZED. SIGNIFICANT EXCITATION TO THE $A^2\Pi_u$ STATE VIA RESONANCE ABSORPTION OF SOLAR RADIATION MAY BE EXPECTED.

THESE EFFECTS MIGHT SIGNIFICANTLY AFFECT THE RECOMBINATION OF O_2^+ IN THE THERMOSPHERE.

MEASUREMENTS OF THE SECOND NEGATIVE BANDS WILL THEREFORE PROVIDE INFORMATION ON THE VIBRATIONAL DISTRIBUTION OF O_2^+

MEASUREMENTS: 0-5 3232,3210 0-6 3421,3397 0-7 3629,3603 ETC.



O_2^+ CONTINUED:

WE ALSO INTEND TO SEARCH FOR EMISSIONS IN THE $O_2^+(a^4\Pi - X^2\Pi_g)$ SYSTEM. THE SOURCE IS VIA CASCADE FROM THE $b^4\Sigma$ STATE VIA THE FIRST NEGATIVE TRANSITIONS.

THE SOURCE WILL BE MONITORED VIA THE FIRST NEGATIVE BANDS WHICH ARE ALL IN THE VISIBLE.

MEASUREMENTS: O_2^+ FIRST NEGATIVE BANDS (b - a) SEE TABLE
(a - X) TRANSITIONS, E.G.
0,6 4531 A, 0,7 4896 A, 0,8 5316 A,
0,9 5803 A, 0,10 6314 A

A SIMPLE SCALING OF AURORAL INTENSITIES SUGGESTS ABOUT 20R FOR THESE BANDS.

THE MEASUREMENTS SHOULD ALLOW US TO STUDY THE SOURCES AND SINKS OF THE METASTABLE $a^4\Pi$ STATE.

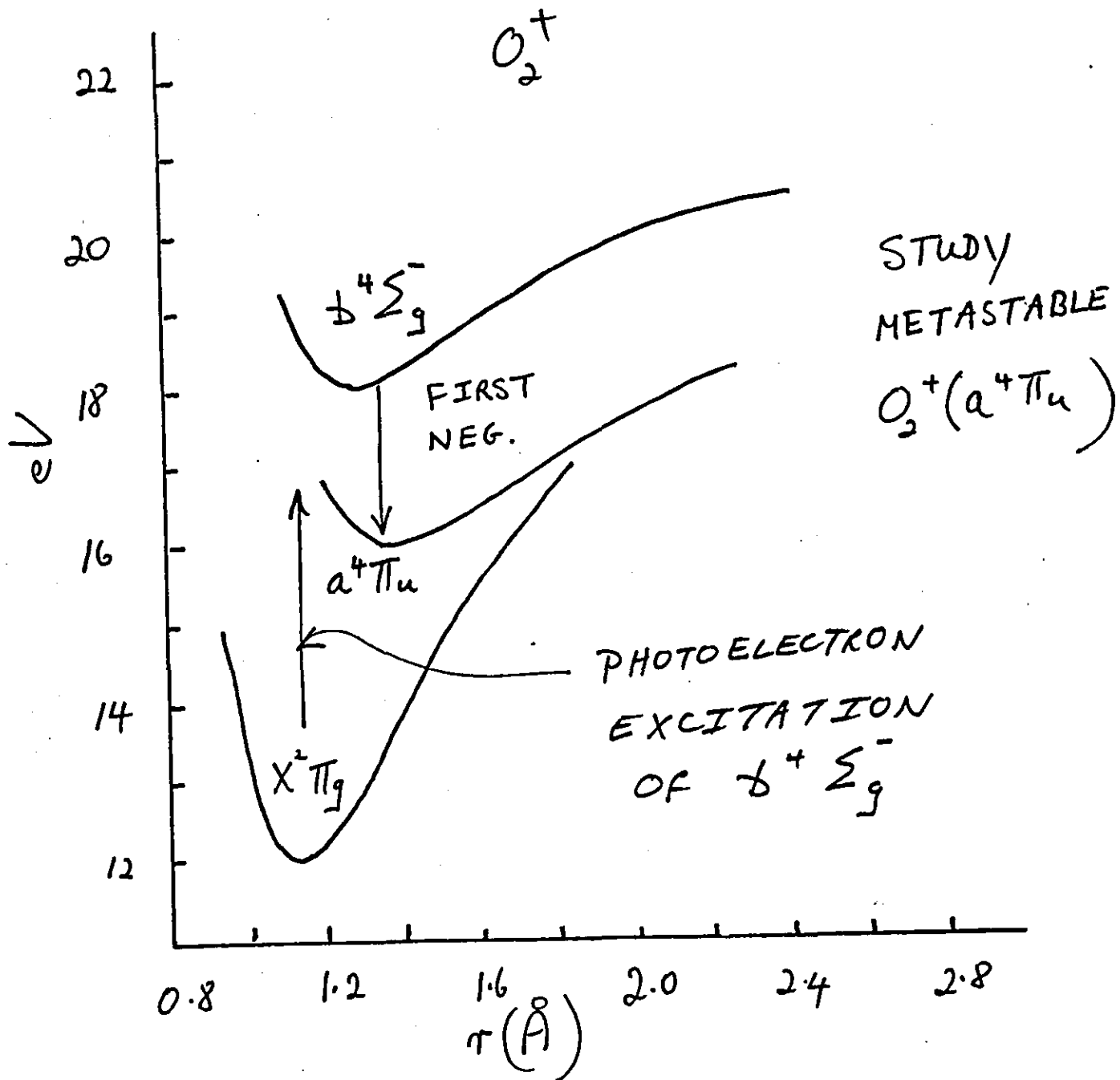


TABLE 3.1 O_2^+ 1N (first negative) band intensities

	v'' 0	1	2	3	4	5	6	7	8
0	<u>5999.9</u> 6.4	<u>6389.0</u> 5.6	6822.3 5.0	7307.6 1.4	7854.4 .6	8474.6 .24			
1	<u>5608.7</u> 9.4	5947.2 .3	6320.9 .6	6735.3 1.4	7197.2 1.2	7714.5 .7	8297.7 .3		
v' 2	<u>5274.8</u> 3.0	5573.2 1.8	5900.1 1.0		6656.6 .16	7096.7 .3	7587.3 .3	8136.9 .16	
3	4987.0 .3	5252.9 1.5							
System intensity - 400R									
v'	v''								
	Wavelength (Å) origin								
	Intensity (R) SZA = 90°								
	Underlined bands observed								

TABLE 3-A

SPECTROMETER UNIT NO.	WAVELENGTH RANGE (Å)	GRATING		PLATE FACTOR (Å)/mm	APPARENT RESOLUTION(Å) (3 PIXELS-90μ)	SPECTRAL RANGE(Å) PER DETECTOR WIDTH (5.7mm)	MINIMUM DETECTOR POSITIONS PER SCAN	PHOTOCATHODE, WINDOW
		GROOVES/mm	BLAZE (Å)					
1	7500-12,000	400	10,000	50	4.5	285	16	CCD Surface (No image tube)
2	4000-8000	450	5500	44	4	253	16	TRIALKALI Glass
3	2200-4100	900	3000	22	2	127	15	BIALKALI Quartz
4	1100-2300	1200	1500	17	1.5	95	13	CsTe MgF ₂
5	300-1200	1200	800	17	9*	95	10	Channel Plate Surface No Window

*18 pixels-540μ
Limited by .045°
FOV collimator

PARTICIPATION IN ACTIVE EXPERIMENTS

- PRELIMINARY COORDINATION WITH SEPAC ON SL-1
- TETHERED SATELLITE EXPERIMENTS
- DIAGNOSTIC FOR CHEMICAL RELEASE EXPERIMENTS
- A SUBSTANTIAL ENHANCEMENT IN THIS CAPABILITY WOULD BE REALIZED BY MOUNTING THE INSTRUMENT ON A POINTING SYSTEM

SUMMARY OF RESOURCE PARAMETERS

WEIGHT: SPECTROMETER ARRAY 239 KGMS
DEP 18 KGMS
257 KGMS

POWER: SPECTROMETER ARRAY ~ 80 WATTS
DEP 85 WATTS
165 WATTS

DIMENSIONS (APPROX.): SPEC. ARRAY: 131 cm X 110 X 74
DEP: 48 cm X 22 X 61

IMAGING SPECTROMETRIC OBSERVATORY

- ARRAY OF 5 IMAGING SPECTROMETERS
- EACH SPECTROMETER AUTONOMOUS
- ISO COVERS BROAD WAVELENGTH RANGE ($\sim 200 - 12,000 \text{ \AA}$)
- RESOLUTION SELECTABLE DOWN TO $\sim 0.5 \text{ \AA}$
- DYNAMIC RANGE: $\sim 10^7$
- SENSITIVITY: MISSION SELECTABLE
SL-1 - 1R IN 60 SEC. WITH S/N = 5

ASPECTS OF DESIGN

- MODULAR CONSTRUCTION PERMITS FLEXIBILITY FOR REFLIGHTS
- SEQUENCES CAN BE CHANGED IN REAL TIME
- ON-BOARD DISPLAYS CAN BE ADDED

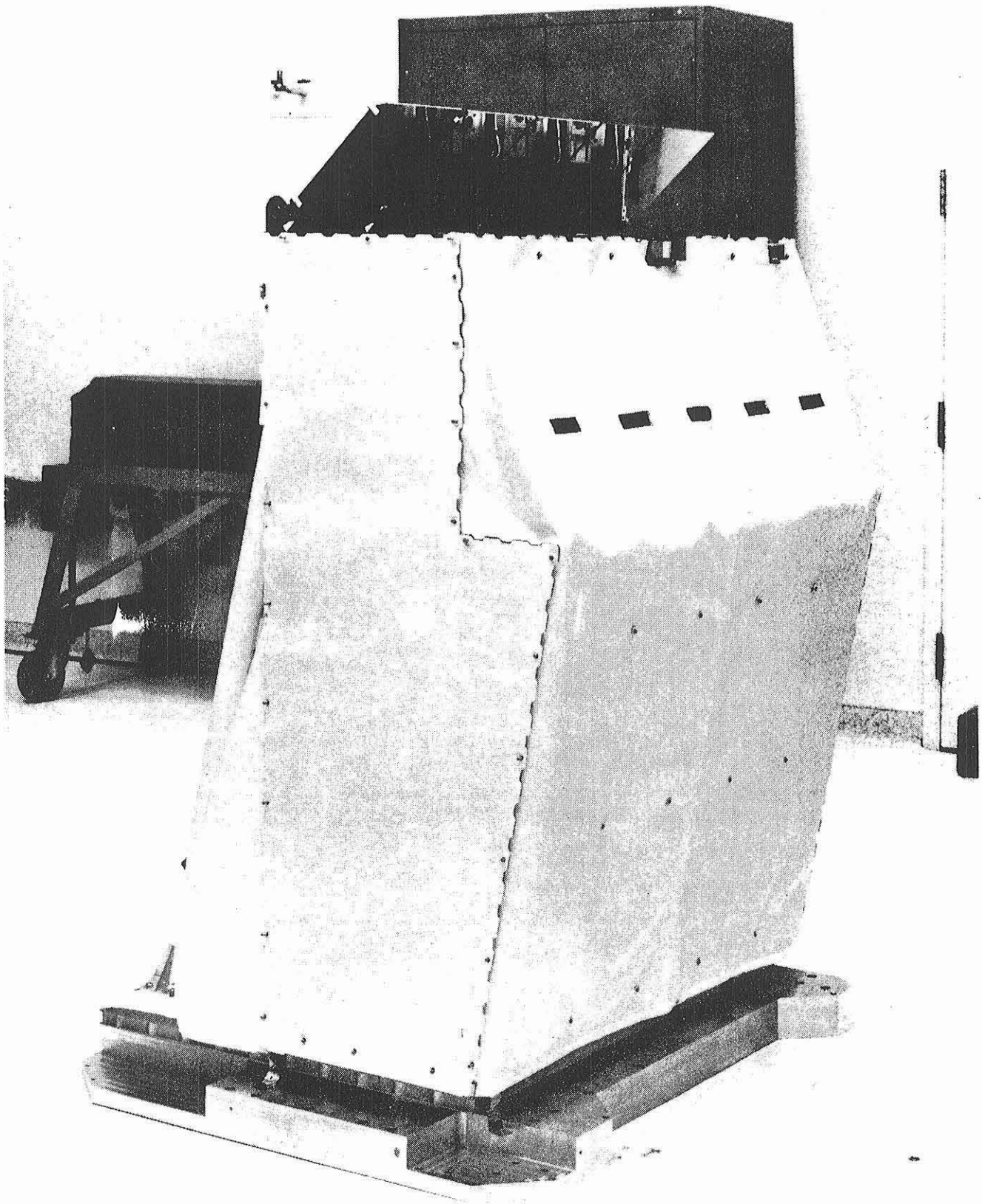
OBJECTIVES

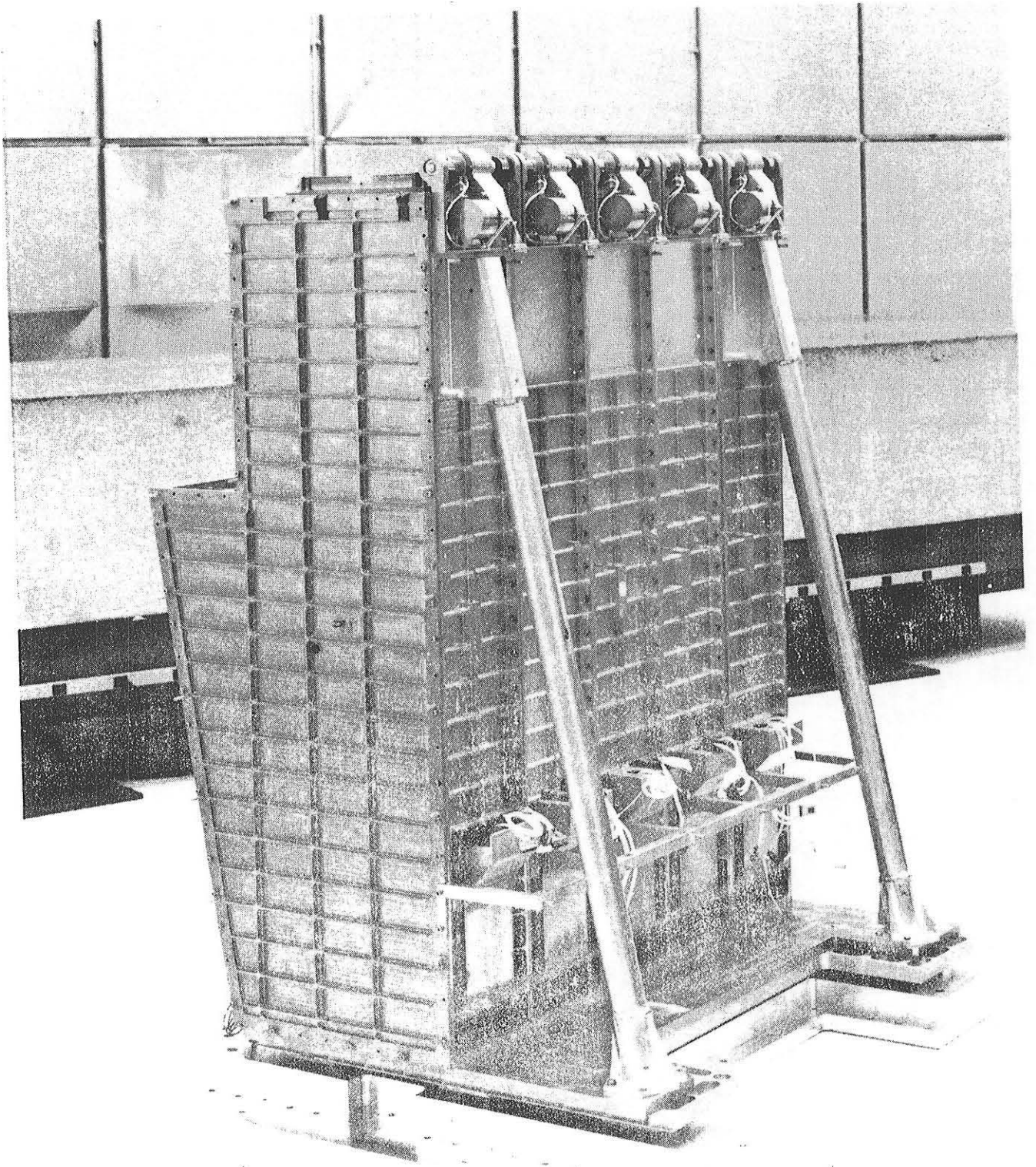
SPACELAB 1

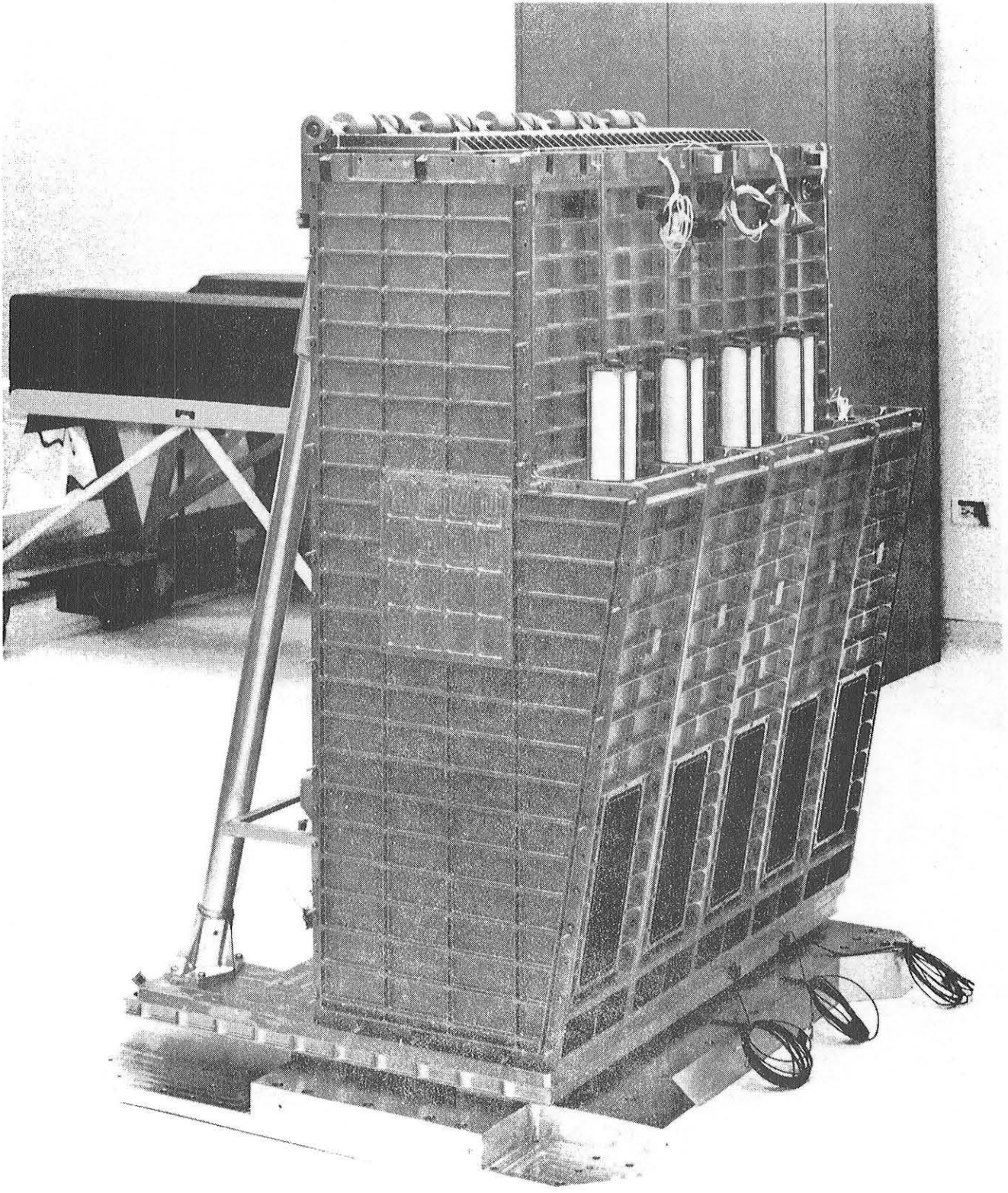
- ATLAS OF THERMOSPHERIC EMISSIONS
- VARIETY OF SPECIFIC STUDIES (DAYSIDE, NIGHTSIDE, TWILIGHT)
- S/C CONTAMINANTS

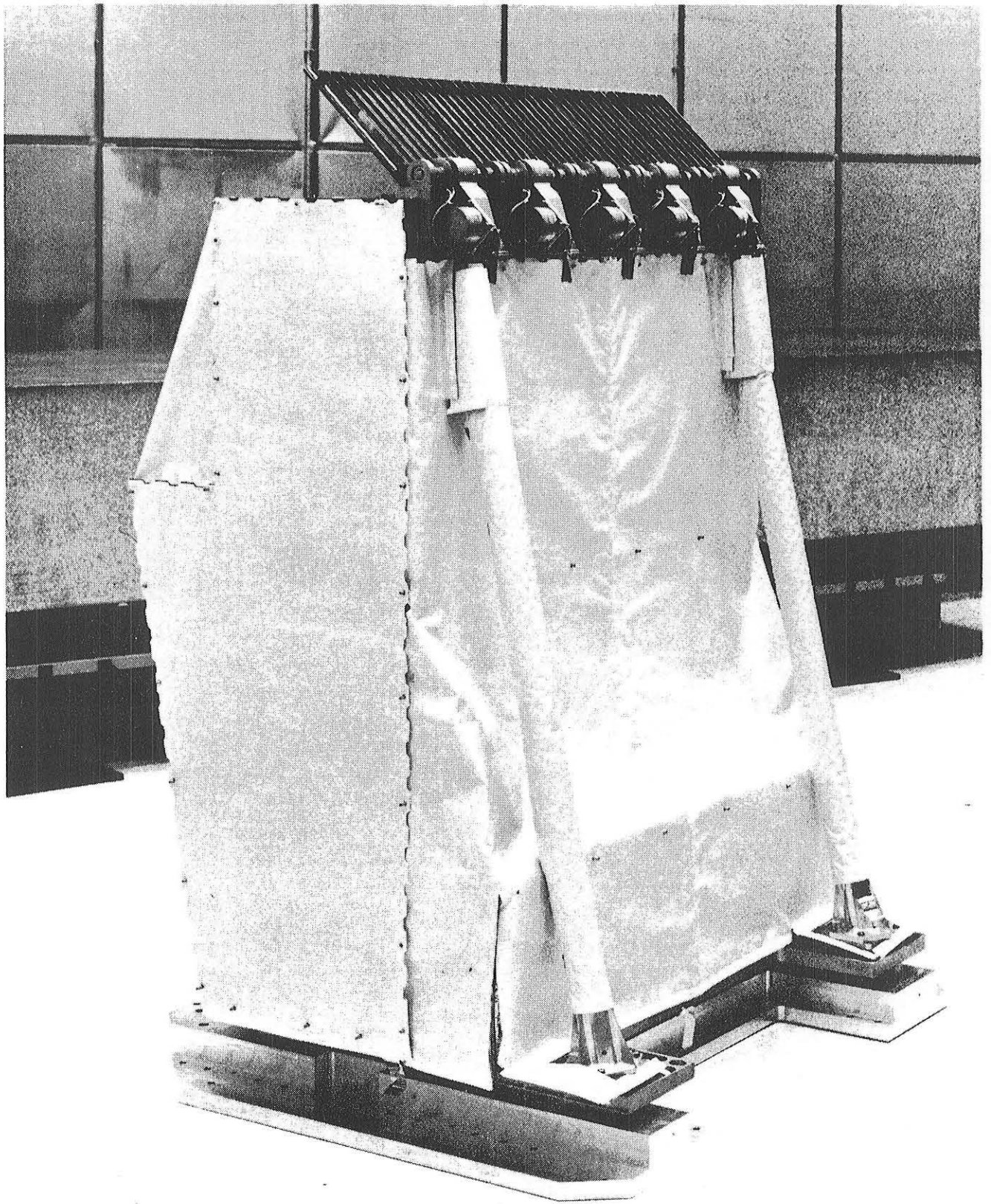
SPACELAB 6

- FURTHER THERMOSPHERIC AND SOME MESOSPHERIC STUDIES









SECTION IV. ENERGETIC NEUTRAL ATOM
PRECIPITATION (ENAP)

ACTIVE EXPERIMENTS WORKING GROUP MEETING

Marshall Space Flight Center
Huntsville

23 - 24 September, 1980

TALK BY BRIAN A. TINSLEY

Measurement of Visible and UV Emission from Energetic Neutral
Atom Precipitation (ENAP), on Spacelab.

INTRODUCTION

This experiment as most of you probably know, uses the Imaging Spectrometric Observatory developed by Marsha Torr, for a set of measurements of the effects on the atmosphere of energetic neutral atom precipitation.

The instrument will first be flown by Marsha on Spacelab 1 in a survey mode. In the reflight for the ENAP experiment it will be used during dark periods of the orbit to look for some faint emissions resulting from the phenomenon of neutral atom precipitation.

I am not discussing the instrument since that is the province of Marsha and Doug Torr, but rather the nature of the experiment, and what can be done with such an instrument in looking for faint emissions in the presence of non-negligible backgrounds.

The precipitation into the thermosphere of energetic neutral atoms results in ionization, optical emission and heating, as the kinetic energy of the atom goes into ionizing collisions, excitation collisions, or momentum transfer collisions. The cross sections for these reactions vary strongly with the species of neutral atom and its kinetic energy. The optical emission is the diagnostic we are using to identify the neutral precipitation, but we would be very interested to collaborate with anyone measuring either

the energetic neutrals themselves; the fraction which get converted again at thermospheric altitudes to energetic ions; or the ionization and heating produced. Figure 1 summarizes the above.

The energetic neutrals arise predominantly from charge exchange of plasmaspheric ions with geocoronal hydrogen at altitudes up to about four earth radii. Figure 2 is a photo of the geocorona, taken from the moon by the Apollo 16 astronauts. The hydrogen is easily detectable to beyond 10 earth radii. Figure 3 is a diagram of the magnetosphere, provided by Heikkila. The ring current source could be described as an atmosphere magnetosphere interaction, in particular as a geocorona - magnetosphere interaction. Because there are always ions in the magnetosphere, with energies from a few eV up to a few MeV, there will always be a flux of precipitating energetic neutral atoms. The flux of energetic neutrals in the 1-100 keV range will be much enhanced during magnetic storms, since the plasmaspheric flux of energetic ions (the ring current) is much enhanced at those times. But even at quiet times there should be measurable effects. There will also be a smaller contribution of energetic neutral atoms from charge exchange of ions in the solar wind with exospheric and interplanetary neutral hydrogen.

We wish to make these measurements for two purposes: to evaluate the heating and ionization effects on the atmosphere, and to evaluate the selective loss of energetic ions from the sources (predominantly ring current). Figure 4 shows a diagram of the source from the plasmasphere. The ions in the ring current which charge exchange to form neutrals are mainly H^+ , He^+ and O^+ , noted on the figure, and so we are looking for emissions due to these

MEASUREMENT OF VISIBLE AND UV EMISSIONS FROM
ENERGETIC NEUTRAL ATOM PRECIPITATION, (ENAP)

UNIVERSITY OF TEXAS AT DALLAS

PRINCIPAL INVESTIGATOR: BRIAN A. TINSLEY

CO INVESTIGATORS: W.B. HANSON

R.P. ROHRBAUGH

UTAH STATE UNIVERSITY

CO INVESTIGATOR: M.R. TORR

INSTRUMENT

IMAGING SPECTROMETRIC OBSERVATORY, BUILT BY MARSHA TORR, UTAH
STATE UNIVERSITY

INTERACTIONS OF PRECIPITATING ATOMS WITH THERMOSPHERE

IONIZATION

EXCITATION AND OPTICAL EMISSION

MOMENTUM TRANSFER (HEATING AND VIBRATIONAL EXCITATION)

SOURCES OF PRECIPITATING NEUTRALS

CHARGE EXCHANGE OF PLASMASPHERIC IONS AND EXOSPHERIC H AND O,

CHARGE EXCHANGE OF SOLAR WIND IONS WITH EXOSPHERIC AND INTER-
PLANETARY HYDROGEN

This figure, which is a print from S-201 frame 40 of a 1-min exposure centered on the earth, wavelength range 1050-1600 Å, was not available in a reproducible form for this document. It may be found in Apollo 16 Preliminary Science Report, NASA SP-315, November 1972, p. 13-8.

Figure 2

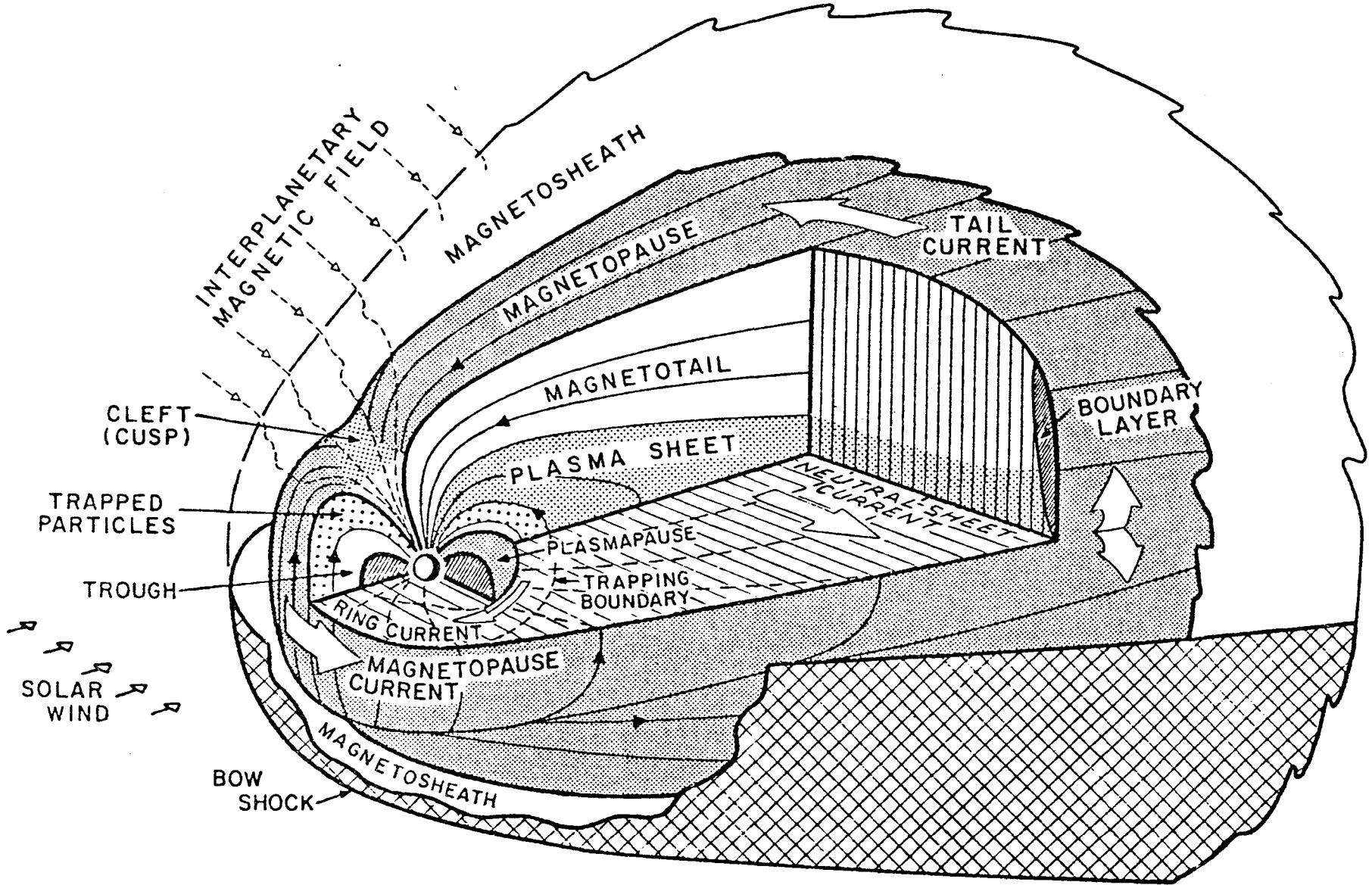
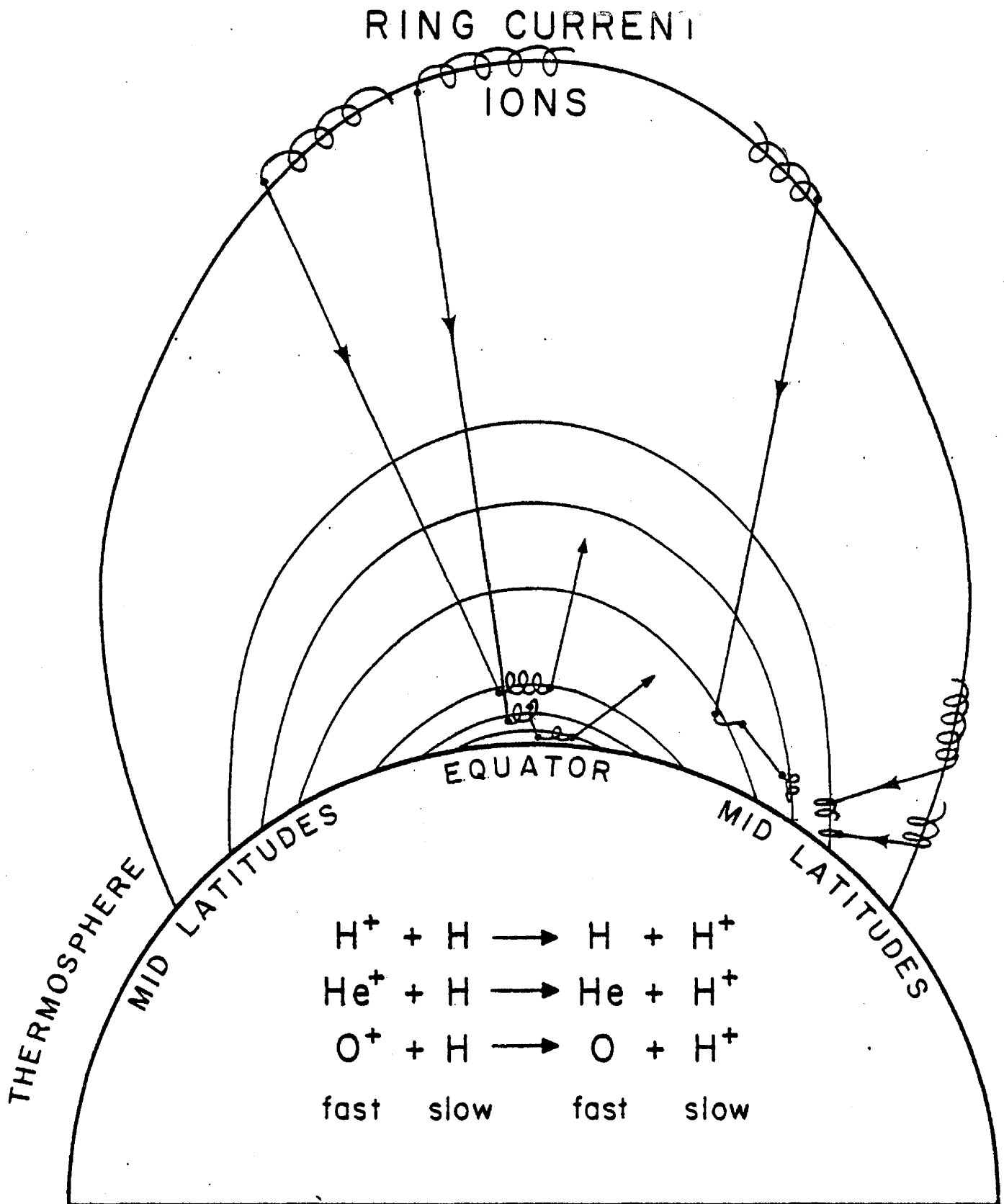


Figure 3

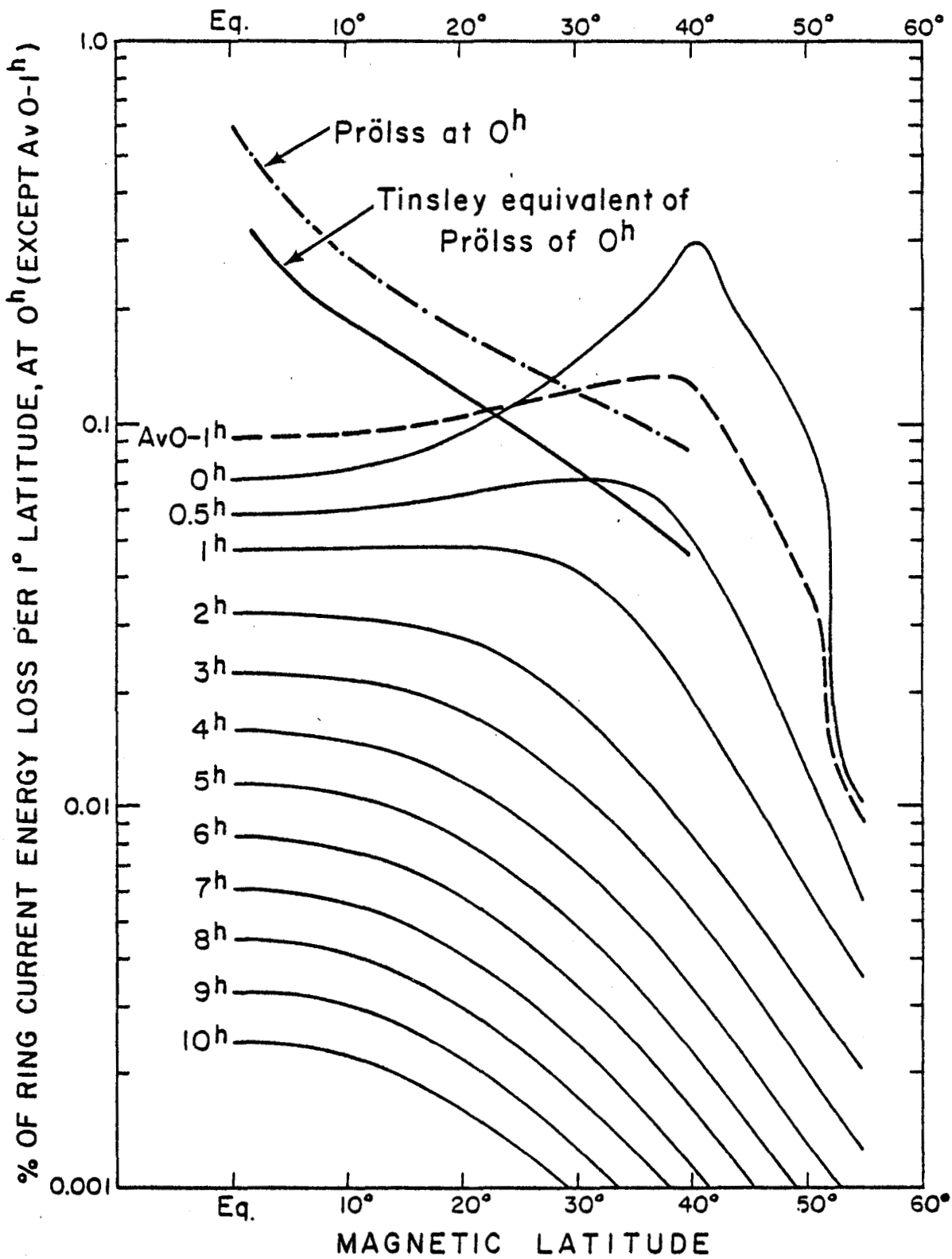


**POLAR SECTION
THROUGH MAGNETOSPHERE**

neutrals impacting the thermosphere. The trajectory of a neutral produced by charge exchange is determined by the direction the ion was moving at the instant of charge exchange - and for energies above a few ev the atoms travel in essentially straight lines. For isotropic ion velocity distributions there will be an isotropic production of neutrals, and most will escape the earth, with less than 10% impacting the thermosphere.

An important feature of the precipitation is that near the magnetic equator atoms moving nearly perpendicular to the magnetic field can become trapped again on their first ionizing collision (for some species and energies the probability of this happening is very low) and a low altitude belt of temporarily trapped ions is set up. Its energy spectrum is approximately that of the high altitude ring current, and its flux tends to rise and fall as the ring current flux changes. These particles go through a succession of charge exchange neutralization and ionization cycles, diffusing vertically in the process, before losing their energy. Such equatorial fluxes of trapped ions have been detected from satellites a number of times.

The latitude distribution of the precipitating neutrals has been calculated and is shown in Figure 5. These calculations are for a population of ions which are initially isotropic and on the L shell defined by $L = 3$ such as the isotropic distributions found where the ring current is interacting with the plasmasphere at the plasmopause. As the ions are lost by charge exchange those which mirror at lowest altitudes are lost fastest (the exospheric hydrogen has a scale height of about 1000 km). Thus the ions with equatorial pitch angles nearest to 0° or 180° are lost fastest, and the pitch angle distribution evolves with time toward a pancake distribution, and the latitude distribution shrinks towards the equator. For a distribution composed of 90°



ISOTROPIC PITCH ANGLE DISTRIBUTION ON L SHELL = 3 AT 0^h

Figure 5

equatorial pitch angle particles, all motion would be confined to the equatorial plane, and all particles would be precipitated essentially at the magnetic equator. The timescale for this figure corresponds to 1-30 keV H^+ ions in the ring current with exospheric hydrogen concentration and altitude distribution for a 950°K exospheric temperature. For other species the charge exchange cross sections are smaller, hence the time scale is longer. Figure 6 shows the variation of reaction rate σv (inversely proportional to lifetime) for several ring current species. Figure 7 shows the latitude distribution of precipitating neutrals for isotropic pitch angle distributions on various L-shells shown. There is a peak influx rate of about 15° equatorward at the foot of the L-shell on which the ring current ions are located. This is particularly interesting since SAR-arcs are found 10-15° inside the latitude of the hydrogen auroral arcs that result from directly precipitating ring current protons. While precipitating neutrals probably don't directly excite easily detectable optical emissions, or the strong 6300 Å emission of SAR-arcs (hot electrons seem to be the cause of that), the precipitating neutrals might heat the atmosphere sufficiently that F-region composition is enhanced in molecular constituents and might also vibrationally excite the molecules, so that dissociative recombination is accelerated, producing the electron density troughs observed. In such low electron density regions the downward conduction by electrons of ring current energy will heat the ionospheric electrons sufficiently to excite 6300 emission.

Most plasmaspheric ions do not have isotropic distributions, however, and for ions at low L values that have been radially transported inward by transverse electric fields, and which have been subject to erosion by charge

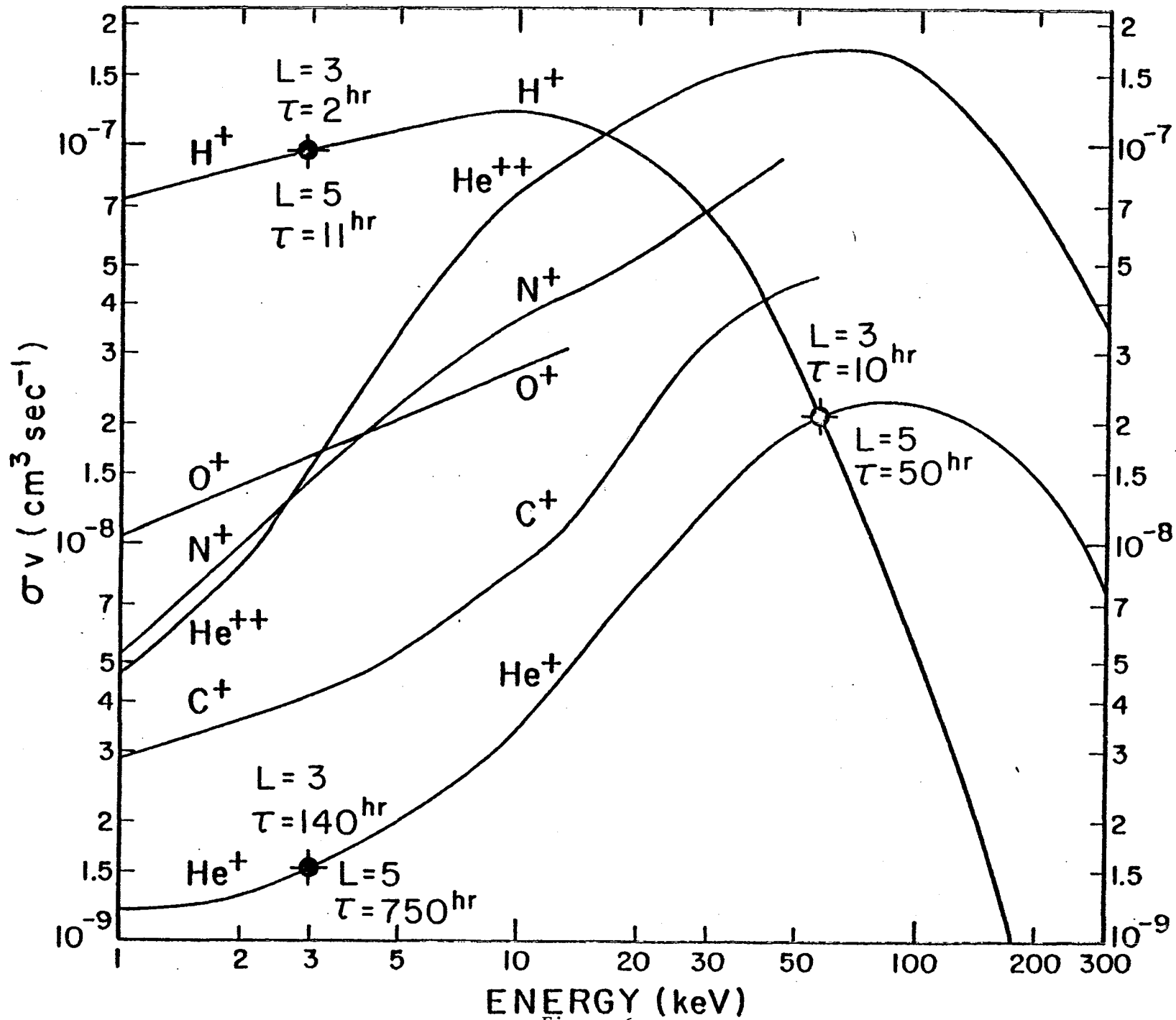
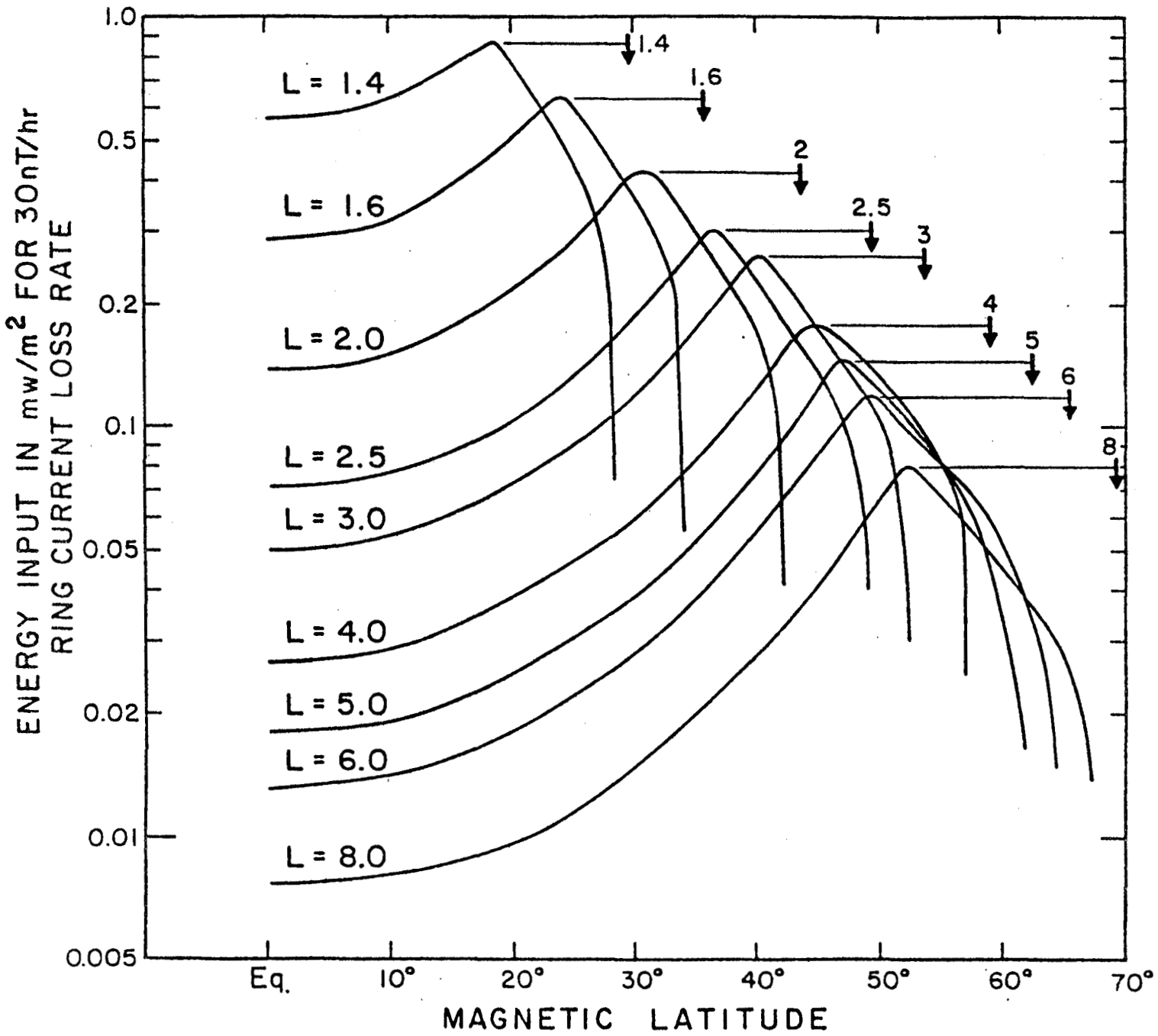


Figure 6



LATITUDE VARIATION OF ENERGETIC NEUTRAL INFLUX FOR ISOTROPIC PITCH ANGLE DISTRIBUTION ON SHELLS OF L-VALUE LISTED THE ARROW MARKS LATITUDE OF FOOT OF L-SHELL

Figure 7

exchange for days or weeks, a very highly anisotropic pancake pitch angle distribution is found. It is apparently a combination of this anisotropic source, together with an increased efficiency of trapping at low altitudes, which results in the equatorial low altitude trapped particles. Fig. 8 shows the latitude variation of several thermospheric manifestations of neutral atom precipitation. The histogram is trapped protons from precipitating MeV H atoms, according to Hovestadt; the smooth curve is $\text{He}^+ 304 \text{ \AA}$ emission from precipitating MeV helium, according to Meier, and the sawtooth curve is the latitude variation of 'probability of occurrence' of H Balmer α emission from precipitating H atoms, according to Levasseur.

With the spacelab observations, we expect to be able to see very faint emissions, of order 10^{-1} to $10^{-2} R$, with time integration, and thus to see the effects of neutral atom precipitation in quiet as well as disturbed times. We will look for emissions not previously detected, and one very important objective is to identify the precipitation of atomic oxygen. We will look for oxygen emissions of higher excitation potential than those produced by recombination, and we will look for lines of hydrogen and helium at low altitudes of intensity greater than that possible from resonant scattering, and for all three for lines of doppler widths greater than could be produced by resonant scattering or chemical excitation. One characteristic of collisional excitation by heavy particles is that they transfer momentum and excite vibrational levels of molecules, thus high vibrational excitation of N_2^+ IRG emissions is a signature of hydrogen atoms or protons below 2 keV, of helium ions or atoms below 8 keV, or oxygen atoms or ions below 30 keV.

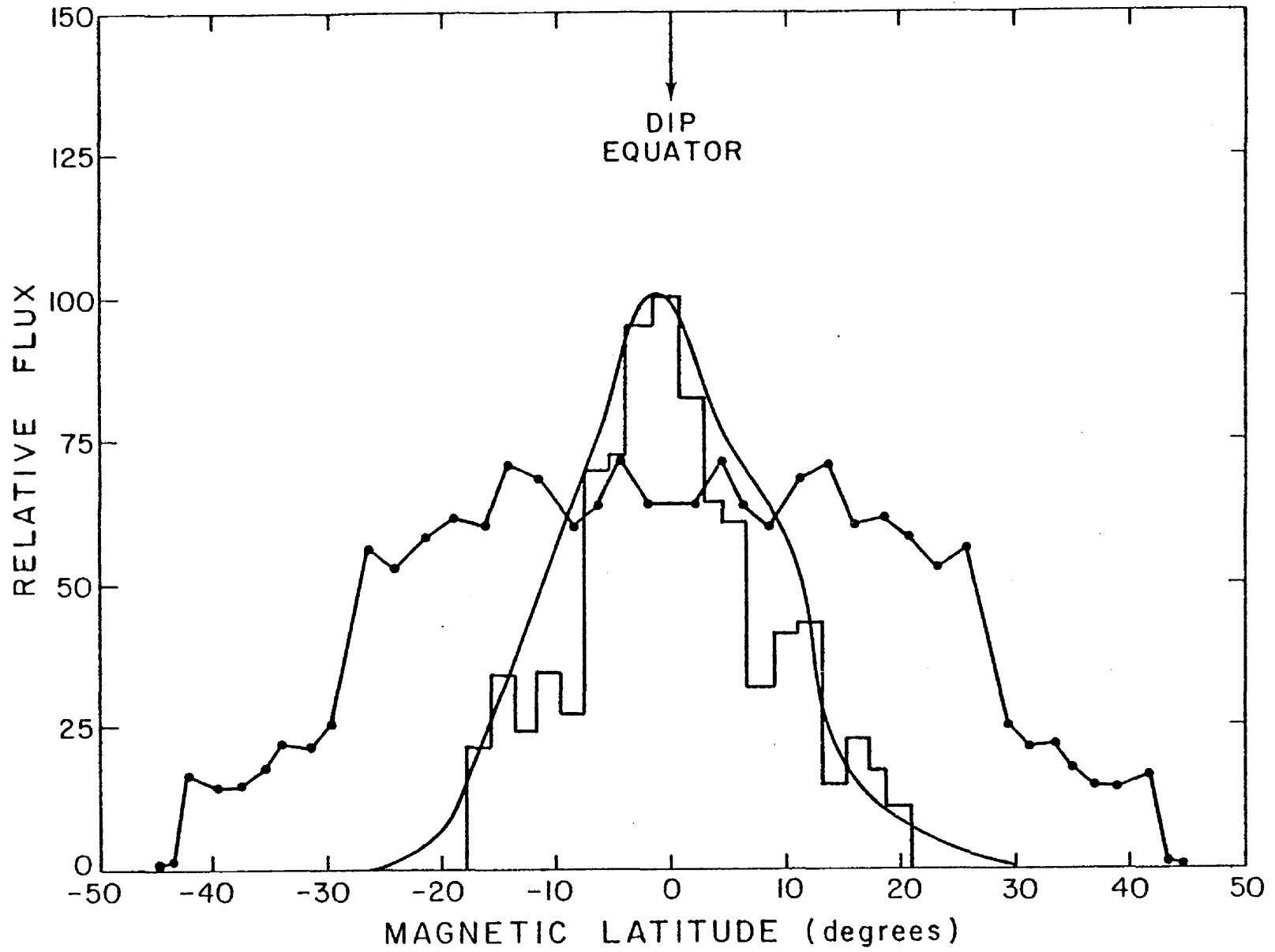


Figure 8

We will be using special techniques to detect the presence of faint lines in the presence of background emissions, such as the zodiacal light and background starlight. One is to minimize the background by selecting viewing directions at high galactic and ecliptic latitudes. This will be somewhat constrained by the need to imaging the limb for altitude profiles of the emissions. However, whatever astronomical backgrounds are present will be viewed at high zenith angles on a different part of the orbit, and subtracted later. Non astronomical backgrounds would be mainly recombination emissions, and as noted earlier, the particle precipitation emissions are distinguishable on the basis of different doppler widths, and different vibrational ratios for molecular emissions.

I am sure that part of the background we will be identifying and subtracting will be emissions due to the artificial environment introduced by the shuttle, and excited by active experiments on the shuttle, so we hope to be of use to other experiments in providing data on these too. The final figure summarizes the functional objectives.

FUNCTIONAL OBJECTIVES OF ENAP

1. EVALUATE RELATIVE FLUXES OF DIFFERENT SPECIES INVOLVED IN NEUTRAL ATOM PRECIPITATION BY MEASURING INTENSITIES OF SPECIFIC EMISSIONS.
2. EVALUATE ENERGY SPECTRUM OF PRECIPITATING NEUTRALS BY MEASURING (A) DOPPLER PROFILES (B) VIBRATIONAL RATIOS (C) ALTITUDE PROFILES FROM LIMB SCANNING OF EMISSIONS.
3. EVALUATE LATITUDE DISTRIBUTION OF PRECIPITATION BY MAKING OBSERVATIONS OVER A RANGE OF LATITUDES, IN FACT THE COMPLETE LATITUDE RANGE DEFINED BY THE ORBIT OF SPACELAB.
4. EVALUATE THE TIME VARIATION OF THE FLUXES OF PRECIPITATING NEUTRALS, AND OF THE LATITUDE DISTRIBUTIONS, PARTICULARLY AS IT IS RELATED TO VARIATIONS IN Dst AND K_p . FOR THIS THE MORE TIME SPENT IN NIGHTTIME OBSERVATION, UP TO THE MAXIMUM DURATION OF THE MISSION, THE BETTER THE SCIENTIFIC RETURN.
5. EVALUATE THE EFFECTS ON THE ATMOSPHERE, PARTICULARLY HEATING, VIBRATIONAL EXCITATION AND PRODUCTION OF IONIZATION, BY OPTICAL OBSERVATIONS AND IF POSSIBLE OTHER SPACELAB. SATELLITE AND GROUND BASED OBSERVATIONS, AND COMPARE WITH EFFECTS CALCULATED FROM EVALUATED FLUXES.
6. EVALUATE THE EFFECTS OF LOSS OF RING CURRENT IONS OF SPECIFIC ENERGIES, SPECIES, AND PITCH ANGLES ON THE EVOLUTION OF THE RING CURRENT, AND COMPARE WITH OTHER SATELLITE AND GROUND BASED (MAGNETIC) OBSERVATIONS.

Figure 9

SECTION V. WIDE ANGLE MICHELSON DOPPLER
IMAGING INTERFEROMETER (WAMDII)

WAMDII - Wide Angle Michelson Doppler Imaging Interferometer

Principal Investigator: G.G. Shepherd, York University, Toronto.

The instrument which we are proposing for Spacelab is a specialized type of optical Michelson interferometer working at sufficiently high resolution to measure line widths and Doppler shifts of naturally occurring atmospheric emissions. With its imaging capability, the WAMDII can potentially supply this information independently for each element of the 100 x 100 detector array. The field of view will be square, measuring 5 to 10° on a side. The objectives of the experiment are (1) to obtain vertical profiles of Atmospheric winds and temperatures as functions of latitude by observing near the limb, (2) to acquire exploratory wind and temperature data on smaller scale structures in airglow irregularities and in auroral forms and (3) to collaborate with other Spacelab experiments, such as barium cloud releases, in providing wind and temperature data.

A schematic view of WAMDII is shown in Fig. 1. It consists of a Michelson of the field-widened type followed by a camera lens and the 100 x 100 CCD photodiode array. An interference filter isolates the emission line being observed and the lens focuses an image of the emission on the CCD array. Thus the CCD camera takes a "picture" of the emission as viewed through the Michelson. The Michelson does not affect the imaging of the lens, but superimposes circular interference fringes, which also focus at the CCD array. The phase of the fringes depends upon the path difference between the two arms of the Michelson and the wavelength of the emission line. By choosing a sufficiently large path difference, even the tiny Doppler shifts caused by atmospheric winds can be made to produce a measurable phase shift in the interference fringes. Obviously the large Doppler shift due to spacecraft motion must be corrected for, and for this the look direction must be known within about 0.03 degrees.

Measurement of Doppler Shift and Temperature with a Michelson

The path difference of the interferometer is very nearly fixed; only enough motion of one reflector is provided to scan over a single fringe, in order to determine its phase. It is actually sufficient to measure three points on a fringe in order to determine its phase and amplitude. The mathematics assumes its simplest form when the points are separated by $\lambda/4$ in path difference. In figure 2, the I's are the three intensities

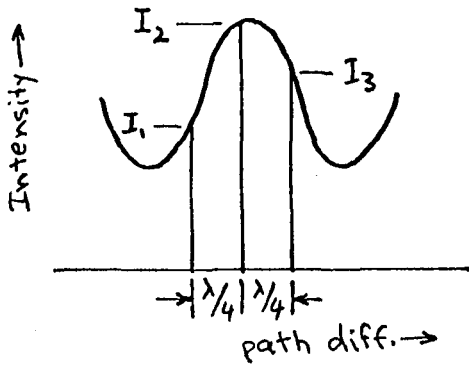


Fig. 2

measured at points on the fringe one-quarter wavelength apart. The phase, ϕ , is then given by

$$\phi = \tan^{-1} \frac{I_1 - I_3}{2I_2 - I_1 - I_3}, \quad (1)$$

referenced to $\phi = 0$ at I_1 . Thus one wind measurement by WAMDII requires that three "pictures" be taken, with the path difference stepped by $\lambda/4$ between

successive exposures. Each exposure yields 10^4 intensities; a set of three exposures therefore yields 10^4 phase values, or Doppler shifts, for the one field of view.

The change in wavelength, $\Delta\lambda$, due to the Doppler shift is related to the relative velocity, v , of the emitting region by

$$v = \frac{\Delta\lambda}{\lambda_0} c,$$

where λ_0 is the wavelength of the unshifted line and c is the velocity of light. In the interferometer, the wavelength shift $\Delta\lambda$ causes a phase shift of $\Delta\phi = 2\pi \frac{\Delta\lambda}{\lambda_0} \frac{D}{\lambda_0} = \frac{2\pi v D}{c \lambda_0}$, (2)

where D is the path difference.

Wind velocity measurement is the primary objective of this experiment, but a secondary interest is the measurement of atmospheric temperature. This, too, can be derived from the three exposures described above without compromising the wind measurements. The fringe contrast, or visibility, V , is given by

$$V = \frac{2[I_2^2 + I_1 I_3 - I_1 I_2 - I_2 I_3]^{1/2}}{I_1 + I_3} \quad (3)$$

This is directly related to the Doppler temperature of the emitting gas through

$$V = \exp[-QTD^2] \quad (4)$$

where T is the temperature

$$Q = 1.82 \times 10^{-12} (\sigma_0^2/M) \text{ K}^{-1} \text{ cm}^{-2}.$$

σ_0 is the central frequency of the emission line in cm^{-1} and M is the mass of the atomic species in amu. This assumes a Gaussian line profile. In graphic terms, V is the ratio of the fringe amplitude to the average value. (see Hilliard and Shepherd, 1966).

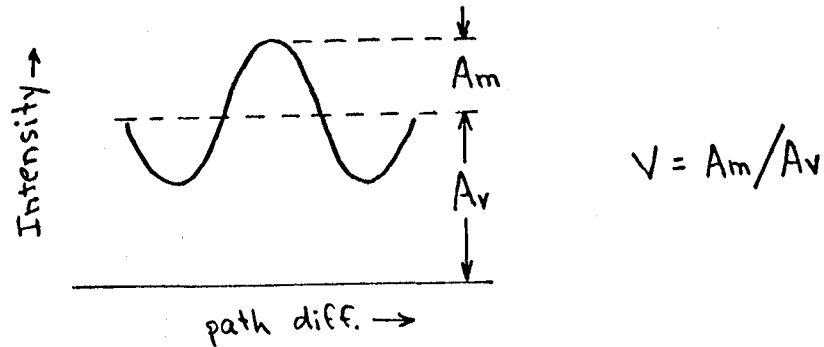


Fig. 3

Figure 4 is a schematic representation of a Gaussian emission line and its "interferogram" (Fourier transform) which would be produced by a scanning Michelson interferometer. The oscillations represent the individual fringes. The envelop causing the amplitude to decrease with path difference (described by equation (4)) is due to the finite width of the emission line. The broader the emission line, the more rapidly the fringe contrast decreases with path difference. Thus, for a given line width, an optimum path difference exists for finding the wind velocity through equation (2). Since several emissions will be observed, a compromise path difference will have to be used, probably in the range 5 to 10 cm. Or it may be possible to have two WAMDII units working at different path differences in the same instrument package, each dedicated to its own set of emissions. Some typical values for line width, visibility and phase shift are given in Table 1.

Figure 5 is another schematic illustrating an interferogram produced by two lines of equal width and intensity. A doublet, or even a more complicated multiplet can be used for the wind measurements if the path difference is chosen so that the fringes from the different components are nearly in phase with each other.

Field Widening

At the large resolving powers involved here ($\sim 10^5$), the fringes of a conventional Michelson are much too narrow to be useful. It is therefore

necessary to use a technique called field widening, or field compensation, to enlarge the fringes to a useful size (Hilliard and Shepherd, 1966). The technique involves placing a refractive plate in one arm of the Michelson and adjusting the positions of the reflectors so that their virtual images are coincident. The resulting symmetry at the beamsplitter results in greatly enlarged interference fringes. In a well-compensated Michelson, the central fringe can be 15° in diameter, compared with 0.18° for a conventional instrument. Figure 6 illustrates the two configurations.

The degree of field widening is wavelength dependent. Because of dispersion in the refractive plate, the location of M_1 (Fig. 1) for maximum field compensation is different for each wavelength. But it is possible, using two plates of different refractivity and dispersion, one in each arm of the Michelson, to make the field widening achromatic enough to be useful over a wide range of the spectrum.

Instrument Description

The design of WAMDII is still evolving and many questions remain to be answered during the Project Definition Phase. Several aspects of the instrument are discussed below under separate headings.

(a) Optical System:

A beamsplitter will probably be a 5 cm cube of fused silica. The Michelson reflectors could be corner prisms or plane mirrors with active parallelism control. An achromatic field compensation system may be needed if the range of wavelengths desired is large. Alternatively, it may be necessary to move one of the reflectors to a different position for each wavelength in order to achieve optimum field compensation. The lens will be well corrected to provide a sharp image at the detector array, and will have an aperture ratio of about $f/1$. Pre-optics could be used to transform the field of view but this is not anticipated.

(b) Stepping Control:

In order to achieve accurate path difference steps of $\lambda/4$ between exposures, one of the reflectors must be moved in steps of $\lambda/8$, and this will be done under servo control using a reference emission line source. Collimated light from the reference lamp is passed through the Michelson in such a way that the field of view of the main detector is not obstructed. The emerging beam is sent to the reference detector and the signal is used to control the position of the reflector through a piezoelectric transducer (Fig. 7). The exact way in which this is done must still be determined,

but one possibility is to use a system similar to the one described by Elsworth and James (1973), in which the emerging reference beam is polarized, the plane of polarization rotating 180° for each wavelength change in path difference. Stepping the reflector a given amount then corresponds to rotating the plane of polarization through a given angle, and the detection system must be designed to detect the angle of polarization.

The reference wavelength can be quite different from that of the line being measured by the main array channel. The filter in front of the array ensures that light from the reference lamp does not reach it.

Another interesting idea which has emerged recently is the possibility of building a completely solid Michelson with no moving parts. The small path difference steps could be provided by a Pockels cell after the beam has emerged from the interferometer. This has great advantages from the point of view of mechanical stability.

(c) Instrument Phase and Modulation Depth:

The reference lamp phase lock applies to only the reference path through the instrument, and cannot be used to characterize the phase over the field of view to the accuracy needed. Therefore a set of phase pictures will be taken of a reference-lamp-illuminated screen, at intervals of a few minutes, and the phase derived and stored for each picture element. The instrument does not yield 100% visibility in the fringes, even for an infinitesimally narrow line, because of imperfections in the optical surfaces and an imperfectly balanced beamsplitter. The instrumental component of the visibility response will be measured and stored in the same operation (the reference line width is finite but known), to be used in the determination of temperature as described by Hilliard and Shepherd (1966).

(d) Array Detector:

Present information suggests that a CCD array be used without an intensifier, which would yield only marginal improvement anyway. Figures available from the Galileo imaging team indicate that we may expect 30% quantum efficiency. The array would have to be cooled, probably to -60°C , to reduce dark current. A 100×100 array with 50μ pixels is possible with present technology. The array might even be somewhat larger than this.

(e) Sun and Horizon Baffles:

The WAMDII will be provided with a sunshade that will allow it to operate with the Spacelab in sunlight and the atmosphere in darkness.

There is also the possibility of horizon viewing with the ground sunlit, but this requires a more sophisticated baffle because the viewed limb and the lower atmosphere are very close together in angle. The problem is eased as the Spacelab altitude is lowered, and a solution is possible, provided the baffle can be made large enough.

(f) Direction Sensor:

The look direction for each exposure must ultimately be known within about 0.03° . Since this cannot be provided as the mission is presently configured, it will be necessary to determine the look direction independently. This can be done by observing the star field with a camera mounted parallel to WAMDII. The camera would use a similar array detector and would be exposed simultaneously with each WAMDII exposure. The actual pointing of the instrument during observations should be carried out within about $\pm 0.5^\circ$ accuracy.

Sensitivity, Measurement Errors, etc.

The signal produced by a single element of the CCD array depends upon the area, A , of the element and the aperture ratio, f , of the camera lens. For one element, the area-solid angle product is

$$A\Omega = \frac{\pi}{4} f^2 A.$$

For a 50μ square pixel and $f/1$ lens, $A\Omega = 2 \times 10^{-5} \text{ cm}^2 \text{ sr}$. With a transmission of 5%, a quantum efficiency of 0.3 and an emission intensity of 5 kR, a pixel produces 120 photoelectrons/s.

An intensity of a few kR is what would be expected for weak airglow viewed tangentially at the limb, or weak aurora viewed directly. It appears from an analysis of errors that the signal from a single pixel would have to be averaged for about 30 sec. to obtain a wind velocity with an error of 10-20 m/s. Individual exposures are likely to last about 1s, so the averaging could be done by adding together the signals from adjacent pixels corresponding to the same altitude. In this way the altitude information would not be lost.

The design proposed here uses a single array, whose simplicity has many advantages. Besides the technical factors, the wind and temperature equations (1) and (3) involve the ratios of intensity differences. This means that for a single detector the dark currents and calibration factors disappear through cancellation and need not even be determined.

References

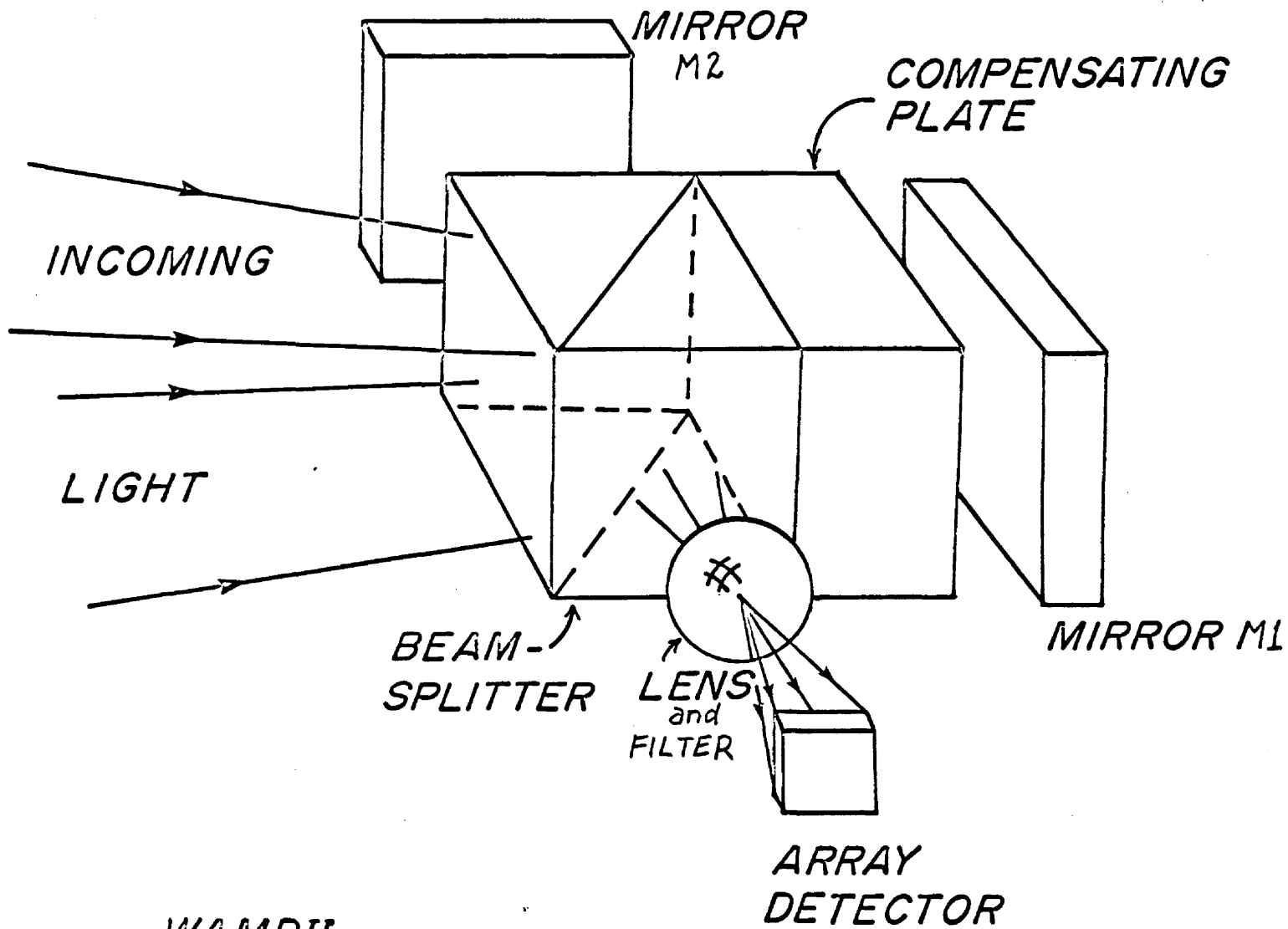
- Elsworth, Y. and James, J.F. 1973. J. Phys. E: Sci. Instrum. 6, 1134.
Hilliard, R.L. and Shepherd, G.G. 1966. J. Opt. Soc. Am. 56, 362.

TABLE 1

Emission	Temp. (K)	Line width (Å)	Visibility at path diff. of 6 cm
OI 6300	750	.031	0.46
	1000	.036	0.36
	1500	.044	0.21
OI 5577	150	.012	0.82
	200	.014	0.77
	300	.017	0.67

Velocity (m/s)	Approx. Doppler shift at 6000 Å	Phase shift at path diff. of 6 cm. (degrees)
10	0.0002	1.2
100	0.002	12
1000	0.02	120
7100	0.14	840

For each line width, there is an optimum path difference which gives greatest accuracy in the wind measurement. For example, for OI 6300 at T = 1000K it is 4.5 cm; for IO 5577 at T = 200 K it is 9.5 cm.



WAMDI

Figure 1

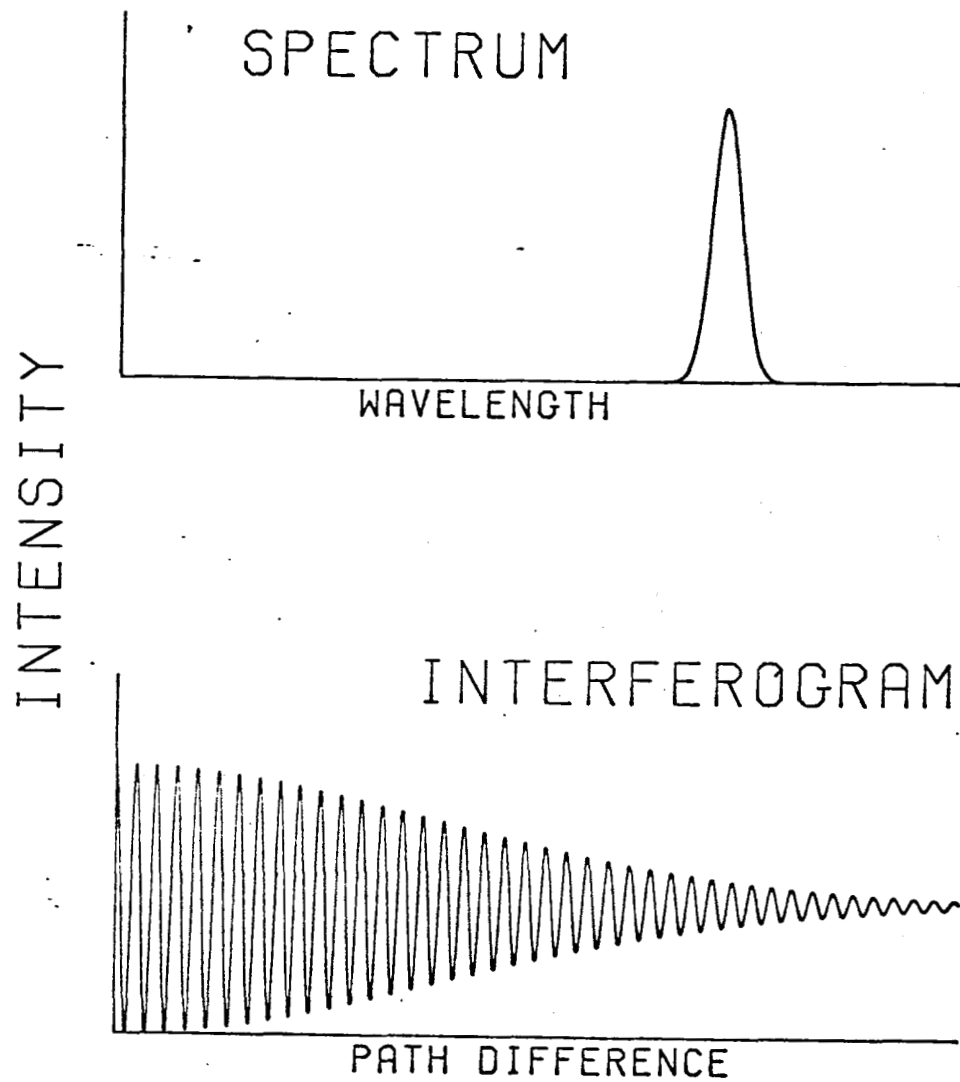


Figure 4.

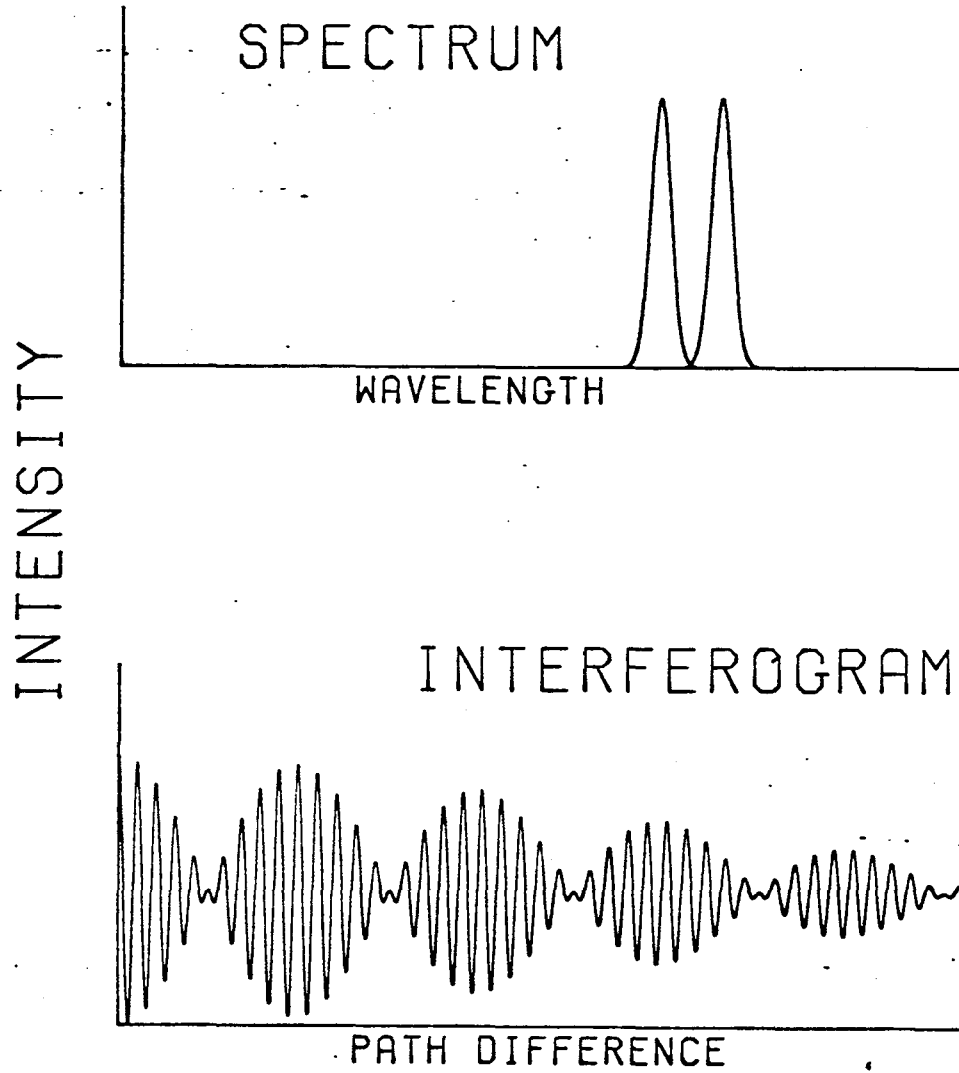
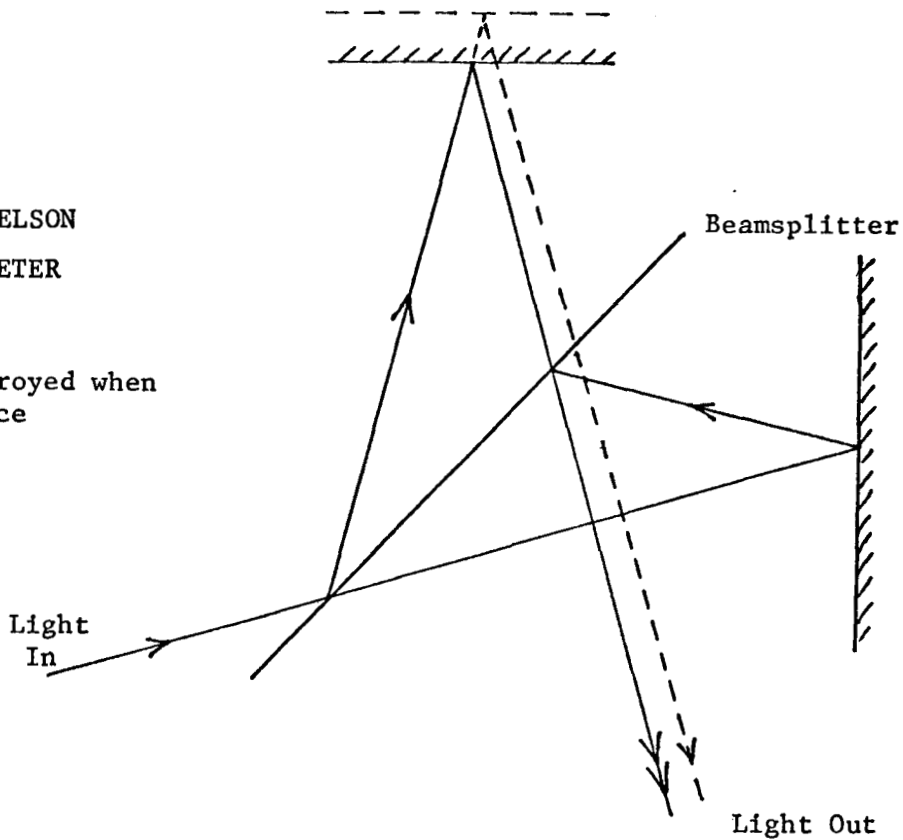


Figure 5

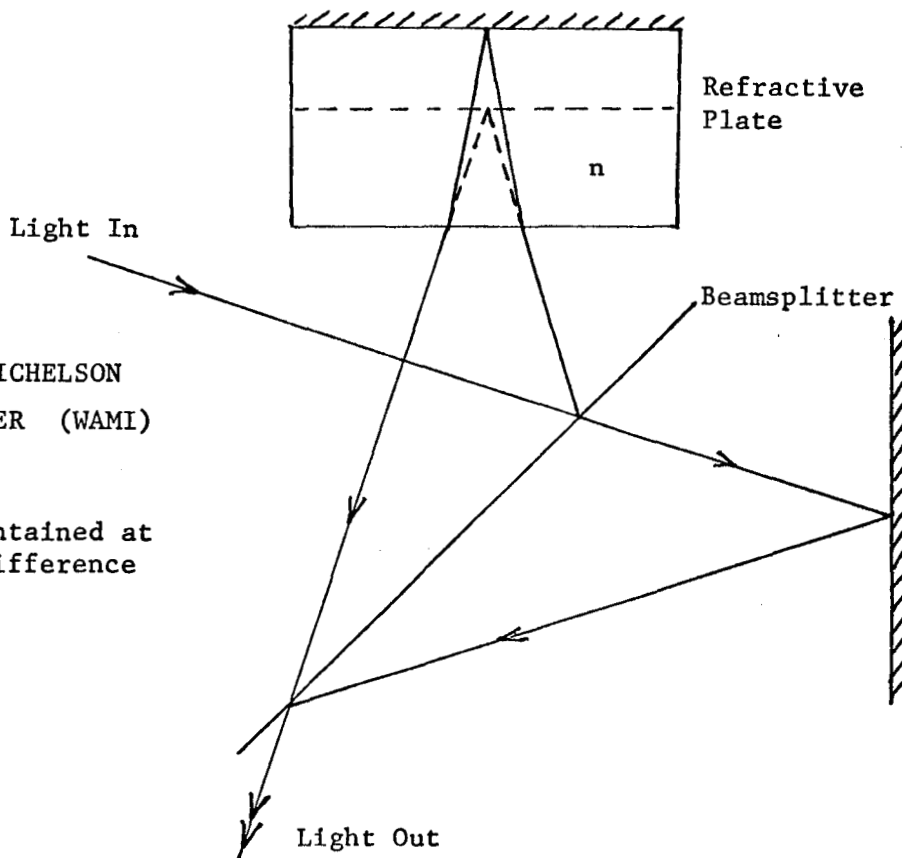
ORDINARY MICHELSON
INTERFEROMETER

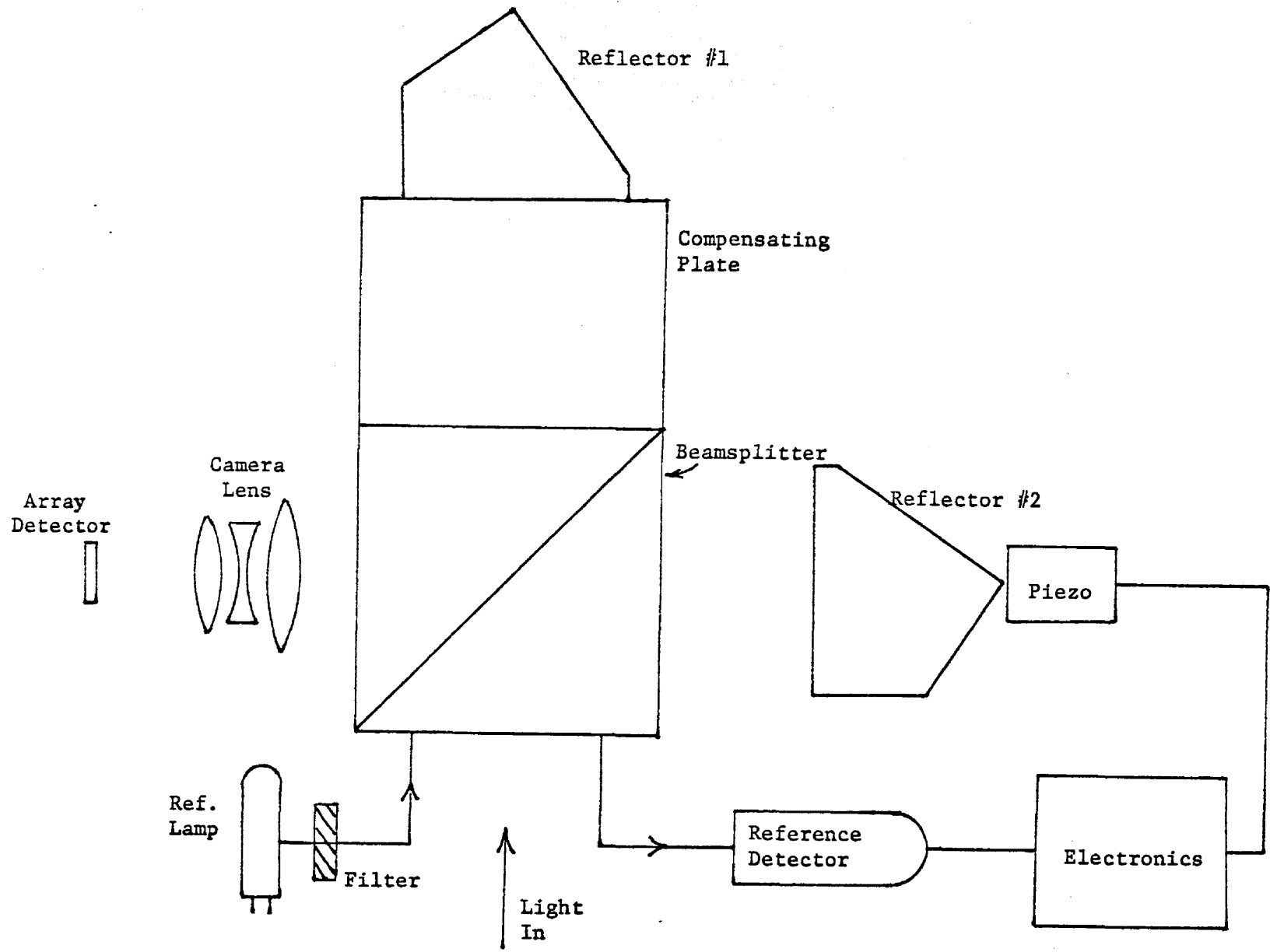
Symmetry destroyed when
path difference
introduced



WIDE ANGLE MICHELSON
INTERFEROMETER (WAMI)

Symmetry maintained at
large path difference





Schematic of Michelson with Reference System

Figure 7

SECTION VI. ENERGETIC ION MASS SPECTROMETER (EIMS)

SPACELAB ENERGETIC ION MASS SPECTROMETER

<u>Principal Investigator:</u>	<u>Organization</u>	<u>Telephone</u>
B.A. Whalen	Herzberg Institute of Astrophysics National Research Council of Canada 100 Sussex Drive Ottawa, Ontario K1A 0R6 Canada	613-992-2734 Telex: 053-3715

Co-Investigators:

I.B. McDiarmid	Herzberg Institute of Astrophysics	613-992-7884
J.R. Burrows	National Research Council of Canada	613-992-2734
R.D. Sharp	Space Sciences Laboratory	Ext. 45479
R.G. Johnson	Department 52-12, Bldg. 205	Ext. 45508
E.G. Shelley	Lockheed Palo Alto Research Lab. 3251 Hanover Street Palo Alto, California 94304 U.S.A. Telephone: (415) 493-4411	Ext. 45508

INVESTIGATION SUMMARY

Energetic Ion Mass Spectrometer

A summary of the proposed energetic ion mass composition experiments for the Spacelab missions is presented in the following. The objectives of the experiments are: 1) to investigate the source region or regions for the energetic ion population in the magnetosphere; 2) to investigate ion energization, transport and loss mechanisms; 3) to detect the minor constituents of the ion population; and 4) to perform active tracer experiments. The instrument proposed for the measurements covers the energy range from thermal energies ($\sim 1/10$ eV) to 40 keV and is capable of resolving ions with rigidities up to 24.5 MV/c ($B\rho = 8.2 \times 10^4$ gauss cm) with a mass resolution $\Delta m/m = 0.1$. The geometric factor is large enough to measure the anticipated fluxes of minor ion species (e.g., O^{6+} , He_3^{++} , He_3^+ if of solar wind origin and He_4^+ , N^+ , N_2^+ , Ne^+ , Fe^+ if of ionospheric origin) in the energetic ion precipitation and will also be used to measure the more rare constituents of the ionospheric plasma.

The instrument proposed for the mission is composed of an electrostatic analyzer followed by a magnetic spectrometer and simultaneously measures the energy per unit charge (E/Q) and mass per unit charge (m/Q) of the ion species. This device is similar in principle to ones used by the NRC group for sounding rocket experiments, but has been scaled up to give a larger geometric factor. An electromagnet is used for momentum analysis to extend the operational energy range over a much wider domain than possible with the permanent magnets used in previous space flights. Retarding potential analysis followed by preacceleration has been added before the cylindrical plate electrostatic analyzer to extend the energy range to thermal energies and to increase the geometric factor for low energy ions. This feature is identical to that used by the Lockheed group on their ISEE and Dynamics Explorer satellite instruments.

The sensitivity and mass resolution capabilities of this instrument exceed by orders of magnitude any previously flown instruments since it is only the large weight carrying capability of the Shuttle which makes this instrument feasible for space experiments. In previous spacecraft experiments the momentum analysis performed by the magnetic field portion of the instrument was compromised by the weight and, to a lesser extent, the power available for any one instrument. This implied that the mass resolution and geometric factor for high rigidity particles was seriously degraded, making high resolution and high sensitivity mass composition measurements of keV to tens of keV heavy ions impossible. The Spacelab mission presents the first opportunity to make such measurements in the region of momentum space which is so important to the understanding of basic magnetospheric processes.

It is anticipated that results from this program will increase our understanding of processes involved in the injection, energization, transport and loss of magnetospheric ions.

1. SCIENTIFIC OBJECTIVES

Mass composition measurements of ambient magnetospheric ions have recently given new insight into magnetospheric processes. We propose to expand and improve on these measurements as well as to use the direct detection of ion tracer releases to improve our understanding of these mechanisms. The major objectives for this mission are outlined below.

a) Energetic Ion Source Regions

Ion mass composition measurements have been made in the past to determine the source regions for energetic magnetospheric ions. The two possible source regions, the solar wind and the ionosphere, have significantly different charge states and minor ion species composition. The dominant ion species in the solar wind are H^+ and He_4^{++} . The next most abundant species is three to four orders of magnitude down in intensity from H^+ . The ionospheric composition at low altitudes is both variable and strongly dependent on magnetic latitude. At latitudes below about 60° , the composition is dominated by H^+ and He_4^+ at altitudes above about 1000 km. At latitudes above about 60° , verticle profile data on the ionospheric composition are limited, but the dominant ion from the F-region peak up to altitudes of about 3000 km is often O^+ . The minor ionospheric ion constituents at high altitudes are not well known; indeed, one of the objectives of this program will be to measure these ions. Recent measurements indicate that Fe^+ ions are sufficiently abundant at ionospheric altitudes to be detectable in the energetic population, assuming an ionospheric source.

Mass composition observations indicative of both solar wind origin and ionospheric origin have been reported in the literature. However, the relative contributions of the two source regions to the hot magnetospheric plasma is uncertain at this time and remains the subject of considerable scientific interest. A major deficiency of the previous measurements has been the lack of adequate sensitivity to observe routinely the minor solar wind constituents which have entered the magnetosphere. One of the goals of this proposal is to utilize the greatly increased sensitivity to expand these investigations and to extend them into as yet unexplored mass and energy regions.

Although the possibility of detecting energetic heavy ion species such as isotopes of Argon, Krypton and Xenon is remote (using the sensor proposed here and assuming normal solar and atmospheric abundances), the cosmological significance of these measurements relating to the earth's accretion rate is important enough to dedicate some time to a search for these elements in the precipitation. A natural evolution of the instrument described here would involve an increase in the instrument geometric factor, and therefore size and weight, to make the detection of these species feasible. A geometric factor increase of one order of magnitude should be adequate and would imply roughly a factor of ten increase

in instrument (magnet) weight. The final design of the scaled-up instrument would depend on results from the first generation experiment.

b) Ion Energization Mechanisms

Several energization mechanisms for solar wind ions appear in the literature and these processes are sensitive to the m/Q of the ion being accelerated. The limited range in energy, mass and rigidity of ions detected until now make conclusive comparisons between theory and observation difficult. The detection of O^+ and He^+ ions in the magnetosphere have added an unexpected complexity to magnetospheric processes. These data indicate that the ionosphere is also an important source for energetic ions. Several theories have been presented which predict the energization of ionospheric ions, the energy source being either the ring current particles or electrostatic acceleration associated with auroral electron energization processes. The relative importance of these energization mechanisms remains uncertain.

The simultaneous measurement of energy spectra of several ions, particularly ones widely spaced in m/Q and rigidity, can be used to test the validity of these mechanisms. To this end the spectrometer described in the following has a greatly increased sensitivity and will have sufficient mass resolution, for high rigidity ions, to make the necessary spectral measurements of the heavy ion population.

c) Field Line Tracing

Naturally occurring heavy ions serve as good tracers of convective electric fields. The heavy ion composition can be used to identify a flux tube since at low energies all heavy ions will remain fixed to a particular field line which can then be identified at some later time by its composition. Using this method of identification, convection of field lines through the magnetosphere may be followed.

For example, assuming a solar wind injection, coordinated solar wind and low altitude observations will allow one to observe the regions and times for solar wind entry into the magnetosphere as a function of ion mass. Similarly, with an ionospheric injection event various ion clouds may be observed as a function of latitude and local time as they are convected and energized in the magnetosphere. As will be discussed later, observations of energetic ions at low altitudes can be significantly perturbed by charge exchange effects and such effects must be considered in modeling the events.

Active experiments involving the injection of easily identified heavy ions (e.g., lithium or barium) into the magnetosphere and solar wind are also planned. This technique offers a method of uniquely tagging field lines in a controlled fashion.

Direct detection of these ions at various times after injection will provide valuable information on both entry, if the release occurs in the solar wind, and energization mechanisms. Hence, a mass spectrometer capable of resolving the tracer ions from the ambient is required. This instrument should obviously have the largest possible geometric factor to maximize the detection probability and a high mass resolution to reduce the background due to the ambient. With such a device the motion and energization of tracer ions can be monitored directly.

As a first step toward successful tracer experiments, a survey of the ambient (background) ions with an instrument suitable for active tracer experiments must be undertaken. To date, this has not been done.

It should be noted that for low altitude injections the average tracer ion energy at injection, using shaped charge techniques, or the spacecraft orbital velocity, would be approximately 10 to 100 eV or of the same order as the ambient thermal plasma high energy tail. The spectrometer must therefore be capable of operating at low energies and, in fact, to complete the ambient ion survey, should be capable of analyzing to thermal (or ram) energies. This instrument has this capability although only the minor or trace ion constituents of the thermal plasma will be monitored. The dominant ion species would saturate the detector and should be measured using standard sensors.

d) Coordinated Investigations

Several spacecraft carrying ion mass spectrometers may be operated during the Spacelab flights (e.g., ISEE, DE, GEOS II, AMPTE, PIE II, etc.). Coordination of observation from these spacecraft along with simultaneous measurements from sounding rockets and ground-based (optical) facilities will be undertaken to investigate the spatial distributions of the various ion populations. These measurements will be conducted during the investigations discussed previously. If tracer ion releases are to be performed during the first mission, efforts will be made to coordinate the mass spectrometer observation periods with the release. Ion releases from the C.R.M. as well as SEPAC will be of particular interest here.

2. ORBIT CONSIDERATIONS

Charge exchange reactions can occur between precipitating ions and atmospheric constituents at low altitudes, thus changing the m/Q of the primary ion beam. Using the mean COSPAR international reference atmosphere, it can be shown that the unperturbed primary ion beam will be observed at 400 km altitude. However, since the atmospheric density may increase or decrease by an order of magnitude at these altitudes, depending on solar activity and latitude, the primary ion beam may or may not reach the sensor in its unperturbed charge state. Valuable observations, therefore, may be made

at 400 km. However, a preferred orbit would be a few atmospheric scale heights higher (i.e., 500-600 km).

It should be noted that contaminant gas surrounding the Spacelab may also cause significant charge exchange effects, hence a monitor of the local gas pressure is required to correct for periods of high ambient pressure associated with engine firings, etc., as well as to define the atmospheric conditions.

Clearly, if high latitude (auroral) data is to be obtained the orbit inclination should be at the maximum allowable. A polar orbiting spacecraft would be ideal; however, even a 57° inclination (launch from K.S.C.) would place the spacecraft in the auroral zone over northern Canada near local midnight.

3. INSTRUMENT DESCRIPTION

The instrument described in this section will be used as the basis for design trade-off studies during the PDP phase. The two groups involved in the study will contribute equally to this portion of the program. The Instrument Control and Data Handling system is to be developed by LMSC and the sensor is to be primarily NRC's responsibility.

As the basic design criteria we have required that the instrument have a mass resolution ($\Delta m/m$) of 0.1 for ions with rigidity (mv/Q) up to that of 20 keV O^+ ions, which is an mv/Q of 24.5 MV/c. Equivalently, in a magnetic field B , since $B\rho = mv/Q$ where ρ is the ion radius of curvature in the field, the maximum ion $B\rho$ will be 8.2×10^4 gauss cm. The instrument must also have an energy resolution $\Delta E/E$ of 0.1 and a geometric factor (G.F.) large enough to allow for detection of the minor constituents of the energetic ion population (G.F. $\sim 10^{-1}$ cm² sr). To perform the energy and mass analysis a combination of electrostatic and magnetic analysers shown in Figure 1 was chosen from among many possible designs considered. This design was selected to take advantage of the large area and near omnidirectional ion source (the magnetosphere). A focusing magnetic deflection system was selected to give both high sensitivity and low background.

a) Momentum Analyzer

To achieve a constant mass resolution independent of particle rigidity and a wide operational range, a magnetic analyzer formed with an electromagnet was chosen. This is a standard configuration for laboratory mass spectrometers. First order focusing using shaped pole pieces is employed to get the maximum geometric factor for a given poleface area (or magnet weight). The magnetic analyzer focuses a parallel beam of particles entering the curved pole face to a point which is at the centre of the channel electron multiplier array shown in Figure 1. Depending on the mass resolution and geometric factor requirements, the CEM elements may be operated either independently or various elements summed. This function is controlled by the instrument control and data handling

section. In the highest mass resolution mode only the centre elements are used while the end elements monitor the "background" rate.

One problem which must be considered in the selection of the sensing element is its response to contamination from Spacelab venting. Channel electron multipliers are less sensitive than other open-ended (discrete dynode) devices to the contaminants expected in the payload bay and thus are the preferred devices; however, we propose to study the response of the sensors to contaminant gases to ensure reliable operation. Ease of replacement of the electron multiplier after each flight is also important in the selection of the sensing elements.

Stray electric and magnetic fields may also interfere with some of the low energy measurements proposed. Ions with energies greater than a few hundred electron volts should, however, be relatively unaffected by the anticipated contaminant fields. To minimize this problem the spectrometer should be located in a region removed from insulating surfaces and high dc electric and magnetic fields.

Stray magnetic fields will also be produced by the electromagnet. A scale model of the analyzer was constructed and some initial tests conducted. The stray field was measured and, when scaled up to the flight unit, will be below the earth's field at a distance of ~ 3 m from the instrument with no magnetic shielding. Some shielding is required for proper operation of the instrument and more may be added as required to reduce the stray field.

A magnetic field strength of 10 k gauss (1 T) is needed in the gap to focus 20 keV O^+ ions. To estimate the peak power and current, the coil was assumed to be wound with #8 AWG wire. Three hundred and twenty turns at 25 amps will produce the 10 kg field. This implies a peak IR power dissipation of 200 Watts. The dissipation averaged over all operating modes and energies would be much lower (~ 50 W). Some savings in power can be made by going to more exotic windings; however, these figures serve as good estimates of the maximum power used by the electromagnet.

Other characteristics such as weight, inductance and time constant are listed in Figure 1. Although only rough estimates, the response time and mass of the system appear to be acceptable from an engineering viewpoint. The analogue control signals for the electromagnet power supply will originate in the instrument control section. The current supply circuit will operate on a feedback system, the primary field sensor being a magnetometer mounted in the gap. Using this type of feedback the coil will be driven to produce an overall response time of the electromagnet system of approximately 1/10 the magnet time constant (50 ms). Rapid changes in field require increased instantaneous power dissipation. To reduce the instantaneous power requirements to < 200 W a small capacitance storage ($\sim 10,000$ μ f

at 100 V) may be required for rapid increases in current. If all rapid changes are limited to decreasing field conditions no energy storage is required.

A drawing indicating the mounting and overall dimensions of the instrument package appears in Figure 2. During the PDP phase consideration will be given to mounting ICDH and some of the power supplies separate from the sensors.

b) Electrostatic Energy Analyzer

The energy analysis is performed using two systems, a retarding potential analyzer (R.P.A.) for low energy (0-50 eV) ions and a cylindrical plate electrostatic analyzer (C.P.E.A.) for high energy ions (less than 40 keV/Q). To retain an energy resolution $\Delta E/E$ of the order of 10% and still keep the deflection plate size to a minimum and the geometric factor at a maximum, as defined by the magnetic spectrometer pole face separation, a set of three concentric cylindrical plates will be used. The centre plate will be operated at roughly the mean of the potentials applied to the two outside plates. Collimators will be inserted between grid G_3 and the C.P.E.A. (see Figure 2) to produce the nearly parallel beam at the exit aperture required for the magnetic analyzer.

The C.P.E.A.-electromagnet system will be designed to be floated up to -3 kV. This option will be used to preaccelerate ions between the R.P.A. and the C.P.E.A., thereby increasing the detection efficiency and geometric factor for low energy ions.

In the high energy modes the R.P.A. is set to repel unwanted low energy ions. In the lowest energy mode the repeller grid (G_2) will be used to integral energy analyse the ions before preacceleration. This approach is identical to that used by the Lockheed group for the ISEE satellite mass spectrometer and is the proposed method for the DE mission. Positive ions entering the R.P.A. are analyzed in the 0 to 20 V range, accelerated by the 3 kV potential drop between G_2 and G_3 and momentum analyzed and detected in the negatively biased C.P.E.A.-magnetic spectrometer system. At this time the C.P.E.A. is set to analyze 3 keV/Q particles and is transparent to all low energy (<50 eV) ions. The R.P.A. will have typically 32 voltage steps and will be controlled by the instrument control logic and by the Spacelab computer.

In the mid-energy range (20-200 eV) two sub-modes can be selected. One uses 3 kV preacceleration and R.P.A. analysis to give pseudo-integral energy spectra, as in the low energy mode. The second mode uses no preacceleration and the C.P.E.A. to give differential energy spectra with $\Delta E/E = 0.1$.

In the high energy mode the R.P.A. is set to repel low energy (50 eV) ions and the C.P.E.A. is used for energy analysis. The preacceleration voltage can be set to either zero or 3 kV, depending on the requirements of the experiment. The preaccelera-

tion mode will be used to increase the effective geometric factor at the expense of energy resolution. With no preacceleration the C.P.E.A. plates are operated in a balanced configuration with the centre plate grounded and the two outside plates at voltages up to ± 6 kV. The plate voltages will be adjusted so that the centre trajectory energy will be the same in each half of the system.

The upper energy limit for heavy ions is set by the magnetic deflection system which was discussed previously. For ions with $m/Q < 16$ the magnetic analyzer is capable of focusing energies greater than 20 keV. Here the upper limit is set by the maximum voltage which may be applied to the electrostatic deflection plates. An upper limit near $E/Q = 40$ kV is estimated for these light ions.

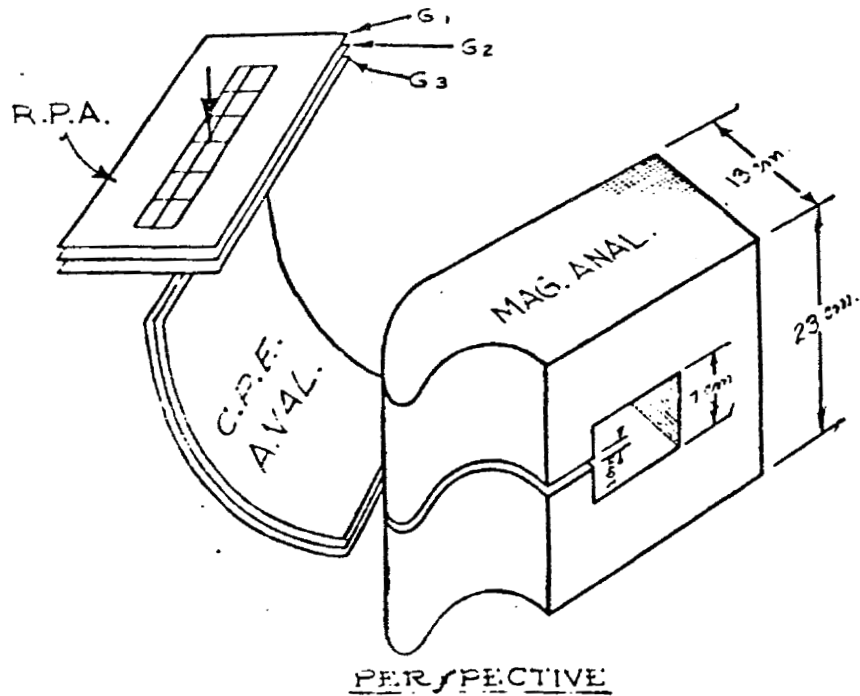
All instrument operational modes are independently programmable via the Spacelab computer and instrument control section; however, a number of preprogrammed scanning routines will be available in the instrument. A typical example involves rapid energy scans from 20 keV to 2 keV at one selected mass. Here the energy would be stepped exponentially and the magnet current would track one particular mass species. The maximum scan rate here would be determined by the maximum allowable magnet dI/dt . The magnetic field current supply will be designed to complete one scan in 50 ms.

A second mode of operation calls for the scanning of a two-dimensional matrix in energy and momentum space. In this mode the magnetic field would remain fixed at a number of steps as the energies are scanned. The maximum scan rate is then defined by the C.P.E.A. high voltage supply rise time which will be 2 ms. As an example an 8×8 energy momentum array may be measured in ~ 200 ms. In many instances the actual dwell times on each element in these arrays will be determined by the requirement for statistical accuracy rather than the instrument capability.

A crude small scale model of the instrument was built and tested at the NRC laboratories. A scan of 2 keV beam emerging from the He^+ ion source is shown in Figure 3. This figure demonstrates some of the strengths of the system as well as the problems. We first note that the half width of the He^+ peak (0.04) is well within specification for single element detection at the focal point. The H^+ peak is due to contaminants in the source. We also note that the background is down by at least 10^{-4} of the peak which is essential for the mission.

The problem area lies in the low mass tail of the distribution which results mostly from inhomogeneities in the magnetic field. This problem will be corrected in the flight unit by magnetic field trimming. Small angle scattering may also be a problem and will be minimized by more careful baffling than present in the model.

Many applications for the instrument require pointing capability, therefore it is proposed that the instrument be mounted on a small, modest accuracy, instrument pointing system. The Spacelab computer will be used in conjunction with the output from the magnetometer sampling the ambient field to either monitor or actively point the mass spectrometer.



CHARACTERISTICS:

EFFECTIVE G.F. = 3.2×10^{-2} to $32 \times 10^{-1} \text{ cm}^2 \text{ sr}$
 MAX. PARTICLE RIGIDITY = $8.2 \times 10^4 \text{ gauss cm}$ (24.5 M/c)
 OR 320 keV H^+
 20 keV O^+

$$\frac{\Delta E}{E} = 0.1$$

$$\frac{\Delta M}{M} = 0.1$$

$$\text{ANG. RES} = 6^\circ$$

WEIGHT = 60 kgms

POWER = 50 W (200 peak)

MAGNET INDUCTANCE = 0.16 h

MAGNET TIME CONST = 0.5 secs

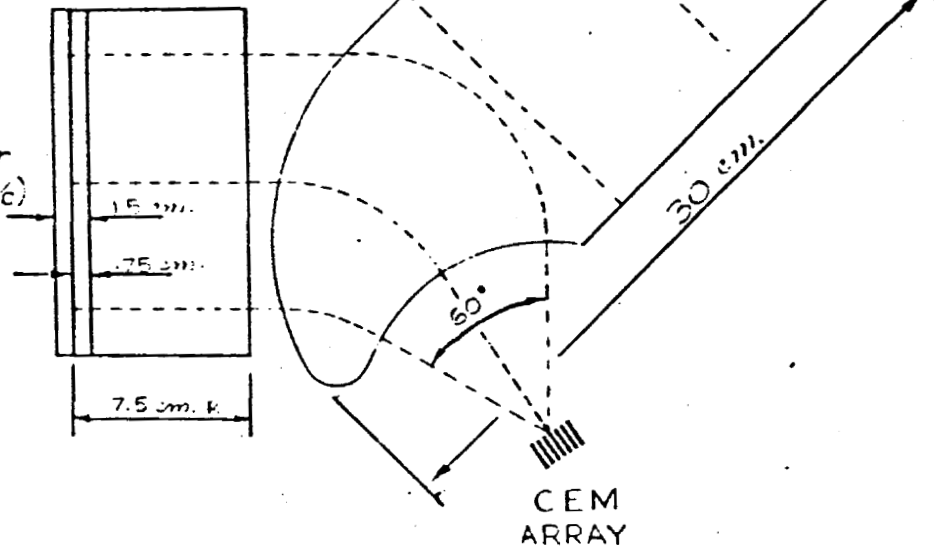


Figure 1

ION MASS SPECTROMETER

BEAM ENERGY - 2.0 KeV

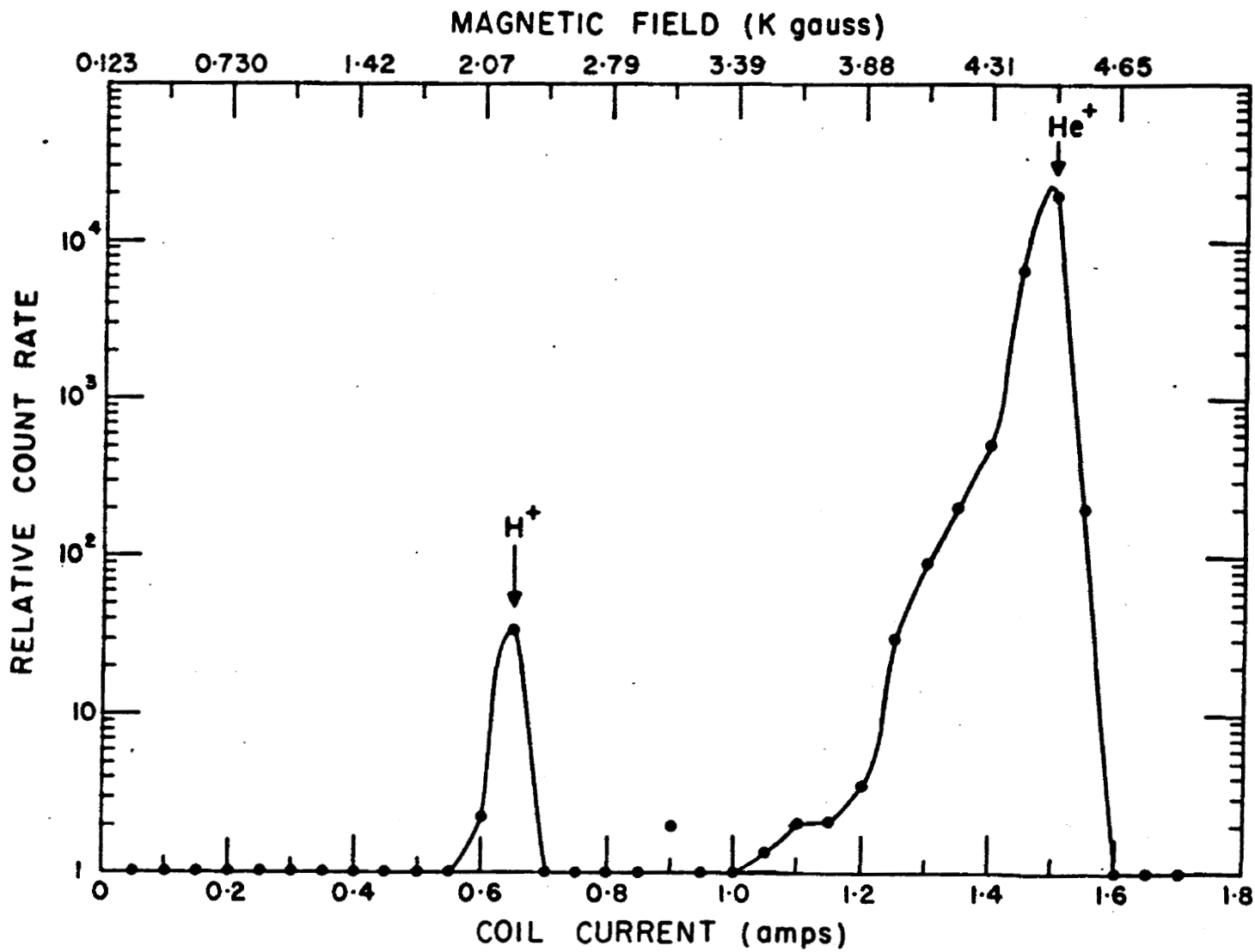


Figure 3

SECTION VII. SPACE EXPERIMENTS WITH
PARTICLE ACCELERATORS (SEPAC)

SPACE EXPERIMENTS WITH PARTICLE ACCELERATORS

SEPAC

STATUS REVIEW

SEPTEMBER 23, 1980

SEPAC DEVELOPMENT RESPONSIBILITIES

INSTITUTE OF SPACE AND AERONAUTICAL SCIENCE (ISAS), UNIVERSITY OF TOKYO

- ACCELERATOR SYSTEMS
 - ELECTRON BEAM ACCELERATOR
 - MAGNETO PLASMA DYNAMIC (MPD) ARCJET
- DIAGNOSTIC SYSTEMS
 - DIAGNOSTIC PACKAGE
 - MONITOR TELEVISION
- POWER SYSTEMS
 - BATTERY AND CHARGER
 - HIGH VOLTAGE CONVERTER

MARSHALL SPACE FLIGHT CENTER

- DEDICATED EXPERIMENT PROCESSOR
- INTERFACE UNIT
- CONTROL PANEL
- ALL FLIGHT SOFTWARE

SEPAC OPERATIONS

- AUTOMATED EXPERIMENTS (UNDER DEP COMMAND CONTROL)
 - 21 INDIVIDUAL EXPERIMENT ELEMENTS
 - EACH EXPERIMENT MAY HAVE PARAMETERS MODIFIED BEFORE THE EXPERIMENT OPERATIONS ARE BEGUN (E.G., PITCH ANGLE, CURRENT, ACCELERATION VOLTAGE, PULSE DURATION, PULSE INTERVAL)
 - TOTAL OF 50 PARAMETERS FOR EACH EXPERIMENT
 - PAYLOAD CREW PERFORMS ALL PARAMETER CHANGES
 - PAYLOAD CREW MONITORS STATUS OF ALL SEPAC INSTRUMENTS
 - PAYLOAD CREW IS INVOLVED IN THE EXPERIMENT PERFORMANCE THROUGH DATA DISPLAYS
 - GRAPHIC DISPLAY OF SAMPLE FROM DIAGNOSTIC INSTRUMENTS
 - TELEVISION MONITOR
- SEPAC MANUAL OPERATIONS (SMO)
 - PAYLOAD CREW MAY CONSTRUCT OTHER EXPERIMENTS USING SMO
 - THE SMO IS PRIMARILY USED TO PERFORM TEST OPERATIONS PRIOR TO EXPERIMENT OPERATIONS
 - THE SMO ALSO PERMITS OTHER EXPERIMENTS TO BE PERFORMED USING FEATURES SUCH AS EBA BEAM MODULATION (1 kHz or \sim 5 kHz)
 - THE SAME DATA DISPLAYS ARE AVAILABLE TO THE PAYLOAD CREW AS DURING AUTOMATED OPERATIONS
 - PAYLOAD CREW SELECTS SEPAC MODE OF SMO BY SETTING UP TO 25 SELECTABLE PARAMETERS

JOINT EXPERIMENTS ON THE FIRST SPACELAB MISSION

AEPI - THIS INSTRUMENT IS USED TO OBSERVE THE HIGH POWER EBA AND MPD FIRINGS (HARD WIRE LINK BETWEEN EXPERIMENTS)

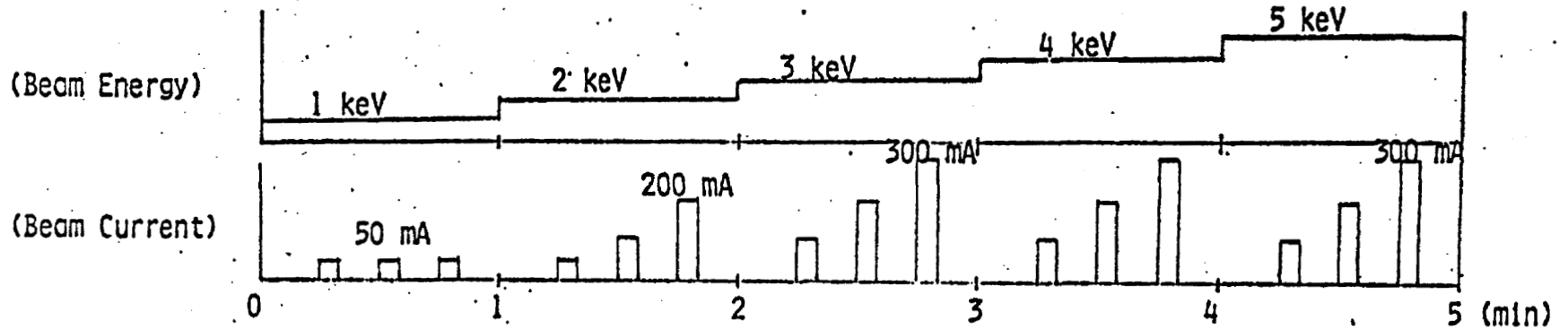
ISO - THIS INSTRUMENT ALSO OBSERVES HIGH POWER EBA FIRINGS (PASSIVE COORDINATION)

ES019 - OBSERVES EBA INDUCED EFFECTS WHEN FIRINGS OCCUR (HARD WIRE LINK BETWEEN EXPERIMENTS)

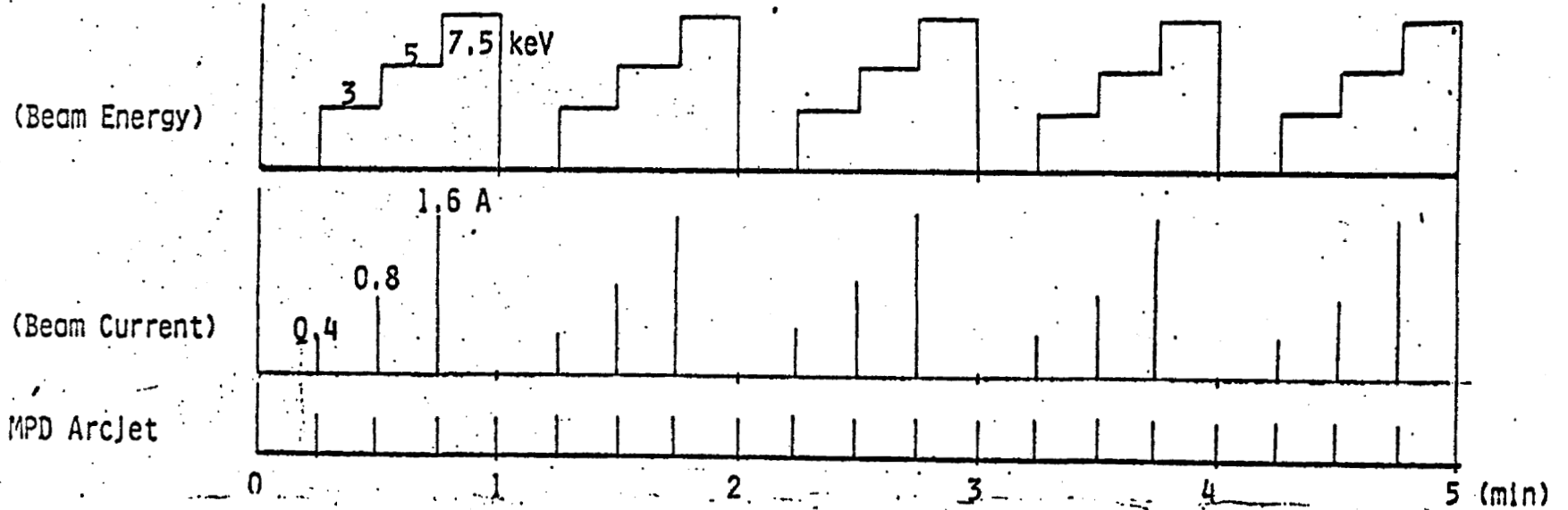
ES020 - SEPAC IS USED IN A DIAGNOSTIC MODE TO OBSERVE E-BEAM FIRINGS BY ES020

Typical Experiments

1) Low Power Electron Beam Experiment (F0-5)



11) High Power Electron Beam Experiment (F0-9 (A-5a))



Operation (Functional Objectives)

F.O.-1	T-0	SEPAC System Checkout
2	T-1	EBA Firing Test (Level I)
3	T-2	MPD Firing Test
4	T-3	EBA Firing Test (Level II)
5	A-1	Electron Beam Experiment 1 (Low Power (1 - 5 keV), CW and Pulse)
6	A-2	Electron Beam Experiment 2 (Low Power (1 - 5 keV), EBA/NGP)
7	A-3	Electron Beam Experiment 3 (Low Power (1 - 5 keV), EBA/MPD)
8	A-4	Plasma Beam Propagation
9	A-5	Artificial Aurora Excitation (High Power (3-7.5 keV) 0.5 sec ON 1.5 sec OFF 3 pulses in series Every 15 sec, EBA/MPD/NGP)
10	A-6	Equatorial Aerochemistry
11	A-7	Electron Echo Experiment (High Power (7.5 keV, 1.6 A) 0.5 sec ON/ Every 15 sec, EBA/MPD)
12	A-8	E// B Experiment (High Power (1 - 7 keV, 0.08 - 1.0 A) 100 msec/Every 1 sec)
13	P-1	Passive Experiment
14	P-2	Passive Experiment (IES020 Support)
15	CFR	SEPAC System Deactivation
16	CHG	Battery Charging

S E P A C Characteristics

Electron Beam Accelerator (EBA)

Beam Energy : 0 - 7.5 keV
Beam Current: 0 - 1.6 A
Pulse Width : 1 msec - 1 sec (High Power)
1 msec - CW (Low Power)

Magneto - Plasma - Dynamic Arcjet (MPD)

Energy Stored 2 kJ
Discharge Pulse Width 1 msec
No. of Ion / electron pairs / shot 10^{19} /shot
Repetition 15 sec
Gas Argon

Neutral Gas Plume Generator (NGP)

Gas Nitrogen

SECTION VIII. THEORETICAL AND EXPERIMENTAL STUDY
OF BEAM PLASMA PHYSICS (TEBPP)

TEBPP

THEORETICAL AND EXPERIMENTAL STUDY OF BEAM-PLASMA-PHYSICS

INVESTIGATORS

HUGH R. ANDERSON, P.I. - RICE UNIVERSITY

WILLIAM BERNSTEIN - RICE UNIVERSITY

LEWIS M. LINSON - SCIENCE APPLICATIONS, INC.

K. PAPADOPOULOS - SCIENCE APPLICATIONS, INC.

PAUL J. KELLOGG - UNIVERSITY OF MINNESOTA

EDWARD P. SZUSZCZEWICZ - NAVAL RESEARCH LABORATORY

THOMAS J. HALLINAN - UNIVERSITY OF ALASKA

HAROLD LEINBACH - NATIONAL OCEANIC AND ATMOSPHERIC ADMINISTRATION
ENVIRONMENTAL RESEARCH LABORATORIES

COLLABORATION WITH:

A. KONRADI - JSC

R. J. JOST - JSC

MSFC TECHNICAL CONTACT:

DRAYTON TALLEY

TEBPP

SCIENTIFIC OBJECTIVE -- TO UNDERSTAND QUANTITATIVELY THE INTERACTION OF AN ELECTRON BEAM (0-10 KEV, 0-1.5 AMP) WITH THE PLASMA AND NEUTRAL ATMOSPHERE AT 200-400 KM ALTITUDE.

APPLICATIONS TO NEAR-EARTH AND COSMICAL PLASMAS.

THE INTERACTION OCCURS IN FOUR SPACE-TIME REGIONS:

- I. NEAR ELECTRON GUN; BEAM COMING INTO EQUILIBRIUM WITH MEDIUM
- II. EQUILIBRIUM PROPAGATION IN IONOSPHERE
- III. AHEAD OF BEAM PULSE; TEMPORAL AND SPATIAL PRECURSORS
- IV. BEHIND A BEAM PULSE

WHILE REGION II IS OF THE GREATEST INTEREST, IT IS ESSENTIAL TO STUDY REGION I BECAUSE IT DETERMINES THE CHARACTERISTICS OF THE BEAM AS IT ENTERS II-IV.

TEBPP

SPECIFICALLY IN THE REGIONS

REGION I - WHAT ARE MECHANISMS FOR CHARGE AND CURRENT NEUTRALIZATION
- OF INJECTED BEAM?
- OF ACCELERATOR AND SPACECRAFT?
- IS BEAM PLASMA DISCHARGE (BPD) AN IMPORTANT MECHANISM?
WHAT ARE DIMENSIONS OF THE REGION?
HOW IS BEAM HEATED BY BPD AND ALTERED BY CHARGING?

REGION II - QUANTITATIVELY WHAT IS
VELOCITY REDISTRIBUTION OF BEAM PARTICLES? PLATEAU?
ALTERATION OF AMBIENT PLASMA DENSITY AND TEMPERATURE?
PRODUCTION OF E-S AND E-M WAVES?
PRODUCTION OF LIGHT?

REGIONS III AND IV - WHAT ARE CHARACTERISTIC TIMES FOR THE ABOVE EFFECTS?

ARE THE REGIONS A GOOD ORDERING OF THE PHENOMENA?

TEBPP

IMPLEMENTATION

THEORETICAL STUDIES

ANALYTICAL AND NUMERICAL SIMULATION OF PHENOMENA SHOULD PROVIDE
MODELS THAT PREDICT QUANTITATIVELY
DESIGN PARAMETERS FOR EXPERIMENTS

INTERPRETATION OF DATA

EXPERIMENTS -- MEASUREMENTS

ROCKET-BORNE

SCEX -- CARRYING ON ELECTRON GUN; KELLOGG IS P.I. 1980-1981
PASSIVE AURORAL PLASMA; ANDERSON IS P.I. 1980-1982
E # B, NRC; BERNSTEIN AND WHALEN 1978; 1979

LABORATORY

LARGE VACUUM FACILITY AT JSC--BERNSTEIN AND ENTIRE GROUP.
THESE ARE ONGOING EXPERIMENTS.

IMPLEMENTATION -- CONTINUED

EXPERIMENTS USING SPACELAB

MISSION MUST CARRY

ELECTRON ACCELERATOR

} SEPAC

NEUTRAL GAS SOURCE

IMAGER

LLLTV

WE BUILD THESE DIAGNOSTICS

PULSED PLASMA PROBE -- SZUSZCZEWICZ

$$3 \times 10^2 < N_E < 10^8 \text{ cm}^{-3}$$

$$.025 < T_E < 3 \text{ eV}$$

PLASMA POTENTIAL, -50 TO +150 VOLTS

PLASMA WAVE RECEIVER (\underline{E} AND \underline{B}) -- KELLOGG

$$10 \text{ Hz} < F < 20 \text{ MHz}$$

CHARGED PARTICLE SPECTROMETER -- ANDERSON

$$10 \text{ eV} < E < 20 \text{ keV}$$

$$\Delta E/E \sim 5\%$$

$$\text{FLUX } 10^6 \text{ TO } 10^{13}$$

PHOTOMETER IF NOT OTHERWISE AVAILABLE.

THESE ARE TO BE MOUNTED ON THE RMS OR A FREE-FLYER TO SCAN ALONG AND
RADIALLY FROM THE BEAM.

WE WILL ALSO CONSIDER OPTICAL AND E-M WAVE MEASUREMENTS FROM SELECTED
GROUND SITES.

TEBPP

ELECTRON BEAM

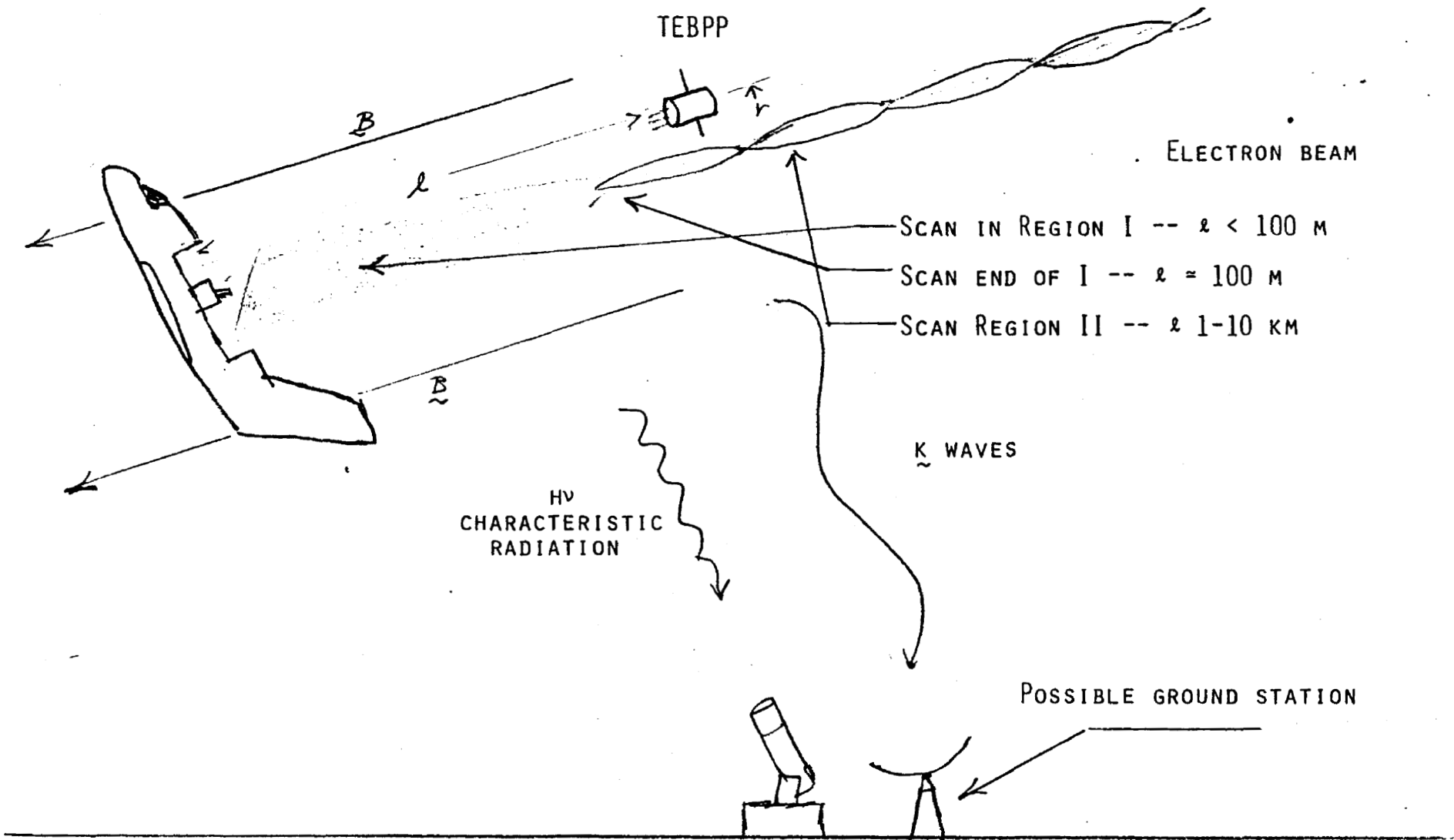
- SCAN IN REGION I -- $\ell < 100$ M
- SCAN END OF I -- $\ell = 100$ M
- SCAN REGION II -- ℓ 1-10 KM

H ν
CHARACTERISTIC
RADIATION

K \sim WAVES

POSSIBLE GROUND STATION

124



RICE UNIVERSITY

23-24 SEPT. 1980

TEBPP

CLOSELY RELATED EXPERIMENTS AND FACILITIES

SEPAC

LLLTV

ALL FREE FLYERS

MMP

PDP

STSS

WISP

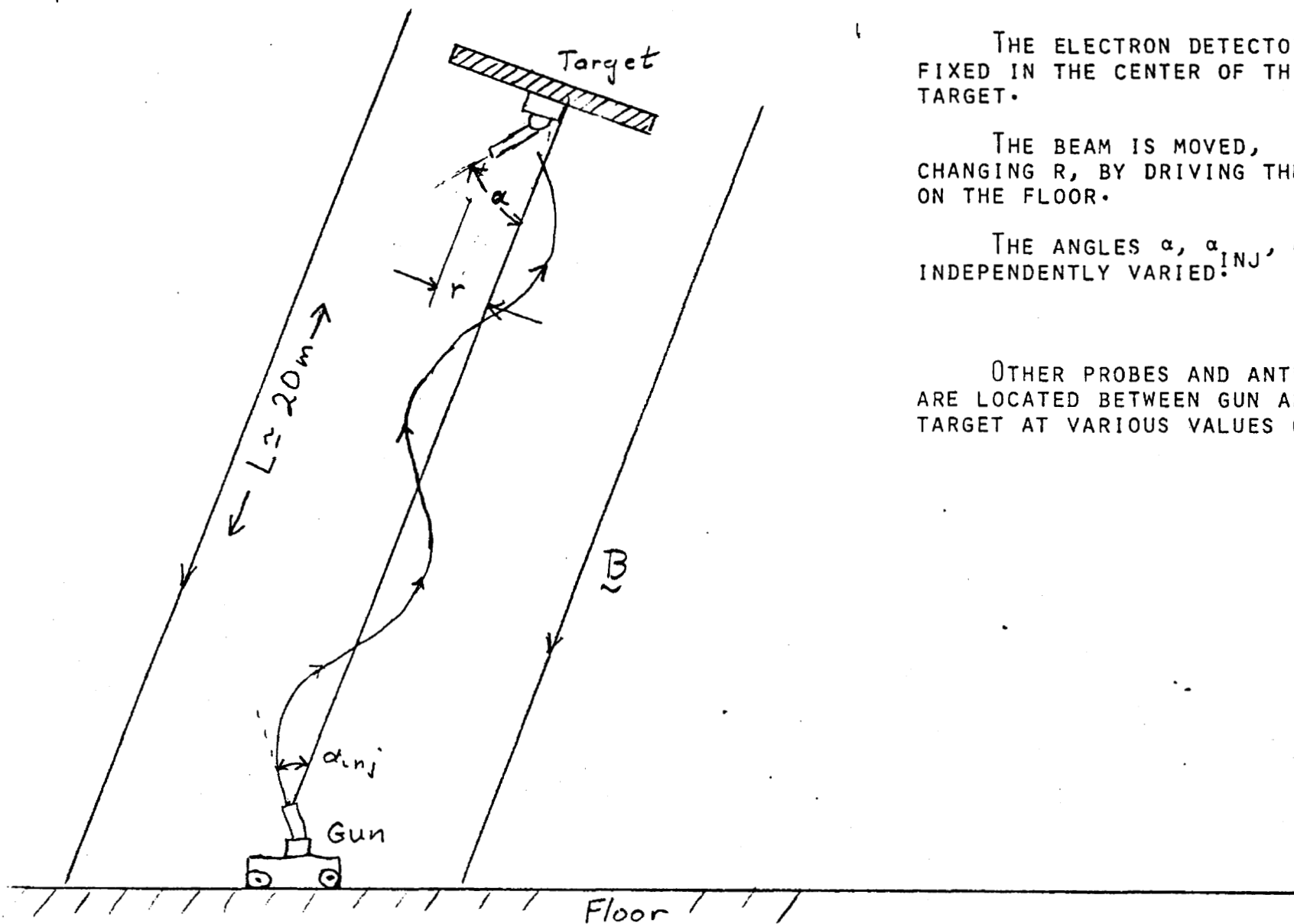
TEBPP
 GEOMETRY OF LAB EXPERIMENTS

THE ELECTRON DETECTOR IS
 FIXED IN THE CENTER OF THE
 TARGET.

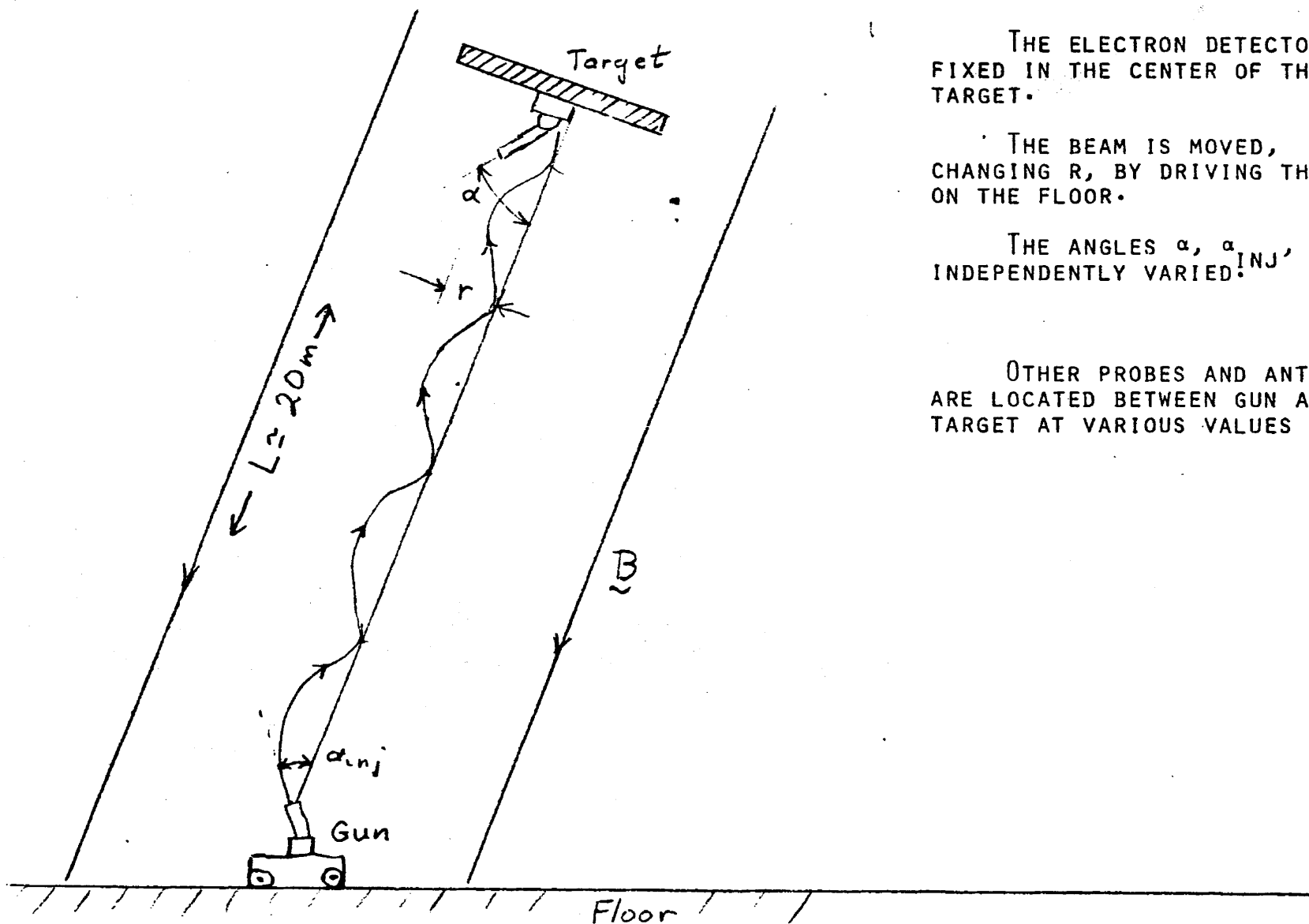
THE BEAM IS MOVED,
 CHANGING R , BY DRIVING THE CART
 ON THE FLOOR.

THE ANGLES α , α_{inj} , CAN BE
 INDEPENDENTLY VARIED.

OTHER PROBES AND ANTENNAS
 ARE LOCATED BETWEEN GUN AND
 TARGET AT VARIOUS VALUES OF R .



TEBPP
 GEOMETRY OF LAB EXPERIMENTS



THE ELECTRON DETECTOR IS FIXED IN THE CENTER OF THE TARGET.

THE BEAM IS MOVED, CHANGING r , BY DRIVING THE CART ON THE FLOOR.

THE ANGLES α , α_{inj} , CAN BE INDEPENDENTLY VARIED.

OTHER PROBES AND ANTENNAS ARE LOCATED BETWEEN GUN AND TARGET AT VARIOUS VALUES OF r .

TEBPP



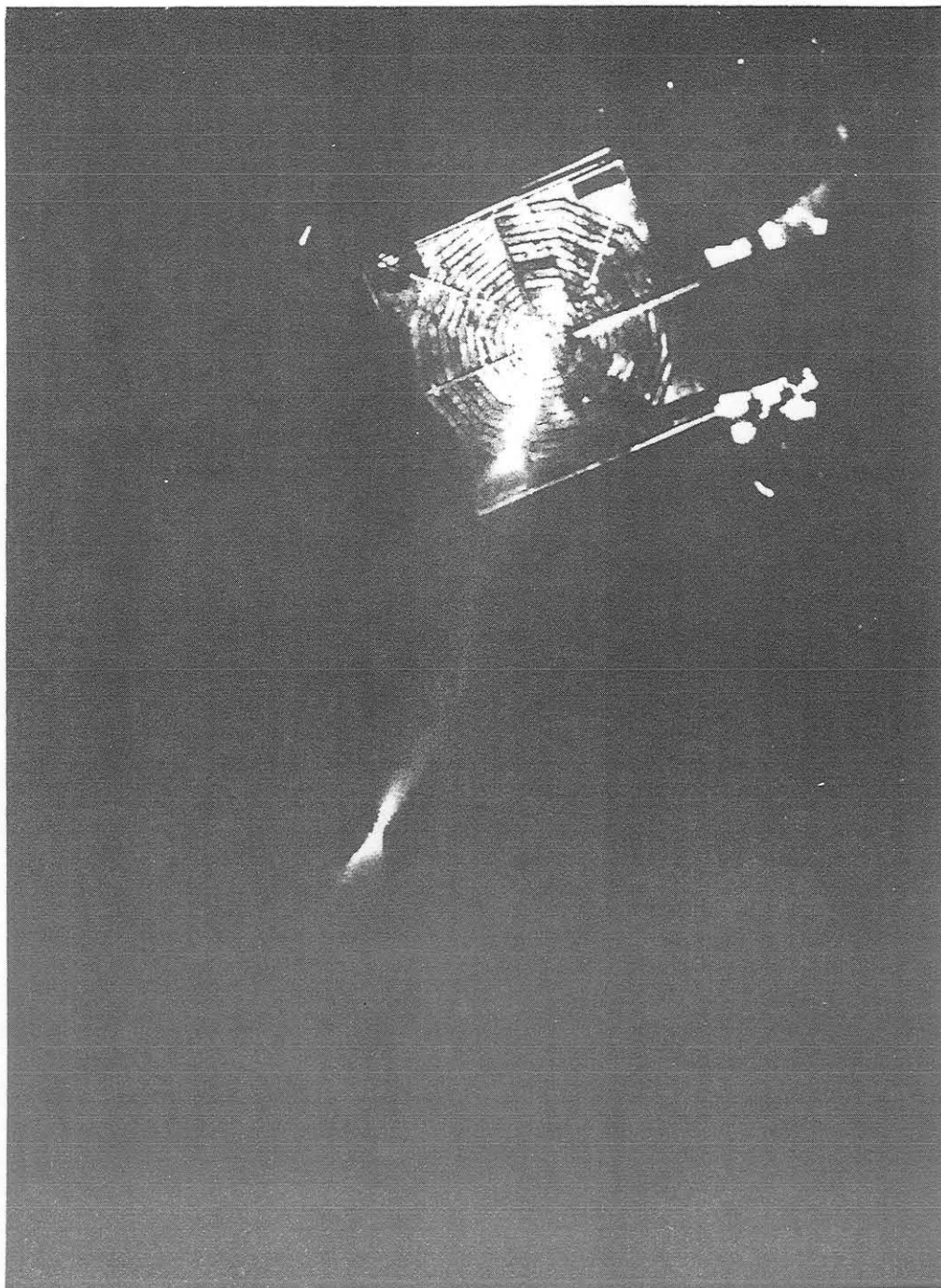
$$P = 7 \times 10^{-6} \text{ TORR}$$

$$B = 1.2 \text{ G}$$

$$V_G = 2000 \text{ VOLTS}$$

$$I = 25 \text{ MA}$$

OBLIQUE INJECTION, $\alpha_{\text{INJ}} = 130^\circ$



TEBPP

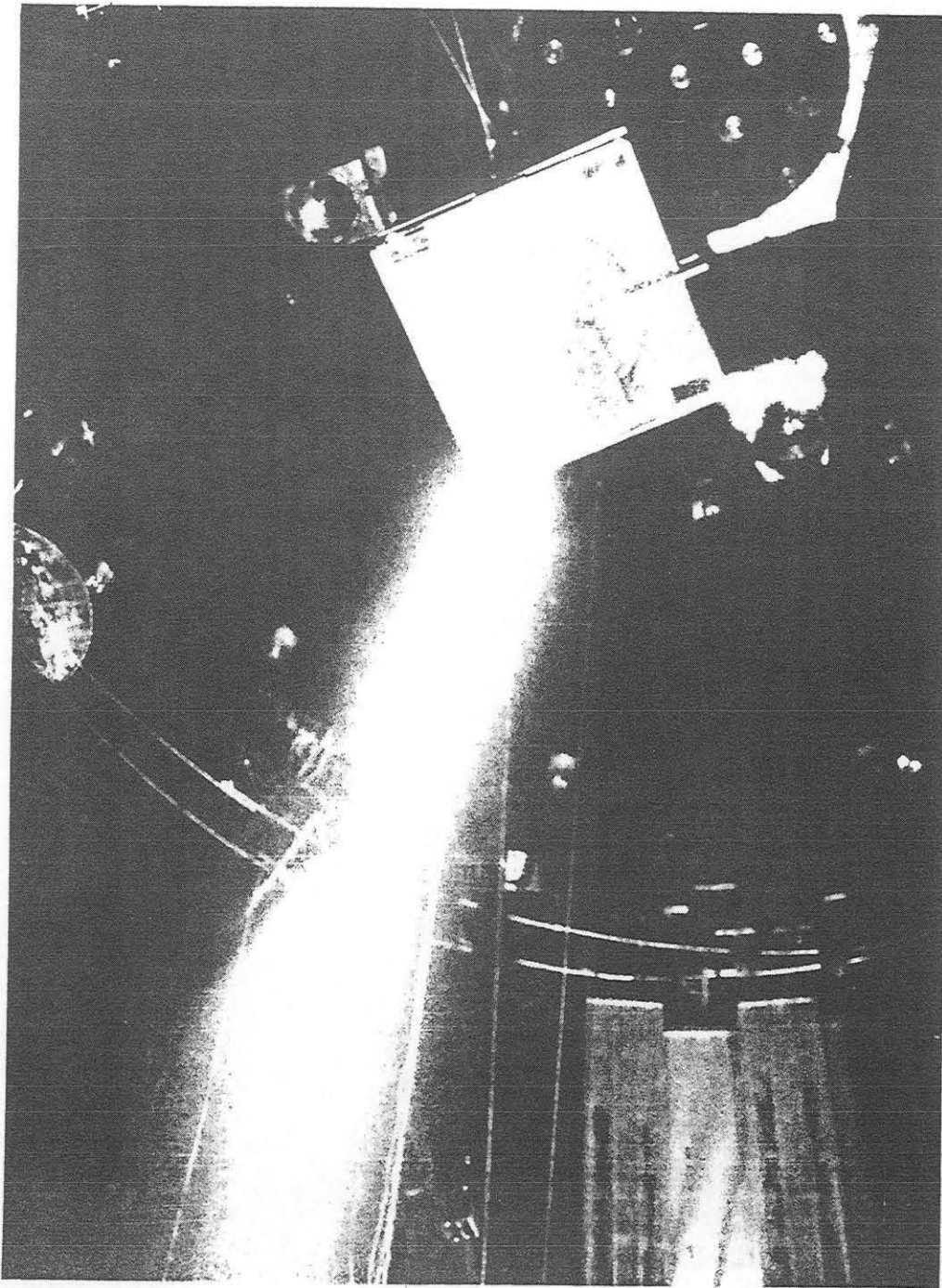
$$P = 7 \times 10^{-6} \text{ TORR}$$

$$B = 1.2 \text{ G}$$

$$V_G = 2000 \text{ VOLTS}$$

$$I = 8 \text{ MA}$$

$$\text{PARALLEL INJECTION, } \alpha_{\text{INJ}} = 180^\circ$$



TEBPP

$$P = 7 \times 10^{-6} \text{ TORR}$$

$$B = 1.2 \text{ G}$$

$$V_G = 2000 \text{ VOLTS}$$

$$I = 40 \text{ MA}$$

$$\text{PARALLEL INJECTION, } \alpha_{\text{INJ}} = 180^\circ$$



TEBPP

$$P = 7 \times 10^{-6} \text{ TORR}$$

$$B = 1.2 \text{ G}$$

$$V_G = 2000 \text{ VOLTS}$$

$$I = 70 \text{ MA}$$

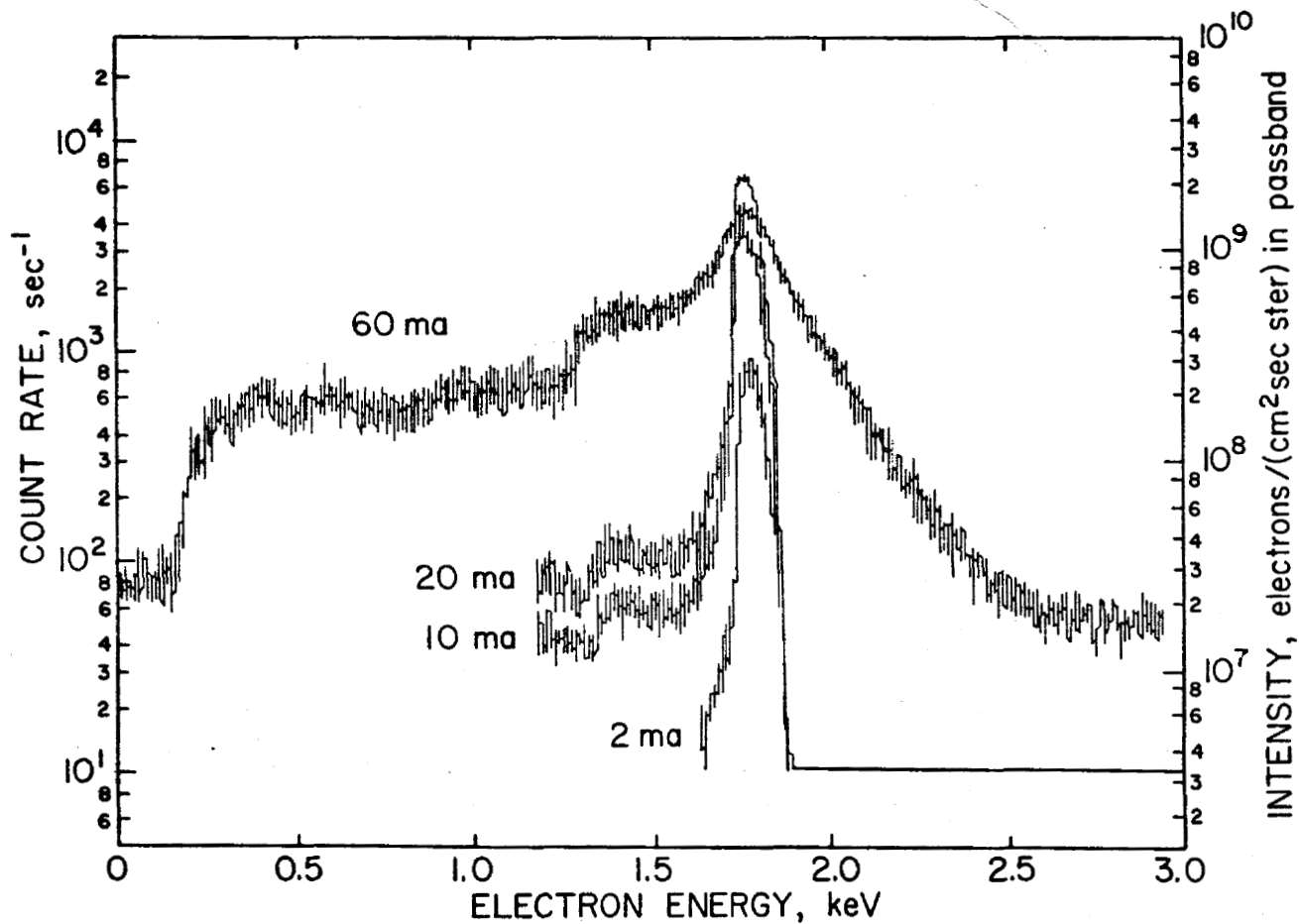
$$\text{PARALLEL INJECTION, } \alpha_{\text{INJ}} = 180^\circ$$

FULL BPD

TEBPP

$P = 3 \times 10^{-6}$ TORR
 $B = 1.2$ G
 $V_G = 1850$ VOLTS
 I AS GIVEN, BPD AT 80 MA
 $\alpha = 125^\circ$ (MAXIMUM FLUX)
 $\alpha_{INJ} = 180^\circ$
 $R = 2.0$ M

132



23-24 SEPT. 1980

TEBPP

$P = 7 \times 10^{-6}$ TORR

$B = 1.2$ G

$V_G = 2100$ VOLTS

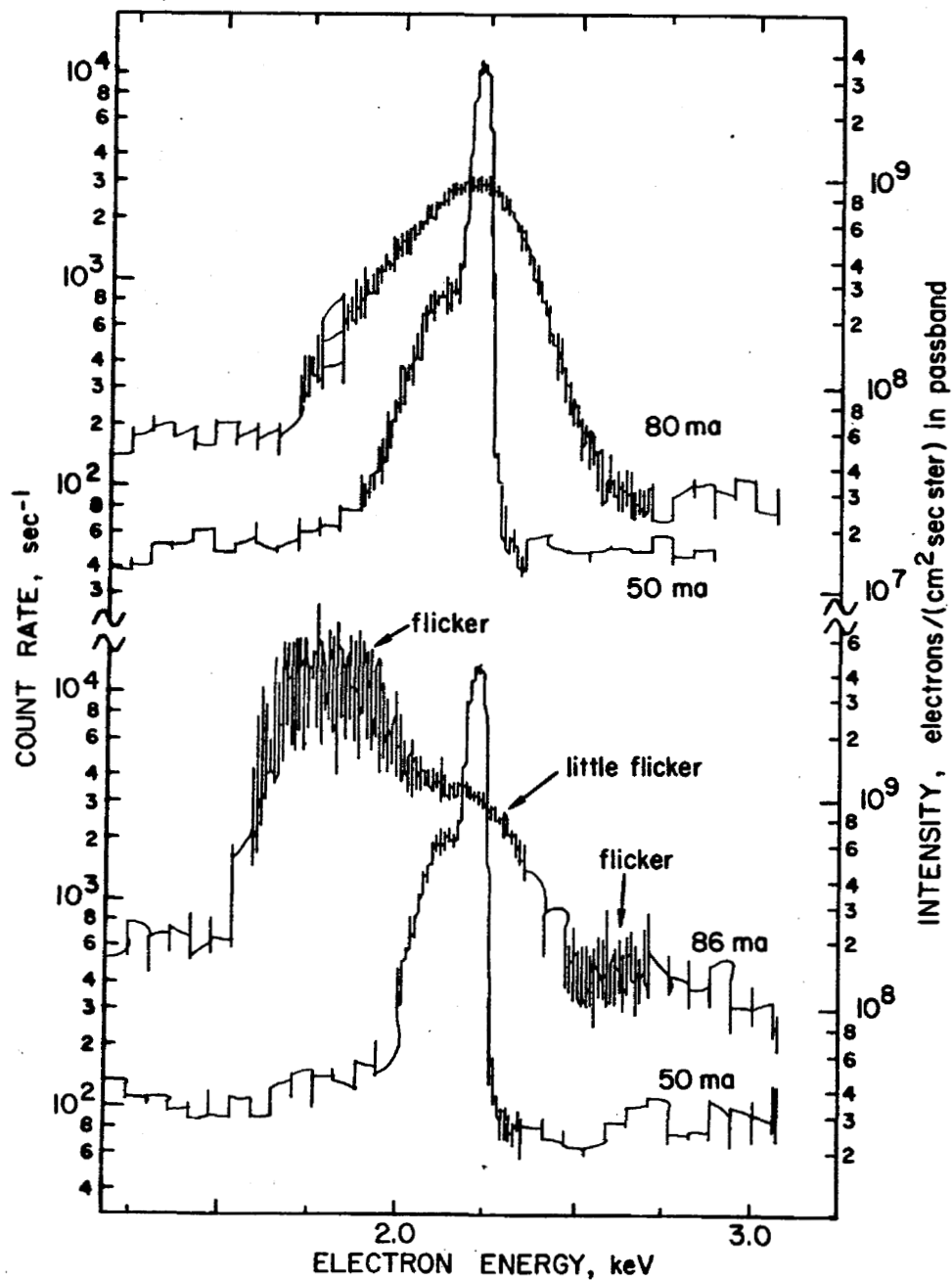
I AS GIVEN, BPD AT HIGHER I .

$\alpha = 180^\circ$

$\alpha_{INJ} = 180^\circ$

$R = 0.9$ M

131



TEBPP

COMMENTS ON PARTICLE MEASUREMENTS

DEPENDING ON ENERGY, FLUX = E^{-R/R_0} WITH $R_0 \sim .4$ M.

WE PRESENTLY HAVE NO DATA AT ENERGIES BETWEEN ~ 10 EV (IONIZATION POTENTIAL) AND ~ 200 EV.

ENERGIES BETWEEN 200 EV AND V_{GUN} ARE RELATIVELY MORE POPULATED IN BPD FOR LARGE R AND $\alpha < 180^\circ$.

A PARTICLE DETECTOR MOUNTED ALONGSIDE THE GUN LOOKING AT $\alpha = 0^\circ$ SAW ONLY A FEATURELESS ENERGY SPECTRUM. CLEAR EVIDENCE OF BPD IS NOT SEEN IN THESE SPECTRA

PRELIMINARY MEASUREMENTS INDICATE THAT THE BPD MAY REQUIRE SEVERAL MSEC TO DEVELOP, DEPENDING ON THE RATIO I/I_C , AND N_E .

TEBPP

GRADIENTS OBSERVED IN VARIOUS PARAMETERS

PARAMETER	E-FOLDING DISTANCE \perp TO BEAM	E-FOLDING DISTANCE \parallel TO BEAM
PLASMA DENSITY	2.0 M	
PLASMA TEMP.	2.5 M	
ENERGETIC PARTICLE FLUX	.43 TO .14 M	
ELECTRIC FIELD STRENGTH		

TEBPP

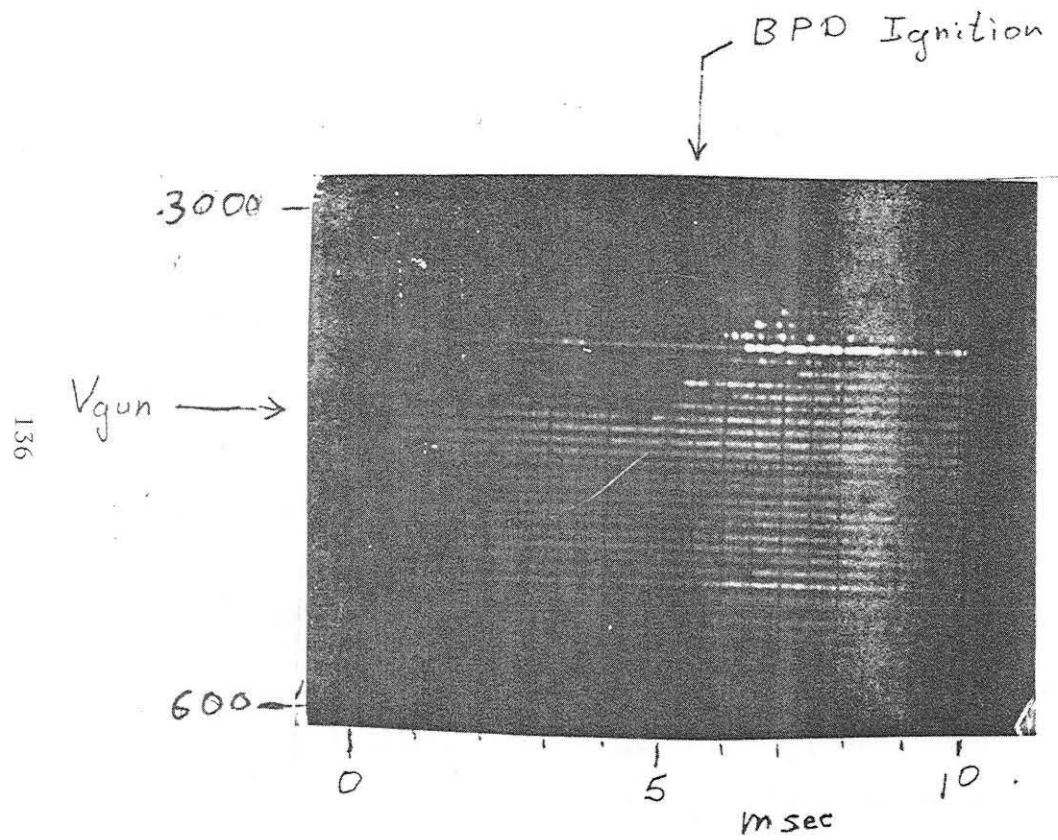
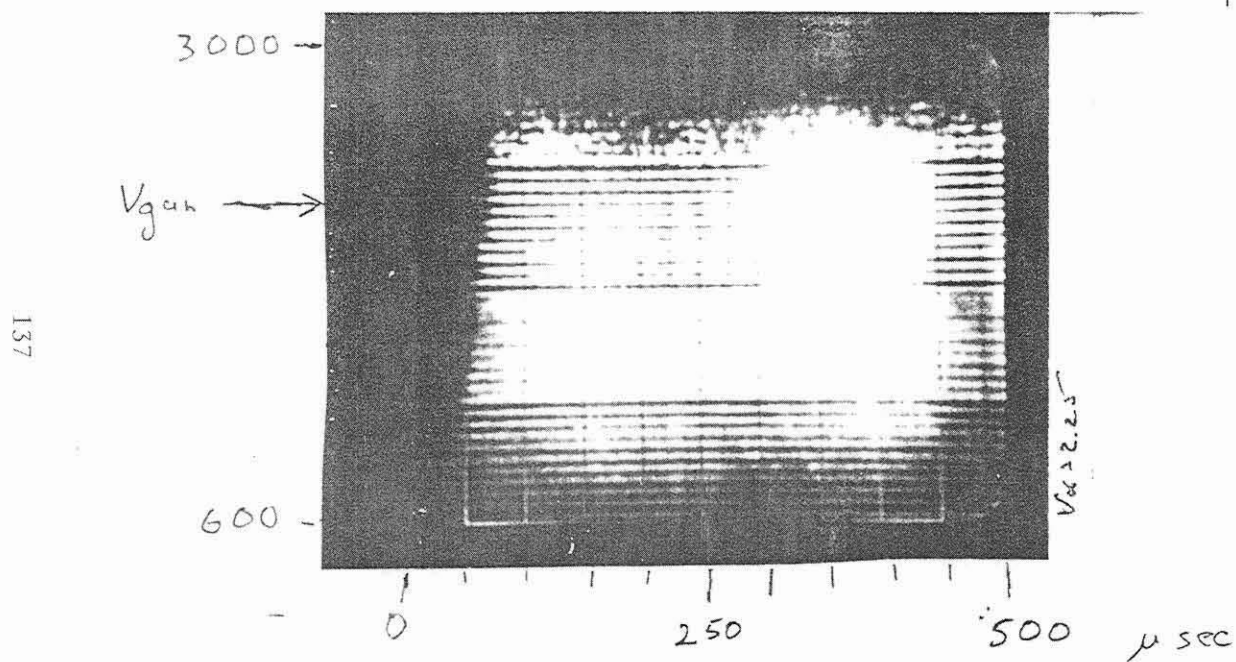


FIGURE 1. BPD IGNITION
OCCURS ~ 5 MS AFTER
INITIATION OF PULSE.
PULSE WIDTH = 30 MS.
INTERPULSE PERIOD = 400 MS

TEBPP

FIGURE 2. BPD IGNITION OCCURS.



SECTION IX. WAVES IN SPACE PLASMAS (WISP)

WAVES IN SPACE PLASMAS (WISP)

PRESENTATION TO

**SPACE PLASMA PHYSICS ACTIVE
EXPERIMENTS WORKING GROUP**

NASA/MSFC 23 SEPT 1980

R.W. FREDRICKS WISP P.I.

VLF WAVE INJECTION EXPERIMENTS

- VLF WAVE-PARTICLE INTERACTIONS
- VLF PROPAGATION

TRAVELING IONOSPHERIC DISTURBANCES AND ATMOSPHERIC GRAVITY WAVES

- HF, VHF REMOTE SOUNDING

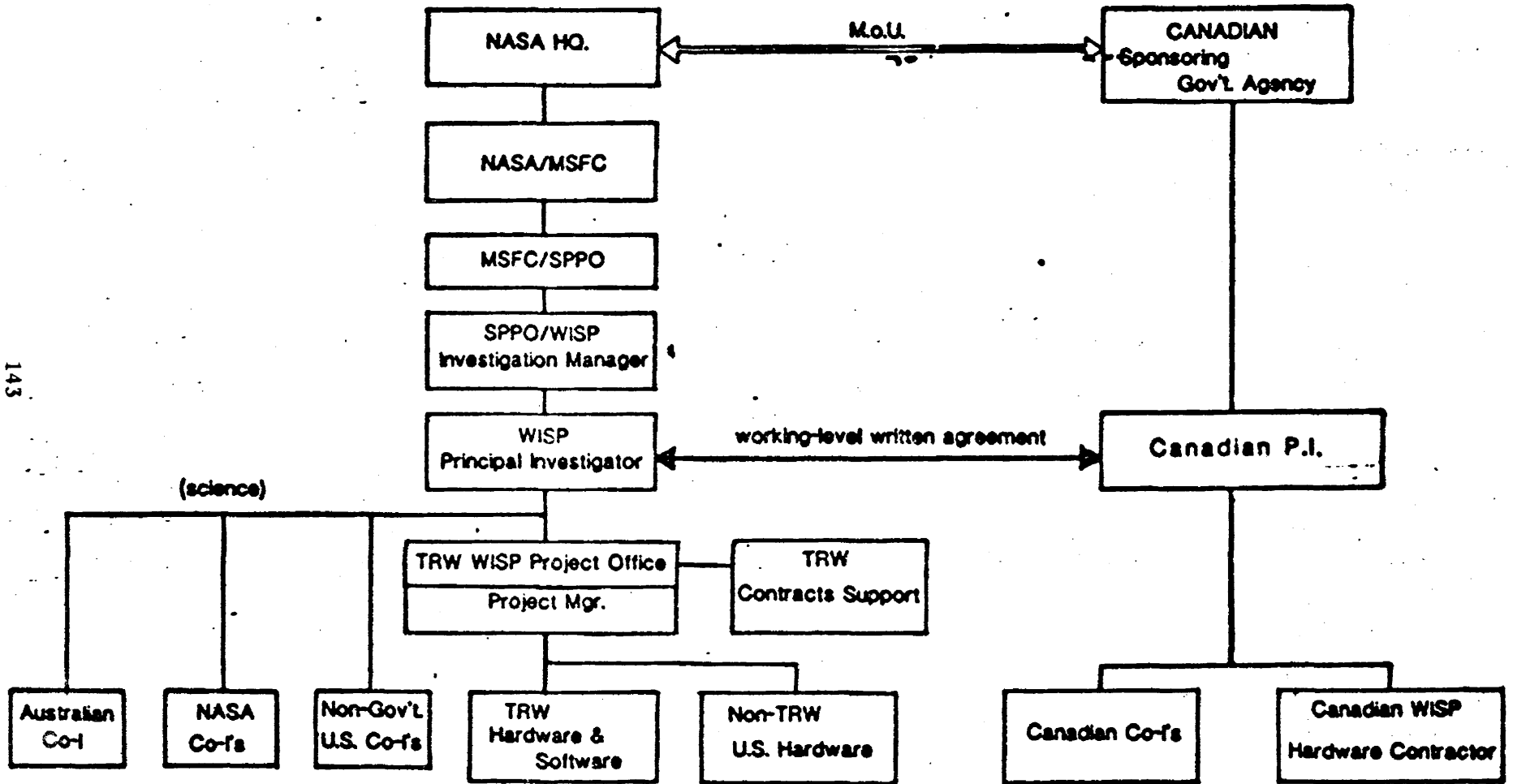
IONOSPHERIC BUBBLES

- HF, VHF REMOTE SOUNDING AND PROPAGATION

PLASMA WAVE PHYSICS

- LINEAR AND NON-LINEAR PLASMA PHYSICS IN SPACE
- ANTENNA-PLASMA INTERACTION STUDIES

WISP INVESTIGATION ORGANIZATION



TRW

- Taylor (RPDP Co-1)
- plasma wave physics and wave/particle interactions

STANFORD - Helliwell and Katsufakis

- VLF/ELF wave propagation and wave/particle interactions

U of IOWA - Shawhan (RPDP P.I.)

- plasma wave physics and wave/particle interactions

NASA/MSFC - Reasoner (RPDP Co-1)

- plasma diagnostics & wave/particle interactions

PINY - Gross

- Traveling ionospheric disturbances and gravity waves

NASA/GSFC - Benson

- Equatorial bubbles and plasma wave physics

SAO - Grossi

- HF & VHF wave propagation and traveling ionospheric disturbances

NASA/JSC - Garriott

- antenna impedance and wave/particle interactions

LaTrobe Univ. (Australia) - Dyson

- equatorial bubbles and simultaneous ground-based measurements

Lockheed - Calvert

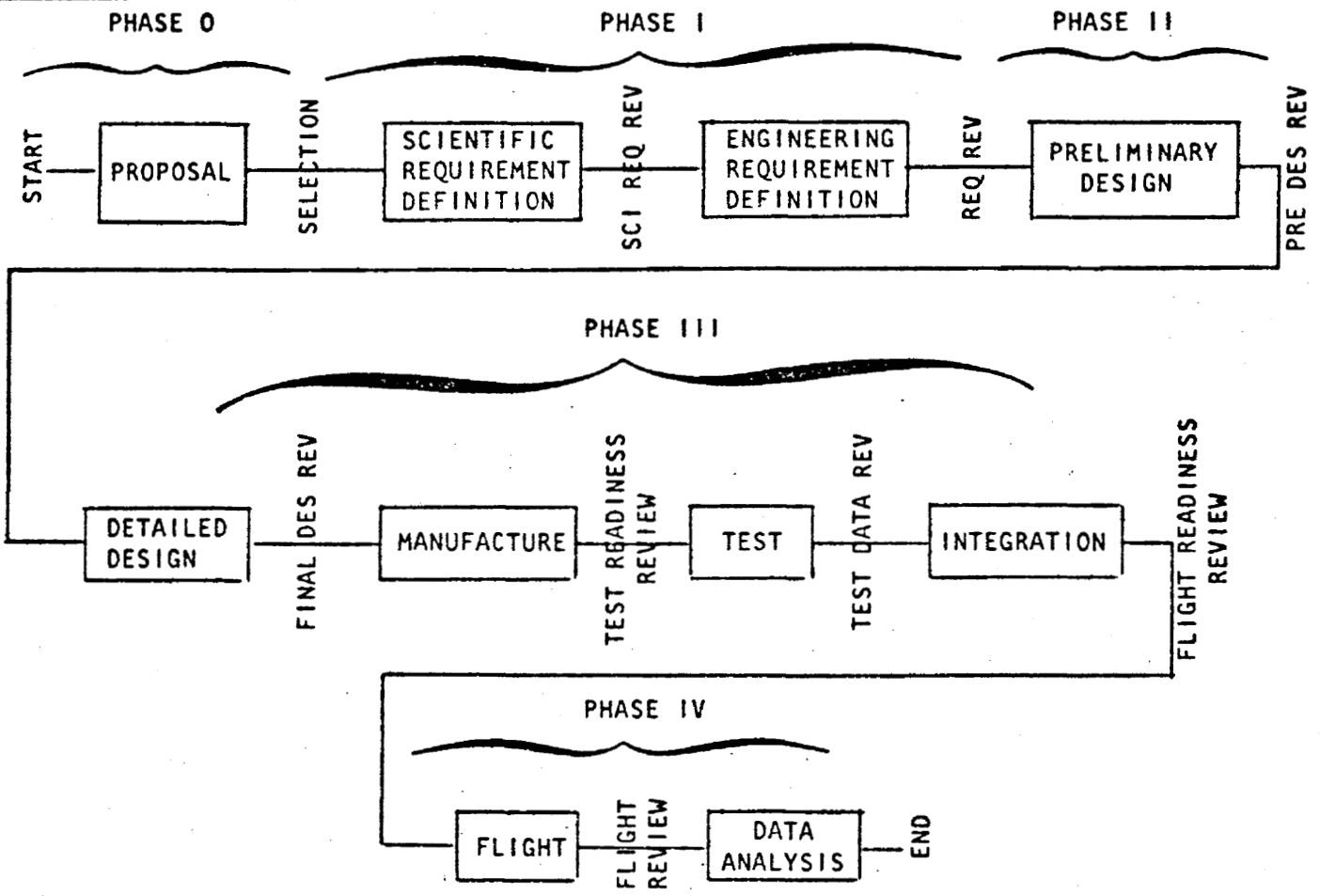
- plasma wave physics in HF regime
- CORE microprocessor definition

SYSTEMS
GROUP
RESEARCH
STAFF

W I S P

WISP PROJECT
LIFE CYCLE

TRW
DEFENSE AND SPACE SYSTEMS GROUP



SYSTEMS
GROUP
RESEARCH
STAFF

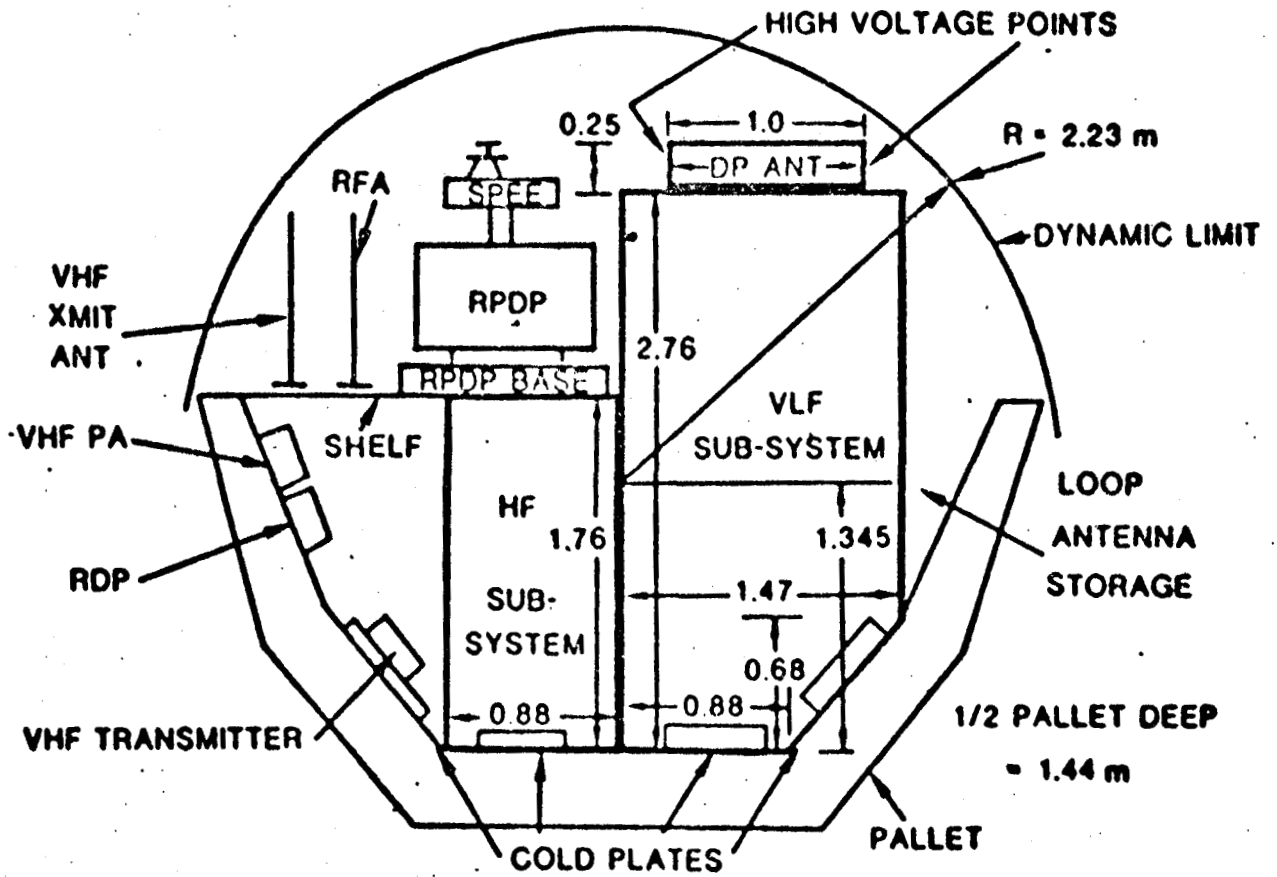
WISP EQUIPMENT
FOR FIRST FLIGHT

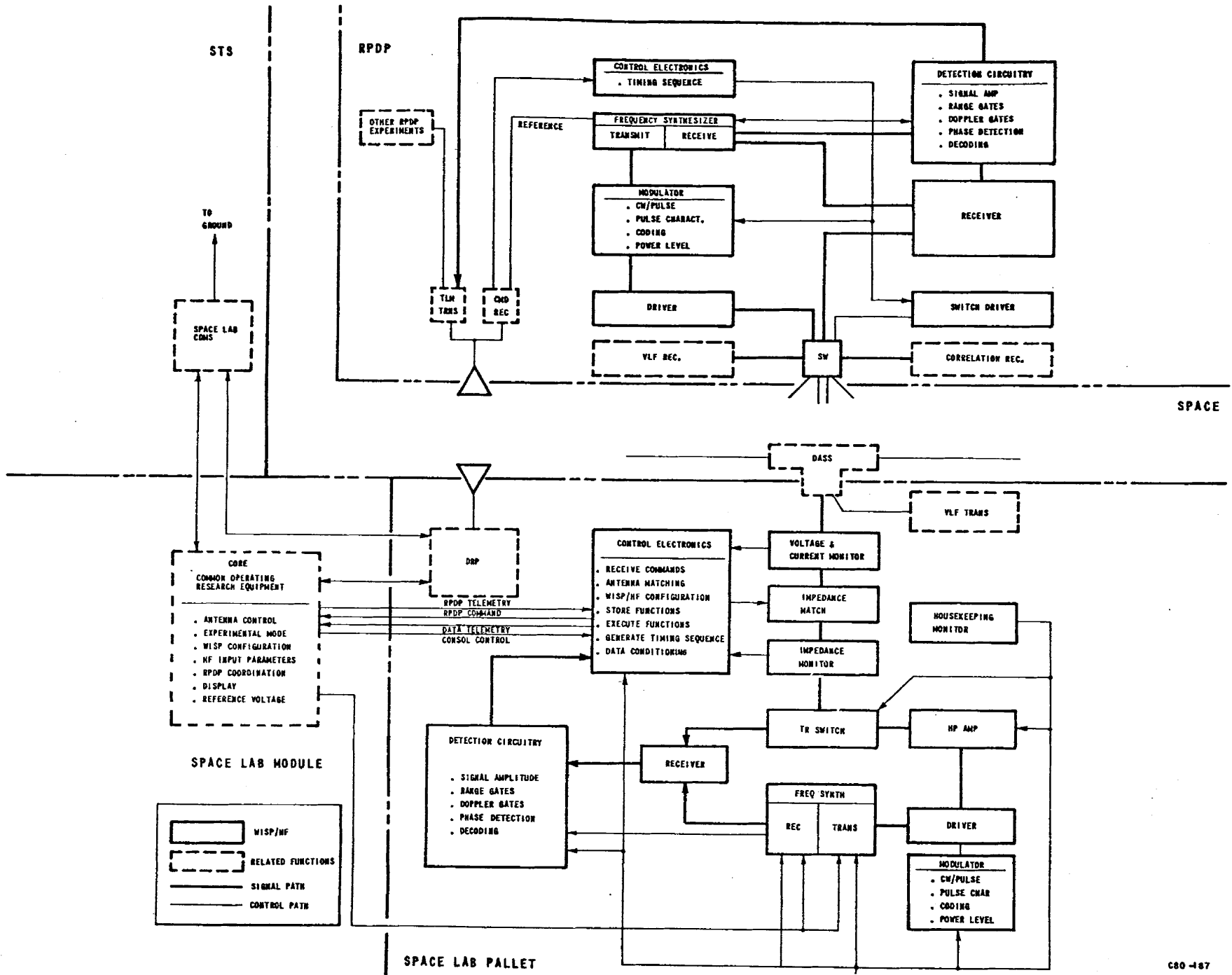


	Flight						
	1	2	3	4	5	6	7
<u>Date (Calendar year)</u>	19 82	83	84	85	85	86	86
<u>Quarter</u>	4	4	3	2	4	2	4
<u>Equipment</u>							
CORE (Common Operating Res'ch Equip.)	X	X	X	X	X	X	X
VLF Transmitter Subsystem	X	X	X			X	X
Extendible Antenna ¹	X	X	X	X	X	X	X
Recoverable Plasma Diagnostics Package (RPDP)	X	X	X	X	X	X	X
Phase 1 RPDP Instrumentation ²	X	X	X			X	X
HF Sounder Receiver	X ³		X ⁴	X ⁴	X ⁴		
HF Sounder Subsystem ⁵		X	X	X	X		
Phase 2 RPDP Instrumentation ⁶		X	X			X	X
Special Display & Analysis Equip. ⁷		X	X	X	X	X	X
Low Light Level TV		X	X			X	X
VHF Sounder Subsystem			X	X	X		
Power Amplifier, 20-40 db gain, 150-350 MHz				X	X		
Loop Transmitting Antenna						X	X
Tether System (conducting tether wire)						X	X

- ¹ 300 m tip-to-tip maximum length dipole pointed in $\pm Y_0$ directions.
- ² Step frequency receiver, electric field antenna, magnetic field antenna (loop), ion retarding potential analyzer, Langmuir probe, ion mass spectrometer.
- ³ On Spacelab.
- ⁴ On RPDP
- ⁵ On Spacelab
- ⁶ Instrumentation added to RPDP: step frequency receiver, correlator, linear receiver, 2 electric field antennas, 2 magnetic field antennas (loop), quadrispherical low energy proton and electron differential energy analyzer.
- ⁷ Spectrum analyzer and oscilloscope with Z modulation and variable persistence.

WISP
NOMINAL SUBSYSTEM SIZES
AS OF DEC 22, 1979





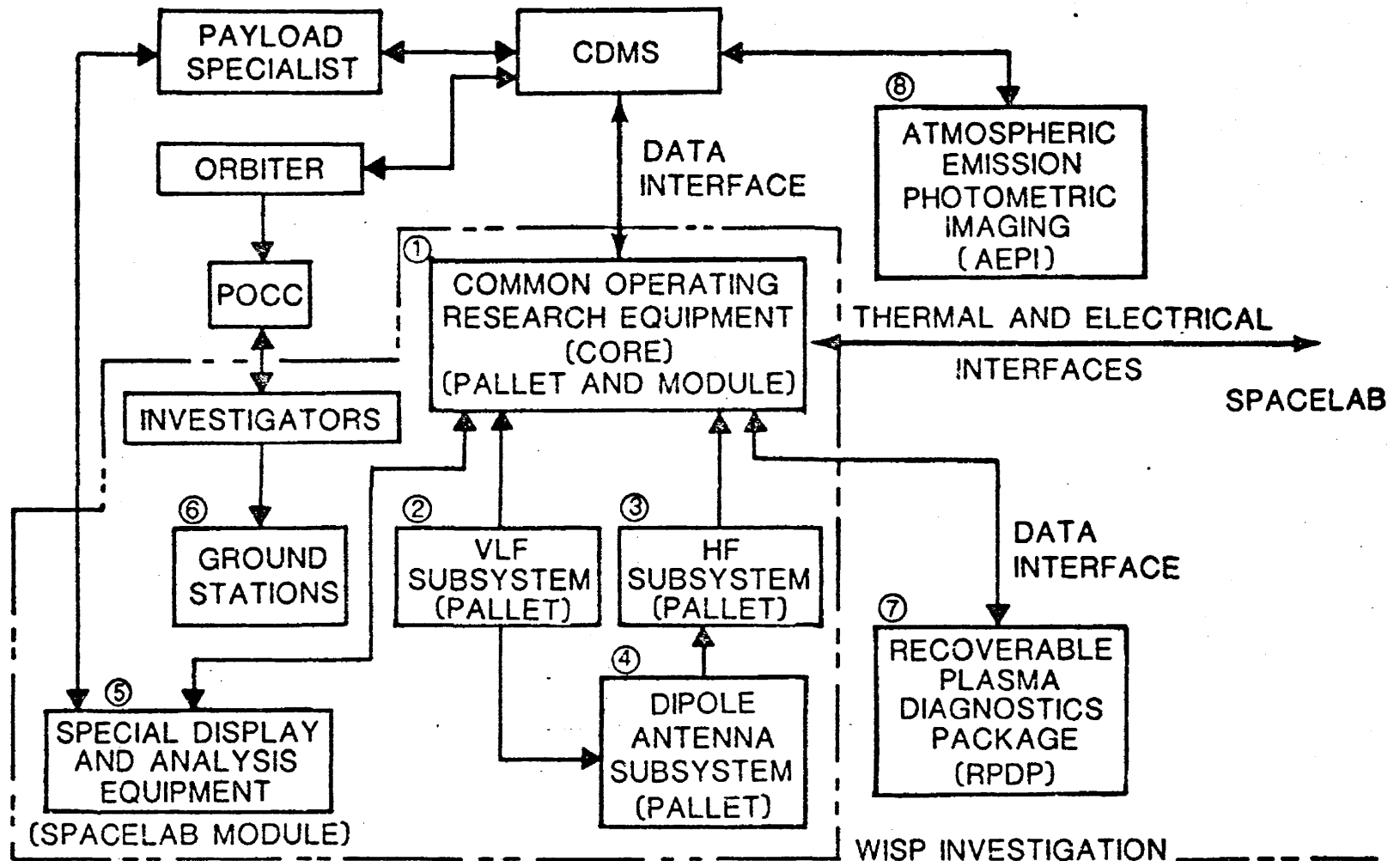
WISP/HF BLOCK DIAGRAM

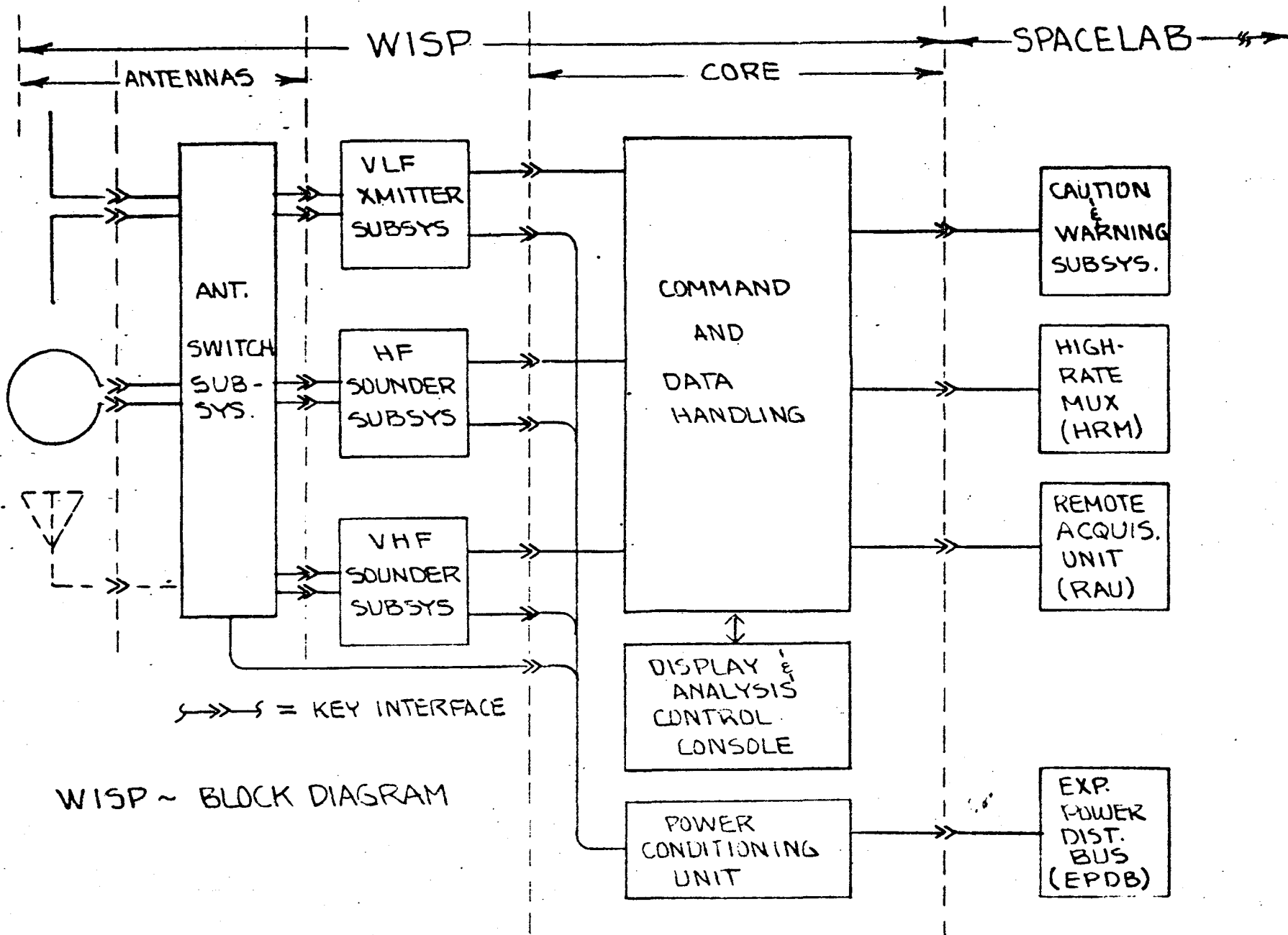
SYSTEMS
GROUP
RESEARCH
STAFF

W I S P

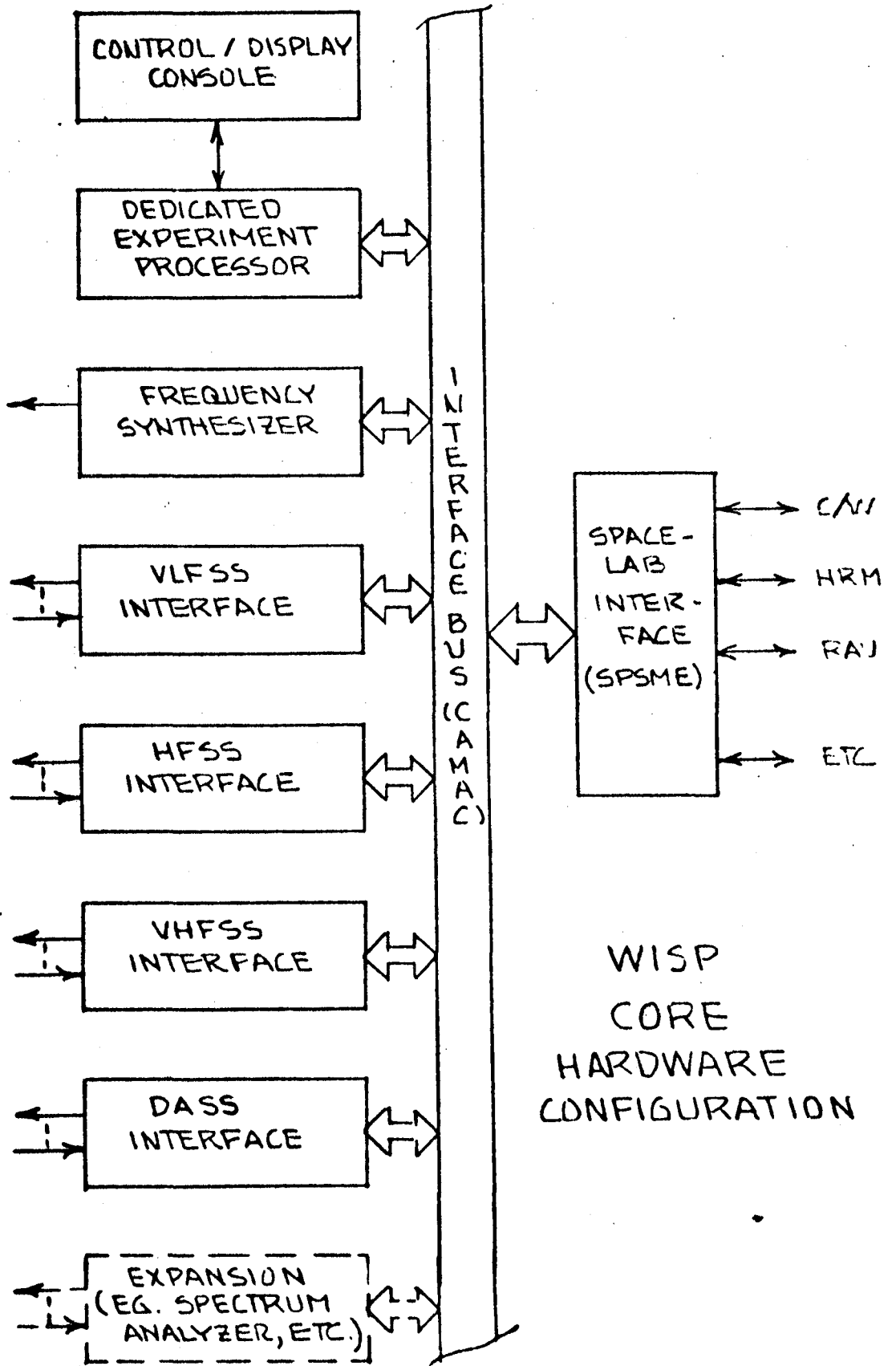
FUNCTIONAL BLOCK DIAGRAM
OF INSTRUMENTATION

TRW
DEFENSE AND SPACE SYSTEMS GROUP





WISP ~ BLOCK DIAGRAM

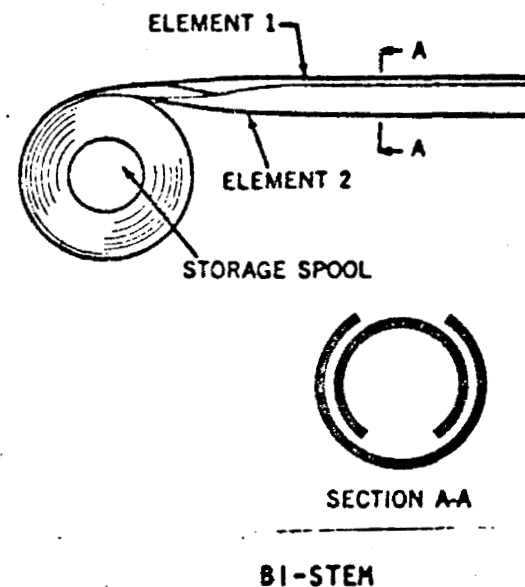


BASIC ANTENNA

- Bi-Stem by Astro
- Nominal length- 300 m tip-to-tip

TRADEOFF STUDY REQUIRED

- Three options identified
 - Bare Bi-Stem from bay
 - Bi-Stem with insulating sleeve from bay
 - Bare Bi-Stem from Astromast
- Analysis Required
 - Dynamics
 - Thermal
 - Electrical
 - Safety
- Decision by end of Phase 1



SYSTEMS
GROUP
RESEARCH
STAFF

W I S P

DIPOLE ANTENNA SUBSYSTEM
DASS

TRW
DEFENSE AND SPACE SYSTEMS GROUP

FUNCTIONS

- MECHANICALLY HOLDS DIPOLE ELEMENTS
- PLACED HIGH IN BAY TO EXTEND ELEMENTS OVER BAY DOORS
- ELECTRICALLY ISOLATE ELEMENTS AND GROUND

PROBLEMS

- CONFIGURATION -- MAST NEEDED?
- RADIATED EMI -- EXEMPTION NEEDED?
- DYNAMICS -- STUDY NEEDED (BY MSFC)?

**SYSTEMS
GROUP
RESEARCH
STAFF**

WISP PRESENTATION TO NASA/MSFC

WISP SCIENCE OBJECTIVES

TRW
DEFENSE AND SPACE SYSTEMS GROUP
11-1-79

VLF WAVE INJECTION EXPERIMENTS

- **VLF WAVE-PARTICLE INTERACTIONS**
- **VLF PROPAGATION**

TRAVELING IONOSPHERIC DISTURBANCES AND ATMOSPHERIC GRAVITY WAVES

- **HF, VHF REMOTE SOUNDING**

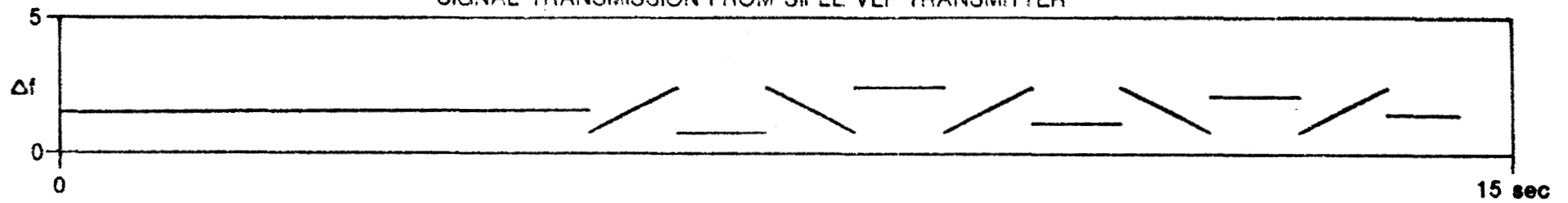
IONOSPHERIC BUBBLES

- **HF, VHF REMOTE SOUNDING AND PROPAGATION**

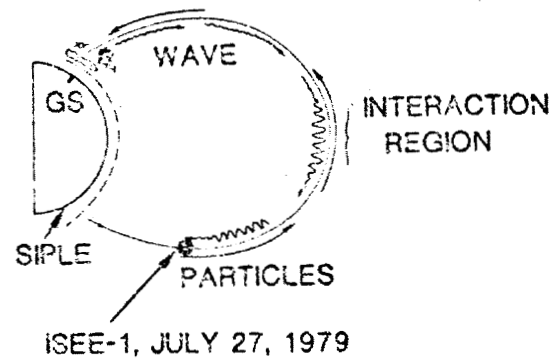
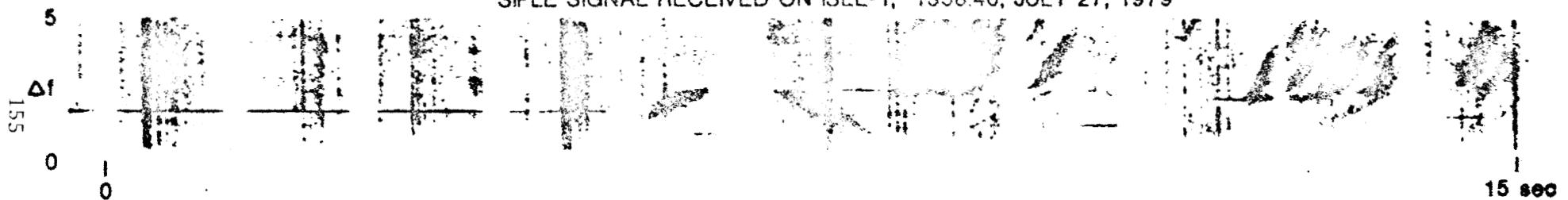
PLASMA WAVE PHYSICS

- **LINEAR AND NON-LINEAR PLASMA PHYSICS IN SPACE**
- **ANTENNA-PLASMA INTERACTION STUDIES**

SIGNAL TRANSMISSION FROM SIPLE VLF TRANSMITTER

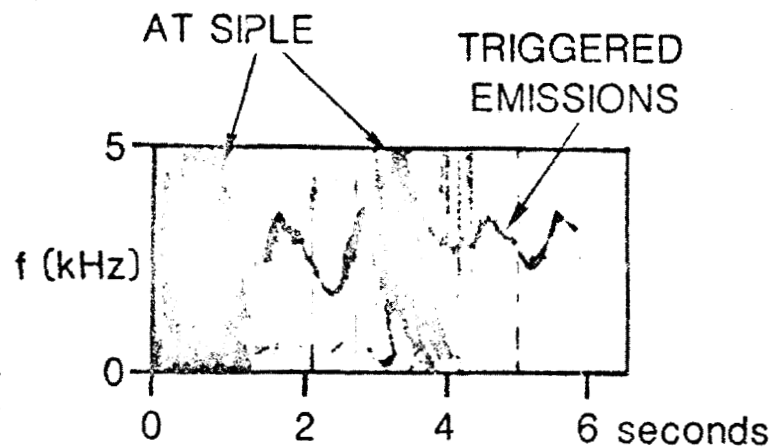


SIPLE SIGNAL RECEIVED ON ISEE-1, 1338:40, JULY 27, 1979

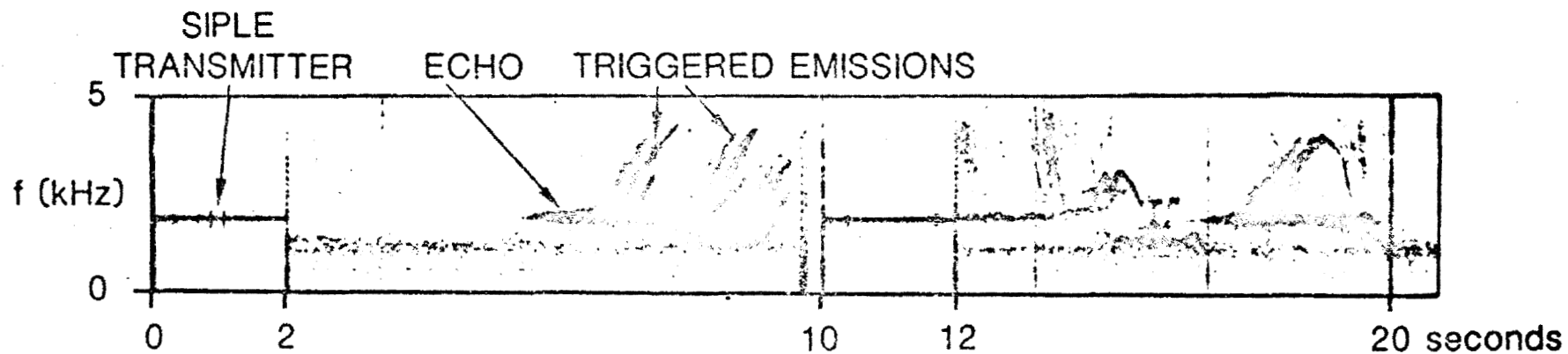
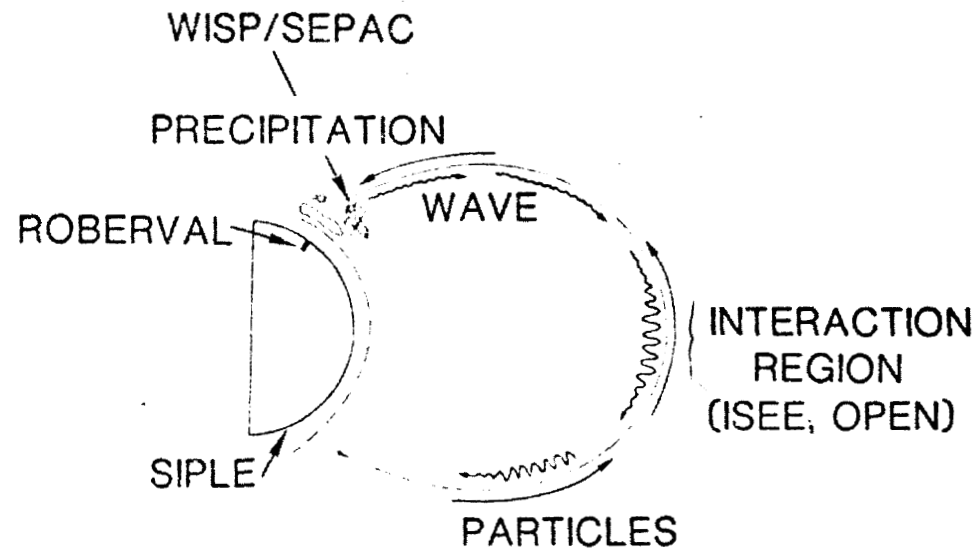


156

LIGHTNING WHISTLERS



1220 UT, JULY 3, 1973, SIPLE STATION



1137 UT, JULY 26, 1977, SIPLE STATION

SYSTEMS
GROUP
RESEARCH
STAFF

W I S P

FIRST TEAM MEETING

OBJECTIVES

TRW
DEFENSE AND SPACE SYSTEMS GROUP

FUNCTIONAL OBJECTIVES AS REQUIRED BY ERD

- UNDERSTAND CONTENT REQUIRED
- UNDERSTAND FO SCIENTIFIC REQUIREMENTS
- REDUCE TO COMMON FORMAT

HARDWARE

- DESCRIBE WISP SUBSYSTEM CONCEPTS
- DESCRIBE OTHER INSTRUMENTATION

ANTENNA IMPEDANCE

- REVIEW AND DISCUSS QUESTION

INTERFACES

- DISCUSS CONCEPTS AND OPTIONS
- MAKE DECISIONS OF PHILOSOPHY

FUNCTIONAL OBJECTIVES - OUTLINE
 CATEGORY, NUMBER, TITLE, AUTHOR/RESPONSIBILITY

CATEGORY I - ENGINEERING [FO 1-9]

<u>FO No.</u>	<u>Short Title</u>	<u>Author/Responsibility</u>
FO 1	System Configuration and Activation	TRW
FO 2	System Checkout (all WISP Systems ON except H.V.)	TRW, Collins, Spar
FO 3	VLSS Checkout (FO 2, except VLSS H.F. ON and transmitter power dumped to antenna simulator)	Collins
FO 4	HFSS Checkout (FO 2, except HFSS H.V. ON and transmitter power dumped to antenna simulator)	Spar
FO 5	Antenna extension or retraction	TRW, MSFC
FO 6	VLSS Interference Tests (FO 3, except power to antenna); secondary objective: measure Z_A propagation	Collins, TRW
FO 7	HFSS Interference Tests (FO 4, except power to antenna); secondary objective: measure Z_A propagation	Spar
FO 8	Antenna Deflection Determination	Garriott, TRW
FO 9	Standby Procedure	TRW, Collins, Spar

CATEGORY II - VLSS, WAVE PARTICLE INTERACTIONS [FO 10-19]

FO 10	Survey of Growth and Triggering	Stanford
FO 11	Detailed Properties of Triggered Emissions (3 or 4 parts)	Stanford
FO 12	Power Line Radiation Simulation	Stanford
FO 13	Induced Particle Precipitation	Stanford
FO 14 } FO 19 }	TBD	Stanford, Investigators

CATEGORY III - VLSS, WAVE PROPAGATION [FO 20-29]

FO 20	Dipole Radiation Pattern for Characteristic Wave Modes; 1 - Whistler Mode	James
FO 21 } FO 26 }	TBD	Stanford, Investigators

CATEGORY III (Cont'd)

FO 27	Field-Aligned VLF Ducts; (a) Siple-to-WISP and (b) WISP-to-Siple	Stanford
FO 28	WISP-to-Ground Beacon Mode	Stanford
FO 29	Plasmapause VLF Propagation	Stanford

CATEGORY IV - VLFSS PLASMA PHYSICS [FO 30-39]

FO 30	Auroral Kilometric Radiation	Stanford
FO 31	TBD	Stanford, Investigators
FO 39		

CATEGORY V - VLFSS, RESERVED [FO 40-49]

FO 40	TBD, Reserved for VLFSS	Stanford, Collins, TRW, Investigators
FO 49		

CATEGORY VI - HFSS, LARGE-SCALE STRUCTURES [FO 50-69]

FO 50	Determine the field-aligned electron density distribution from ducted echoes	Benson
FO 51	Determine the length and stability of field-aligned bubbles by obtaining nearly continuous conjugate echoes while in a ducting region	Benson
FO 52	Determine transverse size of density irregularities within a bubble by obtaining multiple near-end ducted echoes	Benson
FO 53	Determine the electron density at the apex of a field-lined density irregularity by obtaining Z-mode ducted echoes.	Benson
FO 54	Determine the extent of the bottomside density depletion from ground echoes	Benson
FO 55	Determine the changes in the total electron density content between Spacelab and the subsatellite as a bubble region is transversed	Benson
FO 56	Determine background neutral temperature, composition, and wind as well as background plasma temperature, composition and drifts.	Benson
FO 57	Determine AGW and TID wave characteristics, i.e., wave amplitude, phase, angular frequency, and wave vector	Benson

CATEGORY VI (Cont'd)

FO 58	Study the interdependence of AGW's and TID's	Benson
FO 59	Study the source regions of the AGW's and TID's from among the sources: magnetosphere, auroral region, equatorial region, stratosphere-mesosphere, and troposphere	Benson
FO 60	Equatorial Bubbles, Spread F, HF Ducts and Scintillation	Dyson
FO 61	Small Amplitude Discrete Irregularities at the Equator	Dyson
FO 62	Gravity Waves and TID's (HFSS, VHFSS)	Dyson
FO 63	Mid-Latitude Spread F (VHFSS)	Dyson
FO 64	Measurement of Large-Scale Wave Structures in the Ionosphere	Gross
FO 65	Large-Scale Disturbance Structures	Gross
FO 66	Relationships between Wave Structures and Field-Aligned Irregularities	Gross
FO 67	Source Regions for Large-Scale Structures	Gross
FO 68 } FO 69 }	TBD	HF Investigators

CATEGORY VII - HFSS, WAVE PROPAGATION [FO 70-89]

FO 70	Determine the resonance cone structures in the antenna radiation pattern as a function of antenna length	Benson
FO 71	Determine the characteristics of the ionospheric irregularities that give rise to the greatest scattering of whistler and Z-mode signals	Benson
FO 72	Determine the optimum ducting conditions for X, O, Z, and whistler mode signals	Benson
FO 73	Determine the efficiency of wave mode coupling between the Z and O modes	Benson
FO 74	Propagation of Plasma Waves (HFSS)	Taylor
FO 75 } FO 76 } FO 77 } FO 78 } FO 79 }	TBD	HF Investigators

CATEGORY VIII - HFSS, PLASMA PHYSICS [FO 80-109]

FO 80	Determine the characteristics of the f_H resonance as a function of stimulating conditions	Benson
-------	--	--------

CATEGORY VIII (Cont'd)

FO 81	Identify nonlinear wave processes including ion modulation effects on electron plasma waves	Benson
FO 82	Determine the stability of nf_H waves	Benson
FO 83	Determine the domain of stimulated temperature anisotropies	Benson
FO 84	Isolate nonlinear plasma wave processes from instrumental effects, plasma sheath effects and other spacecraft plasma perturbations	Benson
FO 85	Identify the cause of the "floating" nature of some resonances	Benson
FO 86	Explain electrostatic wave propagation phenomena such as the disappearance of the $3f_H$ echo when $f_N/f_H = 4$	Benson
FO 87	Determine the electrostatic to electromagnetic fraction of energy emitted from the antenna under different resonant conditions	Benson
FO 88	Determine electron-beam wave generation in ambient plasma for beam propagation quasi-parallel to magnetic field	Benson
FO 89	Determine electron-beam wave generation in ambient plasma for beam propagation quasi-perpendicular to magnetic field	Benson
FO 90	Determine electron-beam wave generation in ambient plasma for beam oblique propagation	Benson
FO 91	Determine electron-beam wave generation in ambient plasma driven to high anisotropy levels by HFSS/VHFSS for beam propagation quasi-parallel to magnetic field	Benson
FO 92	Determine electron-beam wave generation in ambient plasma driven to high anisotropy levels by HFSS/VHFSS for beam propagation quasi-perpendicular to magnetic field	Benson
FO 93	Determine electron-beam wave generation in ambient plasma driven to high anisotropy levels for oblique beam propagation	Benson
FO 94	Linear Impedance Dependence on Dipole Length	Balmain
FO 95	Linear Impedance Dependence on Dipole Orientation	Balmain
FO 96	Linear Impedance Dependence on Dipole D.C. Bias	Balmain
FO 97	Nonlinear Impedance Dependence on CW Power Level	Balmain

CATEGORY VIII (Cont'd)

FO 98	Linear CW Near-Field Evolution with Distance	Balmain
FO 99	Nonlinear CW Near-Field Evolution with Distance	Balmain
FO 100	Resonance Sounding	James
FO 101	Resonance Interactions using RPDP Diagnostics	Reasoner
FO 102	Stochastic Heating of Plasma and Nonlinear Effects near the Antenna using RPDP Diagnostics	Reasoner
FO 103	TBD	HF Investigators
FO 109		

CATEGORY IX - HFSS, RESERVED [FO 110-129]

FO 110	TBD, Reserved	Investigators
FO 129		

CATEGORY X - VHFSS, GENERAL [FO 130-139]

FO 130	VHF Determinations of Coupled Neutral and Ionospheric Turbulence	Grossi, Gross
FO 131	See FO 62	
FO 132	See FO 63	
FO 134	TBD	Investigators
FO 139		

CATEGORY XI - MISCELLANEOUS [FO 140-149]

FO 140	TBD	TRW, Collins, Spar
FO 147		
FO 148	System Activation	TRW, Collins, Spar
FO 149	Configuration for Return	TRW, Collins, Spar

WISP ACTIVE EXPERIMENT INTERACTIVE MATRIX



AUTHOR	FO No	WISP SS	RDPD	SEPAC	CRM	AEPI	MMP	EIMS	WAMDII	ALAE	ISO	ENAP	TRS
DYSON	T-1	HFSS	X										
TAYLOR	T-2	VLFSS											
STANFORD	T-3	VLFSS	X										
	T-4	"											
	T-5	"	X										
	T-6	"											
	T-7	"	X										
	T-8	"	X										
	T-9	"											
↓	T-10	"	X										
DYSON	T-11	HFSS	X										
BENSON	T-12	HFSS											
	T-13												
	T-14												
	T-15												
	T-16												
	T-17												
	T-18												
	T-19												
	T-20												
↓	T-21	↓											
DYSON	T-22	HFSS											
↓	T-23	↓											
↓	T-24	↓											
DYSON	T-25	HFSS											
GROSS	T-26	HFSS											

GROUND STATION

"

"

"

"

"

"

VLFSS

WISP ACTIVE EXPERIMENT INTERACTIVE MATRIX

AUTHOR	FO No	WISP SS	RPDP	SEPAC	CRM	AEPI	MMP	EIMS	WAMDII	ALAE	ISO	ENAP	TRS
GROSS	T-27	HFSS	X										
	T-28		X										
	T-29		X										
	T-30		X										
	T-31		X										
	T-32		X										
	T-33	↓	X										
GROSS	T-34	VHF	X										
TAYLOR	T-35	HFSS	X										
TAYLOR	T-36	HFSS	X										
GROSSJ	T-37	VHFSS	X										
GARRIOTT	T-38		X	X									
JAMES	T-49	HFSS	X										
↓	T-50		X										
↓	T-51		X										
↓	T-52		X										
↓	T-53		X										
↓	T-54		X										
↓	T-55		X										
↓	T-56	↓	X										
McNamara	T-57	HFSS	X										
↓	T-58	↓	X										
↓	T-59	↓	X										
MOORECRAFT	T-64	HFSS	X										
↓	T-65	↓	X										
↓	T-66	↓	X										

WISP ACTIVE EXPERIMENT INTERACTIVE MATRIX

AUTHOR	FO No	WISP SS	RPDP	SEPAC	CRM	AEPI	MMP	EIMS	WAMDII	ALAE	ISO	ENAP	TRS
MOORCROFT	T-67	HFSS	X										
MULDREW	T-68	HFSS	X										
MULDREW	T-69	↓	X										
	T-70	↓	X										
	T-71	↓	X										
	T-72	↓	X										
	T-73	↓											
	T-74	↓	X										
↓	T-75	↓	X										
BALMAIN	T-76	HFSS											
	T-77	↓											
	T-78	↓											
	T-79	HFSS/ALFS				X							
	T-80	HFSS	X										
	T-81	↓											
	T-82	↓											
	T-83	↓											
	T-84	↓				X							
↓	T-85	↓	X										
McNAMARA	T-86	HFSS	X										
MULDREW	T-87	HFSS	X										
REASONER	T-88	VLFS	X										
	T-89	HFSS	X										

SYSTEMS
GROUP
RESEARCH
STAFF

WISP DEFINITION PHASE

EMI CONSIDERATIONS

TRW
DEFENSE AND SPACE SYSTEMS GROUP

WISP SCIENTIFIC OBJECTIVES:

- depend on energizing antenna to high voltages
- study of the plasma response and loading

PREVIOUS DISCUSSIONS:

- Bob Blount/JSC
- narrow band emissions higher than spec are required by WISP

PROBLEM:

- fear that induced voltages or currents will affect avionics

SOLUTION:

- increase experimental power levels gradually and monitor the avionics

PROCEDURE:

- request appropriate waiver from STS operator

SYSTEMS
GROUP
RESEARCH
STAFF

W I S P

E M I

TRW
DEFENSE AND SPACE SYSTEMS GROUP

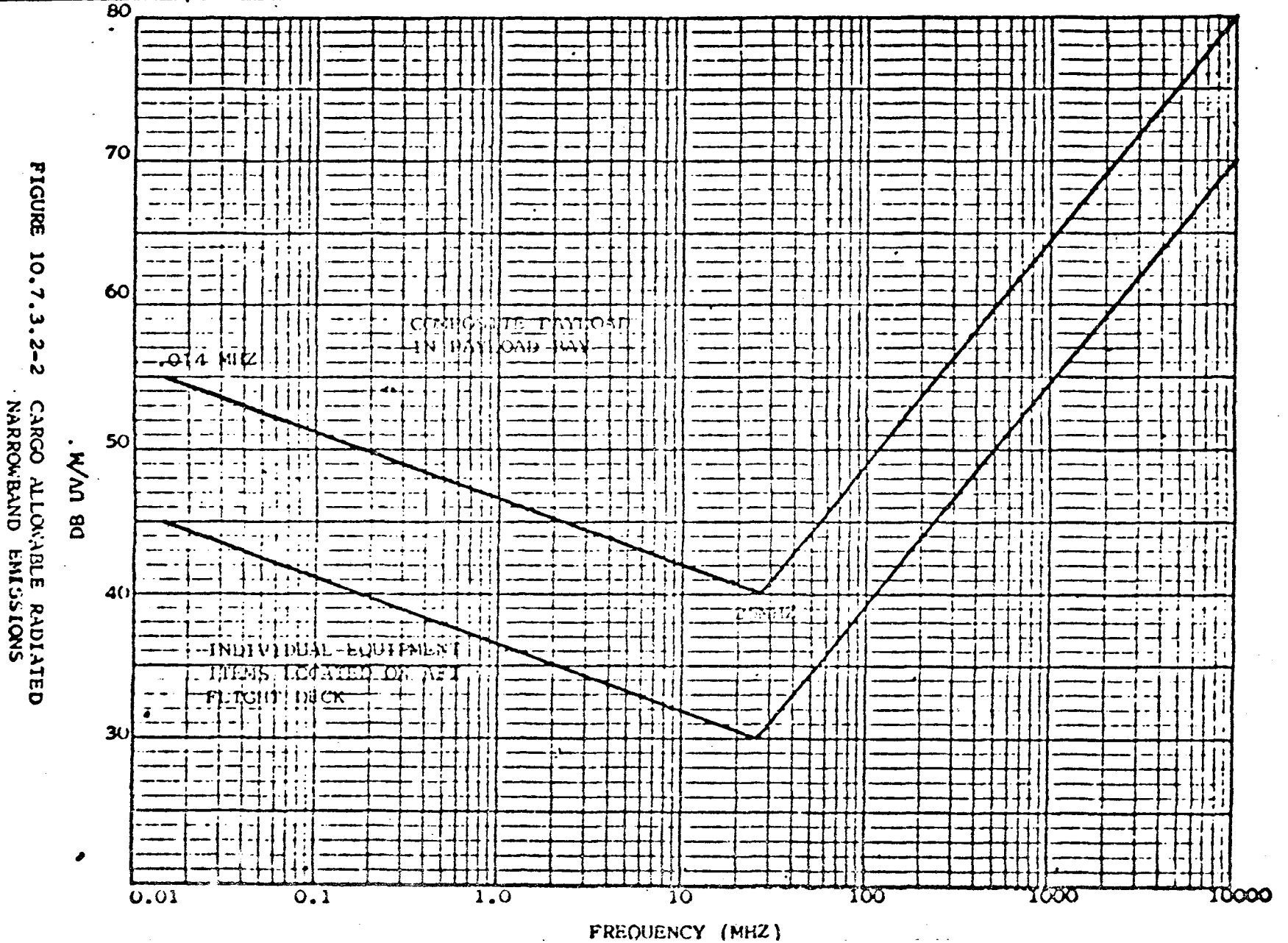
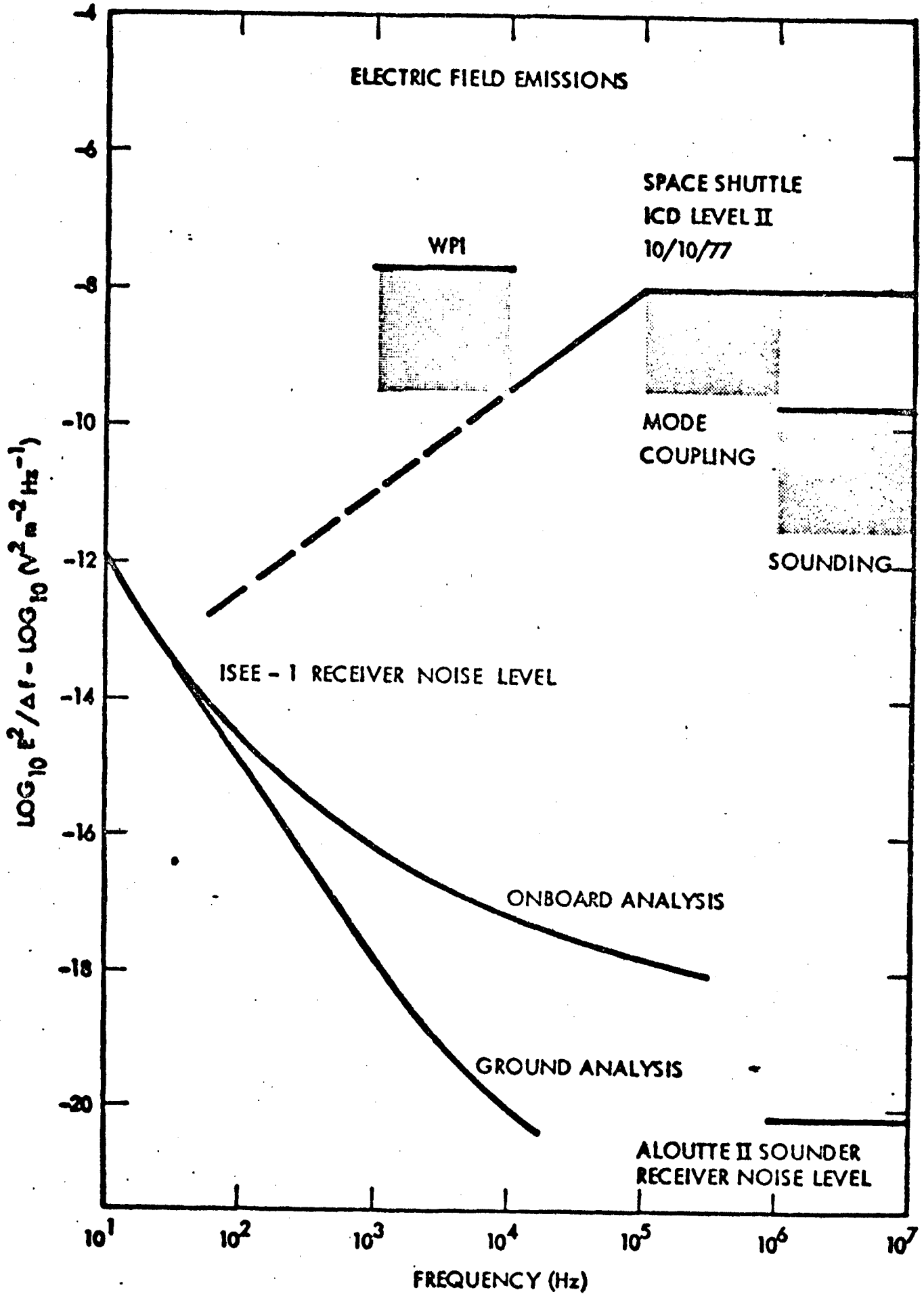


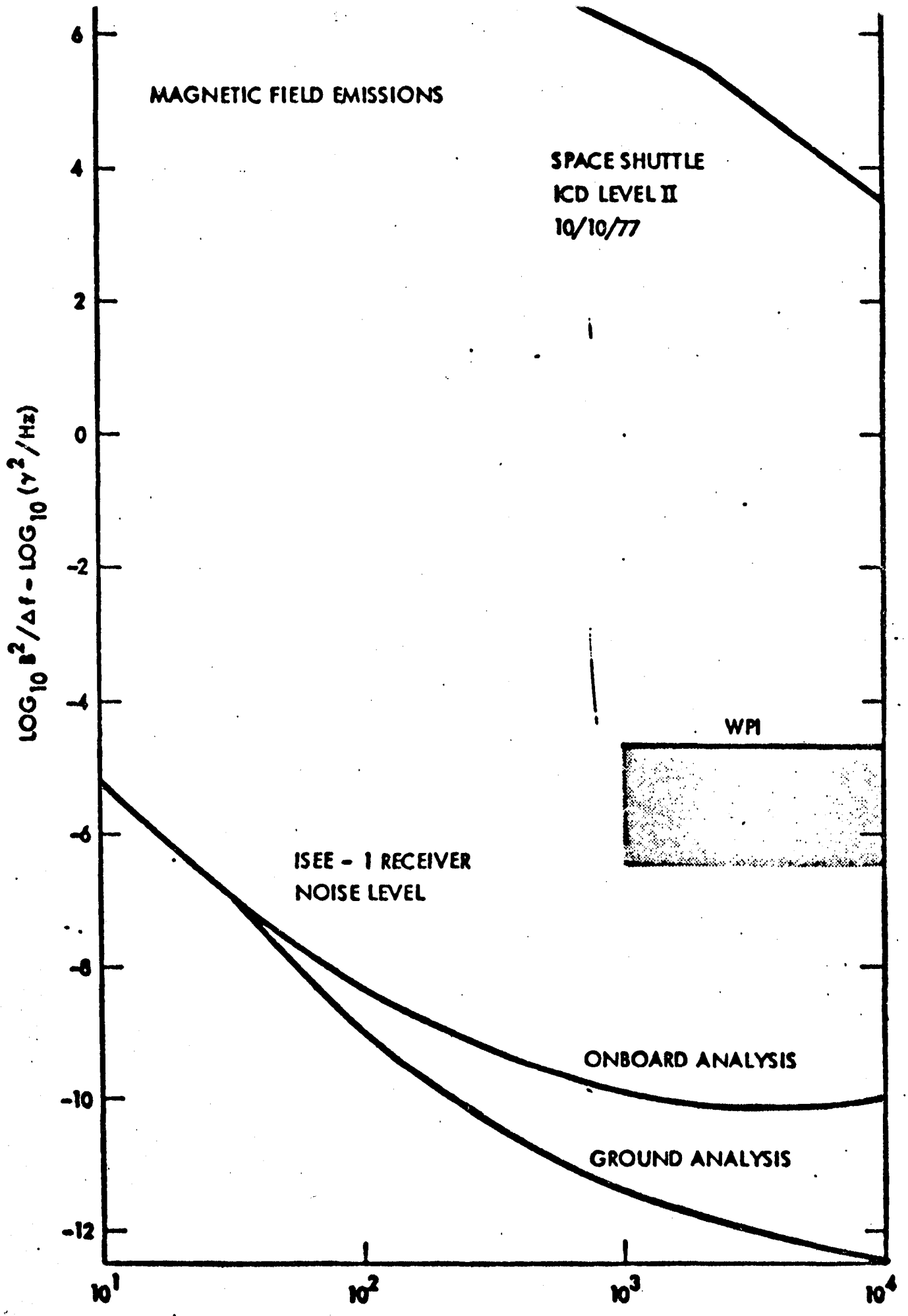
FIGURE 10.7.3.2-2 CARGO ALLOWABLE RADIATED
NARROWBAND EMISSIONS

Attachment 1 (ICD 2-19001)

10-26

CHANGE NO. 2





SECTION X. THE WISP/HF SYSTEM

THE WISP/HF SYSTEM FOR SPACELAB

H. G. James

Communications Research Centre, Department of Communications,
Ottawa, Ontario, K2H8S2 Canada

ABSTRACT

The high-frequency part of the Waves-In-Space Plasmas system, WISP/HF, is a flexible Shuttle/Spacelab instrument for transmitting, receiving and processing signals in the 0.3 to 30 MHz range. It will permit a wide range of plasma wave experiments in the ionosphere including studies of the transmitting antenna, fundamentals of electromagnetic (EM) and electrostatic (ES) waves in magnetoplasmas, instabilities and nonlinearities, and remote sounding of ionospheric structure. Collaborative investigations involving other WISP equipment (e.g. antenna and propagation studies with the WISP/VLF system) or other Spacelab facilities (e.g. beam-plasma interactions using charged-particle guns) are envisaged. A few specific examples illustrate the relevance of WISP/HF to current scientific interest. The overall goal is to help build a comprehensive understanding of plasmaspheric wave physics through group studies.

INTRODUCTION

The National Research Council of Canada (NRCC) has proposed to supply the WISP/HF [1,2] for Spacelab missions to be undertaken by the National Aeronautics and Space Administration (NASA). The system consists essentially of a transmitter and associated phase-coherent receivers, all of which are controlled by a programmable microprocessor. Upon a simple command, the transmitter generates signals with variable frequency, level and modulation. Frequency and amplitude can be swept, stopped or held constant, and are accurately known. The transmitter works into a dipole of variable length (up to 300 m tip-to-tip) and, when matched, can deliver 0.5 kW peak power. The system includes one receiver on the Orbiter and another on the Recoverable Plasma Diagnostics Package (RPDP) subsatellite [3]. Receiver gain, frequency and bandwidth settings are also variable and accurately known.

Figure 1 is one speculative interpretation of the components that will go to make up WISP/HF. They include:

1. A dedicated microprocessor-based Controller permits the Payload Specialist to carry out preprogrammed experiment routines which are stored in its memory. It accepts a simple command from the coordinating system and in turn sends detailed commands to the WISP/HF units. It provides time-base and frequency coordination between the transmitter and the receivers, monitors various circuit parameters or received signal characteristics, and adjusts the operating mode either by calling up preprogrammed responses or by implementing changes requested by the Payload

Specialist or by Payload Operations Control Centre. It detects, processes and formats data for the coordinating system and for CDMS.

2. A Frequency Synthesizer generates the basic RF required in the 0.3 to 30 MHz range and establishes the fixed- or swept-frequency cycles.
3. A Modulator creates pulses with appropriate width, rate, shape and coding.
4. A Driver produces the low-level wave forms.
5. A Power Amplifier amplifies the wave forms from the driver to output levels of at least 0.5 kW in the pulsed mode or 50 W CW.
6. A Transmit-Receive Switch isolates the input of the Orbiter receiver from the Power Amplifier output during transmission.
7. An Antenna Matching network is an electromechanical device which maximizes power transfer to the long dipole antenna during transmission and from that antenna to the Orbiter Receiver during reception. This unit could also control the transmitter power.
8. A Receiver amplifies wanted signals. It has about 100 dB of dynamic range and a bandwidth that is variable by command. One version is located on the Orbiter and has the long transmitting dipole as receiving antenna. The other receiver is on the RPDP where it is assumed that a 10-m dipole will be available for reception. NASA-supplied telecommand and telemetry links between the Orbiter and the RPDP provide control and data liaison between the RPDP receiver and the controller.
9. A Detector digitizes the received signal for processing by the controller. To permit Doppler measurements, it compares the phases of transmitted and received wave forms. It can also serve as a frequency comparator for swept-frequency work.

A working level agreement has been completed between the scientists in the U.S.A. who were responsible for the WISP Proposal [2] and scientists in Canada. The agreement is based on a recognized scientific interest of having an international team work on a comprehensive wave-injection project which encompasses active experimentation at frequencies between the extra-low-frequency range and the very-high-frequency range, inclusively. The team together will provide guidance on matters of general concern. Within this team will be the WISP/HF investigator group who will direct the definition, development and use of the WISP/HF hardware. This group comprises four Canadian scientists, four U.S. scientists and one Australian scientist who have all agreed on their responsibilities in the project. The group encourages scientists outside the team to associate with it in planning experiments.

Present NASA planning calls for a Spacelab mission in mid 1986, with an orbit of 57° inclination at 300 km altitude. The payload would include about a dozen instruments designed for atmospheric, magnetospheric and space-plasma experiments and these would be coordinated in various ways for collaborative investigations. The remainder of this article is a list of the major scientific categories to be addressed with the WISP/HF and includes a few specific illustrations.

ANTENNAS IN PLASMAS

In any radio science experiment, the antenna has a pivotal role, and research on the interaction of an active antenna with a magnetoplasma will be an important constituent of the WISP program. The research will deal first with the basic issues of driving-point impedance and fields of an antenna, in the linear domain. As signal level is increased, more complex descriptions of the antenna and its environment will be required, and a wide variety of phenomena will be investigated.

Figure 2 illustrates some antenna-related measurements. By measuring the voltage and current wave forms and their relative phase at the terminals of the long transmitting dipole, the complex driving-point impedance, Z_A , will be determined. The dependence of Z_A upon frequency, strength and direction of the ambient

magnetic field, plasma composition and density, antenna length and dc bias will be measured. Measurement of current distributions, near and far fields and plasma properties will be carried out with use of detectors mounted on the RPDP as shown in the Figure 2. Current distributions and near fields will normally be made while the RPDP is manoeuvred by the Remote Manipulator System. This work is important to the program because presently there is very little understanding of wave propagation along an antenna in a magnetoplasma. Near-field research would include the investigation of resonance cones, conical high-field regions extending outward from points of high charge accumulation at the centre and ends of the dipole. Cone properties for finite-length dipoles are of special interest because they have never been predicted or measured.

Far-field measurements of antenna radiation patterns (both magnitude and phase) are crucial with respect to wave injection applications of the Orbiter antenna. These will be accomplished using the WISP/HF transmitter and the WISP dipole aboard the Orbiter and receiving antennas and a receiver aboard the free flying RPDP. In cases when the electric and magnetic antennas are available for reception on the RPDP, it will be possible to calculate the Poynting flux. It will be generally desirable to develop techniques for finding power flux, as a step toward the important specific objective determining the antenna radiation efficiency for electromagnetic (EM) and electrostatic (ES) modes at frequencies spanning the resonance frequencies of the plasma.

The nature of the antenna sheath and its contribution to the electrical characteristics of the antenna will first be investigated in the linear regime. Nonlinear phenomena associated with the antenna will also be examined. The impedance, current and field distribution will be measured for increasing signal levels, and will undoubtedly be affected by plasma energization and sheath expansion. Sheath asymmetries may produce rectified rf current to the antenna resulting in the radiation of spurious harmonics. The interactions of particles accelerated by WISP/HF with dielectrics may provide a basis of study of the spacecraft charging [4]. It may also be possible to observe multipactor discharge; this occurs when resonant oscillations of electrons between dipole arms lead to a multiplicative increase in electron density through secondary emission [5].

Measured values of the impedance Z_A , and, eventually of radiated fields at the RPDP will be fed back to the WISP/HF controller (Fig. 2). In turn, the controller will command varactors in the antenna matching unit to maximize power output, optimize some field parameter, or perhaps intentionally set up interesting mismatch conditions.

PROPAGATION AND DISPERSION

WISP/HF will permit tests a number of fundamental concepts of propagation in anisotropic media; these include phase and group delay, polarization and power flux. Under certain conditions, collisional and collisionless damping formulas will be confirmed. Hypotheses about their energy flows can be examined.

The confirmation of the dispersion relations for a number of EM and ES waves can be obtained for hitherto unexplored regimes using the WISP/HF transmitter on Spacelab and a phase-coherent receiver on the RPDP. Of special interest are the ES waves occurring near the fundamental resonances at f_{pe} (plasma frequency) or at mf_{ce} (gyrofrequency harmonics). Figure 3 illustrates the possible geometries and relative sizes of reflected rays. It stresses that the bistatic configuration considerably enlarges the scope of propagation experiments over what has been possible in the past with monostatic systems. In particular, a variety of oblique paths can now be explored. At a given phase of an orbit, the Orbiter-subsatellite geometry will be favourable to at least one of several wave modes, and choices for

operating parameters will be based on real-time information about the plasma conditions and geometry.

Wave mode coupling has been speculated to play important roles in certain laboratory and space plasmas. Coupling will be tested by seeking bistatic geometries that effectively place the transmitter and receiver in different frequency domains and thereby require energy transfer between modes for successful propagation.

INSTABILITIES AND NONLINEARITIES

The flexibility of the WISP systems and associated Spacelab instruments will ensure new understanding of instabilities which occur spontaneously in space plasmas. Unstable waves often grow in amplitude to a point where nonlinear effects become important. Intrinsic plasma nonlinearities can be triggered in a controlled fashion through the use of the variable high output power available from WISP/HF. Nonlinear processes excited for specific wave modes, frequencies and propagation directions typically produce waves with different frequencies, directions and modes. The WISP/HF transmitter and receivers will be independently tunable to specific frequencies of interest, and hence will be able to observe the controlled nonlinear excitation of waves.

Experiments on wave-wave interaction will investigate parametric decay at short range. Attempts will be made to detect both characteristic electron and ion waves resulting from the decay, by judicious use of transmitter geometries and frequencies. Two-frequency pumping to produce ion waves has also been proposed. Work on nonlinearities will include careful diagnosis of the transmitter-heated regions and attempts to clarify all the ES wave modes destabilized in the resulting nonequilibrium plasma. For instance, there is evidence from the topside sounders that temperature anisotropies may be set up which then produce Bernstein waves through the Harris instability.

WISP/HF can be used to investigate wave growth in the presence of streaming charged particles. Once the characteristics of normal propagation in an equilibrium plasma have been established, the transmitter-receiver link can then be applied to the study of net effects of wave growth in nonequilibrium distributions. Natural particle streams in which the stream dimensions greatly exceed propagation path length present an advantage; the assumption of a growth region of infinite extent will simplify analysis. On the other hand, charged-particle guns on Spacelab will have the advantage of complete control over beam parameters (flux magnitude, pitch angle, energy and modulation) and of absence of widespread noise from spontaneous emissions. ES waves like those in Figure 3 have wavelengths of the order of meters and reflect off gradients within about 1 km of the transmitter. This suggests the procedure symbolized in Figure 4. Assuming that the artificial electron beam has a certain radius about a field line, it may be possible to arrange ES ray paths that, after reflection (many wavelengths from the transmitter), cut back across the beam with plane waves. When orbital conditions permit, an RPDP with a receiver located on the ray path just beyond its intersection with the beam should be in a position to monitor incremental wave growth or damping caused by the beam. The shaded areas in Figure 4 indicate that the beam is pulsed. Normal propagation (A) is first studied using rays that are not affected by the streaming particles. The transmitter is off at B and the receiver measures the inherent beam instabilities, if any. Finally, the net results of convective growth or damping of a transmitter pulse can be obtained by measuring the total signal level in the presence of the beam (C), subtracting inherent noise (B) and comparing with ambient propagation (A).

SOUNDING AND SCATTER

The WISP/HF group is strongly interested in research on ionospheric and magnetospheric structure as the basis for understanding the dynamics of the neutral atmosphere and the plasmasphere. Experiments are proposed in remote HF sensing of ionospheric structure in which both the scale size of the structure and the distance to it from Spacelab vary up to thousands of kilometers. New coded-pulse and coherent-transmission methods will be applied to research on traveling ionospheric disturbances and field-aligned irregularities of density. Near the upper-frequency limit of the WISP/HF, scatter from E- and F-region structures can also be studied. In situations where the Orbiter and RPDP fly through structure of interest, simultaneous use of the WISP/HF and other Spacelab systems will help to reduce ambiguities in calculations of density irregularity spectra.

Ionization structures will be measured, both along the orbit and remote from Spacelab. WISP/HF will operate in a number of programmed modes, including survey modes to search for natural phenomena of interest or modes to investigate specific features in detail. Frequency sweep range, pulse width, repetition frequency and power will be variable on command. WISP/HF will be capable of coherent detection, and will permit measurement of time delay, phase, amplitude and Doppler shift of received signals. Real-time data presentations may be used to help the operator focus on structure of particular interest. Since Doppler shift at a given frequency varies as the cosine of the angle between the wave normal and the receiver velocity, the shift is a measure of the angle of arrival of the return ray. This will provide a means of distinguishing returns from different regions with the same delay time.

With a Spacelab orbit in the F-region, WISP/HF will be useful for research on equatorial 'bubbles' [6] and associated field-aligned HF ducts [7]. WISP/HF may be used to find the shape, orientation and dimensions of bubbles, the relationship between bubbles and ducts, and the relationship between bubbles and Spread-F. Doppler data recorded in ducts will provide angle-of-arrival information which could be used to study the electromagnetic trapping mechanism and to distinguish trapped waves from scattered or reflected ones. Apart from bubbles, ducting phenomena deserve extensive study in their own right, and WISP/HF experiments will address wave modes whose guiding cannot be observed on the ground.

Figure 5 illustrates how the coherent bistatic transmitter-receiver could be used to clarify a long-standing question: are ducts of tubular (A) or laminar cross section (B)? In both cases, the transmitter-receiver separation vector is assumed horizontal and passes through the area of minimum density, N_1 , i.e., the inside of the duct. Using the coherence facility, the phase change, $\phi(f)$, is found in a frequency range f_1 to f_2 . The nature of the density contours and the rays consistent with them is such that there is much more dispersion in B than A. Iterative electron density modelling at the analysis stage could be used to deduce the density contours which give the best agreement with the observed $\phi(f)$.

REFERENCES

1. H. G. James, WISP/HF: A proposal for the investigation of medium- and high-frequency waves on Spacelab, Space Science Coordination Office, National Research Council of Canada, Ottawa, Ontario K1A 0R6, Canada, (1980).
2. R. W. Fredricks, Waves In Space Plasmas, TRW Defense and Space Systems Group, Proposal No. 34262.000, Redondo Beach, California, U.S.A. (1978).
3. S. D. Shawhan, A Recoverable Plasma Diagnostics Package (RPDP) for Spacelab, The University of Iowa, Iowa City, Iowa, U.S.A. (1978).

4. A. Rosen, Astronautics and Aeronautics, June, pp. 36, (1975).
5. P. F. Clancy, Microwave J., March, pp. 77, (1978).
6. S. Basu, and M. C. Kelley, J. Atmos. Terr. Phys., 39, 1229, (1977).
7. D. B. Muldrew, J. Geophys. Res., 68(19), 5355, (1963).

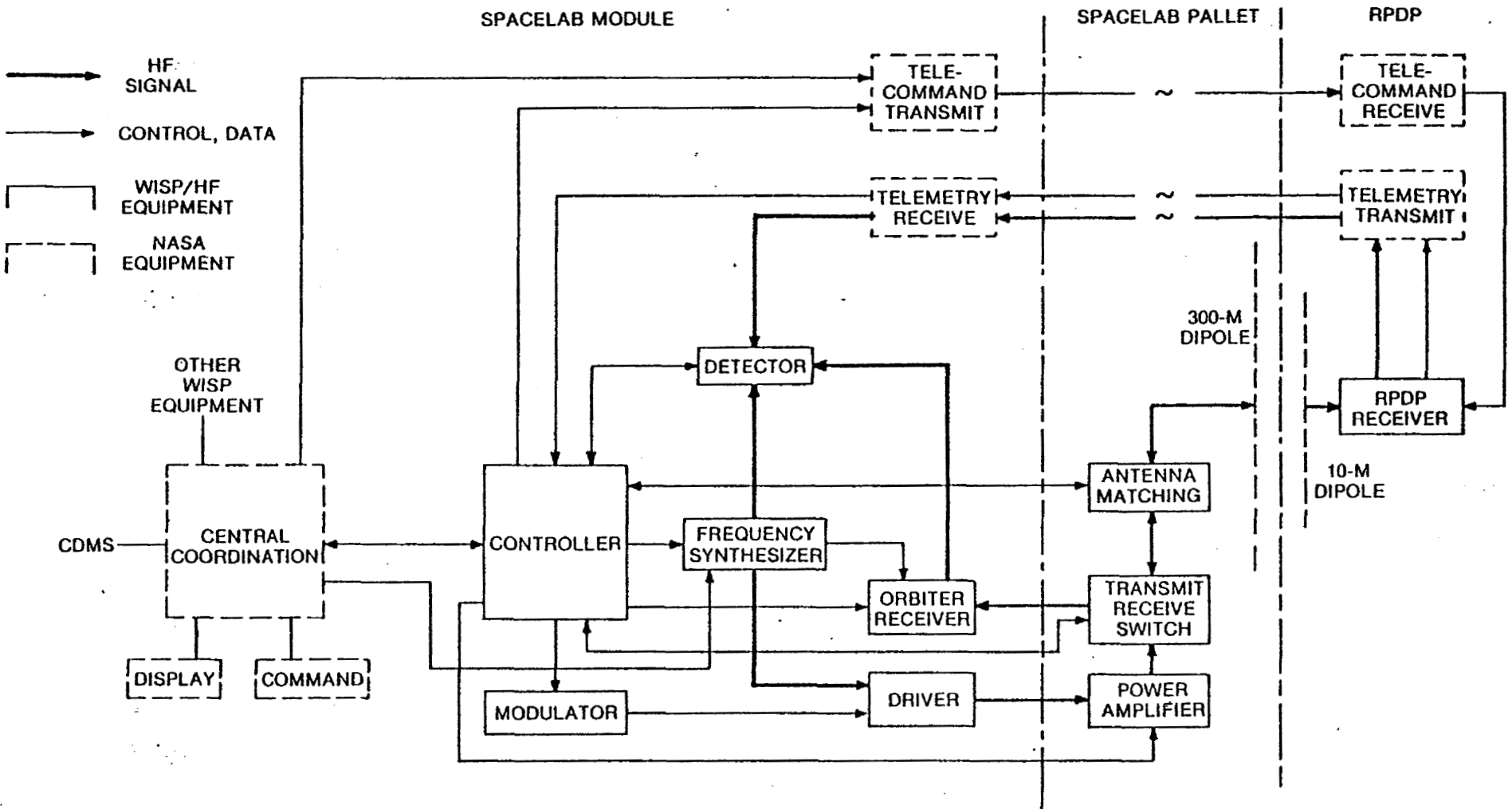


FIG. 1—FUNCTIONS OF WISP/HF

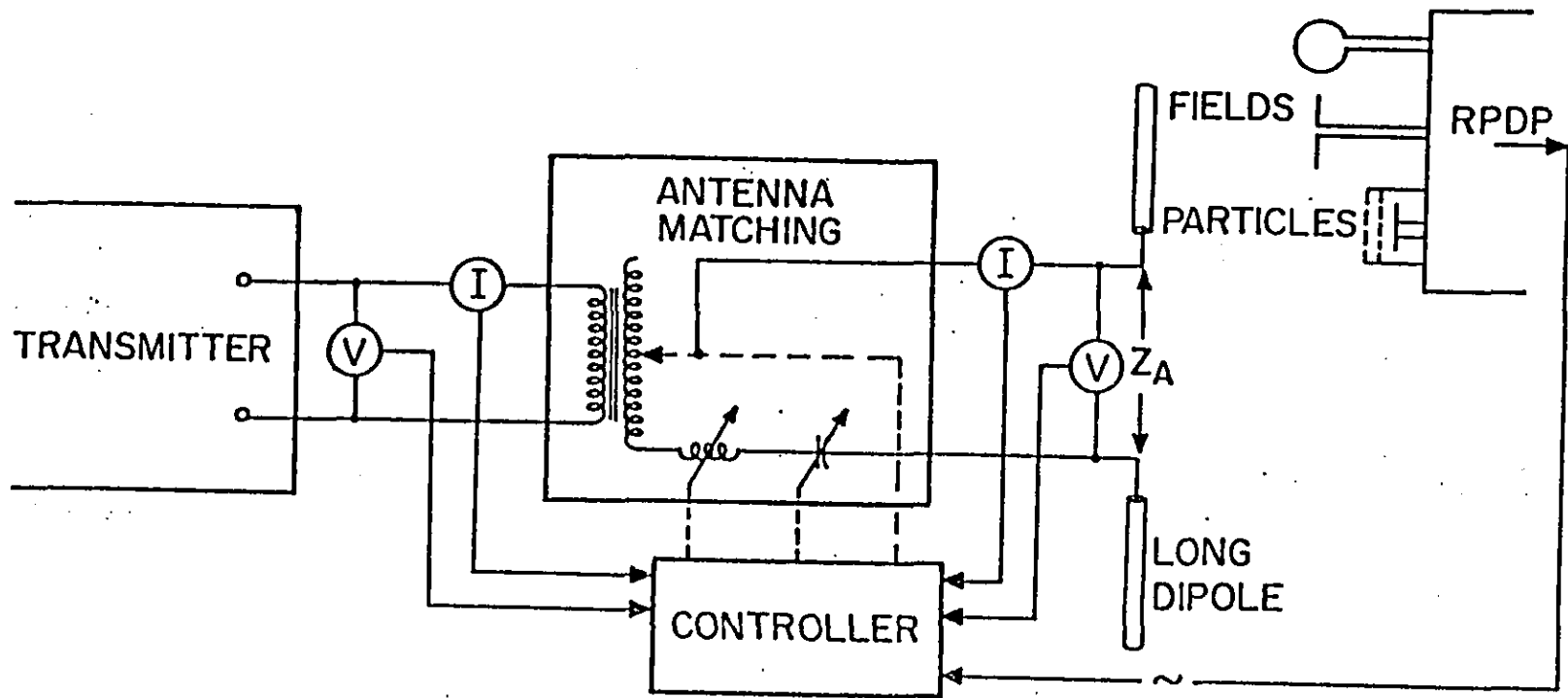


Fig.2

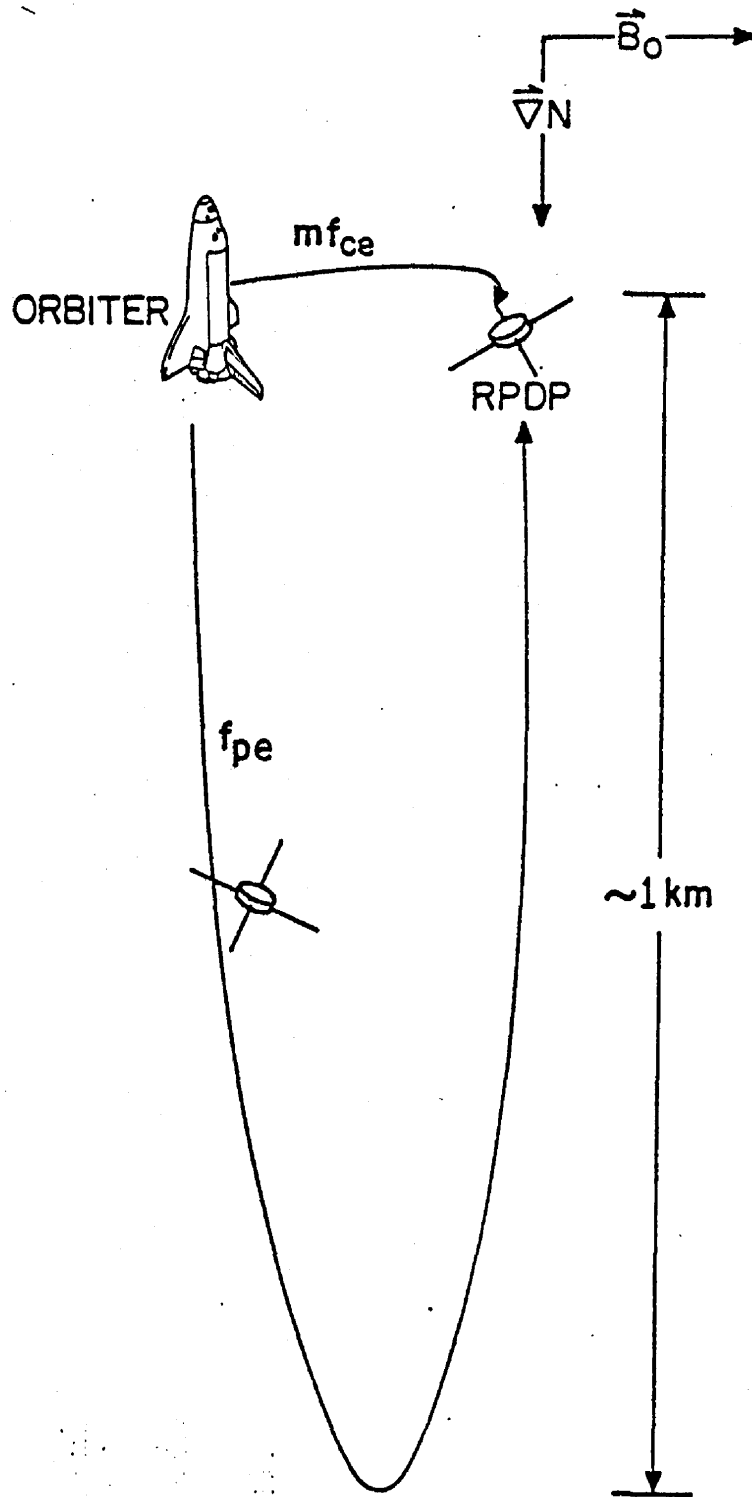


Fig. 3

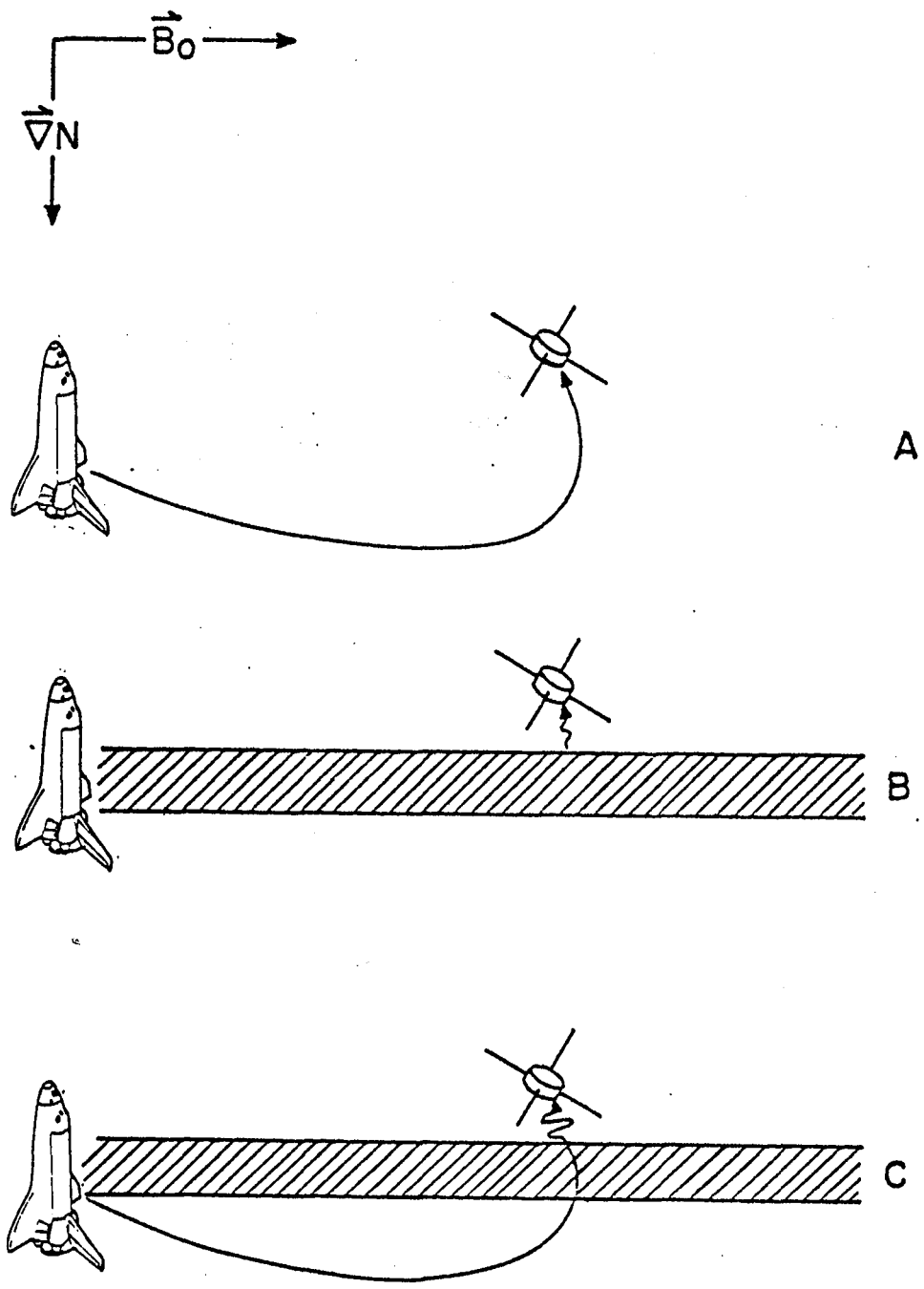


Fig. 4
182

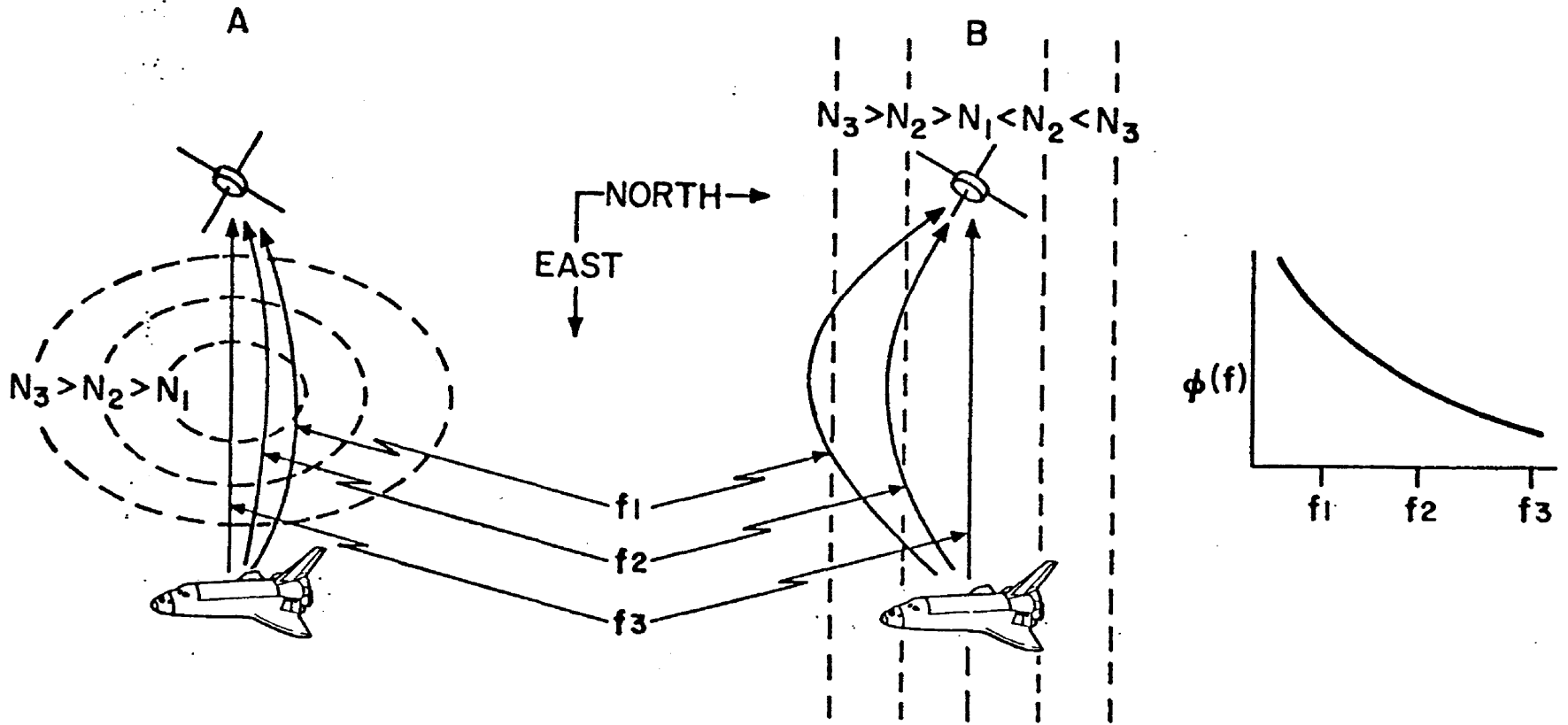


Fig. 5

SECTION XI. MAGNETOSPHERIC MULTIPROBES (MMP)



J. L. BURCH

23 SEPTEMBER 1980

MAGNETOSPHERIC MULTIPROBES
INVESTIGATIONS AND INSTRUMENTATION

SPACELAB ACTIVE EXPERIMENTS WORKING GROUP MEETING
NASA - MARSHALL SPACE FLIGHT CENTER
23 SEPTEMBER 1980



MULTIPROBE INVESTIGATOR TEAM

J. L. BURCH

NOVEMBER 5, 1979

PRINCIPAL INVESTIGATOR:

J. L. BURCH

S W R I

CO-INVESTIGATORS:

C. R. CHAPPELL

M S F C

S. A. FIELDS

C.-G. FÄLTHAMMER

SWEDISH ROYAL INSTITUTE
OF TECHNOLOGY

J. D. WINNINGHAM

S W R I

W. B. HANSON

U T - DALLAS

R. A. HEELIS

W. J. HEIKKILA

M. SUGIURA

G S F C

W. H. FARTHING

S. D. SHAWHAN

S U I

H. R. ANDERSON

R I C E



MULTIPROBE SCIENTIFIC OBJECTIVES

J. L. BURCH

NOVEMBER 5, 1979

- o DETERMINE THE SPATIAL STRUCTURE OF PLASMA PHENOMENA SUCH AS THE AURORA, CONVECTION REVERSALS, AND ION TROUGHS

- o SEPARATE SPATIAL AND TEMPORAL VARIATIONS IN THESE PHENOMENA

- o DETERMINE FIELD-ALIGNED CURRENT DENSITIES BY MEASURING CURL \bar{B} AND APPLYING THE MAXWELL EQUATION $\text{CURL } \bar{B} = \mu_0 \bar{J}$

- o PERFORM MULTIPLE-POINT ANALYSES OF PARTICLE BEAMS, WAVE FIELDS AND PLASMA CLOUDS THAT ARE INJECTED INTO THE IONOSPHERE AND MAGNETOSPHERE BY SPACELAB ACTIVE EXPERIMENT FACILITIES



MULTIPROBE SPATIAL CONFIGURATIONS

J. L. BURCH

NOVEMBER 5, 1979

o MISSION A

INITIAL: A CLUSTER COVERING A VOLUME WITH DIMENSIONS IN THE RANGE
OF 1 km TO 20 km.

FINAL: LINEAR TRAIL WITH INTERPROBE SPACINGS OF 1 km TO 100 km.

o MISSION B

LINEAR TRAIL WITH INTERPROBE SPACINGS OF 600 km TO 6000 km.

o POSITION DETERMINATION

200 METERS (MISSION A)

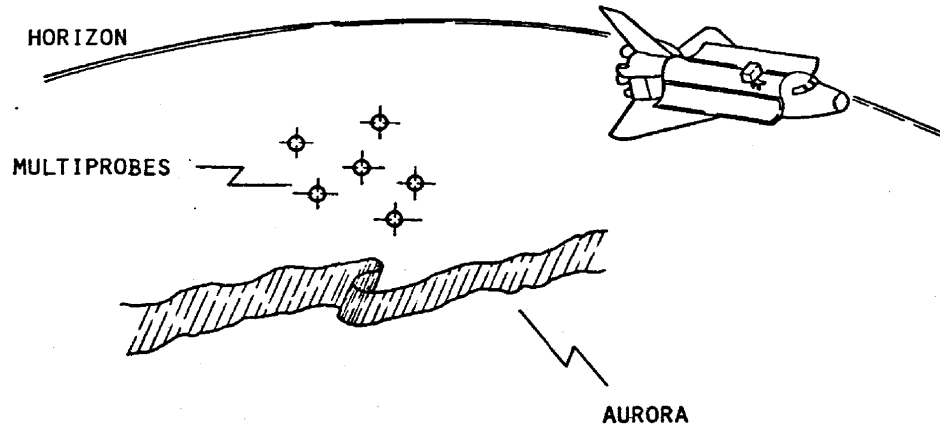
1 KILOMETER (MISSION B)



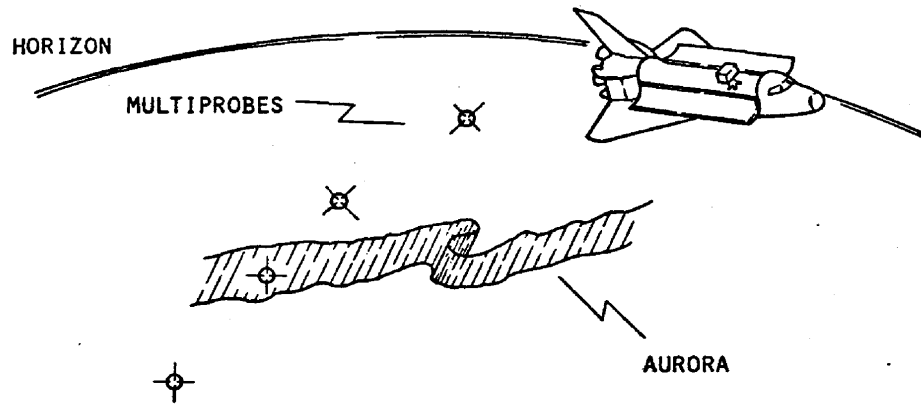
MULTIPROBE MISSION A SPATIAL CONFIGURATIONS

J. L. BURCH

NOVEMBER 5, 1979



MISSION A (CONFIGURATION 1)



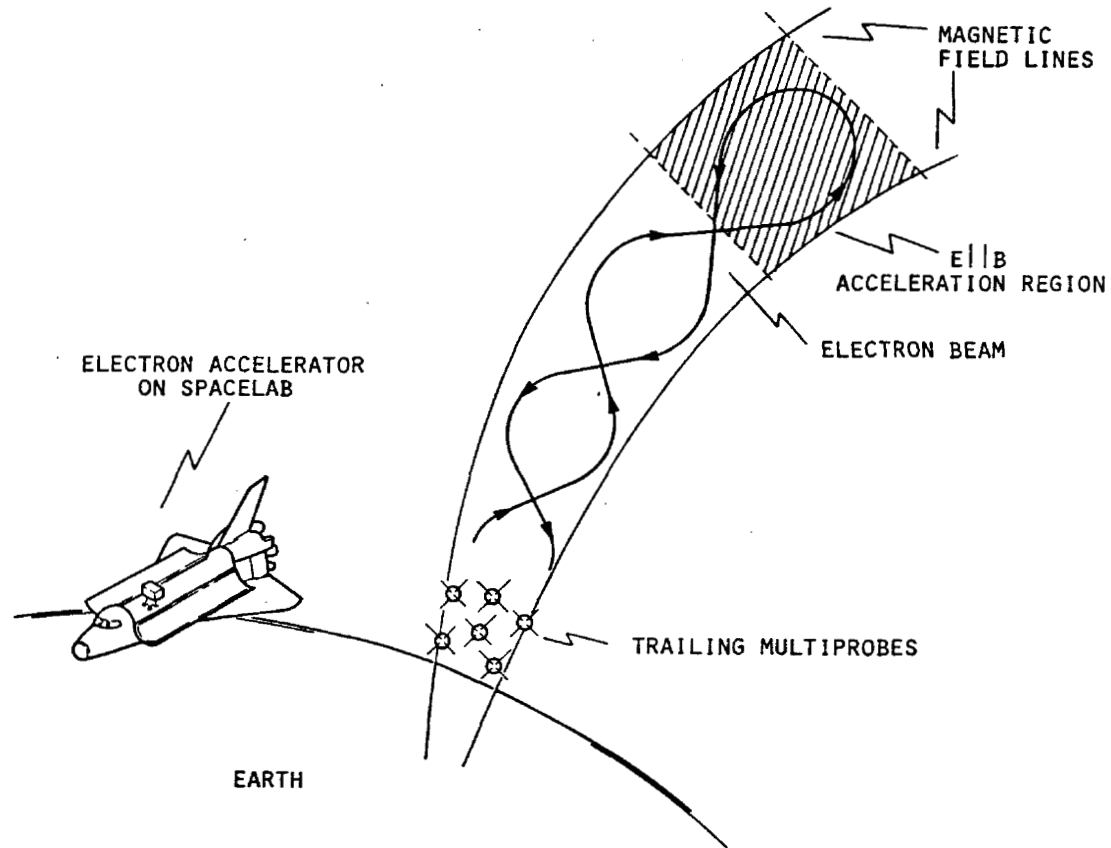
MISSION A (CONFIGURATION 2)



ELECTRON BEAM INJECTION EXPERIMENT
WITH MULTIPROBES

J. L. BURCH

NOVEMBER 5, 1979





MULTIPROBE SCIENTIFIC MEASUREMENTS

J. L. BURCH

NOVEMBER 5, 1979

BASIC COMPLEMENT

- o VECTOR MAGNETIC FIELD WITH ACCURACY OF 50 nT AND SPATIAL RESOLUTION OF 200 METERS.
- o VECTOR ELECTRIC FIELD WITH ACCURACY OF 5 mV/m AND SPATIAL RESOLUTION OF 200 METERS.
- o ELECTRON DENSITY AND TEMPERATURE WITH SPATIAL RESOLUTION OF LESS THAN 1 km.
- o ENERGY SPECTRA AND PITCH-ANGLE DISTRIBUTIONS OF SUPRATHERMAL ELECTRONS FOR ENERGIES OF 5 eV TO 30 keV WITH AT LEAST TEN COMPLETE ENERGY SCANS PER SPIN PERIOD.

OPTIONS

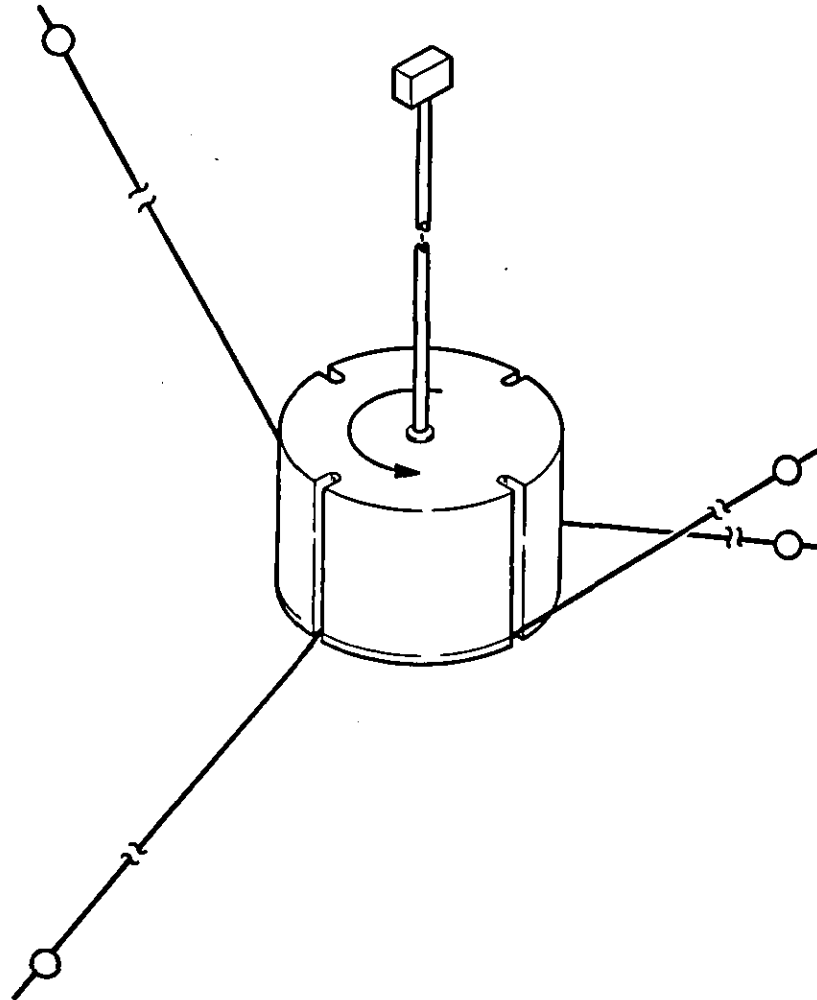
- o VECTOR ION DRIFT WITH ACCURACY OF 100 m/s, AND SPATIAL RESOLUTION OF LESS THAN 10 km.
- o THERMAL ION TEMPERATURE AND COMPOSITION OVER MASS RANGE OF 1 TO 56 AMU.



MULTIPROBE WITH DEPLOYED BOOMS AND ANTENNAS

J. L. BURCH

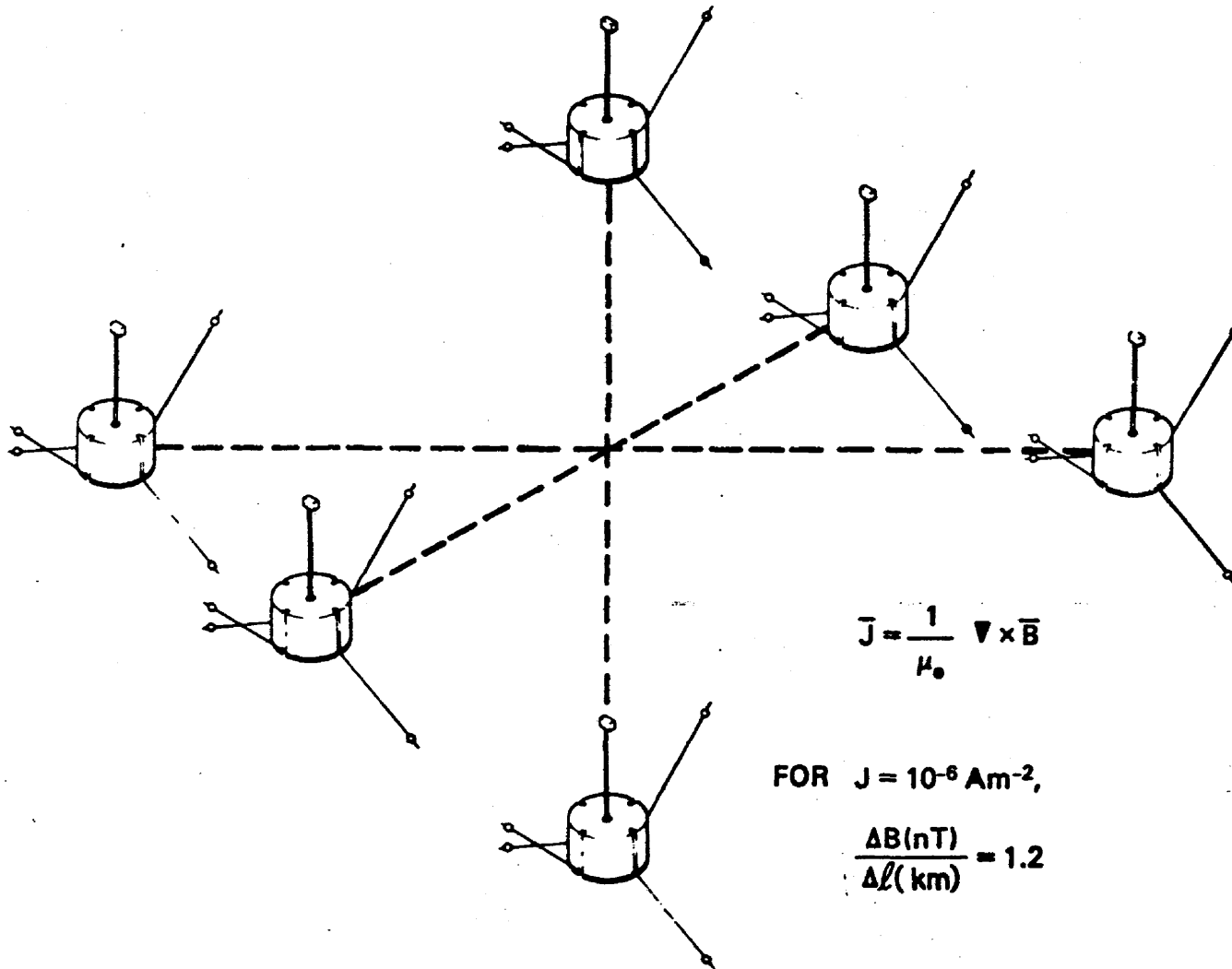
NOVEMBER 5, 1979





MULTIPROBE CLUSTER FOR CURRENT MEASUREMENTS

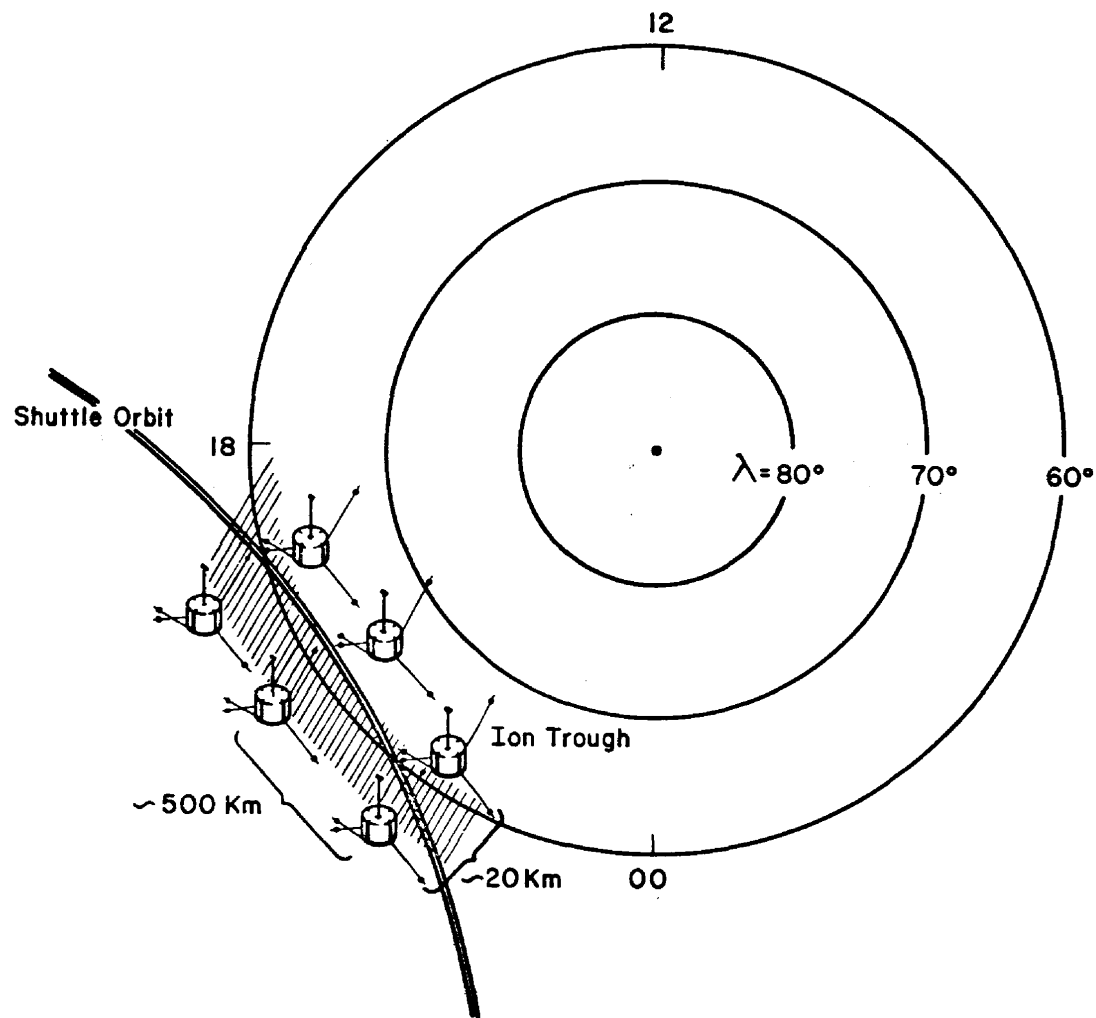
J. L. BURCH
23 SEPTEMBER 1980





MULTIPROBE INVESTIGATION OF STRUCTURE
AND DYNAMICS OF ION TROUGH

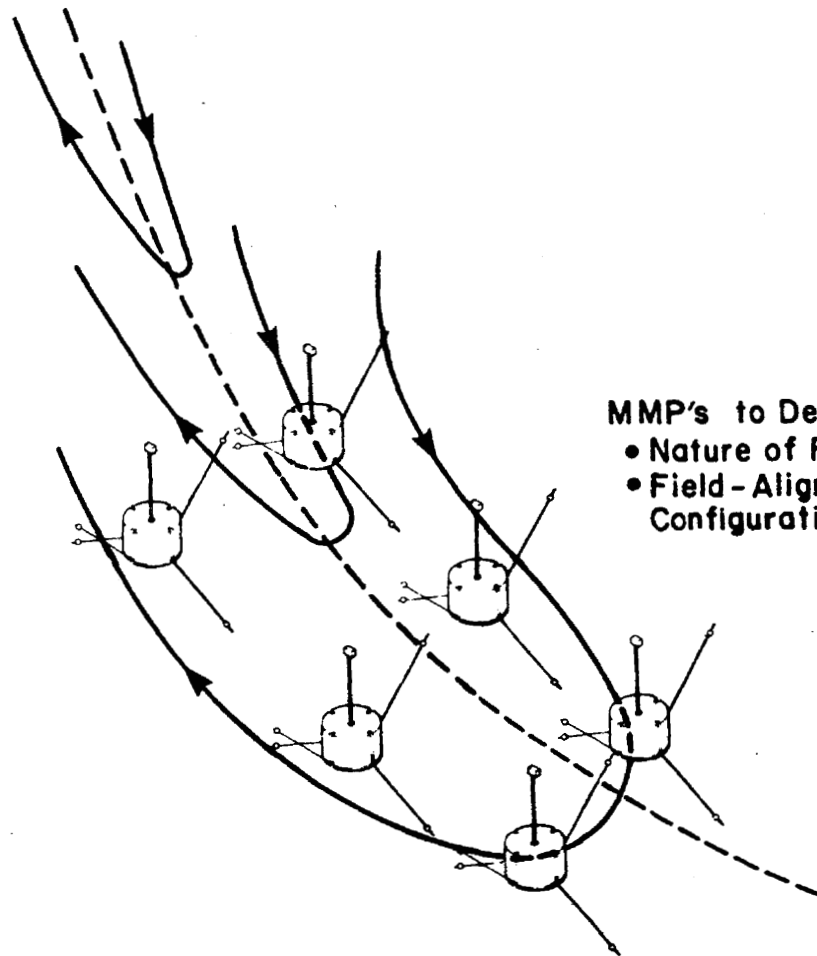
J. L. BURCH
23 SEPTEMBER 1980





**MMP INVESTIGATION OF FLOW REVERSALS
(CLEFT AND HARANG DISCONTINUITIES)**

J. L. BURCH
23 SEPTEMBER 1980

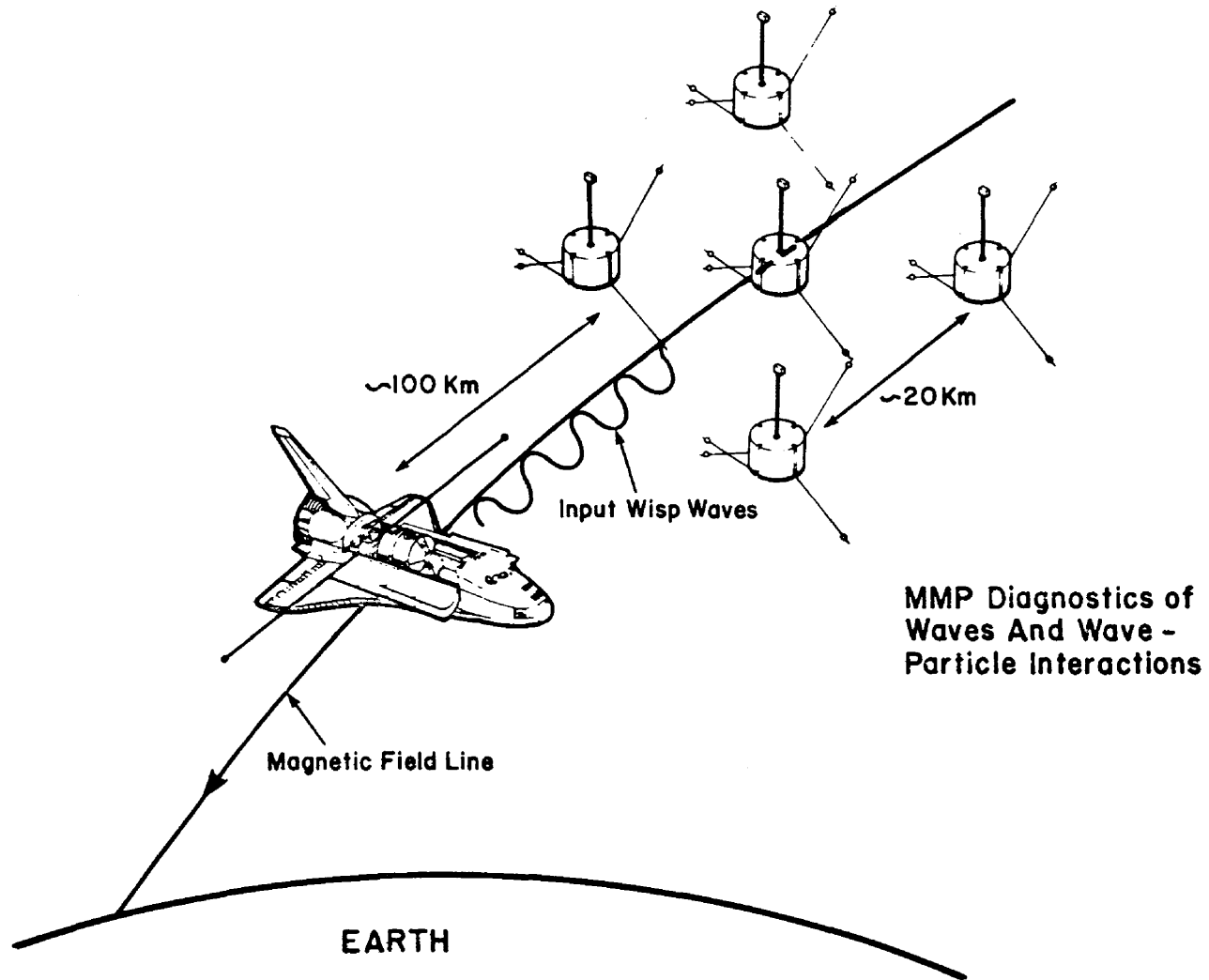


MMP's to Determine
• Nature of Flow Reversal
• Field-Aligned Current Configuration



USE OF MULTIPROBES IN WISP WAVE INJECTION EXPERIMENTS

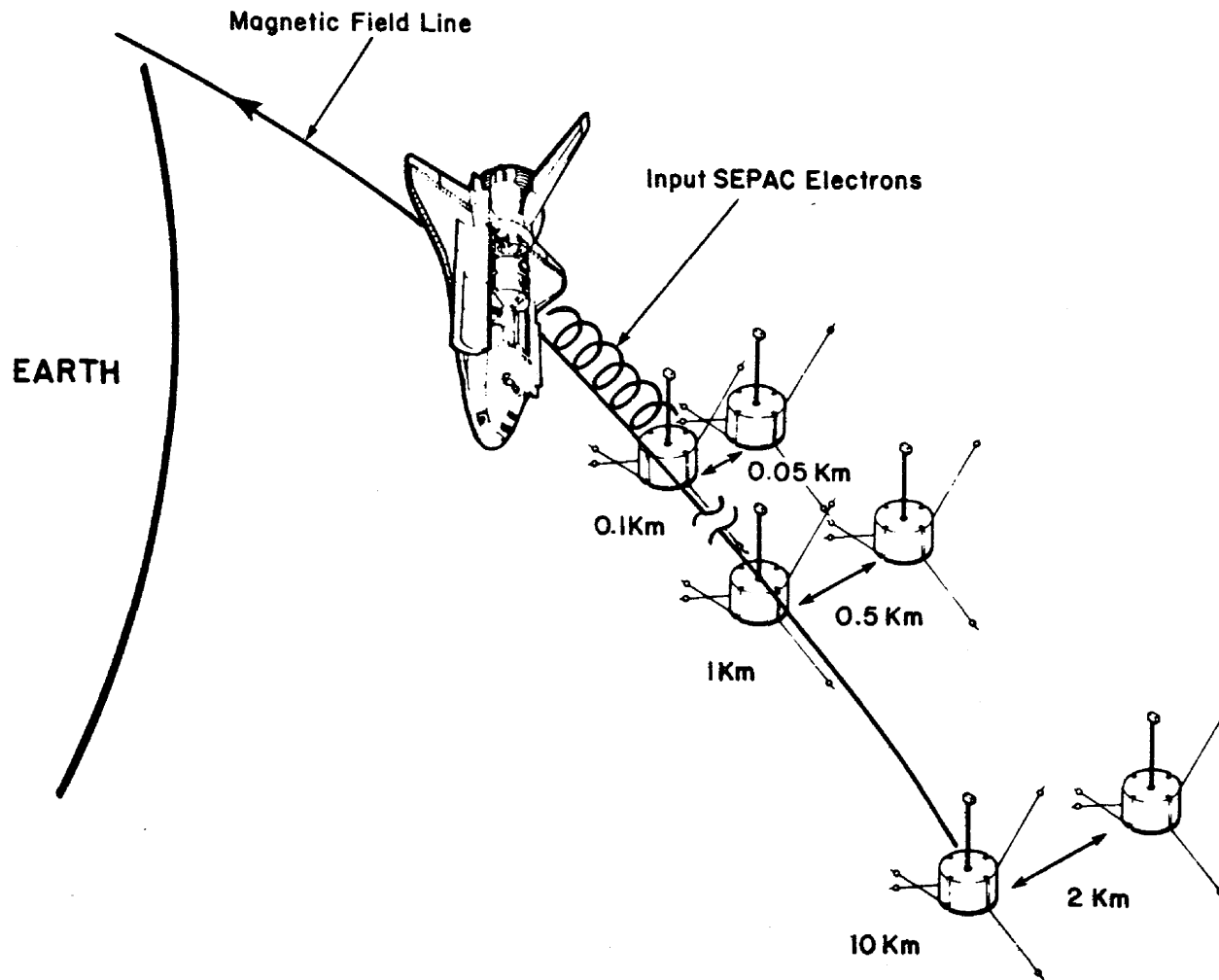
J. L. BURCH
23 SEPTEMBER 1980





USE OF MULTIPROBES IN SEPAC BEAM-PLASMA EXPERIMENTS

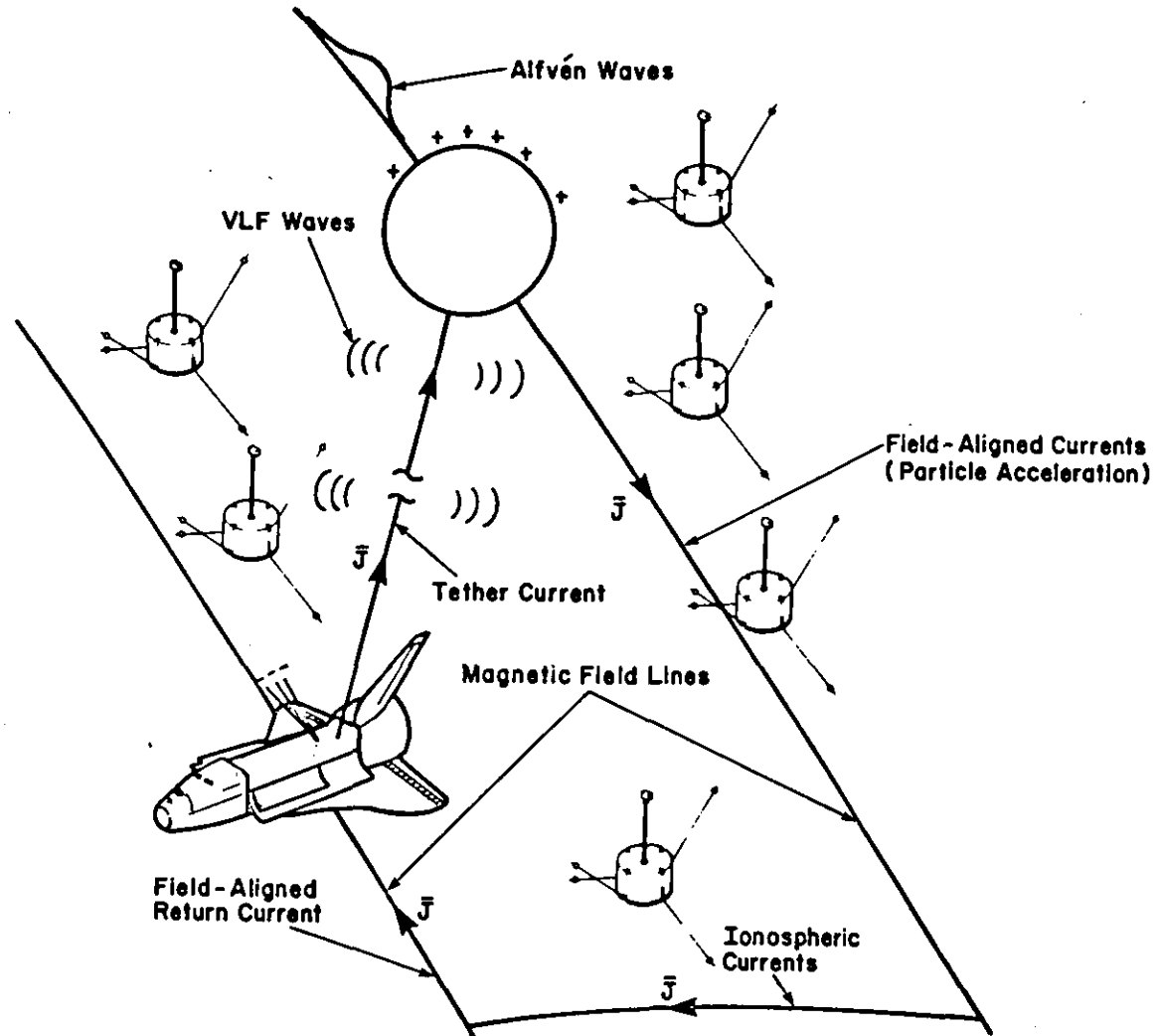
J. L. BURCH
23 SEPTEMBER 1980





USE OF MULTIPROBES WITH ELECTRODYNAMIC TETHER

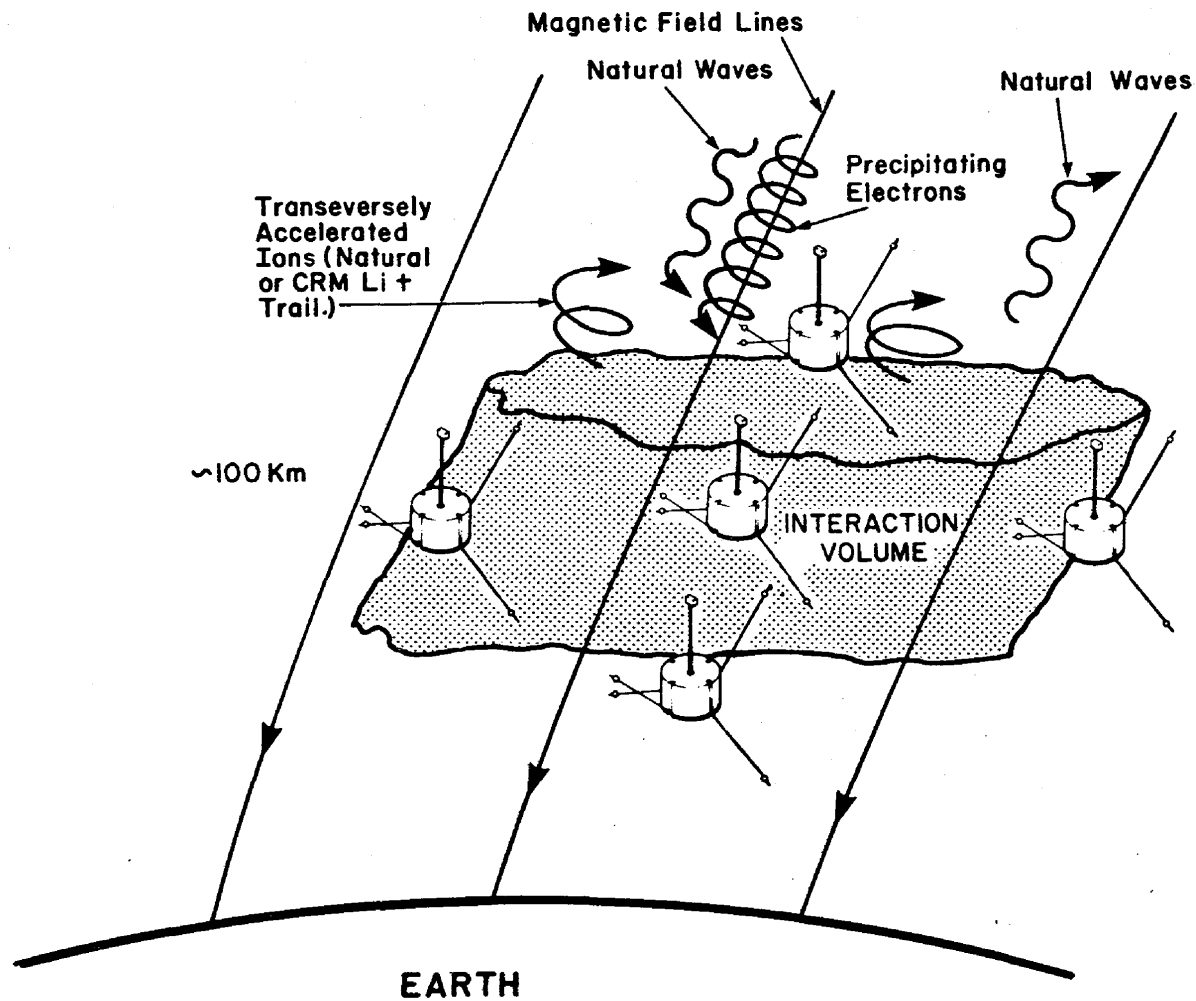
J. L. BURCH
23 SEPTEMBER 1980





MULTIPROBE INVESTIGATION OF TRANSVERSE ION ACCELERATION

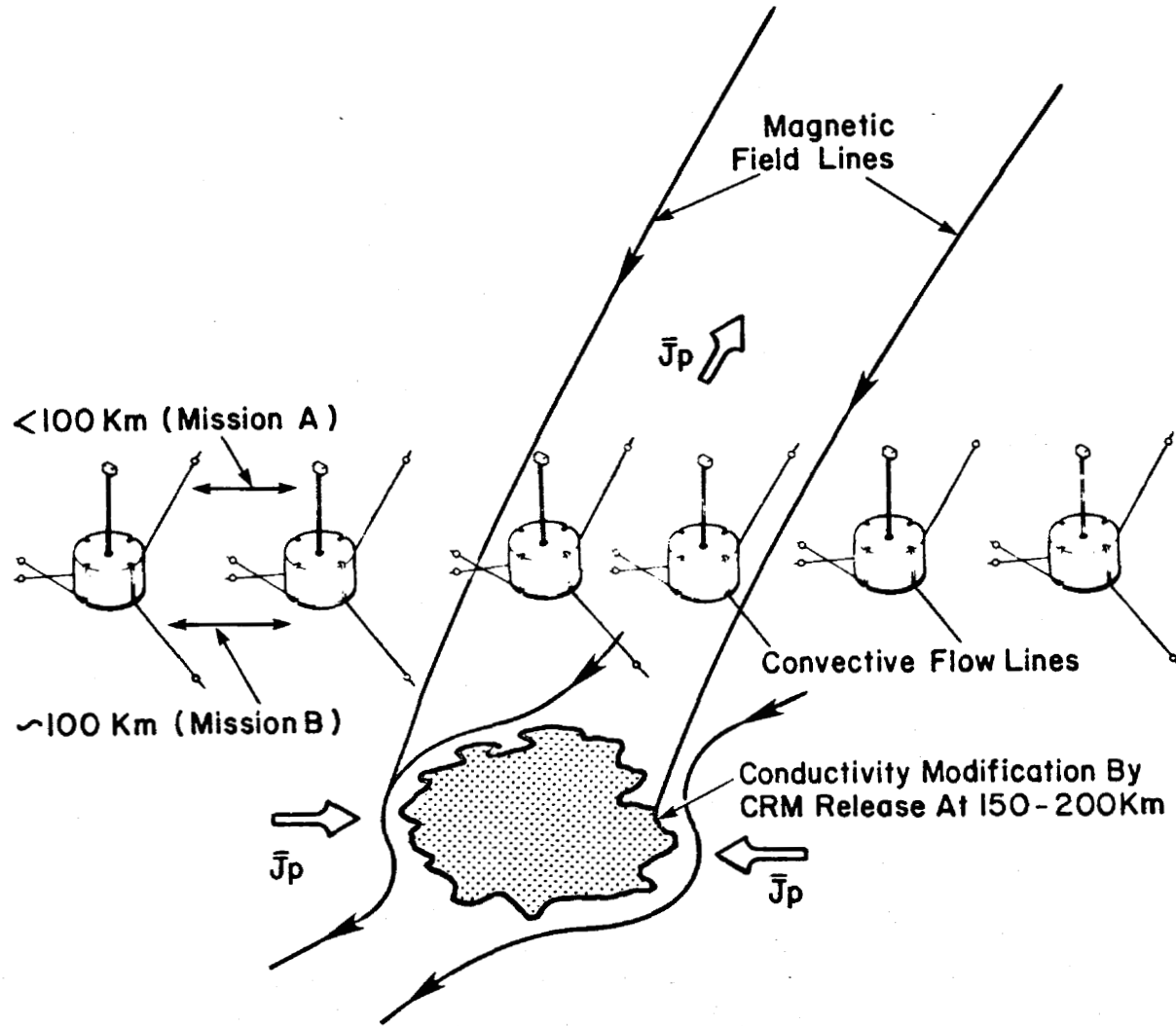
J. L. BURCH
23 SEPTEMBER 1980





USE OF MULTIPROBES IN CRM CONDUCTIVITY
MODIFICATION EXPERIMENTS

J. L. BURCH
23 SEPTEMBER 1980

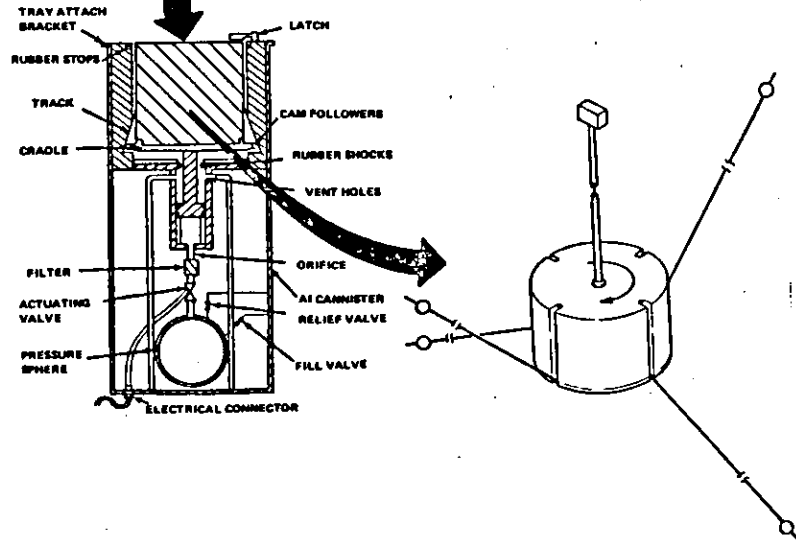
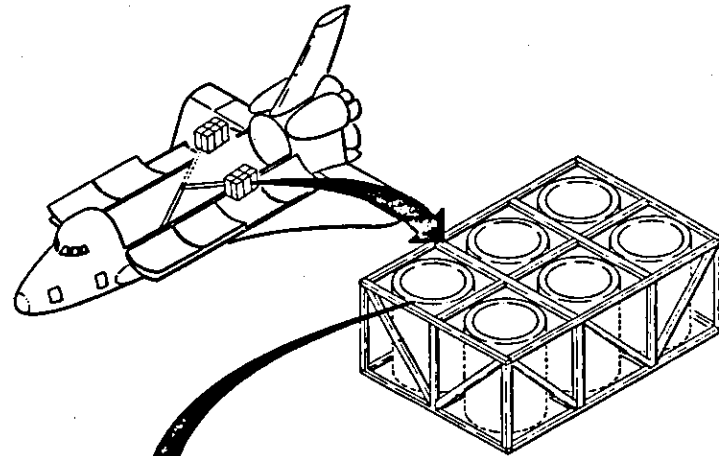




MULTIPROBE STOWAGE AND EJECTION SYSTEM

J. L. BURCH

NOVEMBER 5, 1979

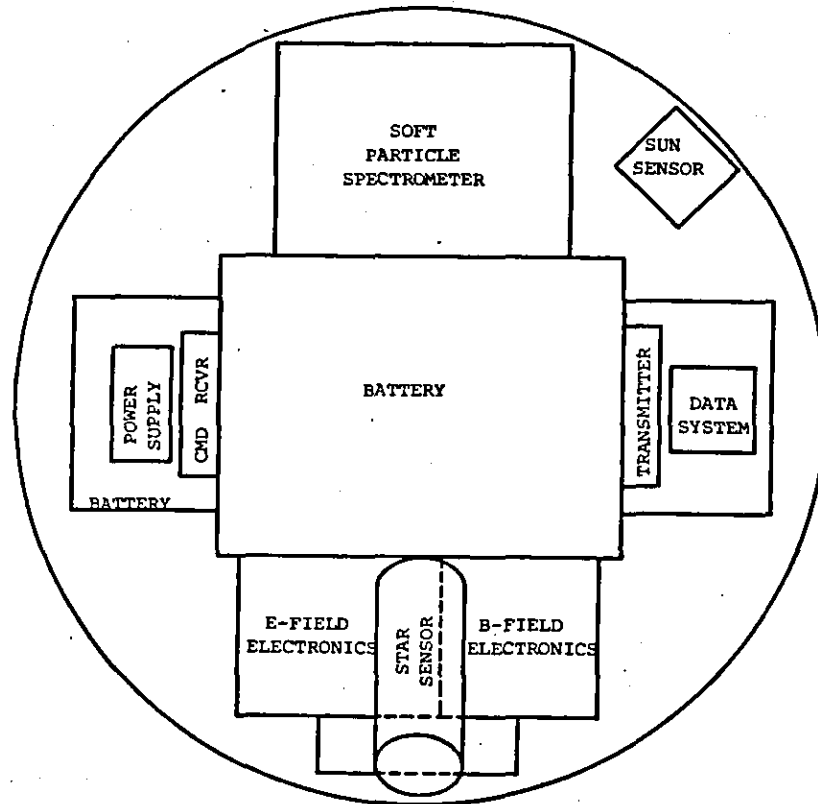




PLAN VIEW OF ASSEMBLED MULTIPROBE SUBSYSTEMS

J. L. BURCH

NOVEMBER 5, 1979

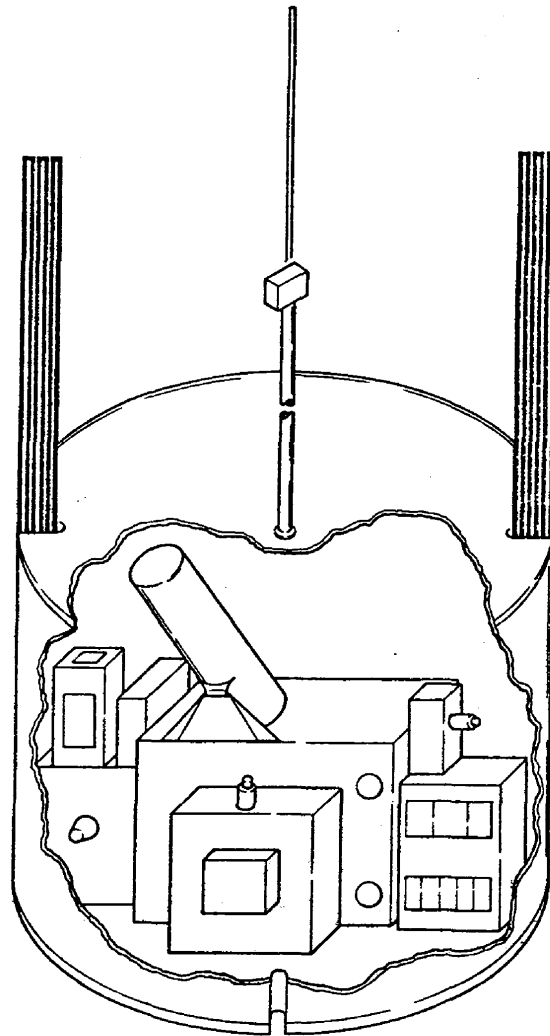




CUTAWAY VIEW OF ASSEMBLED MULTIPROBE

J. L. BURCH

NOVEMBER 5, 1979



DIAM: 60 cm

HEIGHT: 38 cm

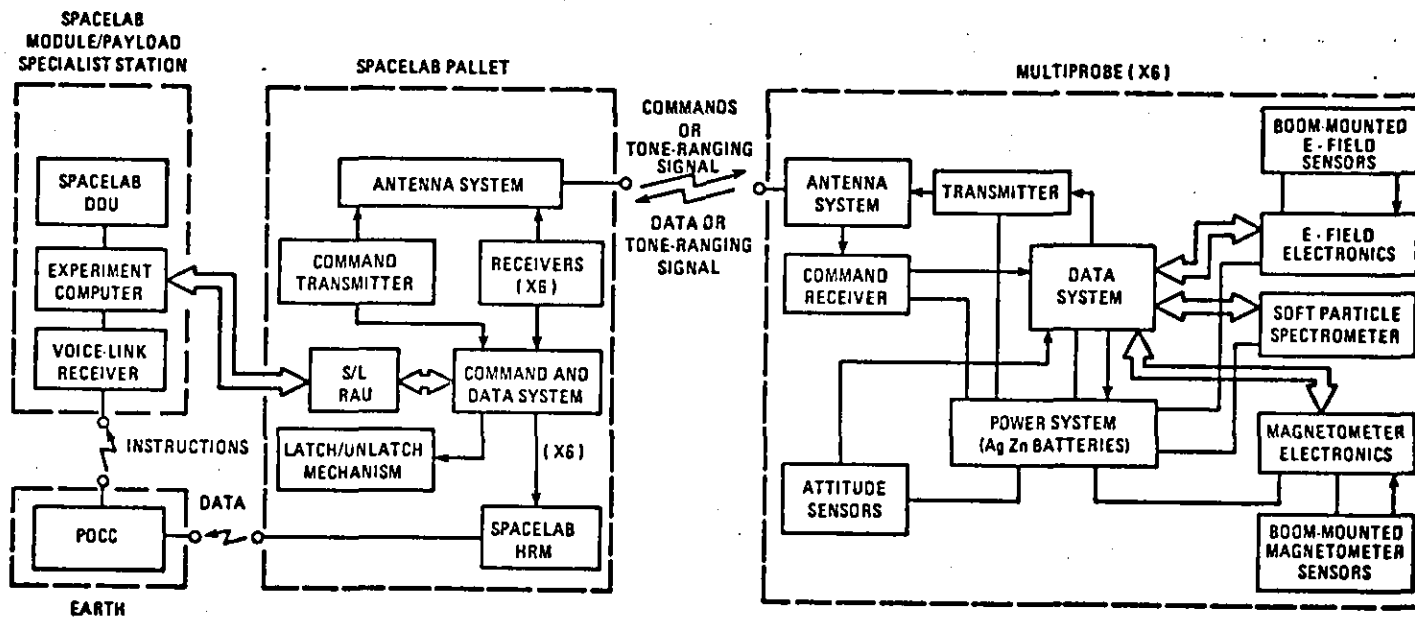
MASS: 50 kg



MULTIPROBE SYSTEM BLOCK DIAGRAM

J. L. BURCH

NOVEMBER 5, 1979

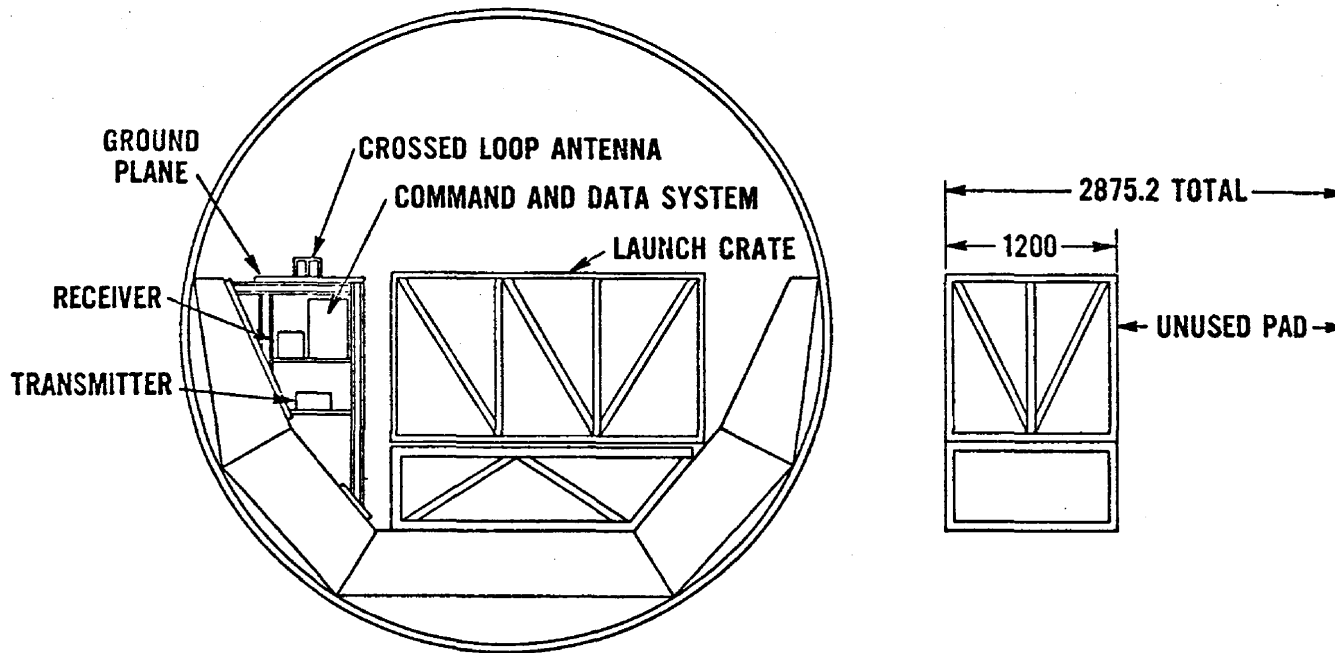




MULTIPROBE SYSTEM MOUNTED ON SPACELAB PALLET

J. L. BURCH

NOVEMBER 5, 1979



INSTRUMENT ACCOMMODATIONS

- EVALUATE MEANS OF PROVIDING MECHANICAL MOUNTING FIXTURES FOR EACH INSTRUMENT WITH SERVICEABILITY AS A CONSIDERATION
- EVALUATE ELECTRICAL INTERFACE CIRCUITS NECESSARY TO PROVIDE COMMAND AND DATA SUPPORT TO EACH INSTRUMENT
- EVALUATE POWER CIRCUIT INTERFACE REQUIREMENTS FOR FUSING AND CONTROL CONSIDERATIONS
- EVALUATE EMI ENVIRONMENT FOR INSTRUMENT CONTAMINATION CONSIDERATIONS

POWER

- EVALUATE THE SUITABILITY OF VARIOUS BATTERY TECHNOLOGIES (INCLUDING LITHIUM, AgZn, AND NiCd BATTERIES) FOR THE MULTIPROBE POWER SUBSYSTEM

ATTITUDE DETERMINATION

- EVALUATE THE USE OF SUN SENSORS, HORIZON SENSORS, AND STAR SENSORS FOR DETERMINING 3-AXIS ATTITUDE TO THE REQUIRED 0.1°

ELECTRIC FIELD ANTENNAS

- EVALUATE THE SUITABILITY OF VARIOUS TYPES OF ANTENNAS, INCLUDING HINGED, TAPE AND WIRE



MULTIPROBE TRADE STUDIES

J. L. BURCH

NOVEMBER 5, 1979

STOWAGE AND EJECTION

• EVALUATE THE FOLLOWING ALTERNATIVE MEANS OF STOWING AND EJECTING MULTIPROBES AT SPACELAB:

- (1) COLD-GAS DRIVEN PISTON EJECTION FROM A MODIFIED IECM FRAME
- (2) SPIN-UP AND EJECTION BY A SPECIAL PURPOSE END EFFECTOR ON THE RMS, AS IN THE PDP
- (3) SPIN-UP AND EJECTION FROM THE RMS BY A COLD-GAS SYSTEM INTERNAL TO EACH MULTIPROBE

THERMAL CONTROL

- EVALUATE VARIOUS PASSIVE AND ACTIVE MEANS OF CONTROLLING THE THERMAL ENVIRONMENT OF THE ENTIRE PALLET-MOUNTED MULTIPROBE SYSTEM AND OF EACH INDIVIDUAL DEPLOYED MULTIPROBE.

TRACKING

- EVALUATE THE FOLLOWING ALTERNATIVE METHODS FOR OBTAINING POSITION DETERMINATION TO AN ACCURACY OF 200 m:
 - (1) TONE-RANGING WITH DIRECTIONAL ANTENNAS
 - (2) TONE-RANGING WITH OPTICAL FIXES AND ORBITAL MECHANICS CALCULATIONS
 - (3) GLOBAL POSITIONING SYSTEM
 - (4) ORBITER RENDEZVOUS RADAR WITH TRANSPONDERS

COMMUNICATIONS

- EVALUATE USE OF THE 401 TO 402 MHz BAND WITH DEDICATED MULTIPROBE TRANSMITTER AND RECEIVERS ON SPACELAB AND, ALTERNATIVELY, S-BAND COMMUNICATIONS WITH THE ORBITER PAYLOAD INTERROGATOR.

COMMAND AND DATA MANAGEMENT

- EVALUATE OPTIONS FOR THE PROCESSING OF COMMANDS AND DATA ON BOARD SPACELAB AND AT EACH MULTIPROBE. IDENTIFY THE NEED FOR AND THE UTILIZATION OF THE SPACELAB DDU AND EXPERIMENT COMPUTER, A SPACELAB-BASED DEP, COMMAND ENCODER, AND DATA ACQUISITION SYSTEM, AND A MULTIPROBE-BASED COMMAND DECODER AND DATA ACQUISITION SYSTEM.



MULTIPROBE TRADE STUDIES

J. L. BURCH

NOVEMBER 5, 1979

PAYLOAD AND MISSION SPECIALIST SUPPORT

- DEFINE THE ROLE OF CREW MEMBERS IN EJECTING AND TRACKING MULTIPROBES
- DEFINE THE ROLE OF CREW MEMBERS IN CONTROLLING THE MULTIPROBES IN ORBIT IN COORDINATION WITH OTHER SPACELAB FACILITIES SUCH AS WISP AND SEPAC

FUNCTIONAL OBJECTIVES

- DEFINE SCIENTIFIC EXPERIMENTS TO BE CARRIED OUT WITH THE MULTIPROBES AND IDENTIFY OTHER REQUIRED SPACELAB FACILITIES
- DEVELOP A STRAWMAN MISSION TIMELINE TO INCLUDE EFFECTS OF MULTIPROBE ORBITAL MECHANICS AND SEPAC AND WISP BEAM AND WAVE INJECTION CHARACTERISTICS

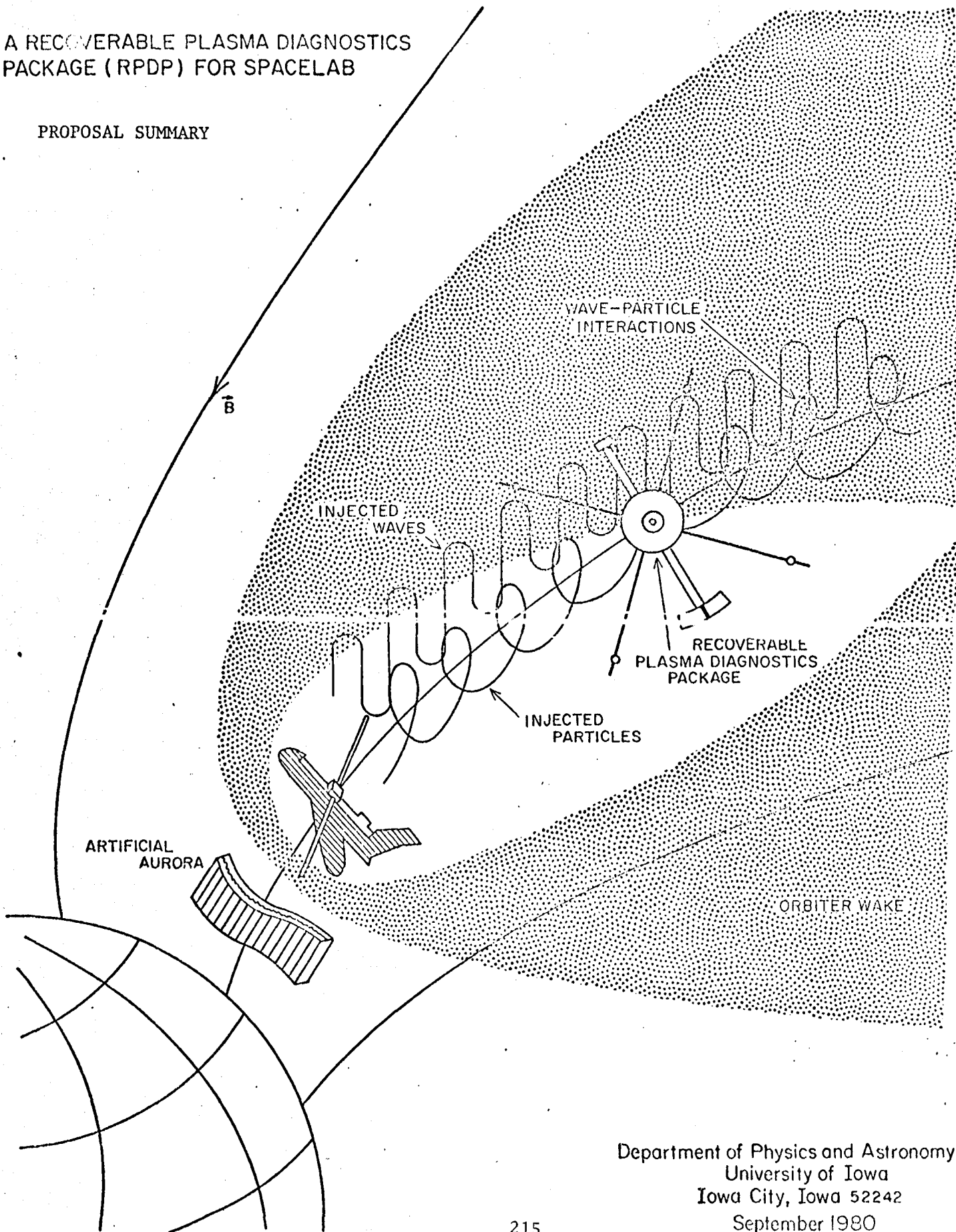
ORBITAL ANALYSIS

- EVALUATE FEASIBILITY OF ACHIEVING THE REQUIRED RELATIVE POSITIONS AMONG THE MULTIPROBES AND SPACELAB.
- DETERMINE OPTIMUM DRAG COEFFICIENTS FOR MULTIPROBES
- DETERMINE OPTIMUM LAUNCH CONDITIONS AND ORBITAL PARAMETERS TO MEET THE MULTIPROBE FUNCTIONAL OBJECTIVES

SECTION XII. RECOVERABLE PLASMA DIAGNOSTICS
PACKAGE (RPDP)

A RECOVERABLE PLASMA DIAGNOSTICS PACKAGE (RPDP) FOR SPACELAB

PROPOSAL SUMMARY



Department of Physics and Astronomy
University of Iowa
Iowa City, Iowa 52242
September 1980

A RECOVERABLE PLASMA DIAGNOSTICS
PACKAGE (RPDP) FOR SPACELAB

PRINCIPAL INVESTIGATOR:
STANLEY D. SHAWHAN
DEPARTMENT OF PHYSICS & ASTRONOMY
THE UNIVERSITY OF IOWA
IOWA CITY, IOWA 52242
PHONE: 319/353-3294

SUBMITTING INSTITUTION:
DEPARTMENT OF PHYSICS & ASTRONOMY
THE UNIVERSITY OF IOWA
IOWA CITY, IOWA 52242
HEAD: PROF. JAMES A. VAN ALLEN
PHONE: 319/353-4531

CO-INVESTIGATORS:

K. L. Ackerson
R. R. Anderson
J. D. Craven
N. D'Angelo
L. A. Frank
D. A. Gurnett
R. R. Shaw
Dept. of Physics & Astronomy
The University of Iowa
Iowa City, Iowa

L. P. Block
C.-G. Falthammar
Department of Plasma Physics
Royal Institute of Technology
Stockholm, Sweden

M. Sugiura
Electrodynamics Branch
NASA/GSFC
Greenbelt, Maryland

J. H. Hoffman
Center for Space Sciences
University of Texas at Dallas
Richardson, Texas

W. W. L. Taylor
TRW Defense & Space Systems
Group
Redondo Beach, California
(Coordinator for WISP)

T. Obayashi
Institute for Space & Aeronau-
tical Science
University of Tokyo
Tokyo, Japan
(Coordinator for SEPAC)

P. M. Banks
Department of Physics
Utah State University
Logan, Utah
(Coordinator for VCAP)

N. H. Stone
Space Sciences Laboratory
NASA/MSFC
Huntsville, AL

U. Samir
Space Physics Research
Laboratory
University of Michigan
Ann Arbor, Michigan

INVESTIGATION SUMMARY
RECOVERABLE PLASMA DIAGNOSTICS PACKAGE

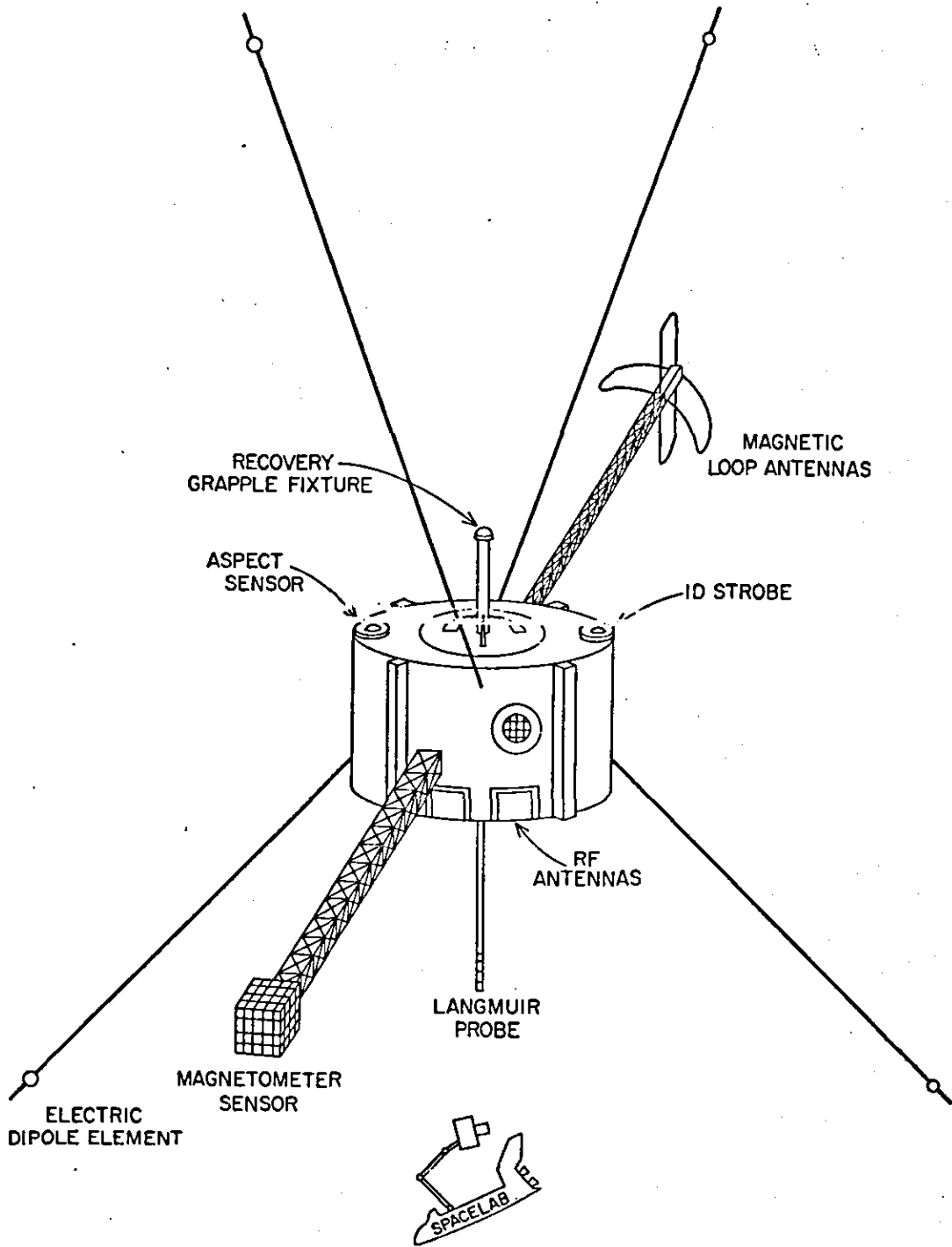
In response to NASA AO-OSS-2-78, the University of Iowa proposed a Recoverable Plasma Diagnostics Package (RPDP) as an essential element for the cost-effective use of the Space Shuttle to conduct research in space plasma physics and related disciplines on the Spacelab Missions. This RPDP program is a continuation of the ejectable Plasma Diagnostics Package investigation under development for the OSS-1 and Spacelab 2 Missions.

The RPDP is a fully instrumented, ejectable and recoverable unit with flight and ground support systems so that it can be utilized attached to the Orbiter Remote Manipulator System, tethered from the Orbiter, or as an Orbiter Subsatellite to (200 km range with an operation time up to 200 hours from batteries. Core instruments on the RPDP are flight-proven hardware which provide diagnostics measurements of energetic particles (electrons and ions, 2eV to 50keV), AC electromagnetic and electrostatic waves (5 Hz to 30 MHz), vector magnetic field signatures of current systems ($> 2\gamma$), vector electric field signatures associated with plasma flow and particle acceleration (> 1 mV/m), thermal plasma ion composition and density ($1-64$ AMU $> 1\text{cm}^{-3}$), thermal plasma electron density and temperature (10^2 to 10^7 cm^{-3} , 1×10^2 to 1×10^4 K) and images of optical emission regions in UV (1100-1700A) or visible (3900-6300A) wavelengths.

Two investigations utilizing the RPDP are the basis for the definition phase: diagnosing the dynamics and consequences of particle beams injected into the magnetosphere from an Orbiter-borne accelerator (SEPAC system by Obayashi et al.) and diagnosing the emission and propagation characteristics of waves injected from an Orbiter-borne transmitter (WISP system by Fredricks et al.) or by means of a conducting tether. Studies, initiated by the PDP on OSS-1 and Spacelab 2, are to be continued for wave, particle and field effects stimulated by the motion of the large-sized Orbiter through the magnetized plasma and for naturally occurring magnetospheric phenomena.

Based on the OSS-1 and Spacelab 2 design, a new PDP unit is to be developed which can accommodate a more flexible complement of instruments and the necessary hardware and electronics subsystems to make the PDP recoverable. Existing PDP flight support and ground support equipment are to be modified to accommodate the RPDP. The major development item is the Special Purpose End Effector which is to effect ejection and recovery of the spinning RPDP (5 to 20 RPM).

Once in existence, the RPDP can provide a cost-effective and comprehensive means of diagnostics for Spacelab experiments such as the Shuttle electrodynamics tether, plasma flow around bodies, magnetospheric multiprobes, chemical release modules, plasma depletion experiments, sheaths around large structures in space, auroral electrodynamics and tethered atmospheric probes. For such follow-on missions several additional instruments can be accommodated.



A. GENERAL SCIENTIFIC OBJECTIVES

- § Continue to study the Orbiter-magnetoplasma interactions such as density wakes, energized plasmas, dc electric fields, and wave-particle instabilities.
- § Investigate the dynamics of the primary particle beams ejected from the Orbiter via SEPAC and the characteristics of the secondary and tertiary energetic plasma below 50 keV by measurement of the particle distribution functions with the quadrispherical low energy proton and electron differential energy analyzer (LEPEDEA) within 100km range of the Orbiter. Characterize the induced wave and optical emissions, the current systems and the electric field regions both in the vicinity of the Orbiter and remote to it.
- § Measure the transmitting antenna radiation pattern and the propagation and mode coupling characteristics of electrostatic and electromagnetic waves injected by the Orbiter, via WISP, in the range of 0.3 kHz -30 MHz with a step frequency correlator receiver and antennas. Characterize the ambient plasma and induced modifications such as particle acceleration and precipitation.
- § Within a range of 100 km from the Orbiter, probe the microscale properties of wave-particle interactions induced by joint operations of wave and particle beam injectors and the RPDP.
- § Support investigations which may be carried out with the Magnetospheric Multiprobes, Chemical Release Module and Tether System investigations.

B. RECOVERABLE PLASMA DIAGNOSTICS PACKAGE DESCRIPTION

1. General Description of the Recoverable PDP and Operating Scheme

The major subsystems which make up the RPDP Flight and Operations system are identified in Figure 1. In Table 1 the function of each major subsystem is stated and its performance characteristics are specified.

Taken together the RPDP systems provide for a plasma diagnostics package which can be operated on the RMS, tethered to the Orbiter or released from and recovered by the Orbiter to serve as a reusable subsatellite. Figure 2 depicts the interfaces to Spacelab. The Recoverable Plasma Diagnostics Package (RPDP), shown as an artist's conception as part of the Summary, is latched to the Spacelab pallet structure by the Release Mechanism (REM) which is controlled via the Payload Retention Panel in the aft flight deck (AFD). The Recovery Special Purpose End Effector (RSPEE) provides the mechanical and electrical interface to the Remote Manipulator System which allows the RSPEE to be controlled from the Standard Switch Panel in location L12 in the AFD. Spin-up, deployment on-orbit and retrieval of the RPDP are effected by the RSPEE. Once the RPDP is released from the REM it operates on batteries and commands are transmitted and data received through the 400 MHz RF antenna (RFA) located on the pallet. Commands and data processing are controlled by the Receiver and Data Processing Electronics (RDP) which are mounted under the pallet shelf on a cold plate. This unit contains the command generator

FIGURE 1. FLIGHT HARDWARE ITEMS¹

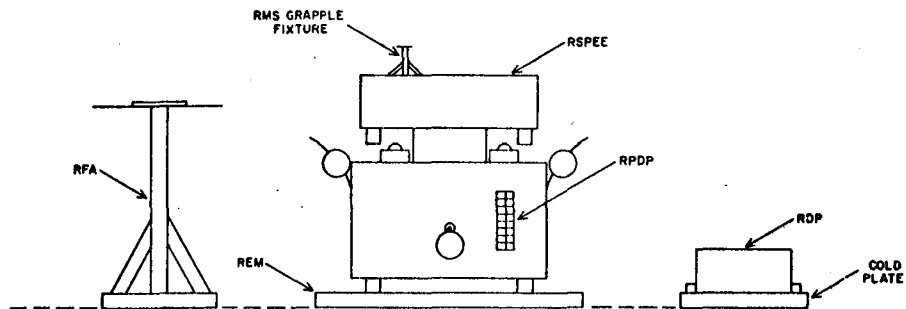
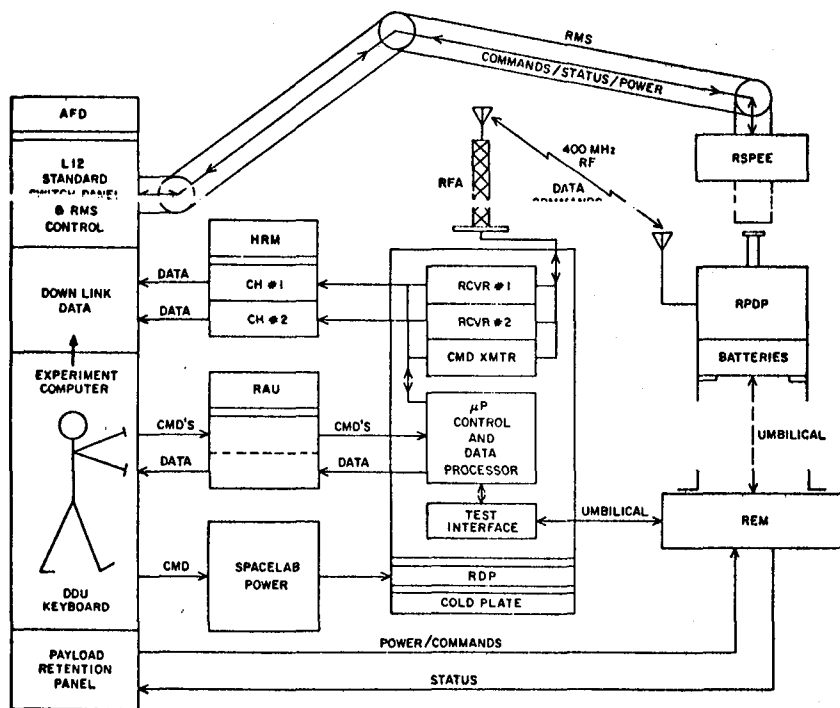


FIGURE 2. SPACELAB/RPDP INTERFACES¹



- ¹KEY
- RPDP : RECOVERABLE PLASMA DIAGNOSTICS PACKAGE
 - RFA : RADIO FREQUENCY ANTENNA
 - REM : RELEASE MECHANISM
 - RSPEE : RECOVERY SPECIAL PURPOSE END EFFECTOR FOR RMS
 - RMS : REMOTE MANIPULATOR SYSTEM
 - RDP : RECEIVER, COMMAND TRANSMITTER AND DATA PROCESSING ELECTRONICS

TABLE 1. SPECIFICATIONS FOR RPDP SUBSYSTEMS

SUBSYSTEM: FUNCTION	PARAMETER: SPECIFICATION
<p><u>Recoverable Plasma Diagnostics Package (RPLP):</u> Houses scientific instruments and subsystems on RMS and as subsatellite</p>	<p>Size 107 cm dia x 66 cm high Weight 250 kg Energy 9 KWH from batteries Power. 45-90 watts Operating Life 100-200 hours Accommodations 6-10 scientific instruments Telemetry. 400-402 MHz UHF band, 1 watt Downlink #1 32 kbps PCM data Downlink #2 50 kHz analog data Uplink. Commands, sync signal, tone ranging Telemetry Range. 100-200 km Commands 32 for S/C functions & data mode Data System. RCA 1802 μP based Antennas 4 of 15 m - tubular type/retractable Booms. 2 of 3 m - telescoping/retractable Aspect Star sensor, sun sensor, triaxial magnetometer for $\pm 0.1^\circ$ accuracy ID Strobe. 1 or 2 - 40 flashes/minute</p>
<p><u>Recovery Special Purpose End Effector (RSPEE):</u> Provides mechanical and electrical interface to the RMS and spin-up, release and recovery of the RPDP</p>	<p>Size 91 cm x 91 cm x 45 cm Weight 100 kg Power. 50 W average, 150 W peak DC RMS Interface. Electrical grapple fixture Control & Status Standard switch panel L12/AFD Spin-up Range. 5-20 RPM $\pm 10\%$ in < 1 minute</p>
<p><u>Release Mechanism Assembly (REM):</u> Mechanically latches RPDP to Spacelab pallet and provides electrical umbilical connection to test RPDP (Developed by MSFC for EECM)</p>	<p>Size 120 cm x 142 cm x 16 cm Weight 53 kg Power. 118 W peak DC; 450 W peak AC Technique. Guide rails for x, y location; secured by motor-driven screws Control & Status Packaged reception panel in AFD</p>
<p><u>Receiver and Data Processing Electronics (RDP):</u> Houses RF data receivers and command transmitter; interfaces to RAU and HRM; processes data and commands</p>	<p>Size 33 cm x 50 cm x 30 cm Weight 20 kg Power. 50 W DC Thermal Control. Cold plate mounted RAU Interface. Analog Inputs - 32 Discrete Outputs - 40 Discrete Inputs - 40 Serial Commands - 1 Serial Inputs - 1 All data available to DDU & POCC HRM Interface. Channel 1 - 1.2 Mbps Channel 2 - 32 kbps Data/Control System. Intel 8085 μP based</p>
<p><u>RF Antenna Assembly (RFA):</u> Receives 400 MHz telemetry data from RPDP and transmits 400 MHz uplink commands & sync signals</p>	<p>Size 40 cm x 40 cm x 2 cm plate on top of ~ 150 cm mast Weight 15 kg Power. None Technique. Dual polarized microstrip Pattern. +8 dBI along +Z, -30 dBI along -Z</p>
<p><u>Experiment Ground Support Equipment (EGSE):</u> Processes RPDP data from HRM, RAU and OI stream in POCC</p>	<p>Complement 2 Chromeco Z-80 microcomputers with peripherals for controlling RPDP, displaying, listing and tape recording data.</p>

and transmitter and the data receivers for the RF links to the RPDP. Included also are a microprocessor and interface electronics for command and data processing to provide two data streams to the High Rate Multiplexer (HRM) and to exchange data and commands with the Remote Acquisition Unit (RAU). Commands to the RPDP can be issued either by the POCC or by the crew through the keyboard and experiment computer. Data and housekeeping parameters from the RDP are available for display on the DDU via the RAU and experiment computer.

The Definition Phase study will include tasks to verify the following proposal assumptions: The REM will exist as part of both the MSFC IECM program and the U of Iowa PDP on OSS-1 and Spacelab 2 programs. It can be used without modification. On Spacelab 2 the PDP is to be released and not recovered so that the RPDP must be fabricated based on the PDP structural and electrical subsystem designs with modifications to accommodate the recovery mechanism, several more scientific instruments and more complex, but more flexible, subsystems such as the command/sync signal uplink and the microprocessor-based data system. A SPEE for spin-up and deployment of the Spacelab 2 PDP will exist, however, because of cost constraints, it will not be capable of effecting recovery. The added capability of recovery requires careful design and consideration because of the safety aspects; this design and fabrication is to be subcontracted. The RF Antenna can probably be used without modification. It provides hemispherical coverage about the Orbiter +Z axis with good suppression of Orbiter EMI in the -Z hemisphere. Data receivers, the microprocessor data processing elements, and RAU and HRM interface circuits from the Spacelab 2 RDP can be utilized. Additions to the RDP include the command generator and command transmitter as well as expansion of the RAU interface and the microprocessor ROM and RAM.

Once on-orbit, the Payload Specialist will be required to carry out a functional check of the RPDP by issuing commands through the keyboard and monitoring housekeeping and scientific parameters on the DDU. To deploy the RPDP, the RMS operation grapples the electrical grapple fixture on the RSPEE using the CCTV; the REM is then operated to release the combined RPDP and RSPEE units; Orbiter attitude is adjusted and the RMS articulates the RPDP so that it will be deployed in the cartwheel mode--the RPDP spin plane is parallel to the Orbiter's orbital plane. The RSPEE is controlled and monitored via the L12 Standard Switch Panel; functions include heater, spin-up to preset rate in the 5-20 RPM range and separation. Commands sent to the RPDP prior to spin-up are used to partially extend the booms and antennas to establish a stable dynamic configuration for the RPDP. Once spin-up and separation are effected, the Orbiter is flown away from the RPDP to a prescribed position in order to carry out experiments. The Payload Specialist will be required to carry out predefined experimental programs by operating the particle beam and/or wave injectors and by monitoring the results from the RPDP. The Payload Specialist will then make adjustments in parameters such as RPDP location, transmitter frequency, etc., to optimize the results. After completion of the mission objectives, the Orbiter is to rendezvous with the RPDP. Commands are sent to retract the booms and antennas and the RSPEE spin rate is matched to that of the RPDP. Recovery is monitored through use of the CCTV, the RPDP is restowed on the REM and the RMS is ungrappled and stowed.

2. Orbiter Resource Requirements

Orbiter resource requirements in terms of size, weight, power, command, and data handling and operating modes are given in Table 1.

3. PDP Launch/Recovery System Concept

The launch/recovery system for the RPDP represents a somewhat new development item which may represent a safety hazard especially during recovery operations. A Special Purpose End Effector (SPEE) for the RMS is being developed by Ball Aerospace Systems Division for launch of the Spacelab 2 PDP which provides a design base and relevant experience with qualification tests and safety aspects.

Two feasible launch/recovery concepts developed by Ball Aerospace and Spar Aerospace were included in the original proposal. Highlights of the concepts are as follows:

- § *Ball--The Spacelab 2 SPEE is modified to handle multiple satellites. The SPEE latches to a cone and probe device on the RPDP that is similar to the standard grapple fixture. This SPEE provides spin-up and launch. For recovery the RPDP is yo-yo despun to 5 RPM or less and grasped by the standard end effector.*
- § *Spar--A spin joint is to be inserted between the standard end effector and the wrist roll joint of the Remote Manipulator System. This approach is possible because the SEE is a "Line Replaceable Unit". This spin joint provides the spin-up and spin-down function while the SEE provides the release and recapture functions. Only a standard grapple fixture is required on the RPDP.*

Iowa proposes to issue three design contracts for this SPEE during the definition phase and one development and testing contract to a selected aerospace vendor during the development phase.

In order to recover the PDP, the deployed booms and antennas must be retracted or severed. Of concern is the possibility that the RPDP batteries would be depleted of energy before recovery is possible. To avoid this situation, it is proposed to provide a separate battery pack with sufficient energy to continually operate a command receiver and to operate motors and/or pyrotechnics as required to ready the RPDP for recovery. Since there is a possibility that the RPDP might have to be stored on-orbit between Spacelab flights due to a contingency situation, consideration will be given to using a small solar cell array to keep this recovery battery pack charged.

4. Objectives For Possible RPDP Follow-on Missions

With minor refurbishment and the addition or change of instrumentation the RPDP can be used on many different sorts of investigations. Some of these are depicted in Figure 3. Note that the RPDP might be combined with the teleoperator or IUS to attain an orbit significantly different from the Orbiter.

Three possible follow-on investigations are described as follows:

RECOVERABLE PLASMA DIAGNOSTICS PACKAGE FOLLOW-ON MISSIONS

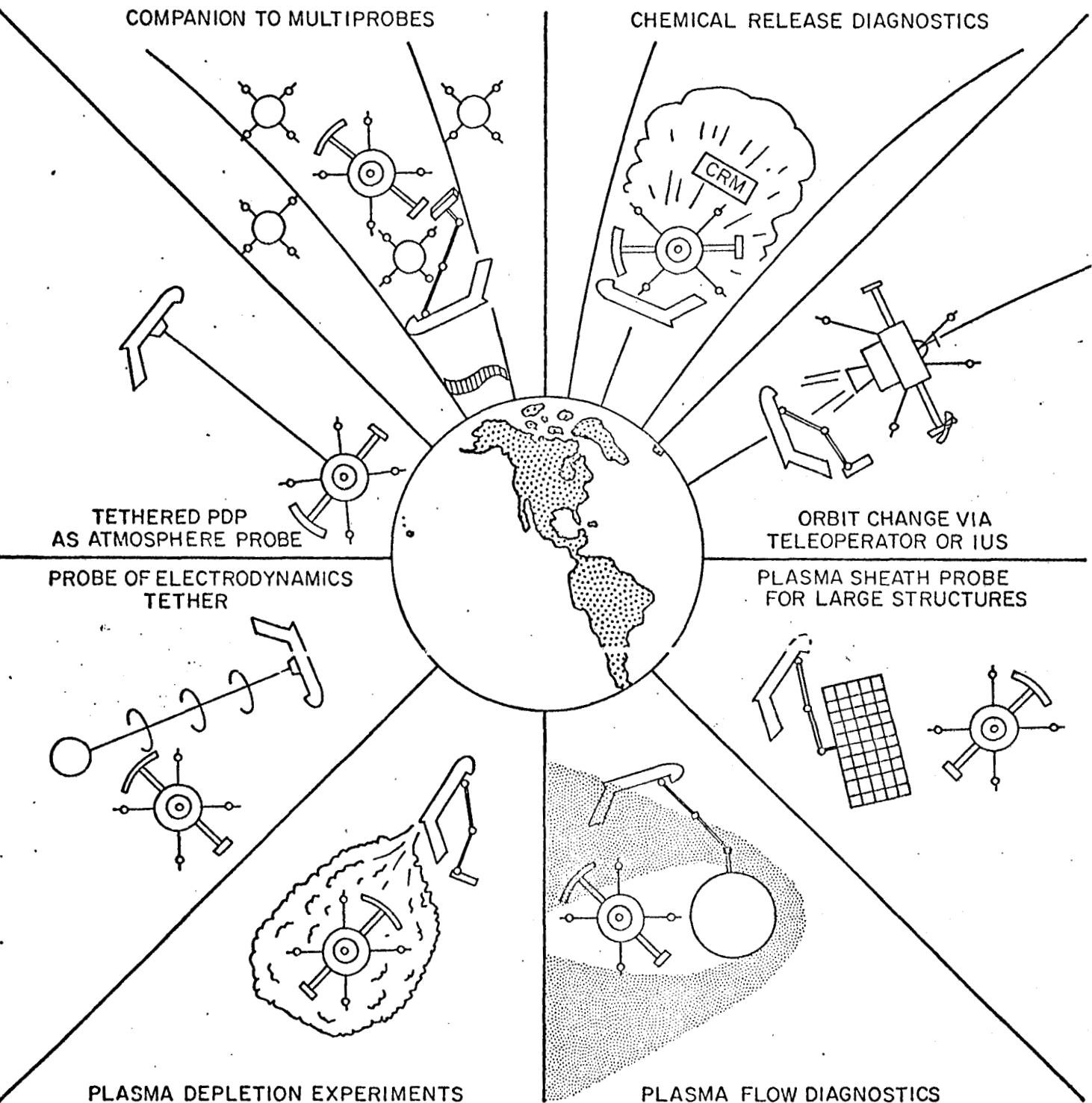


FIGURE 3

(a) Plasma Flow Investigation and Required Instrumentation (N. H. Stone/MSFC)

The Space Shuttle and its payload are capable of serving as a near-earth plasma laboratory which uses the ionospheric plasma as a natural collisionless and unbounded working medium. The use of the methods of laboratory plasma physics in earth-orbit will provide a great stride forward in experimental capabilities: Opening up a new range of parameter space, previously unattainable, and alleviating a number of problems inherent in earth-bound laboratories.

As a result a variety of physical processes, some of which are qualitatively similar to processes important to solar system plasma physics, can be studied over a wide range of scale sizes and plasma conditions. For example, supersonic sub-Alfvenic plasma flow can be studied in a collisionless regime; the range of scale sizes will enable a direct comparison of the continuum-MHD and kinetic theories, thereby establishing the range of applicability of single fluid MHD models, possibly determined quantitatively by the ratio of the body sizes to the ion Larmor Radius ($R_0/L+$); and the interaction of the satellite, I_0 , with the Jovian magnetosphere can be qualitatively simulated in order to study the nature of the plasma sheath in the presence of a substantial voltage drop, the possibility of an associated charged particle acceleration mechanism, and the resulting field aligned circuit system--all of which are thought to be characteristic of the I_0 interaction. Such an extrapolation from experiments conducted in the ionosphere to the plasma physics of the solar system is analogous to the extrapolation from heliospheric plasma processes to astrophysical phenomena advocated by the Space Science Board.

This application of the Shuttle as a near-earth plasma laboratory will be the subject of a proposal to be submitted next year by N. H. Stone, U. Samir, and others. It should be emphasized here that the PDP will be a necessary component of these studies.

To conduct these experiments, it will be necessary to have a test body to generate the plasma disturbance and a set of diagnostic instruments to measure the characteristics of the disturbed plasma flow. Control of the relative position of the instrument package with respect to the test body is required to effect a mapping of the flow field. It is also desirable to simultaneously monitor certain characteristics of the ambient atmosphere.

The required diagnostic instrumentation can be carried on the PDP. This would include instruments to measure the ion and electron temperatures and densities, the ion drift velocity (magnitude and direction), the ion mass, and the local space potential. The space potential should be measured with sufficient temporal resolution to detect oscillations in the range of the ion plasma and ion cyclotron frequencies. With the exception of the vector flow velocity, all of these measurements can be made by standard plasma diagnostic instruments. The vector velocity measurements can be made with the Differential Ion Flux Probe (DIFP) which has recently been developed at MSFC and will fly as part of the Spacelab 2 PDP experiment. It may be decided that this instrument should be included on the RPDP proposed here.

A small (one-meter diameter) spherical conducting body mounted on the Shuttle RMS is being proposed by P. M. Banks, et al. This body would be available for these experiments and would provide the lower-end of the range of scale size needed for the comparison of the continuum and kinetic theories (i.e., $R_0/L+\ll 1$). In addition, Banks' proposal will include diagnostics which can measure ion and electron densities and temperatures out to two meters from the body surface. This would combine ideally with the PDP instrumentation

which would be used to measure the disturbed flow field at larger distances (out to ~100 m) while the instrumentation from the Banks' experiment would be used to monitor the ambient conditions. A mapping of the flow field would be effected by a combination of varying the stand-off distance to the free-flying PDP, downstream from the test body, by maneuvering the Shuttle and manipulation of the test body position normal to the flow direction with the RMS.

In later experiments, bodies with diameters of ~10 m ($R_0/L \approx 1$) and ~100 m ($R_0/L \gg 1$) would be used to complete the desired range of scale sizes. The 10 m diameter body can be manipulated by the RMS in conjunction with a free-flying PDP as described above for the 1 m body. However, the 100 m body will require a tether system and some capability to maneuver the PDP-- possibly with the MSFC teleoperator.

In summary, the PDP is a necessary component for experimental investigations of plasma flow interactions with obstacles in earth-orbit which are applicable to space plasma physics, and in particular to solar system plasma physics. The PDP can be used directly in initial small-body studies, and possibly with some modification to allow maneuverability in later large-body studies. A reusable PDP is particularly cost effective in this class of experiments, since the complete investigation will involve an evolutionary series of experiments carried out over a number of different Shuttle missions.

(b) Neutral Atmosphere Wind, Composition and Temperature (W. R. Hoegy and N. W. Spencer/GSFC)

In the recent past, measurement of neutral gravity wave properties have provided only a few of the parameters necessary to determine the wave characteristics. Some of the neutral wave parameters have been indirectly inferred from the observations of traveling ionospheric disturbances (TID's). A unique specification of the neutral waves (period, wavelengths and direction of propagation) is possible only with simultaneous in situ measurements of neutral wind, temperature, and composition data (Hoegy et al., 1978). A spectral analysis of the data gives wave amplitudes and phases for one component of the wind, temperature and composition. Linear gravity wave theory is used to convert the amplitudes and phases into the wave parameters ω and k , which are needed to compute the velocity of wave energy propagation and eventually the wave source. Flights of an instrument which provides wind, temperature, and composition data are needed for a complete and accurate determination of gravity wave characteristics, and for comparison with simultaneous TID observations.

Instruments meeting these requirements will be employed on the Dynamics Explorer B and San Marco D1 spacecraft. Three components of the winds (vertical, orbit plane normal, and horizontal in-plane) will be measured in situ on these spacecraft using an advanced design based on first generation instruments providing similar data on AE. In situ kinetic temperature (N_2 and O) as well as composition are time sequenced measurements. The temperature measurement technique involves determination of the velocity distribution among the particles of a particular gas, usually N_2 , from which the kinetic temperature is calculated. The wind velocity components are determined through the use of a baffle which modulates the stream of gas entering the mass spectrometer allowing determination of the angle of entry with respect to the spacecraft velocity vector. The vertical and orbit normal components are measured in this way, but the in-plane component is determined in an "rpa"

manner by decelerating the ionized component of the incoming gas stream and computing the resulting velocity effect. Composition is determined using the instrument in the usual mass spectrometer mode.

References:

Hoegy, W. R., P. L. Dyson, L. E. Wharton, and N. W. Spencer, Neutral atmosphere waves determined from Atmosphere Explorer measurements, NASA TM #79670, November 1978.

Spencer et al., Geophys. Res. Ltrs., Vol. 3, #6, 1976.

Spencer et al., The midnight neutral (N_2) temperature maximum, (in preparation).

(c) The Cornell DELTA N Experiment (M. Kelley/Cornell)

The Cornell University DELTA N experiment is designed to detect the fluctuating density component of electrostatic waves generated both naturally in the near space region of the Earth and artificially by active experiments conducted from the Space Shuttle. The detector is sensitive to waves with frequencies from dc to 10 kHz which corresponds to wavelengths from zero order background scale lengths to a few Debye lengths. Such waves are very important in a low temperature plasma such as the ionosphere and low altitude magnetosphere since their phase velocities are comparable to either the thermal velocity of the constituents or to the drift velocity of species due to applied forces such as electric fields, pressure gradients and gravitational fields. Their role is equally important in active experiments since they can be directly produced by beams, antennas, and chemical releases or be generated in a multi-step process by instabilities or parametric decay of large amplitude electromagnetic or electrostatic waves. In addition to the direct production of electrostatic waves in active experiments, there are important processes in the background plasma which can feed back on the primary beam or wave. An example is the self-focusing effect on electromagnetic waves near the electron plasma frequency observed in the ground based HF heating experiments. This is caused by plasma heating which reduces the density locally and which in turn causes a focusing effect on the waves and creates more heating. The DELTA N experiment is ideally suited for detection of such induced structures with wave number perpendicular to the magnetic field. Effects of naturally occurring plasma gradients and irregularities will also be measurable with the detector.

The sensor is a cylinder 15 cm long and 1 cm in diameter deployed parallel to the spin axis on a rigid BeCu boom a distance of 3 m. The collecting surface is coated with a colloidal suspension of carbon with excellent surface properties. Guard rings 1 cm in length are located at each end of the active surface. A 15 cm long cylindrical section of the boom located .5 cm from the sensor is free of the insulating surface and acts as a floating reference potential for the sensor bias. The high data rate channel has automatic gain control to maintain a good signal to noise ratio and is proportional to the relative fluctuations in plasma density, $\delta n/n$, independent of n . This covers the frequency range 1-10,000 Hz. A dc coupled output, proportional to the log of the plasma density, covers the range from 0-50 Hz. The latter yields an accurate relative density measurement in fluctuations due

to long wavelength irregularities or waves and absolute density with an accuracy of 50%.

The basic electronics weighs 2 kg, package occupies a volume of 1500 cm³ and consumes 2.6 watts of electrical power at 28 volts. The boom system is deployed with a typical pyrotechnic firing pulse of short duration. The stowed outline dimensions of the boom system are a 10 cm diameter cylindrical volume 50 cm in length with long axis parallel to the spin axis. It could be mounted on the outside of the spacecraft. If other than real time wave data is necessary or desirable a spectrum analyzer can be provided with an increase in power of 2 watts and 1 kg in weight.

C. RPDP INSTRUMENT DESCRIPTIONS

A core set of instruments essential to the particle beam and wave injection investigations are to be defined. These instruments are identified and briefly described along with a detailed specification of the measured parameters in Table 2 "Performance Characteristics for RPDP Core Instruments." The heritage and operating principles of each of these instruments are as follows:

1. Correlating Step Frequency Receiver (Gurnett, Shaw, Anderson/Iowa)

For ISEE-1 a four band step frequency receiver was developed. For the Dynamics Explorer-A (DE-A) mission, two of these receivers are being combined with correlating detectors to produce a step frequency correlator covering the range of 100 Hz to 400 kHz.

For the RPDP it is desired to add two bands of 400 kHz to 3.2 MHz and 3.2 MHz to 25.6 MHz to cover the gyrofrequency ((1 MHz) and plasma frequency ((10 MHz) and harmonics in the upper ionosphere. This development is to make the receivers step faster and to extend the dynamic range of each band as well. Also this receiver is to utilize a microprocessor for control of the receiver parameters such as bandwidth, sweep rate, sweep range and antenna selection.

In the present scheme, a master 4 MHz oscillator is divided down to provide the intermediate mixing frequency. The divide-by circuit is controlled by a ROM. Within each band an 8:1 frequency range is covered. A second mixing frequency of 1 MHz is common to all the receivers. These conversion processes are single sideband so that the phase information is preserved and the two receivers for the same band are phase-locked. The output for each band is fed to a log compressor to give amplitude information over (110 dB range and then to a quadrature phase shift network to produce in-phase and quadrature phase components. These components from each band receiver are correlated to produce sine and cosine correlation coefficients from which the relative phase and correlation between signals from two different antennas can be obtained at 192 frequencies from 100 Hz to 25 MHz.

Correlation between the two magnetic antennas can provide the wave normal vector; between two electric antennas the wave polarization and the phase velocity of electrostatic waves; and between electric and magnetic antennas the Poynting vector and the discrimination between electromagnetic and electrostatic waves. Also, the correlation between a single antenna and a reference signal uplinked from the Orbiter can be used for doppler sounding. Measurement of these wave characteristics are necessary to carry out the wave injection investigation and to assess waves generated by beam-plasma interactions. Sample ISEE results are shown in Figure 4A.

TABLE 2. PERFORMANCE CHARACTERISTICS FOR RPD CORE INSTRUMENTS

INSTRUMENT: MEASUREMENT	PARAMETER: SPECIFICATION
<p><u>Step Frequency Correlator:</u> Measures amplitude and phase between signals from any two sensors; sensors include 4 electric monopoles combined electronically to give triaxial dipoles and crossed magnetic loops to provide 3 magnetic components in 1/4 spin period.</p>	<p>Frequency Range 6 bands: 100-780 Hz, 780-6250 Hz, 6.25-50 kHz, 50-400 kHz, 0.1-3.2 MHz, 3.2-25.6 MHz Frequency Step 32 frequencies/band; log spaced Frequency Resolution ~1% Time Resolution 4 spectra/second Dynamic Range 110 dB Amplitude Resolution 0.5 dB E-range 10^{-8} to $3 \times 10^{-3} \text{ Vm}^{-1} \text{ Hz}^{-1/2}$ B-range 10^{-6} to $3\gamma \text{ Hz}^{-1/2}$ Phase $0-360^\circ \pm 5^\circ$ Correlation $\pm 1.0, \pm 5\%$</p>
<p><u>Quadrispherical LEPEDA:</u> Measures distribution function for supra-thermal electrons and ions</p>	<p>Energy Range 2 eV-50 keV in 48 steps Field of View $6^\circ \times 162^\circ$ Angular Resolution 7 detectors: $9-18^\circ, 18-39^\circ, 39-71^\circ, 71-109^\circ, 109-141^\circ, 141-162^\circ, 162-171^\circ$ Energy Resolution 34% Geometric Factors $10^{-3} \text{ cm}^2\text{-sr}$ electrons, $4 \times 10^{-4} \text{ cm}^2\text{-sr}$ prot. Time Resolution 1 sec for energy-angle scan 1 spin period for distribution function</p>
<p><u>Ion Mass Spectrometer:</u> Measures ion composition of ambient plasma</p>	<p>Density Range 1 to 10^8 ions cm^{-3} Mass Range 1-64 AMU in 3 channels Time Resolution 0.2 sec/channel</p>
<p><u>Triaxial Magnetometer (Fluxgate):</u> Measures vector components of geomagnetic field and perturbations to the field caused by localized current systems</p>	<p>Frequency range DC to 5 Hz each axis Range ± 0.6 gauss each axis Dynamic Range 15 bits = $\pm 2\gamma$ resolution Aspect knowledge $10:1 - 100:1$ absolute perturbation vector</p>
<p><u>DC Electric Field/Langmuir Probe:</u> Measures vector components of electric fields in plasma associated with localized space charge regions or plasma convection. Also sweeps sensors to determine characteristics of thermal electron plasma.</p>	<p>Electric Field Range 1 mV/m to 1 V/m Time Resolution 16 samples/second each axis Density 10^3-10^7 electrons cm^{-3} Temperature Range 500-10,000°K for electrons Sample Resolution 10 probe sweeps/second</p>
<p><u>Spin-Scan Imaging System:</u> Measures light intensity as a function of position for a selected wavelength range in the UV or visible (but not both) to produce an image of the emitting region.</p>	<p>Pixel Size $0^\circ 25 \times 0^\circ 25$ Collimator Field of View $36^\circ \times 3^\circ$ Frame Size $36^\circ \times 360^\circ$ Visible System Sensitivity (at 20 RPM) ~ 1.5 counts $(\text{kR-pixel})^{-1}$, 3914Å (N_2^+), 5577Å (OI), 6300Å (OI) Ultra-Violet System* ~ 1.0 counts $(\text{kR-pixel})^{-1}$ Sensitivity (at 20 RPM) 1170-1240Å (Hα, 1216Å) 1240-1370Å (OI, 1304Å and 1356Å) 1370-1700Å (N_2, LBH Band) *option</p>
<p><u>Recoverable Plasma Diagnostics Package (RPDP):</u> Houses scientific instruments and subsystems on RMS and as subsatellite.</p>	<p>Size 107 cm dia x 66 cm high Weight 250 kg Energy 9 KWH from batteries Operating Life 100-200 hours at 90-45 watts Telemetry Up & Down 400-402 MHz UHF band, ~ 1 watt Telemetry Range 100-200 km Commands 32 for S/C functions & data mode Data System RCA 1802 μP based Antennas 4 of 15 m-tubular type/retractable Booms 2 of 3m-telescoping/retractable Aspect Star sensor, sun sensor, triaxial magnetometer for $\pm 0.1^\circ$ accuracy ID Strobe 1 or 2 @ 40 flashes/minute</p>

2. Quadrispherical LEPDEA (Frank and Ackerson/Iowa)

The quadrispherical low energy proton and electron differential energy analyzer (LEPEDEA) is being flown on ISEE-1 and 2. Another unit is being prepared for the OSS-1/Spacelab 2 PDP. Three quadrispherical, concentric plates with radii of curvature 10.8 cm, 11.2 cm, and 11.7 cm form two 90° electrostatic analyzers for proton (positive ion) and electron spectra, separately and simultaneously. The two outer plates are tied to circuit ground and the center plate is supplied with a variable positive potential which ranges from 0.15 V to 3500 V. This geometry of the electrostatic analyzers was chosen primarily because of its versatility and mechanical simplicity. Thus, only one curved plate with high voltage is required for two electrostatic analyzers, large energy bandwidths and geometric factors, and ability to provide angular distributions of particle intensities within a fan-shaped solid angle of view, 162° × 6°, via the introduction of multiple detectors. Within this field of view two sets of seven detectors are placed to obtain fluxes simultaneously at seven angles with respect to the satellite spin vector.

A new development is to add microprocessor control to this instrument based on the controller being designed for Galileo. Especially for the RPDP usage this controller would give the flexibility to change sweep rates, energy steps and energy ranges. Also it will be possible to sync the sweep to an external pulse such as a particle beam firing pulse. As an example, the quadrispherical LEPDEA can be operated in a single comprehensive mode for which the plate voltage is an exponentially decreasing ramp from 3500V to 0.15V. The repetition rate of this ramped voltage is once per second. Thus the differential, directional intensities of protons and electrons are sampled over the energy range 50,000 eV to 2 eV once each second. The responses of each of the fourteen electron multipliers are sampled with a 13-bit to 8-bit digital compressor and fed into the spacecraft telemetry stream. These compressors are sampled 48 times per second and hence 48-passband spectra of electron and proton intensities, each in seven directions, are acquired each second. For a spacecraft spin rate of 5 RPM there are 12 such scans of the spectra per spacecraft revolution. Complete velocity distributions of protons and electrons are gained once each 12 seconds and each comprise 4032 individual intensity samples. The inherent energy resolution of the analyzer $\Delta E/E = 0.17$, and the geometrical factors, $1.0 \times 10^{-3} \text{ cm}^2\text{-sr}$ for protons and $4.0 \times 10^{-4} \text{ cm}^2\text{-sr}$ for electrons, are considered generously adequate for measurements of low-altitude plasmas on the basis of previous applications of LEPDEA instruments on the Injun-5 and Ariel-4 missions. The geometric factors can be adjusted to detect monoenergetic, directional beams of (1 amp(m)^{-2}) from an ion or electron gun by adding a collimator with a pinhole at the entrance aperture of an electron multiplier. Sample ISEE results are shown in Figure 4B.

3. Ion Mass Spectrometer (Hoffman/UTD)

As one of the core instruments on the RPDP, an ion mass spectrometer, similar to that to be flown on the Dynamics Explorer-A spacecraft, will be used to determine the composition and density of the plasma in the vicinity of the spacecraft.

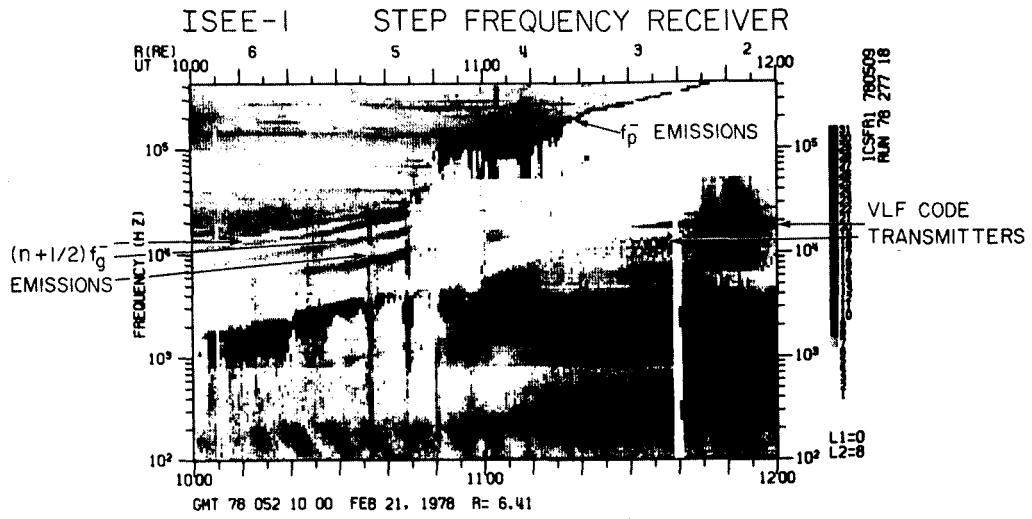


FIGURE 4A

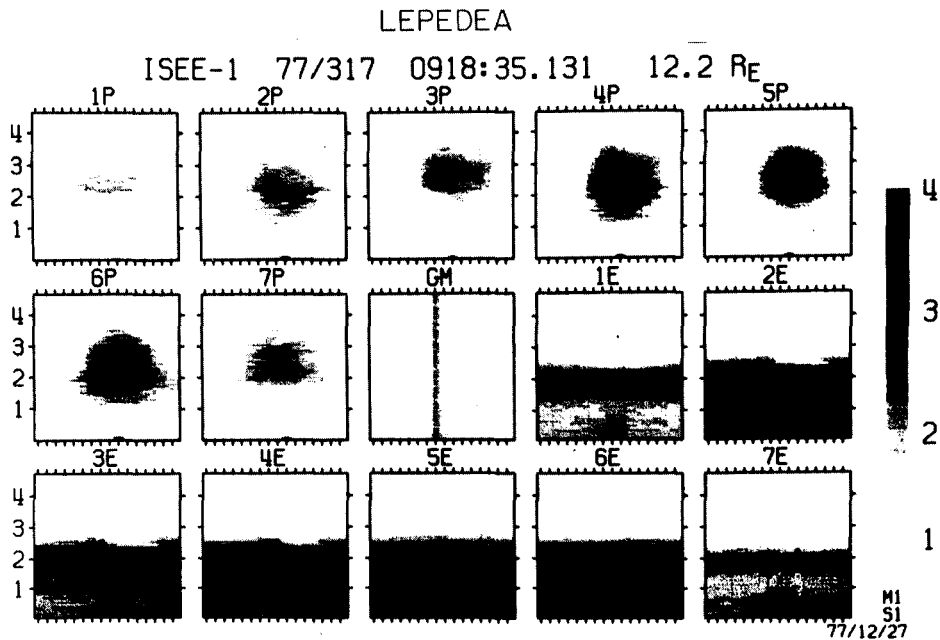


FIGURE 4B

The principal parts of each sensor are the entrance aperture containing the ion trap, magnetic analyzer, and electron multipliers. The entrance aperture is preceded by a 3-inch diameter screen flush mounted with the spacecraft skin looking out in its equatorial plane. Ambient ions entering the aperture due to the ram velocity of the satellite are collected in part on the ion trap collector which has a small hole in its center. This collector current is proportional to the total ion density. Those ions passing through the hole are post accelerated, collimated and passed through a magnetic analyzer. Three allowed trajectories lead to 3 collector slits which simultaneously collect ions in the mass ratio 1:7:14. Signal detection is by electron multipliers and log electrometer amplifiers. A useful dynamic range of over 7 decades results from a commandable multiplier gain range of 10^3 and a 5 decade log amplifier. The ion post acceleration voltage may be divided into 3 segments which may be repeatedly scanned separately or in any combination. The table below gives the ion species measured by each collector channel during each segment of the scan. Any single range is scanned in 200 ms.

<u>CHANNEL</u>	<u>RANGE 1</u>	<u>RANGE 2</u>	<u>RANGE 3</u>
A	H ⁺	D ⁺	He ⁺
B	Li ⁺ , N ⁺⁺ , O ⁺⁺	N ⁺ , O ⁺	Mg ⁺ , Al ⁺ , Si ⁺ , N ₂ ⁺ , NO ⁺ , O ₂ ⁺
C	N ⁺ , O ⁺	Mg ⁺ , Al ⁺ , Si ⁺ , N ₂ ⁺ , NO ⁺ , O ₂ ⁺	Fe ⁺

Comparison between the ion trap collector signal, which is a measure of total ion density, and the summation of all mass spectrometer output current provides an in-flight calibration of the mass spectrometer. If this is done under various conditions of ionospheric composition, calibrations are obtained for the several major ionospheric constituents. This technique has been used successfully between the RPA and IMS on the Atmospheric Explorer satellites, between the topside sounder and IMS on the ISIS-II satellite, and will be used for the RIMS on Dynamics Explorer-A, which is an RPA and IMS in tandem, similar to that proposed for RPDP. Overall accuracy is expected to be approximately 10% for the major ion species.

4. Triaxial Fluxgate Magnetometer (Sugiura/GSFC)

The fluxgate sensor planned for RPDP is a modification of the instrument being flown on Dynamics Explorer (DE). The Dynamics Explorer instrument is a hybrid consisting of a four bit digitally controlled current source and twelve bit internal analog-to-digital converter operating on a }6000 gamma (1 gamma = 1 nT) analog signal. The instrument planned for RPDP will incorporate the same sensor design with the range modified to produce a }64000 gamma analog signal fed into a 14 bit A-D converter to give a resolution of }2 gamma.

Errors include the noise level of the instrument of approximately 0.1 gamma peak to peak, the temperature coefficient of sensitivity which is less than 10 ppm/°C, and the temperature stability of the sensor magnetic axis, which is less than 3 arc seconds/°C. The latter two sources convert to

maximum error sources of .64 gamma/°C and .93 gamma/°C respectively. They are controllable by ground calibration and/or inflight thermal control, and in the case of the sensitivity, by inflight calibration. As is almost always the case with magnetometers, the ultimate accuracy of measurement will be determined by the degree to which spacecraft fields can be eliminated at the sensor, and by the accuracy of attitude determination provided.

5. DC Electric Field/Langmuir Probe (Block and Falthammar/KTH, Gurnett/Iowa)

The electric field instrument developed by the Swedish Royal Institute of Technology (KTH) has been flown on numerous sounding rocket and balloon missions. This unit combines voltages from the four monopole antenna elements with summing and difference amplifiers to produce vector components of the electric field from dc up to 1 kHz. At the end of each antenna element is a 7 cm diameter specially coated spherical probe to minimize the effect of photoemission. This unit is microprocessor controlled so that it is adaptive in case an antenna element fails to open and programmable so that periodically the sensors can be swept with a voltage ramp to produce the Langmuir probe I vs. V characteristics. From this sweep the electron density and temperature can be obtained. This sweep can be initiated up to 10 times/second if desired.

The final design and the fabrication of flight hardware is to be carried out at Iowa based on the KTH design.

6. Spin-Scan Imaging System (Frank and Craven/Iowa)

Two spin-scan imaging systems are being developed for the Dynamics Explorer-A Mission. One of these systems responds in the visible wavelength range at 391.4, 557.7, and 630.0 nm due to the selected interference filters and the other responds in the vacuum ultraviolet region at 117-124, 124-137, and 137-170 nm. It is proposed to fabricate only one of these imagers at this time. The one selected will depend on the specific mission objectives to be accomplished.

Both imaging systems have a similar scheme. Light enters through a collimator which defines the field of view to $36^\circ \times 3^\circ$ and reflects off a mirror which is positioned in angle by a stepping motor. Light from the stepped mirror is focused by a parabolic mirror onto a pinhole aperture. This (4mm diameter light beam passes through a selected interference filter in a filter wheel and is incident on the photocathode of a photomultiplier tube. The PM tube output gives the light intensity. As the RPDP spins, the imager scans a 360° circle producing a line of 1440 pixels. After each scan the stepping mirror changes angle to produce an image field of 144 lines. At a spin rate of 20 RPM it takes 7.2 minutes to form a complete image of $360^\circ \times 36^\circ$. Scans of smaller fields of view can be obtained in less time by command or by programmed sequence.

7. Additional Instruments for WISP

The RPDP is to be designed so that several additional instruments can be accommodated. For SEPAC, Magnetospheric Multiprobes, CRM, and Tether it

may be that the investigations will provide instruments for RPDP. For WISP there have been two sets of instruments selected for accommodation on RPDP:

- + WISP Plasma Analysis Package (D. L. Reasoner/MSFC). The knowledge of the background plasma composition and density is required to estimate critical parameters in plasma dispersion relations such as ion plasma frequencies and acoustic speeds. In situ plasma measurements will augment sounder observations of F-region plasma bubbles. The RPDP will carry an ion mass spectrometer, a retarding potential analyzer, and a Langmuir probe, all similar to instruments developed for flight on the DOD SCATHA and on satellites or rockets by MSFC. The ion mass spectrometer is a magnetic focussing analyzer which will be able to measure the densities of H^+ , He^+ , O^+ , the N_2^+ , NO^+ , O_2^+ heavy ion group, and the heavier ions up to mass 56 (Fe^+). The retarding potential analyzer and Langmuir probe feature high frequency responses (≈ 1 kHz), important for analyzing transient perturbations caused by wave plasma interactions.
- + WISP HF Sounder (W. W. L. Taylor/TRW). The HF Sounder subsystem is an active, remote radio frequency sensor of considerable flexibility capable of coherent detection and range and Doppler measurements. It will be used to determine ionization structures and motions of TID's. It measures the time delay between transmitted and received pulses and the phase, amplitude and Doppler shift of the received signals. The structure and location of irregularities will be measured, both along the orbit and remote from Spacelab.

The HF Sounder Subsystem will operate in a number of preprogrammed modes, including a survey mode. This is a search operation for natural phenomena of interest which will recognize the local plasma frequency and the condition of the ionosphere (quiescent or disturbed). Subsequent HF Sounder activity will follow to investigate some feature in greater detail by means of another mode of operation, which will usually provide information of interest in a more magnified form. Other modes may change the frequency range of operation, pulse width, pulse repetition frequency and/or the power radiated. Modes may determine Doppler shifts or operate at a single frequency for monitoring the strength and variation of the received signals. Several types of data presentations are possible, including displays of propagation time vs. frequency, Doppler vs. time for selected frequencies, Doppler vs. range at selected frequencies, and range vs. time at selected frequencies.

RPDP QUESTIONS RELATED TO JOINT OPERATIONS

- Other Required/Desired Instruments
- Maximum Range of Operation
- Maximum Spatial/Temporal Resolution (Data Rate)
- Absolute RPDP Attitude Information
 - Real Time
 - Post Mission
- Absolute RPDP Position Information
 - With Respect to Orbiter
 - With Respect to Earth/Magnetic Field
 - Performance of Ku-Band Radar
 - Availability of Global Positioning System
 - Real Time
 - Post Mission
- Operation On-Orbit Between STS Flights
- Multiple Joint Operations on One Mission
 - Total Energy
 - Conflicting Requirements

SECTION XIII. CHEMICAL RELEASE MODULE (CRM)

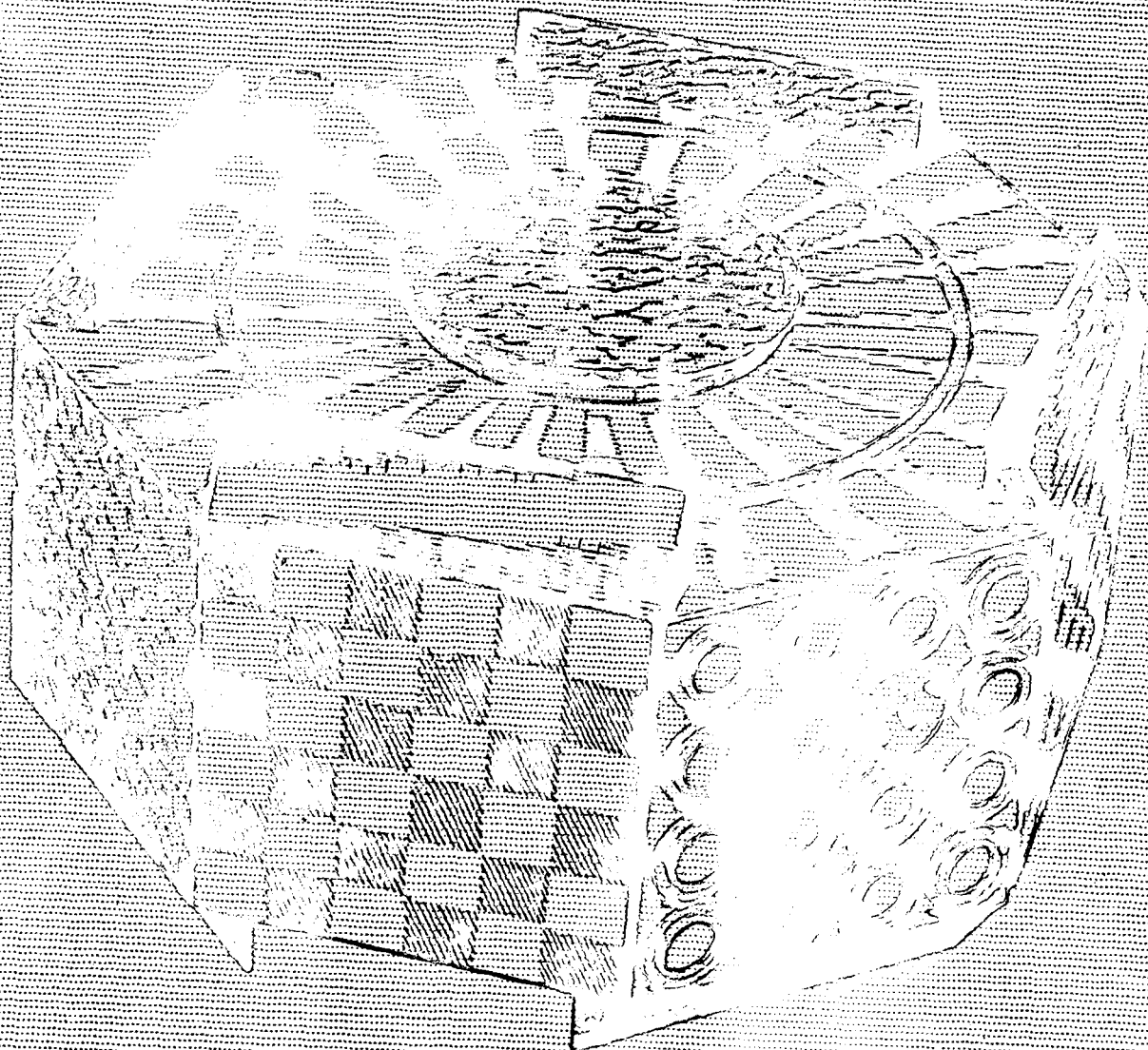
CHEMICAL RELEASE MODULE FACILITY

Presentation To

ACTIVE EXPERIMENTS WORKING GROUP

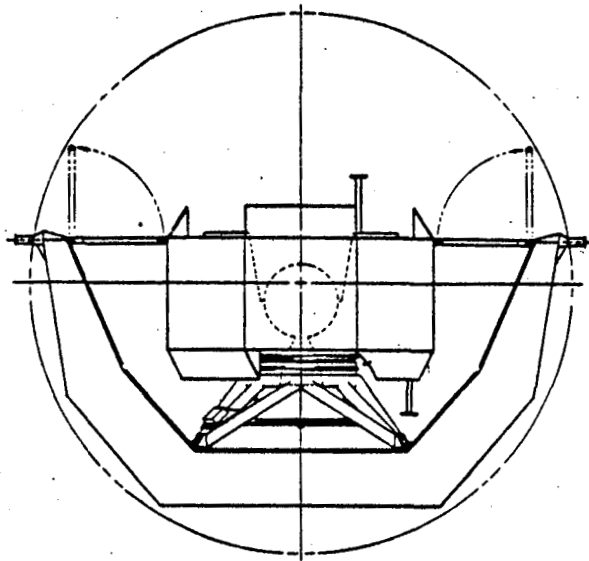
September 23, 1980

**David L. Reasoner
ES53
Marshall Space Flight Center**

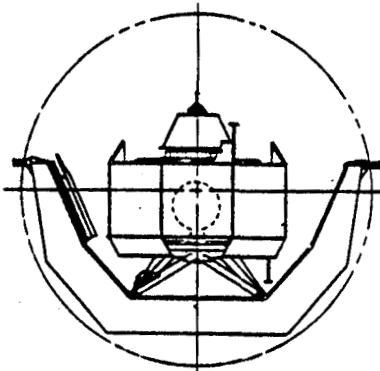


CHEMICAL RELEASE MODULE FACILITY (CRMF)

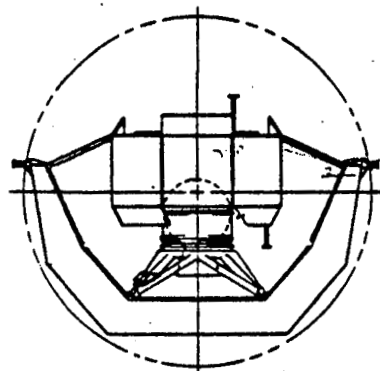
BASD



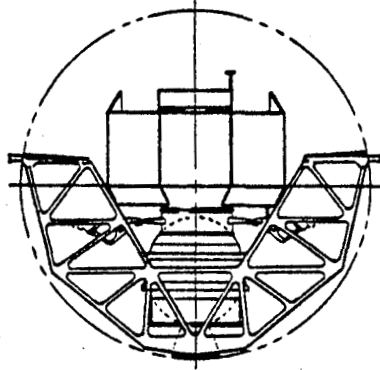
CRMF-1 CONFIGURATION



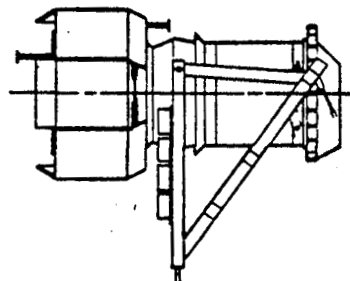
SPEE DEPLOYMENT COMPATIBILITY



94cm-DIA PKM COMPATIBILITY



SSUS-D COMPATIBILITY



SSUS-A COMPATIBILITY

Figure 2 CRMS Launch Arrangements

ORGANIZATION:	MARSHALL SPACE FLIGHT CENTER CHEMICAL RELEASE MODULE FACILITY	NAME: DATE:
---------------	--	--------------------

MILESTONE DATES

MARCH, 1979	CRM FACILITY ASSIGNED TO MSFC FOR PHASE C/D
NOVEMBER, 1979	RFP ISSUED FOR DESIGN AND FABRICATION OF CRM
MAY, 1980	ENVIRONMENTAL ASSESSMENT OF CRM COMPLETED
JULY, 1980	CRM DESIGN ,DEVELOPMENT, AND FABRICATION CONTRACT AWARDED TO BALL AEROSPACE SYSTEMS DIVISION, BOULDER, CO.
OCTOBER, 1980	RELEASE OF ANNOUNCEMENT OF OPPORTUNITY

242.

CRM DESIGN PROPERTIES

1. PROVIDES THE CAPABILITY TO CONDUCT:

- A. THERMITE-BASED METAL VAPOR RELEASES
 - B. PRESSURIZED GAS RELEASES
 - C. DISPERSED LIQUID RELEASES
 - D. SHAPED CHARGE RELEASES FROM EJECTED SUB-MODULES
 - E. DIAGNOSTIC MEASUREMENTS WITH PI SUPPLIED INSTRUMENTS
(ON-BOARD OR FROM EJECTED SUB-MODULES)
- } FROM EITHER
ON-BOARD OR EJECTED
CONTAINERS

2. PROVIDES A BASIC R-F AND ELECTRICAL SYSTEM:

- A. FOR RECEIVING AND EXECUTING COMMANDS
- B. FOR TELEMETERING HOUSEKEEPING (OR OTHER) DATA
- C. FOR TRACKING
- D. FOR MONITORING HOUSEKEEPING AND CONTROL UNITS
- E. FOR ULTRA-SAFE DIS-ARMING AND CONTROL MONITORING

FIGURE 22(a)

57° INCLINED ORBIT RELATIVE TO L-SHELLS AT 250 km

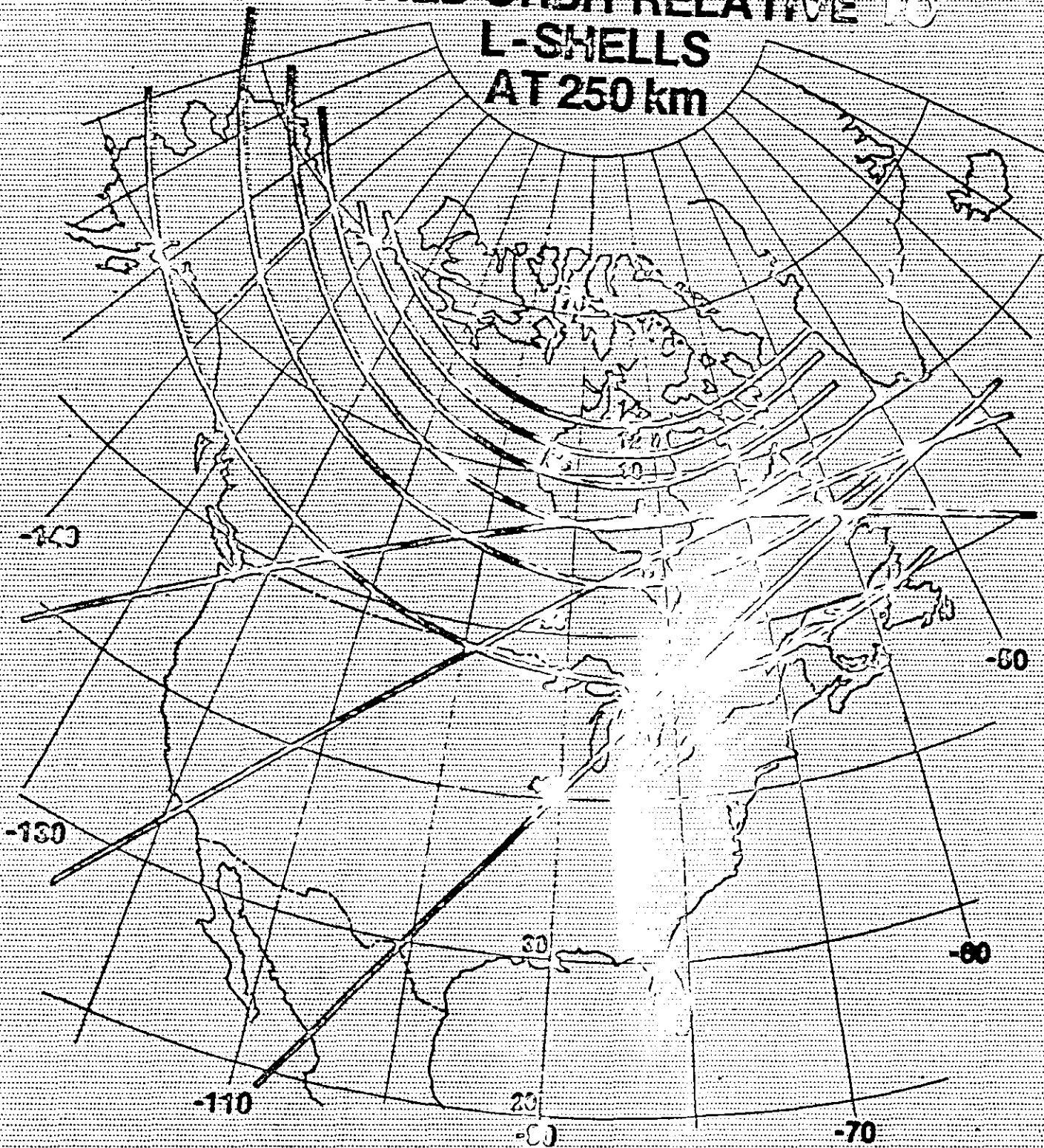


FIGURE 20

ORGANIZATION:

MARSHALL SPACE FLIGHT CENTER

NAME:

ES53

CHEMICAL RELEASE TECHNIQUES

D. J. REASONER

DATE:

• THERMITE REACTIONS: $n\text{Ba} + \text{CuO} \rightarrow \text{BaO} + \text{Cu} + (n-1)\text{Ba}$

• LIQUID RELEASES FOLLOWED BY FLASH VAPORIZATIONS: TMA $[\text{Al}(\text{CH}_3)_3]$

• GAS RELEASES: N_2 , Ar, SF_6 , etc.

• $\text{Ba} + h\nu \rightarrow \text{Ba}^* + e$ $\tau = 20-30 \text{ sec.}$

Ba^* has resonance line 5535 \AA

Sr has resonance line at 4607 \AA

• $\text{Li} + h\nu \rightarrow \text{Li}^* + e$ $\tau = 30 \text{ min.}$

Li has resonance line at 6708 \AA

Li^* has resonance line in Far U.V.

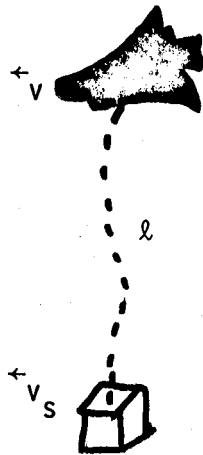
• $\text{TMA} + \text{O} \rightarrow \text{Al}_2\text{O} + h\nu$

SECTION XIV. TETHER FACILITY

TETHER FACILITY PRESENTATION

Peter Banks

BASIC MECHANICAL PRINCIPLES



$$\uparrow mv^2/r$$

300 km

$$\downarrow mg_0(r_0/r)^2$$

$v \sim 7.8$ km/sec

$$T \uparrow \uparrow \frac{m_s v_s^2}{r_s}$$

200 km

$$\downarrow m_s g_0 (r_0/r)^2$$

$v_s \sim v + 59$ m/sec

If tether is acting to constrain the satellite, then

$$\Omega_{\text{Shuttle}} = \Omega_{\text{satellite}}$$

and

$$T = \frac{3l}{r} m_s g$$

NOTE: There are 2 stable points of equilibrium.

If $l = 100$ km

$r = 6670$ km (300 km altitude)

$m_s = 500$ kg ,

then

$$T \sim 200 \text{ N} \quad (\sim 91 \text{ lbs force}) .$$

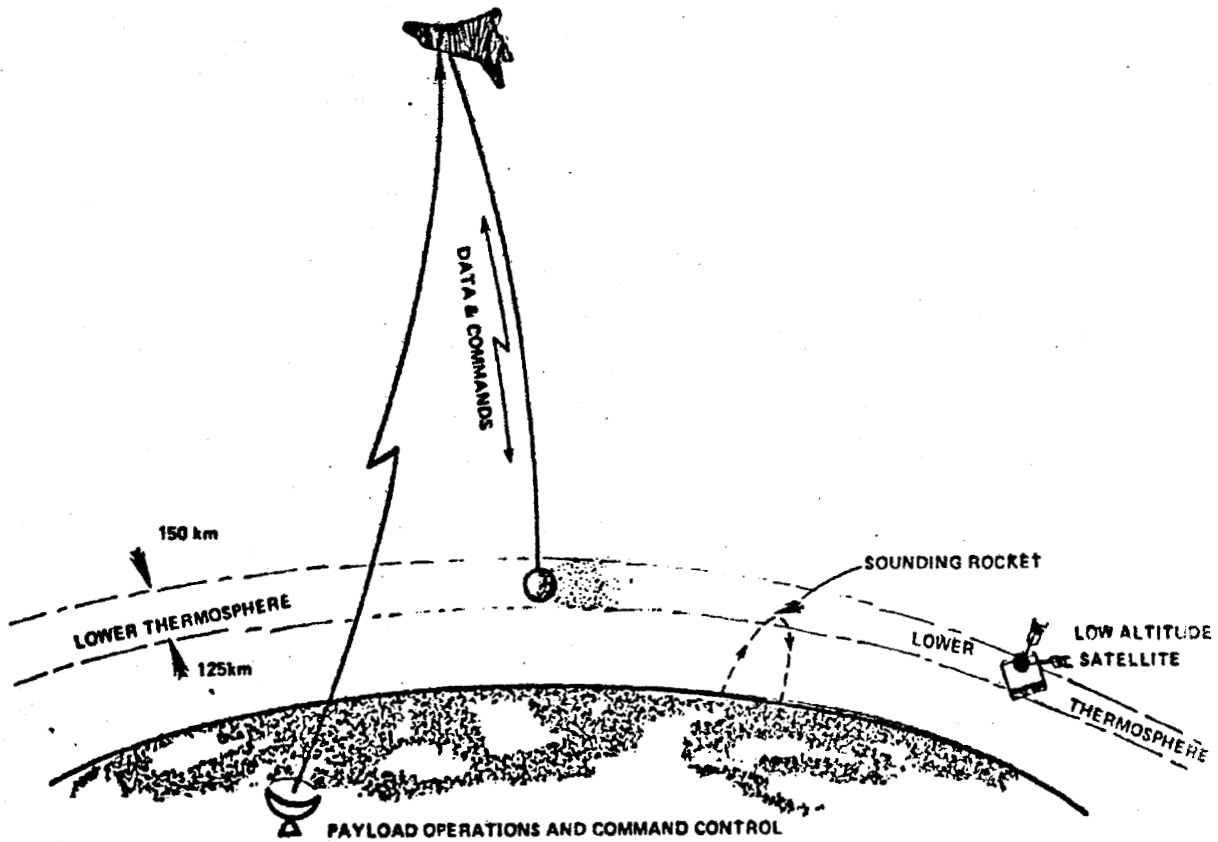
WAVES

$$v_{\omega} \sim \sqrt{\frac{T}{\rho_{\ell}}}$$

If $T \sim 200 \text{ N}$

$$\rho_{\ell} \sim 5 \times 10^{-3} \text{ kg/m ,}$$

then $v_{\omega} \sim 200 \text{ m/sec .}$

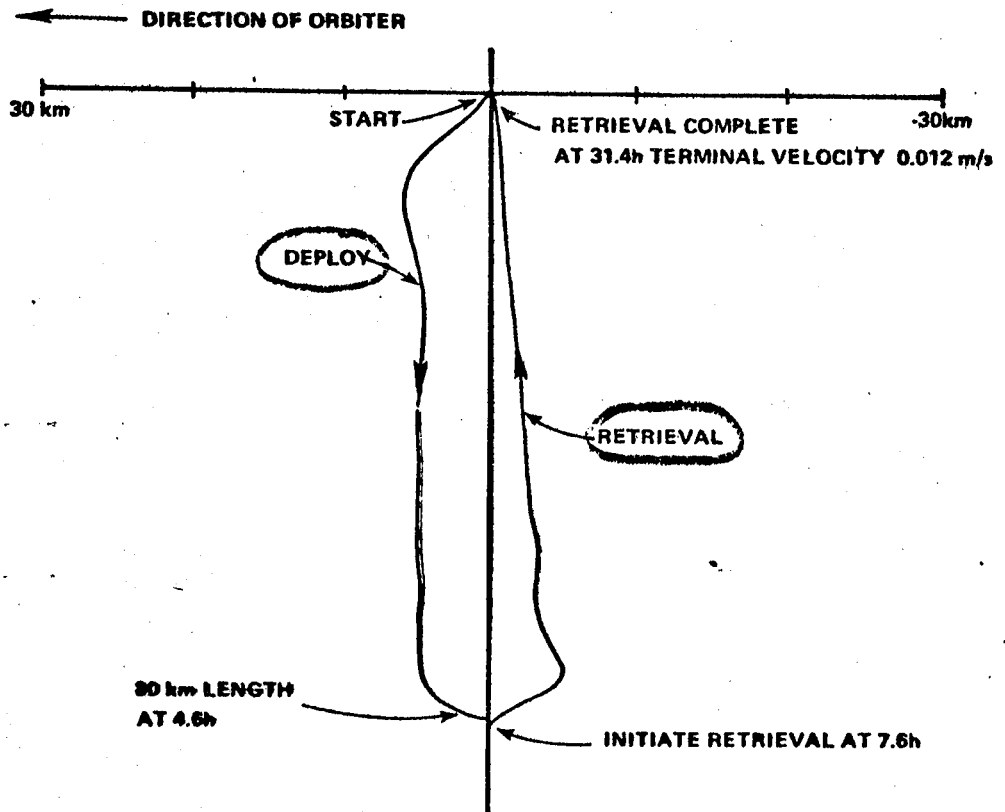
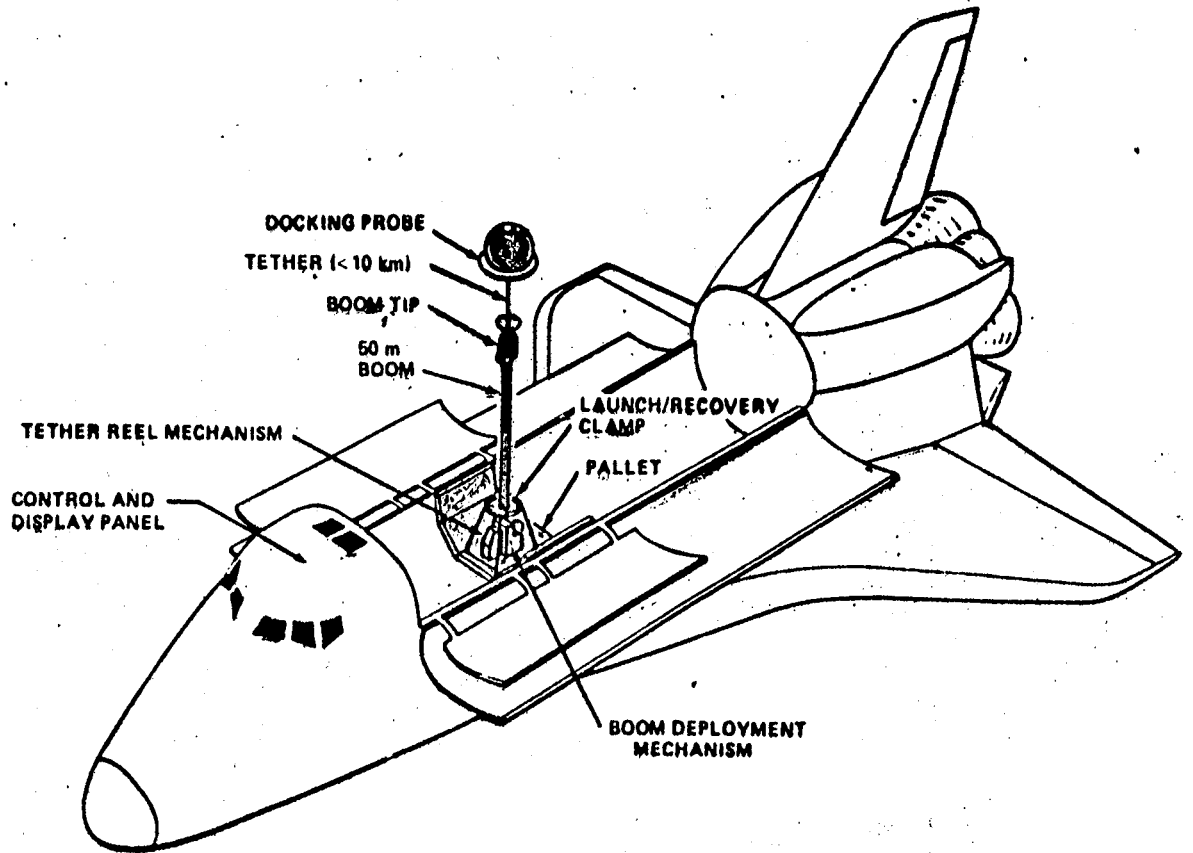


TETHERED SATELLITE SYSTEM

FRDT STUDY

HISTORY

- INITIAL IDEA OF TSS PRESENTED BY M. GROSSI AND G. COLOMBO (SMITHSONIAN ASTROPHYSICAL OBSERVATORY) TO MSFC (1973, 1974).
- AMPS STUDY PRESENTATIONS AT MSFC AND GSFC (1974-1976).
- MSFC STUDIES (1975-PRESENT).
- SAO STUDIES (1974-PRESENT).
- UTAH STATE UNIVERSITY, ELECTRODYNAMIC TETHER SYSTEM STUDIES (1976-PRESENT).
- ADVANCED SYSTEM DEFINITION STUDIES BY BALL AEROSPACE AND MARTIN-MARIETTA (1979-PRESENT).
- FRDT ESTABLISHED APRIL, 1979. TEAM MEETINGS HELD IN MAY, JULY AND OCTOBER, 1979.
- FRDT FINAL REPORT COMPLETED IN MAY, 1980



TETHERED SATELLITE SYSTEM

FUTURE USES

GEOPHYSICS

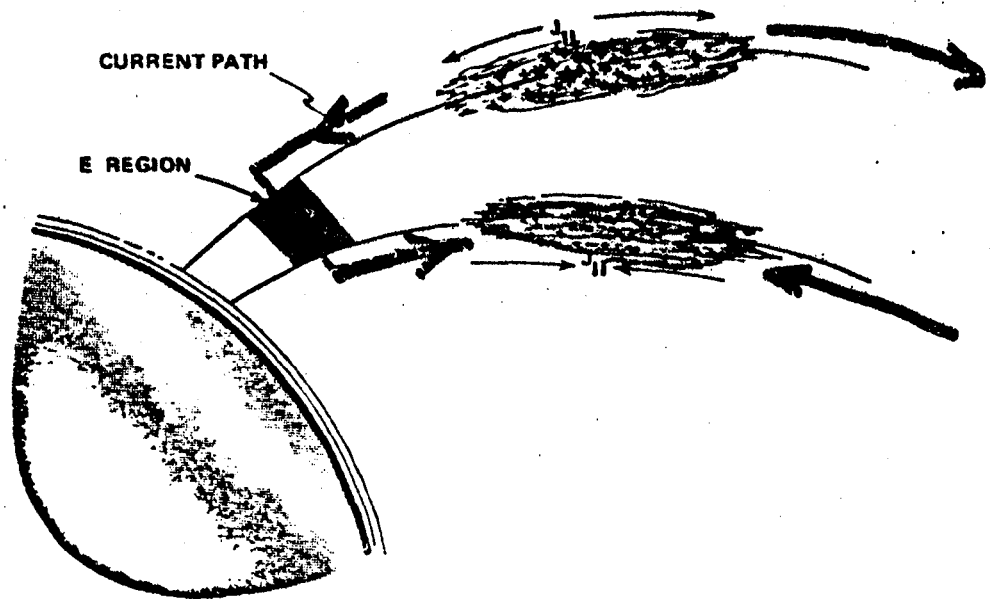
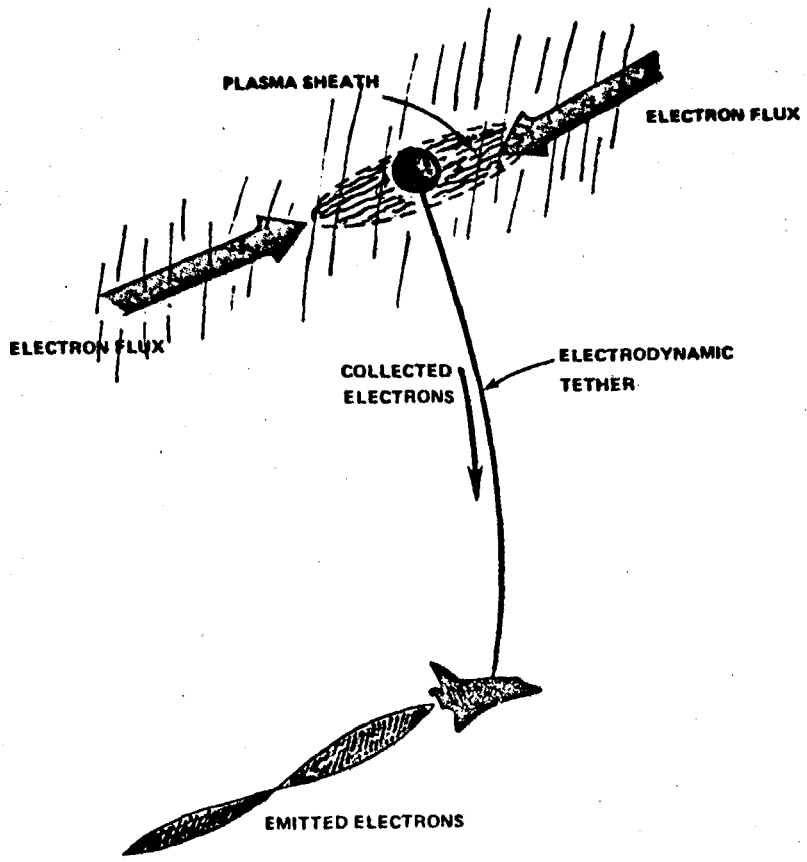
THERMOSPHERE ELECTRODYNAMICS
THERMOSPHERE DYNAMICS
THERMOSPHERE COMPOSITION
METASTABLE SPECIES DYNAMICS
DEEP ATMOSPHERE PROBES
GEOMAGNETIC ANOMALIES

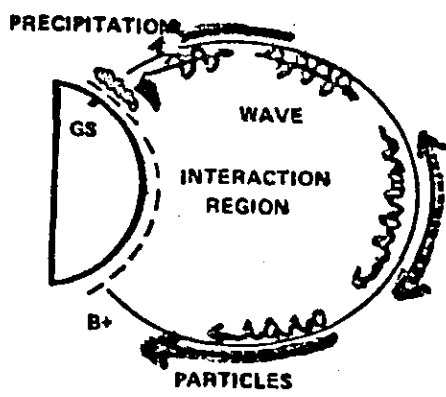
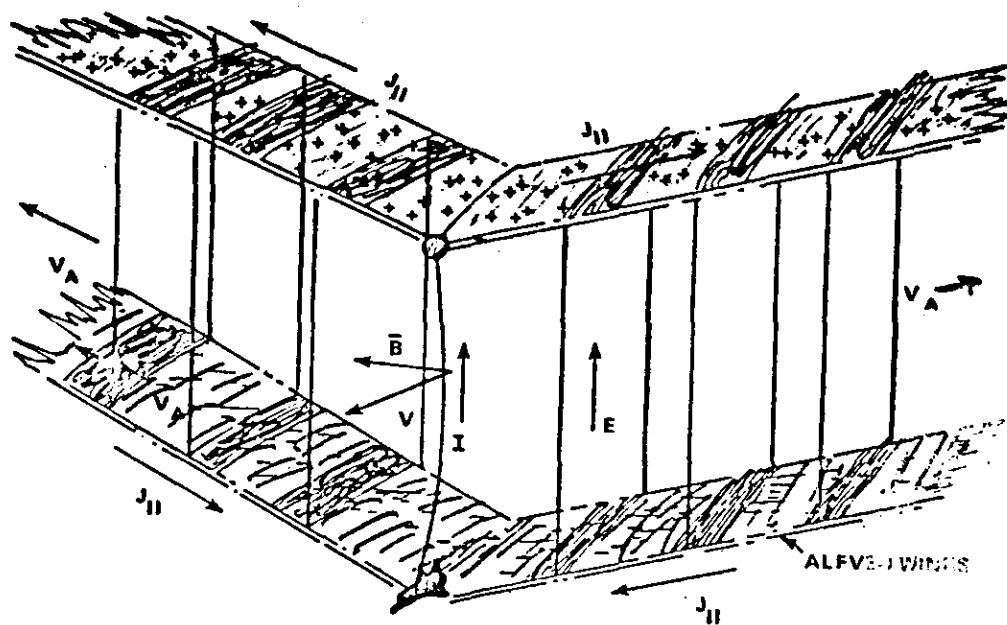
PLASMAS

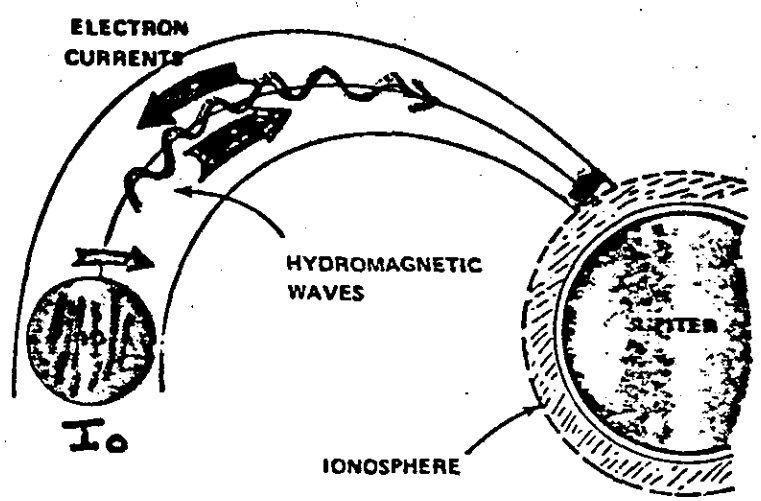
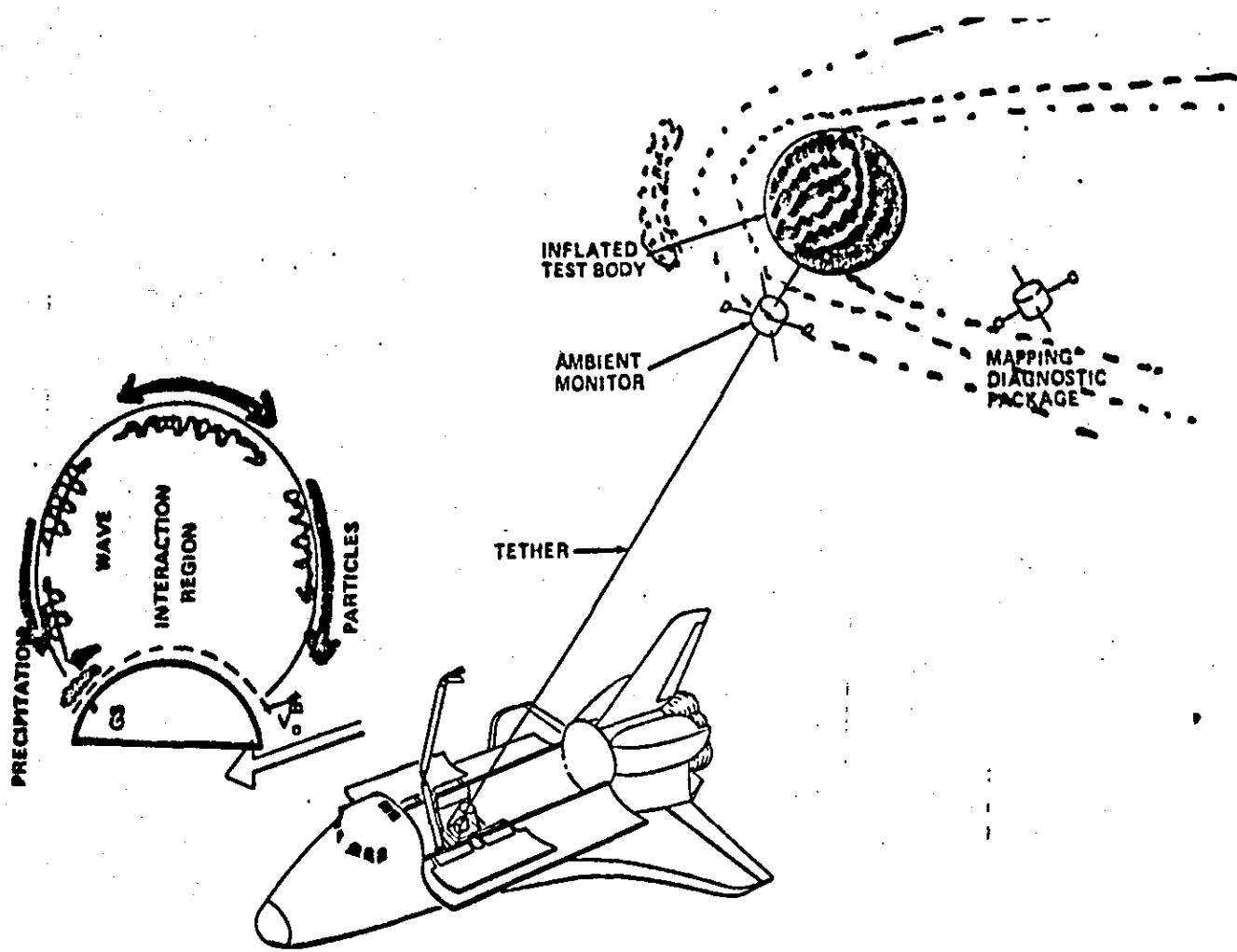
PLASMA SHEATH STUDIES
PLASMA WAVE GENERATION
PLASMADYNAMIC STUDIES
VLF WAVE GENERATION
CHARGE NEUTRALIZATION

SUPPORT ACTIVITIES

TETHERED CHEMICAL RELEASES
TETHERED ELECTRON/ION ACCELERATOR
SUPPORTING MEASUREMENTS PLATFORM







FRDT RECOMMENDATIONS

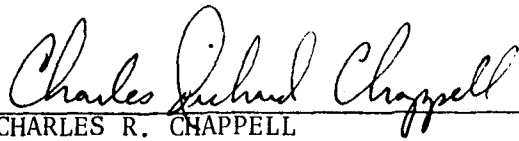
- SCIENTIFIC USE OF THE TSS SHOULD BE GOVERNED BY COMPETITIVE PEER GROUP SELECTION.
- THE TSS FACILITY SHOULD BE DESIGNED TO ACCOMMODATE A BROAD RANGE OF POTENTIAL USERS.
- THE TSS FACILITY SHOULD PROVIDE FOR INTERACTIVE EXPERIMENTS INVOLVING ORBITER AND GROUND SCIENTIFIC PERSONNEL.
- ACCOMMODATIONS SHOULD BE MADE TO PERMIT PALLET-BASED EXPERIMENTS TO OPERATE IN CONJUNCTION WITH TSS EXPERIMENTS.
- SCIENTIFIC PLANNING FOR THE TSS WILL BENEFIT FROM A TSS SCIENCE WORKING GROUP.
- A TSS SUPPORT GROUP TO AID SCIENTIFIC INVESTIGATORS SHOULD BE ESTABLISHED AT A NASA CENTER.
- TWO RE-USABLE, MULTIPLE INSTRUMENT PLATFORMS SHOULD BE DEVELOPED FOR ELECTRODYNAMIC TETHER AND GEOPHYSICAL OBSERVATIONS,

APPROVAL

SPACE PLASMA PHYSICS ACTIVE EXPERIMENTS

Edited by W. T. Roberts

The information in this report has been reviewed for technical content. Review of any information concerning Department of Defense or nuclear energy activities or programs has been made by the MSFC Security Classification Officer. This report, in its entirety, has been determined to be unclassified.



CHARLES R. CHAPPELL

Chief, Solar-Terrestrial Physics Division



CHARLES A. LUNDQUIST

Director, Space Sciences Laboratory

